Continuous production of rhamnolipids by means of process integration

Dissertation

zur Erlangung des akademischen Grades eines
Doktors der Ingenieurwissenschaften (Dr.-Ing.)

vorgelegt an der
**Fakultät für Chemieingenieurwesen und Verfahrenstechnik der
Universität Fridericiana Karlsruhe**

von

Dipl.-Ing. Miriam Heyd

geb. 26. Mai 1981 in Sindelfingen

Tag des Kolloquiums: 29. 01. 2009
Referent: PD. Dr.-Ing. habil. M. Franzreb
Korreferent: Prof. Dr. rer. nat. C. Syldatk

Institut für Technische Chemie
Bereich Wasser- und Geotechnologie
Forschungszentrum Karlsruhe

Karlsruhe 2009

Danksagung

Die vorliegende Arbeit entstand im Rahmen meiner wissenschaftlichen Arbeiten von 2005 bis 2008 am Institut für Technische Chemie, Bereich Wasser- und Geotechnologie im Forschungszentrum Karlsruhe GmbH. An dieser Stelle bedanke ich mich herzlich bei den Personen, die zum Gelingen dieser Arbeit beigetragen haben.

Meiner Betreuerin Frau Prof. Dr. Sonja Berensmeier gilt mein ganz besonderer Dank für die Unterstützung, Beratung und wegweisenden Diskussionen während der einzelnen Phasen meiner Arbeit, ohne mich dabei in meiner Gestaltungsfreiheit einzuschränken.
Herrn PD Dr. Matthias Franzreb danke ich für seinen fachlichen Beitrag und dass er mir jederzeit mit Rat und Tat beistand, wenn ich Hilfe benötigte. Ferner bin ich Herrn Prof. Dr. Wolfgang Höll für die Aufnahme in seinem Institut und die Ermöglichung meiner Doktorarbeit dankbar.

Herrn Prof. Dr. Syldatk danke ich herzlich für die Übernahme des Koreferats und die Koordination des Rhamnolipidprojektes, sowie allen weiteren Projektpartnern für hilfreiche Diskussionen. Hierbei bin ich außerdem Herrn Dipl.-Ing. Michael Nusser, Dipl.-Ing. Frank Kirschhöfer und Silke Kirchen für ihre wertvolle Mitarbeit und Beratung bei Fragen der Rhamnolipidanalytik und der Mikrobiologie sehr dankbar.

In diesem Rahmen bin ich insbesondere auch meinen vielen DiplomandInnen, PraktikantInnen und Studienarbeitern zu Dank verpflichtet, ohne die diese Arbeit nie in dem Umfang möglich gewesen wäre. Der Dank geht an Dennis Ungan, Tze Heng Tan, Antje Kohnert, Marieke Dreiling, Stefan Raffelt, Helena Ernst, Stephanie Trauth und Pascal Weigold.

Letztlich hätte mir diese Arbeit bei weitem nicht so viel Freude bereitet, wenn mich nicht meine Arbeitskollegen und -kolleginnen unserer Abteilung für Physikalisch-chemische Interaktionen an Grenzflächen tagtäglich begleitet hätten. Ihnen danke ich für die tolle Arbeitsatmosphäre, die vielfachen Unterstützungen im Laboralltag, die Kaffeerunden und die kleinen Aufmunterungen zwischendurch, insbesondere wenn es abends mal wieder etwas später wurde.

Abschließend gilt mein größter Dank meinem Freund und meiner Familie, die mir stets viel Geduld und Verständnis entgegengebracht und an mich geglaubt haben. In diesem Sinne möchte ich mich auch bei allen Freunden und Bekannten bedanken, die auf direkte oder indirekte Weise zum Gelingen meiner Arbeit beigetragen haben.

„DANKE"

Table of contents

1 Summary and outlook

Motivation

In view of the current discussion of remaining petrochemical resources and sustainability of production processes, industrial biocatalysis based on fermentation processes and renewable feedstocks offers a great potential for production of chemical and biotechnological products and intermediates and will considerably increase during the next few years. As regards surfactants which are widely applied in detergents, pharmaceuticals, cosmetics as well as in food industry, mainly petrochemistry-based compounds are still used in industry. In general, they are only partly biodegradable and may permanently pollute the environment. Biosurfactants, for example rhamnolipids, by contrast, show a high effectiveness coupled with a good biodegradability and low toxicities. Rhamnolipids are mostly produced by *Pseudomonas aeruginosa* and composed of one or two rhamnose molecules and up to three molecules of hydroxy fatty acids. Their chain length may vary from 8 up to 14 carbon molecules. The rhamnolipids most commonly produced by *P. aeruginosa* are Rha-C_{10}-C_{10} and Rha-Rha-C_{10}-C_{10}. Even though biotechnological production of biosurfactants has been established for several years, high production costs due to intense foaming, expensive downstream processing, and high substrate costs have impeded their bulk use up to now.

Integrated rhamnolipid production and purification

The aim of the work covered by this thesis was to produce rhamnolipids by *P. aeruginosa* DSM 2874 in an integrated reactor system. By this process integration of continuous rhamnolipid synthesis and subsequent purification, production costs were to be reduced. As rhamnolipids are secondary metabolites of *P. aeruginosa,* a separation of biomass and rhamnolipid production was possible for continuous rhamnolipid synthesis. The same 10 L bioreactor was used first for biomass production and then for rhamnolipid formation with magnetically immobilised bacteria. In the first step biomass from *P. aeruginosa* DSM 2874 was produced by means of an exponential feeding concept. Then, the biomass obtained was immobilised in magnetic matrices that will allow retention of the biocatalyst by magnetic separation. In a second fermentation step rhamnolipids were produced with immobilised bacteria using a continuous process with *in situ* product removal through foam fractionation. As immobilisates were also carried along with the foam, a high-gradient magnetic separator was integrated downstream of the foam fractionation column to retain them in the fermentation process. Glycerol from biodiesel production was used as a carbon source from renewable raw material to reduce process charges. Reliable rhamnolipid analysis and further purification steps also have to be considered for process optimisation. In principle, feasibility

of the integrated rhamnolipid production concept was demonstrated. In the following paragraphs, the different process steps with the main results will be summarised.

Biomass production: As rhamnolipid synthesis is quorum sensing regulated, higher rhamnolipid yields of continuous rhamnolipid formation requires the production of high biomass concentrations. A fed-batch fermentation step in a 10 L bioreactor based on an exponential feed concept of the carbon source glycerol was needed to achieve the desired cell concentrations, since the production strain is sensitive to higher salt concentrations. Final concentrations of cell dry weights of 15 $g^.L^{-1}$ were obtained, which are higher than the values reported in literature for the growth of *P. aeruginosa* on glycerol (see chapter 4).

Cell immobilisation: It was demonstrated that immobilisation of *P. aeruginosa* cells in magnetic hydrogel beads may be a good means for continuous biosurfactant production by retention of the biocatalyst in the production process through high-gradient magnetic separation and in situ product removal by foam fractionation. For this purpose, different immobilisation matrices, magnetic materials, and immobilisation processes were investigated with regard to their application potential in a continuous rhamnolipid production process. Properties analysed included the particle size distribution, stability, diffusion properties, and, of course, their influence on rhamnolipid production.

As far as the immobilisation process for the materials studied is concerned, suspension polymerisation with facilitated bead separation from the suspension medium by an oil/water emulsion revealed certain advantages compared to droplet extrusion by the JetCutting® device. Smaller bead sizes were possible. Entrapment of magnetite particles was easier and especially at higher bead quantities, no plugging problems occurred.

Of the materials investigated, Bayoxide® magnetite and MagPrep® Silica magnetite were homogeneously embedded in alginate beads. They also showed the best properties with highest saturation magnetisation for good magnetic separation, an almost neutral zeta potential at working pH for reduced interactions with rhamnolipids, and good diffusion properties not changing the product composition of effused rhamnolipids.

Alginate immobilisates with embedded magnetite possessed an improved mechanical as well as chemical stability compared to pure alginate beads, but their stability still was inferior to polyurethane beads which stayed elastic even with relatively high deformations and were inert to all kinds of chemical agents. However, rhamnolipid synthesis by polyurethane beads was lower than for alginate immobilisates with embedded MagPrep® Silica magnetite, which revealed highest rhamnolipid production closely followed by Bayoxide® magnetite (see chapter 3).

For continuous rhamnolipid production, the biomass from fed-batch fermentation was subsequently immobilised in calcium alginate beads with concurrently embedded ferrimagnetic Bayoxide® magnetite in a suspension polymerisation process which was simple to handle and yielded large quantities of immobilisates in a short time. These immobilisates had the following properties: a medium bead size ($\overline{x}_{AV}$) of about 240 µm, a saturation magnetisation of 5 $A^.m^{2.}kg^{-1}$ for the humid beads, and improved mechanical properties compared to pure alginate beads.

Rhamnolipid synthesis, analysis, and purification: Based on the following integrated reactor concept, rhamnolipids were continuously produced with the immobilised bacteria in a modified 10 L bioreactor. Due to their ability to form micelles, *in situ* removal of rhamnolipids did only seem to be possible by foam fractionation. Fractionation tests with cell-free immobilisates revealed an antithetic behaviour of rhamnolipid enrichment and mass flow rate, thus resulting in an optimisation task. However, rhamnolipid enrichment was principally influenced by rhamnolipid concentrations in the production medium. It was highest for very low concentrations. In practice, fermentation conditions were therefore chosen such that the rhamnolipids produced were completely separated from the production medium with minimum stirrer speeds and gas flow rates, yielding higher rhamnolipid enrichments through lower rhamnolipid concentrations in the medium.

As immobilisates were also entrained with the foam, their magnetic separation by a high-gradient magnetic separator from foam turned out to be well suited. In practice, the HGF 10 separator operated in a cyclic mode using "switchable" permanent magnets permitted a reliable separation over long production times. However, optimisations are still required with respect to the backflushing of ferrimagnetic immobilisates.

According to the integrated reactor concept, rhamnolipid production required re-induction and cell growth of immobilised bacteria after a certain production time, as rhamnolipid synthesis slowed down. In contrast to this, specific rhamnolipid synthesis rates related to the viable cell concentration remained at the initial level over several production cycles. By this process management, complete and continuous separation of rhamnolipids from the production medium was achieved with average enrichment ratios of approximately 15 in the collapsed foam. A total rhamnolipid yield of 70 g over four production cycles revealed the feasibility of a continuous rhamnolipid production, yet leaving potential for further improvements regarding constantly high cell concentrations and lower substrate wastage (see chapter 4).

Effective process optimisation of rhamnolipid synthesis also needs a credible and quick product analysis. Rhamnolipid analysis methods in literature generally range from simple colorimetric tests to sophisticated chromatographic separation, coupled with detection

systems like mass spectrometry to provide detailed structural information and will be reviewed in chapter 2. In this case, HPLC coupled with mass spectrometry represents the most precise method for rhamnolipid identification and quantification at the moment. Most commonly, rhamnolipids are extracted from culture broth and then subjected to HPLC analysis. Recently, efforts were made to accelerate rhamnolipid quantification for a better control of biosurfactant production. Suitable approaches are HPLC analysis directly from culture broth by adding an internal standard or FTIR-ATR measurements of culture broth as quasi-online quantification method. The search for alternative rhamnolipid-producing strains makes a structure analysis and constant adaptation of the existing quantification methods necessary. Simple colorimetric tests based on the total rhamnolipid content may provide a useful tool for strain and medium screening.

Conclusions & outlook

It was demonstrated that continuous rhamnolipid production with intermediate growth periods is possible when using an integrated reactor design. In this case, magnetic immobilisates of the bacteria are a promising tool for easier handling of biocatalysts in a continuous biological production process.

However, a lot of efforts still remain to be undertaken to increase rhamnolipid yields for an economically efficient production process. New approaches will be based on a better understanding of rhamnolipid regulation in *P. aeruginosa* cells, which may also provide tools for process regulation or even transfer of the rhamnolipid synthesis system to heterologous hosts. Additionally, hyperproducing strains can be produced by genetic or metabolic engineering. Another aspect towards industrial application consists in the utilisation of non-pathogenic production strains, for example from *Pseudomonas chlororaphis* or *Burkholderia plantarii*.

2 Zusammenfassung und Ausblick

Motivation

In den letzten Jahren kam vermehrt eine Diskussion über verbleibende Erdölreserven und die nachhaltige Nutzung von Rohstoffen auf. In diesem Kontext bietet die industrielle Biokatalyse auf Basis nachwachsender Rohstoffe ein großartiges Potenzial für die Produktion von chemischen und biotechnologischen Produkten und wird in den kommenden Jahren noch deutlich an Bedeutung gewinnen. Im Fall von Tensiden, die vielfältige Anwendungen in Detergenzien, Pharmazeutika, Kosmetika sowie in der Nahrungsmittelindustrie besitzen, basiert die absolute Mehrheit der Tenside nach wie vor auf petrochemischen Herstellprozessen. Dies hat zur Konsequenz, dass durch die häufig nur teilweise Abbaubarkeit der Tenside nachhaltig die Umwelt geschädigt wird. Biotenside, als Beispiel Rhamnolipide, zeigen eine hohe Wirkeffizienz bei gleichzeitig guter biologischer Abbaubarkeit und geringer Toxizität. Rhamnolipide, die in erster Linie durch *Pseudomonas aeruginosa* als Sekundärmetabolite gebildet werden, bestehen aus ein bis zwei Rhamnosemolekülen und bis zu drei Hydroxyfettsäureeinheiten. Die Fettsäuren können hierbei in der Kettenlänge von 8 bis 14 Kohlenstoffatomen variieren. Die am häufigsten von *P. aeruginosa* synthetisierten Rhamnolipide sind Rha-C_{10}-C_{10} und Rha-Rha-C_{10}-C_{10}. Obwohl die biotechnologische Herstellung von Biotensiden bereits seit einiger Zeit etabliert ist, werden Biotenside aufgrund der hohen Produktionskosten bisher nur in Nischenbereichen eingesetzt. Die Produktkosten werden im Wesentlichen von den eingesetzten Produktions-verfahren, insbesondere durch die Produktaufarbeitung, bestimmt, so dass sich hier Ansatzpunkte zur gezielten Verfahrensoptimierung bieten.

Integrierte Rhamnolipidproduktion und -aufreinigung

Ziel dieser Arbeit war die Produktion von Rhamnolipiden durch *P. aeruginosa* DSM 2874 in einem integrierten Reaktorsystem. Durch die Prozessintegration von kontinuierlicher Rhamnolipidsynthese und anschließender Aufreinigung sollte die Prozessführung vereinfacht und eine Senkung der Produktionskosten erreicht werden. Da Rhamnolipide als Sekundärmetabolite von *P. aeruginosa* gebildet werden, war eine Trennung von Biomasse- und Rhamnolipidproduktion für die kontinuierliche Biotensidherstellung möglich. Derselbe 10 L Bioreaktor wurde zuerst für die Biomassefermentation und anschließend leicht modifiziert für die Rhamnolipidbildung mit magnetischen Zellimmobilisaten eingesetzt. Im ersten Schritt wurde Biomasse von *P. aeruginosa* DSM 2874 in einem Fed-Batch-Verfahren zur Erreichung höherer Zellkonzentrationen kultiviert. Diese Biomasse wurde anschließend in magnetischen Hydrogelen immobilisiert, um sie über Magnetseparation im Bioreaktor zurückhalten zu können. Ein darauffolgender zweiter Fermentationsschritt mit den

magnetisch immobilisierten Bakterien diente der kontinuierlichen Rhamnolipidproduktion mittels *in situ* Produktentfernung durch Schaumfraktionierung. Da auch Immobilisate mit dem Schaum ausgetragen wurden, wurde ein Hochgradienten-Magnetseparator hinter das Fraktionierungsrohr geschaltet, der die Immobilisate im Produktionsprozess hielt. Als Kohlenstoffquelle wurde Glycerin verwendet, das als nachwachsender Rohstoff beispielsweise in größeren Mengen während der Biodieselherstellung anfällt. Des Weiteren sind eine verlässliche Rhamnolipidanalytik sowie die Betrachtung weiterer Aufreinigungsschritte unabdingbar für die Prozessoptimierung. Grundsätzlich konnte die Machbarkeit der integrierten kontinuierlichen Rhamnolipidproduktion demonstriert werden. In den folgenden Abschnitten werden nun die Vorgehensweisen in den einzelnen Prozessschritten und die wichtigsten Ergebnisse kurz dargestellt.

Biomasseproduktion: Da die Rhamnolipidsynthese durch *P. aeruginosa* Quorum sensing reguliert ist, stellt der Einsatz höherer Zellkonzentrationen während der Rhamnlipidproduktion die Grundlage für gute Rhamnolipidausbeuten dar. Um diese höheren Zellkonzentrationen während der Biomassefermentation trotz einer gewissen Sensibilität des Produktionsstammes gegenüber höheren Salzkonzentrationen zu erreichen, wurde eine Fed-Batch-Kultivierung mit exponentiellem Feed der Kohlenstoffquelle Glycerin im 10 L Bioreaktor durchgeführt. Hierbei wurden Endkonzentrationen an Biotrockenmasse von $15\ \text{g·L}^{-1}$ bei einer maximalen Wachstumsrate von $0.15\ \text{h}^{-1}$ erreicht. Diese überschreiten bisher in der Literatur berichtete Werte für das Wachstum von *P. aeruginosa* mit Glycerin als Kohlenstoffquelle und anschließender Rhamnolipidproduktion, die von ca. $4 - 12\ \text{g·L}^{-1}$ reichen (siehe Kapitel 4).

Zellimmobilisierung: Es wurde demonstriert, dass die Immobilisierung von *P. aeruginosa* Zellen in magnetischen Hydrogelen ein gutes Werkzeug zur kontinuierlichen Biotensidproduktion mit Rückhaltung des Biokatalysators über Hochgradienten-Magnetseparation und *in situ* Produktentfernung durch Schaumfraktionierung darstellt. Zur Optimierung des Prozesses wurden verschiedene Matrices, Magnetitarten und Immobilisierungsverfahren in Hinblick auf ihr Anwendungspotenzial zur kontinuierlichen Rhamnolipidproduktion untersucht. Analysierte Eigenschaften waren hierbei die Partikelgrößenverteilung, die Stabilität, die Diffusionseigenschaften und natürlich die Beeinflussung der Rhamnolipidproduktion.
In Bezug auf den Immobilisierungsprozess zeigte die Suspensionspolymerisation mit erleichterter Immobilisatseparation vom Suspensionsmedium über eine Wasser-in-Öl Emulsion gewisse Vorteile gegenüber der Tropfenextrusion mittels des JetCutter®-Verfahrens. Neben kleineren möglichen Partikelgrößen erwies sich insbesondere der

Einschluss von Magnetitteilchen bei der Suspensionspolymerisation als einfacher und führte nicht zu Verstopfungen von Filtern oder Düsen bei größeren Polymermengen wie im Falle des JetCutter®-Apparates.

Von den untersuchten Magnetitpartikeln, ließen sich Bayoxide® Magnetit und MagPrep® Silica Magnetit besonders homogen in den Alginatimmobilisaten einschließen. Außerdem zeigten sie mit hohen Sättigungsmagnetisierungen, einem nahezu neutralen Zetapotenzial beim verwendeten pH-Wert und damit verbundenen geringen Wechselwirkungen mit Rhamnolipiden sowie guten Diffusionseigenschaften die besten Voraussetzungen für die integrierte Rhamnolipidherstellung.

Des Weiteren konnte eine generelle Verbesserung der mechanischen sowie chemischen Stabilität durch gleichzeitigen Einschluss von Magnetpartikeln in Calciumalginatperlen im Vergleich zu reinem Calciumalginat beobachtet werden. Die erreichten Stabilitäten blieben jedoch immer noch unterhalb derjenigen von Polyurethanimmobilisaten, die selbst bei hohen Deformierungen noch elastisches Verhalten aufwiesen und inert gegenüber allen verwendeten Chemikalien waren. Allerdings war die Rhamnolipidsynthese von immobilisierten *P. aeruginosa* in Polyurethan deutlich geringer als in Calciumalginat mit eingeschlossenem MagPrep® Silica oder Bayoxide® Magnetit (siehe Kapitel 3).

Für die kontinuierliche Rhamnolipidproduktion wurde die Biomasse aus der Fed-Batch Fermentation in Calciumalginat mit gleichzeitig eingeschlossenem ferrimagnetischem Bayoxide® Magnetit immobilisiert. Die Herstellung sphärischer Partikel erfolgte durch Suspensionspolymerisation, welche eine leichte Handhabbarkeit des Prozesses auch mit magnetischen Einschlüssen und die Produktion großer Immobilisatemengen in kurzer Zeit ermöglichte. Die erzielten Immobilisate wiesen folgende Eigenschaften auf: mittlere Partikelgröße ($\overline{x}_{AV}$) von 240 µm, eine Sättigungsmagnetisierung von 5 $A \cdot m^2 \cdot kg^{-1}$ der feuchten Immobilisate und verbesserte mechanische Eigenschaften gegenüber reinen Alginatimmobilisaten.

Rhamnolipidsynthese, -analyse and -aufreinigung: In einem anschließenden integrierten Reaktorkonzept wurden Rhamnolipide kontinuierlich im 10 L Bioreaktor mit den immobilisierten *P. aeruginosa* produziert und abgetrennt. Aufgrund ihrer Eigenschaft, oberhalb einer bestimmten Konzentration Mizellen zu bilden, erschien eine kontinuierliche Produktentfernung *in situ* nur über Schaumfraktionierung möglich, da Rhamnolipide über Membranen zurückgehalten werden. Schaumfraktionierungsversuche im Batch-Verfahren ließen ein gegenläufiges Verhalten von Rhamnolipidanreicherung im Schaum und Separationsrate erkennen, die prinzipiell eine Optimierung der Separationsparameter erforderlich machte. In erster Linie war jedoch die Anreicherung von Rhamnolipiden im Schaum von der Rhamnolipidkonzentration im Produktionsmedium abhängig und erzielte

höchste Werte für sehr geringe Konzentrationen im Medium. In der Praxis bewährte sich daher die Einstellung der Rührerdrehzahl und Begasungsrate, die gerade noch eine komplette Separation der Rhamnolipide vom Produktionsmedium ermöglichte. Bei diesen Bedingungen waren gleichzeitig durch die niedrigen Rhamnolipidkonzentrationen im Medium höhere Anreicherungen im Schaum möglich.

Da ebenfalls Immobilisate mit dem Schaum ausgetragen wurden, erwies sich deren Rückhaltung über Hochgradienten-Magnetseparation als besonders geeignet. Der verwendete HGF 10 Separator, welcher zyklisch mit „schaltbaren" Permanentmagneten arbeitet, erlaubte eine verlässliche Separation über lange Produktionszeiten hinweg. In Bezug auf die Rückspülung der ferrimagnetischen Immobilisate sind jedoch noch Optimierungen erforderlich, um ein Verstopfen der Filtermatrix nach langen Laufzeiten zu vermeiden.

Nach einer gewissen Kultivierungsdauer ließ die Rhamnolipidproduktion im 10 L Bioreaktor etwas nach, wodurch eine erneute Induktion der Rhamnolipidbildung sowie Wachstum der Zellen erforderlich wurde. Da die spezifische Rhamnolipidsynthese bezogen auf die Lebendzellzahl über mehrere Produktionszyklen hinweg auf dem anfänglichen Niveau blieb, war das Nachlassen der Rhamnolipidproduktion auf Zell- sowie Immobilisatverluste zurückzuführen. Durch diese Prozessführung mit Schaumfraktionierung und Magnetseparation war es möglich, Rhamnolipide vollständig und kontinuierlich mit einer durchschnittlichen Anreicherung im kollabierten Schaum von 15 aus dem Produktionsmedium zu entfernen. Hierbei wurden über vier Produktionszyklen hinweg 70 g Rhamnolipid mit einer Raum-Zeit-Ausbeute von 0.023 $g \cdot L^{-1} \cdot h^{-1}$ erzielt. Damit konnte die Machbarkeit einer kontinuierlichen Rhamnolipidproduktion über Prozessintegration gezeigt werden. Jedoch sind bezüglich Raum-Zeit-Ausbeuten, Zellwachstum und geringerem Substratverbrauch noch Verbesserungen nötig (siehe Kapitel 4).

Eine effektive Prozessoptimierung beruht auch auf einer schnellen und verlässlichen Produktanalyse. Rhamnolipid-Analysemethoden reichen in der Literatur von einfachen Farbtests hin zu anspruchsvoller chromatographischer Auftrennung, gekoppelt mit Detektionssystemen wie beispielsweise der Massenspektrometrie. Diese dient neben der Quantifizierung von Analyten auch der Ermittlung von detaillierten Strukturinformationen über Massenspektra. Die Kopplung von HPLC mit Massenspektrometrie stellt im Augenblick die Methode der Wahl dar, wenn es um präzise Identifizierung und Quantifizierung von Rhamnolipiden geht. In der Regel werden Rhamnolipide aus der Kulturbrühe extrahiert und danach über HPLC analysiert. In letzter Zeit wurden einige Anstrengungen unternommen, um die Rhamnolipidanalyse für eine bessere Steuerung der Biotensidproduktion zu beschleunigen. Geeignete Ansätze finden sich in der HPLC-Messung direkt aus

Kulturmedium mithilfe der Zugabe eines internen Standards oder in FTIR-ATR Messungen ebenfalls direkt im Produktionsmedium als quasi-online Analytik. Die Suche nach alternativen nicht-pathogenen Rhamnolipid-produzierenden Stämmen erfordert eine genaue Strukturanalyse gebildeter oberflächenaktiver Substanzen sowie eine ständige Anpassung der vorhandenen Quantifizierungsmethoden an neue Rhamnolipidspezies. In diesem Fall können auch einfache Farbtests, basierend auf dem Gesamtgehalt an Rhamnosemolekülen, einen wertvollen Beitrag zum Screenen von neuen Produktionsstämmen und geeigneten Medienzusammensetzungen leisten (siehe Kapitel 2).

Fazit & Ausblick

Es wurde demonstriert, dass eine kontinuierliche Rhamnolipidproduktion mit zwischenzeitlichen Regenerationsphasen der Bakterien durch das integrierte Reaktorkonzept möglich ist. Für diese Prozessintegration bieten sich magnetische Zellimmobilisate als ein Erfolg versprechendes Werkzeug an, das eine einfachere Handhabung des Biokatalysators in einem kontinuierlichen Fermentationsprozess erlaubt.

Dennoch sind noch einige Anstrengungen auf Seiten des Upstreams zu unternehmen, um Rhamnolipidausbeuten zu steigern und damit einen ökonomisch effizienten Produktionsprozess zu erreichen. Dafür ist ein besseres Verständnis der Rhamnolipidregulation in *P. aeruginosa* notwendig, um eine gezielte Regulation der Synthese zu ermöglichen. Zusätzlich ist die Gewinnung von Überexpressionsstämmen durch genetische Modifikationen oder Metabolic-engineering denkbar. Ein weiterer Aspekt in Richtung kommerzielle Produktion besteht in der Verwendung und Optimierung von nicht-pathogenen Produktionsstämmen wie beispielsweise *Pseudomonas chlororaphis* oder *Burkholderia plantarii*.

3 Theoretical basics and research project

3.1 Introduction and outline of this thesis

Surfactants are widely used in larger quantities in detergents, pharmaceuticals, cosmetics and in food industry. As traditionally used surfactants are based on petrochemistry, they are only partially biodegradable and pollute enduringly the environment. Biosurfactants, for example rhamnolipids, show high effectiveness coupled with good biodegradability [90]. Even though biotechnological production of biosurfactants is already established for several years, high production costs due to intense foaming, expensive downstream processing and high substrate costs impede their bulk use up to now [93].

The aim of this thesis is the continuous production of rhamnolipids (RL) by *P. aeruginosa* in an integrated reactor system, consisting of a three step process: biomass production (A), immobilisation (B) and rhamnolipid formation (C). The same bioreactor is used first for biomass production and then for rhamnolipid formation with magnetically immobilised bacteria (see Fig. 3-1).
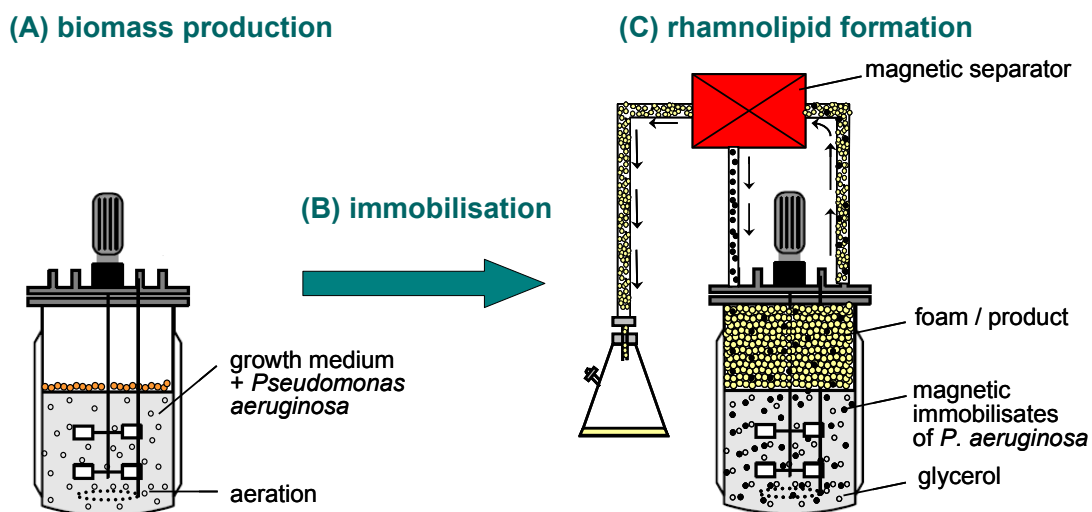
Fig. 3-1: Process design for rhamnolipid production

For the first step an exponential feeding-concept was developed to yield high cell densities. Then, the obtained biomass is immobilised in magnetic matrices that allow retention of the biocatalyst in the bioreactor by magnetic separation. The used material, the immobilisation method as well as the entrapped magnetite have been optimised with respect to particle size distribution, stability, diffusion properties, biocompatibility, etc (see chapter 4).

In a second cultivation step rhamnolipid production with immobilised bacteria in a 10 L bioreactor were studied for implementation of a continuous process with *in situ* product removal (see chapter 5). The product, available as foam, is continuously removed by foam

fractionation and the liquid level completed by a controlled substrate feed. As immobilisates are also carried along with the foam, a high gradient magnetic separator is interconnected after the fractionation tube to retain them in the fermentation process. Utilisation of renewable raw materials such as glycerol from biodiesel production as substrate should furthermore reduce process charges. The realisation of this process also included the installation of an effective rhamnolipid analysis as well as rhamnolipid purification procedures, which are presented in chapter 6. This thesis is part of the cooperation project "Neue Verfahren zur preisgünstige Herstellung mikrobieller Rhamnolipide auf Basis nachwachsender Rohstoffe" supported by the Fachagentur Nachwachsende Rohstoffe e.V.

3.2 Biosurfactants

3.2.1 Properties and applications of biosurfactants

Biosurfactants are amphiphilic molecules of biological origin with both hydrophilic and hydrophobic moieties. They partition preferentially at the interface between fluid phases with different degrees of polarity and hydrogen bonding such as oil/water or air/water interfaces. These properties render surfactants capable of reducing surface and interfacial tension and forming microemulsions. The solubility limit of surfactants is described by the critical micelle concentration (cmc). Exceeding this limit, micelles, double layers and vesicles are formed which entail a couple of physiological properties.

Tab. 3-1: Potential applications of biosurfactants as fine and speciality chemicals [9]

No.	Function	Application field
1	Emulsifiers and dispersants	Cosmetics, paints, additives for rolling oil
2	Solubilisers and microemulsions	Toiletriesm pharmaceuticals
3	Wetting and penetrating agents	Pharmaceuticals, textile industy, paints
4	Detergents	Household, agriculture products, high tch products
5	Foaming agents	Toiletries, cosmetics, ore floatation
6	Thickening agents	Paints
7	Metal sequestering agents	Mining
8	Vesicle forming agents	Cosmetics, drug delivery systems
9	Microbial growth enhancers	Sewage sludge treatments for oily wastes, fermentation
10	Demulsifiers	Waste treatment
11	Viscosity reducing agents	Pipeline transportation
12	Dispersants	Coal-oil mixture, coal-water slurry
13	Resource recovery agents	Tertiary recovery of oil

Biosurfactants exhibit excellent emulsification and wetting characteristics for application in detergents, cosmetics and nutrition. An overview of possible applications fields of biosurfactants is given in Tab. 3-1. As they emulsify long chain fatty acids and enhance cell membrane hydrophobicity through excretion of lipopolysaccharides, hexadecane assimilation by microorganisms is facilitated and offers therefore a big potential for hexadecane degradation in petrochemical industries [8]. Metal complexation of biotensides permits the bioremediation of contaminated soils [39, 121, 165]. Additional applications potentials are in agriculture, construction, plastics production as well as metal, paper and textile processing industries profiting of properties such as corrosion inhibition, phase separation, flotation and viscosity reduction [9].

In the case of rhamnolipids, fabrication of rhamnose, which serves as flavour, is relatively simple on the basis of rhamnolipids compared to chemical synthesis [54]. Also characteristic for biotensides are their high effectiveness with high selectivities and specific activities even at extreme temperatures, pH and salinities [24]. Furthermore, they have the advantages over chemical surfactants that they show lower toxicities, better environmental compatibility and higher biodegradability as well as the ability to be synthesised from renewable feedstocks [38].

3.2.2 Rhamnolipids

Rhamnolipids are the biosurfactants studied in this work. In the following paragraphs, all aspects of rhamnolipids, beginning with their structure and their biological functions, followed by biosynthesis pathways and genetics, as well as rhamnolipid production and recovery are discussed. The chapter closes with strategies towards commercial application of rhamnolipids.

3.2.2.1 Structure and biological functions

Unlike chemically synthesised surfactants, which are classified according to the nature of their polar grouping, biosurfactants are categorised mainly by their chemical composition and their microbial origin. In general, their structure includes a hydrophilic moiety consisting of amino acids, peptides or mono-, di-, or polysaccharides and a hydrophobic moiety consisting of unsaturated or saturated fatty acids. Accordingly, the major classes of biosurfactants include glycolipids, lipopeptides and lipoproteins, phospholipids and fatty acids, polymeric surfactants, and particulate surfactants.

Rhamnolipids are one kind of glycolipids produced by *Pseudomonas aeruginosa* and some other bacterial strains from *P. chlororaphis*, *P. putida*, *B. planarii*, *B. glumae* [58]. They consist of hydrophilic rhamnose molecules (Rha) and hydrophobic β-hydroxy fatty acids (C_{10}, C_{12}, etc.) which have already been observed by LC-MS (liquid chromatography coupled to mass spectrometry) to vary from 8 carbon molecules to 14 [113]. Analysis of fermentation

broths from *P. aeruginosa* revealed a great variety of rhamnolipid species which differed in their number of rhamnose molecules and fatty acid chains as well as in their fatty acid chain lengths [40]. The synthesised rhamnolipid spectrum depends on the bacterial strain, the available substrates and the living stadium of the bacterium. The most commonly produced rhamnolipids from *P. aeruginosa* are described by Syldatk et *al.* [153] as rhamnolipid 1 (L-rhamnosyl-*β*-hydroxydecanoyl-*β*-hydroxydecanoate) and rhamnolipid 3 (L-rhamnosyl-L-rhamnosyl-*β*-hydroxydecanoyl-*β*-hydroxydecanoate; often referred to as RL 2). The rhamnolipids of the Pseudomonas strain used in this work are illustrated in Fig. 3-2.

m, n = 8, 10, 12 or 12-1
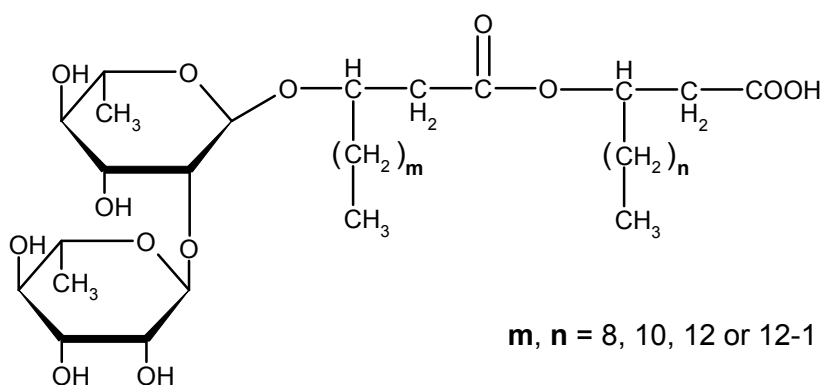
Fig. 3-2: General structure of di-rhamnolipids from *Pseudomonas aeruginosa* DSM 2874

P. aeruginosa, a gram-negative aerobic rod, is ubiquitous and can be found in water and soils either in planktonic form or in biofilms. In natural environment rhamnolipids entail different functions which are still poorly understood. Quite established is the supported susceptibility of hydrophobic substrates by two mechanisms. On the one hand rhamnolipids emulsify hydrophobic substances better in water and make them thus accessible. On the other hand rhamnolipids are supposed to unhitch lipopolysaccharides from the outer cell membrane of bacteria or even to be part of the membrane and to render it so more hydrophobic [3, 4, 175]. This facilitates contact with hydrocarbon droplets and assimilation of insoluble substrates. Concerning biofilms, rhamnolipids are involved in biofilm architecture and cell-to-cell signalling [23, 35]. As reported by Caiazza et *al.* [23] rhamnolipids modulate swarming motility patterns of *P. aeruginosa*. Translocation by swarming occurs on semisolid surfaces and requires functional flagella and biosurfactant production. It seems that surfactants may be able to maintain open channels in biofilms by affecting cell-cell interactions and the attachment of bacterial cells to surfaces. These channels permit a better nutrition supply in biofilms. Communication between cells, the so-called quorum sensing, is generally used by bacteria to coordinate processes. The rhamnolipid synthesis is mainly regulated by quorum sensing through the gene *rhlR* [126] (see Fig. 3-4). In addition, biosurfactants have been shown to be involved in cell adherence which imparts greater

stability under hostile environmental conditions and virulence [140], in cell desorption to find new habitats for survival and in antagonistic effects toward other microbes in the environment [91].

3.2.2.2 Biosynthesis and genetics

As rhamnolipids are amphiphilic molecules two primary metabolic pathways (hydrocarbon and carbohydrate) and therefore a specific set of enzymes are involved in their synthesis.

Fig. 3-3: Possible rhamnolipid biosynthesis pathways from triglycerides or glycerol [92]

Dependent on the furnished substrate either the carbohydrate moiety or the fatty acid chains or even both are synthesised de novo. A general scheme for rhamnolipid synthesis with triglycerides or glycerol as substrate is illustrated in Fig. 3-3.

Fig. 3-4: Model for the regulation of the rhamnolipid production in *P. aeruginosa* [126]

Studies by Burger et *al.* [22] with radioactive labelled precursor molecules revealed the assembly of the separate synthesised moieties to the final rhamnolipids according to

Fig. 3-4. Thymidine-diphosphate(TDP)-L-rhamnose provides the precursor for the rhamnolipid and is connected by specific rhamnosyltransferases with the *β*-hydroxydecanoyl-*β*-hydroxydecanoate.
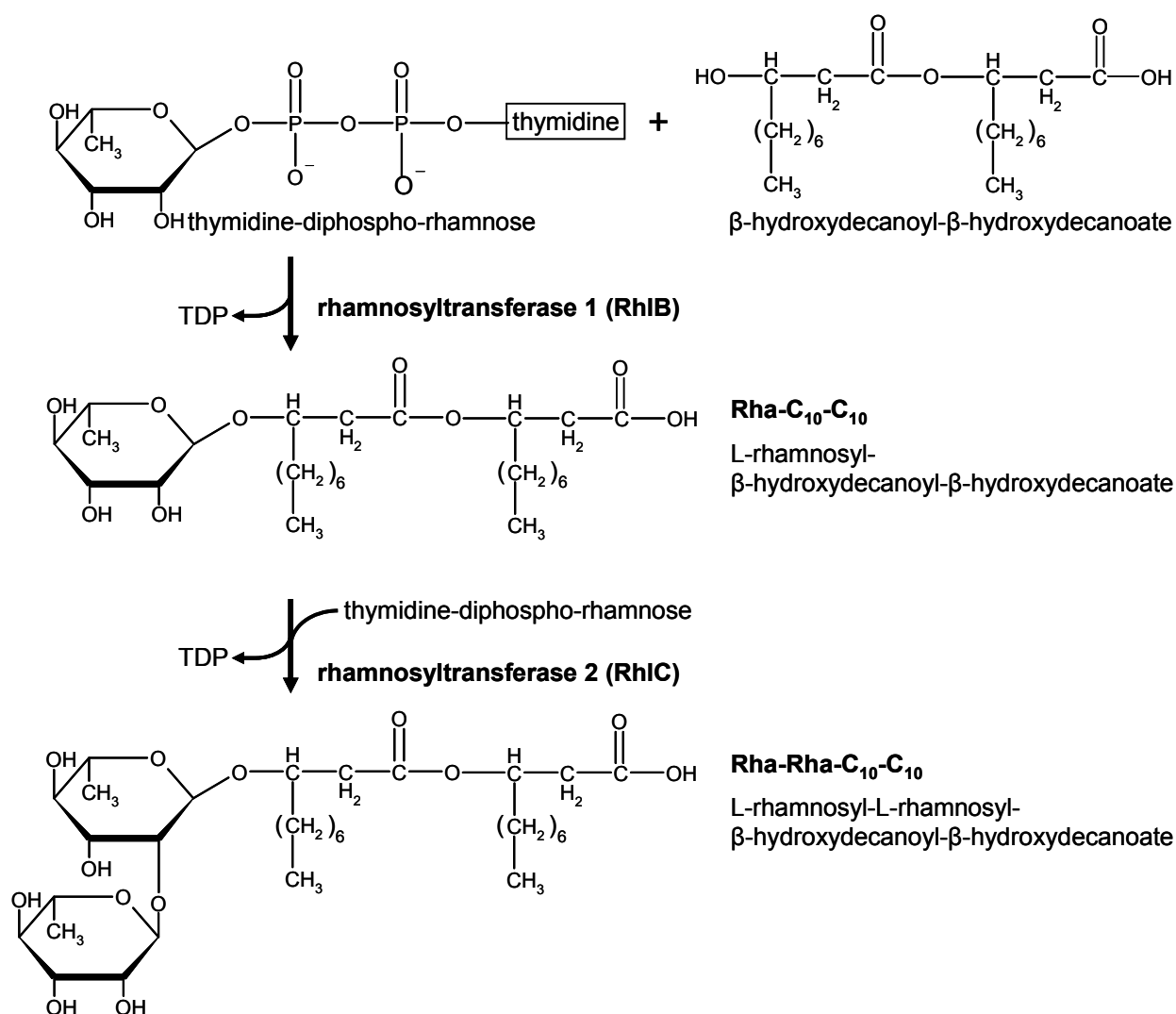
Fig. 3-5: Biosynthesis pathway of rhamnolipid Rha-C$_{10}$-C$_{10}$ and Rha-Rha-C$_{10}$-C$_{10}$ [22]

The most important work on genetics of rhamnolipid synthesis derives from Ochsner et *al.* [125, 126]. His group revealed the *rhlABR* gene cluster to be responsible for the synthesis of RhlR regulatory protein and rhamnosyltransferase 1, both essential for rhamnolipid synthesis. Rhamnosyltransferase 1 is encoded by *rhlAB* genes, which are organised in one operon (see Fig. 3-4). The *rhlR* and *rhlI* genes are arranged in sequence and act as regulators of the expression of the *rhlAB* genes. This regulation is cell density dependent and depends on the quorum sensing response. A second quorum-sensing (QS) system coding for the genes *lasR* and *lasI* also controls the *rhl*-system. The activity of the RhlR and LasR regulator proteins is influenced by the autoinducers butanoyl-homoserine lactone (C$_4$-HSL) and 3-oxo-dodecanoyl-homoserinelactone (3-oxo-C$_{12}$-HSL), which are synthesised by the RhlI and LasI proteins. The *rhlC* gene coding for the second rhamnosyltransferase involved

in the assembly of di-rhamnolipid molecules is part of a separate operon and also regulated by QS [133].

3.2.2.3 Production regulation

In general, three mechanisms, namely, induction, repression, and nitrogen or multivalent ions limitation, operate in the regulation of biosurfactant production. Rhamnolipid synthesis can be induced by addition of hydrophobic substrates such as long chain fatty acids, hydrocarbons or glycerides. In contrast, addition of hydrophilic compounds like D-glucose, acetate and tricarboxylic acids leads to reduced synthesis of rhamnolipids by *P. aeruginosa* [63, 64]. For this reason, highest rhamnolipid concentrations in solution up to almost 100 g·L^{-1} have been achieved with vegetable oils [54]. These high concentrations are also supposed to be influenced by the adsorption of rhamnolipids to the oil/water-interface [98]. Repression of alkane and hexadecane biodegradation in *P. aeruginosa* by glucose, glycerol and palmitic acid has been observed [62]. Nitrogen- or metal ion-dependent regulation also influences the synthesis of biosurfactants. Rhamnolipids are so-called "secondary metabolites", and as such, their production starts with the beginning of the stationary phase when the nitrogen source is exhausted [56, 135, 154]. Moreover, the addition of a nitrogen source caused an inhibition of rhamnolipid synthesis in resting cells of *P. aeruginosa* [154]. Generally, it has been observed that higher rhamnolipid concentrations can be achieved with previous growth of *P. aeruginosa* on a nitrate than on ammonium [105, 131]. If nitrogen source is limited, phosphate and carbon source should be available abundantly. At the beginning of rhamnolipid production, the metabolism change from *P. aeruginosa* implicates an increased generation of glutamine and higher phosphate consumption [118]. The limitation of multivalent cations also causes overproduction of biosurfactants [27, 56, 154]. Guerra-Santos et *al.* [57] demonstrated that by limiting the concentrations of salts of magnesium, calcium, potassium, sodium, and trace elements, a higher yield of rhamnolipid can be achieved.

Apart from rhamnolipid yields, substrates and environmental factors can also influence the synthesised product spectrum. Concerning the carbon source, Syldatk et *al.* [154] and Edmonds and Cooney [46] demonstrated that although different carbon sources in the medium affected the composition of biosurfactant production in *Pseudomonas spp.*, substrates with different chain lengths exhibited no effect on the chain lengths of fatty acid moieties in rhamnolipids.

Environmental factors and growth conditions such as pH, temperature, and oxygen availability also affect biosurfactant production through their effects on cellular growth or activity. Rhamnolipid production in *Pseudomonas spp.* is at its maximum at a pH range from 6 to 6.5 or 7, depending on the strain used [56, 153]. In *Pseudomonas sp.* strain DSM 2874 [154], temperature causes alteration in the composition of the produced rhamnolipids. The

impact of dissolved oxygen in solution still is not resolved. Sabra et *al.* [141] recently proposed that *P. aeruginosa* is producing rhamnolipids to reduce the oxygen transfer rate as a means of protection from oxidative stress, and it appears that this mechanism is activated by iron deficiency [84]. However, rhamnolipid production is also obtained in the absence of oxygen [27].

3.2.2.4 Fermentation strategies

For microbial production of rhamnolipids in bioreactors different fermentation strategies have been studied during the last decades [56, 111, 154]. An essential precondition for overproduction of rhamnolipids is growth limitation, induced by appropriately limiting the concentration of nitrogen sources or of multivalent ions, and an excess of the carbon source. These important limiting conditions can be maintained by the following production methods:

1. (Fed-)batch cultivation under growth-limiting conditions,
2. Batch cultivation under resting cell conditions,
3. Semi-continuous production with immobilised cells (without N source), and
4. Continuous cultivation and production with free cells.

Fed-batch cultivation of *P. aeruginosa* with rhamnolipid production after exhaustion of nitrogen source has extensively been used for screening of bacterial strains, medium composition and study of environmental factors in shake flask experiments [1, 2, 153]. For higher rhamnolipid yields and further industrial application generally stirred tank reactors are used [11, 54, 96]. High yield coefficients ($Y_{P/S}$ and $Y_{P/X}$) have been achieved in particular with n-alkanes, vegetable oils and ethanol in fed-batch cultures. Yields of more than 100 $g^.L^{-1}$ and comparably high productivities have been described in a patent from Hoechst AG [54]. A general difficulty in these systems is avoidance and if necessary abatement of foam which can be resolved by foam recycle systems [11] or special feeding strategies of hydrophobic substrates in addition to efficient foam brakers and surface aeration [54, 98].

As rhamnolipids are only synthesised by *P. aeruginosa* after reaching the late exponential phase with growth limiting conditions, a separation of biomass and rhamnolipid production into two separated steps is possible. Possible cost reduction and the ability to intensify the process by immobilisation of the bacteria favour utilisation of resting cells. Production by resting cells is a type of rhamnolipid production in which there is no cell multiplication, but bacteria nevertheless continue to utilise the carbon source for synthesis of rhamnolipids. Works from Syldatk et *al.* [153] showed an improved rhamnolipid yield compared to nitrogen-limiting cultivation. However, concerning the synthesised rhamnolipid spectrum, more different types of rhamnolipids were detected in the culture suspension of resting cells compared to a simple step process [153].

In general, semi-continuous production with immobilised cells also uses resting cell conditions [79, 111, 147]. In some cases small amounts of nutrients are supplemented in the beginning to increase cell loading of immobilisates or to overcome the straining conditions of immobilisation. Advantages of immobilisation are the possibilities of an intensified and continuous rhamnolipid production over longer time periods with reuse of the biocatalyst and easier product removal. Screening of the carbon substrates and the immobilisation system for *Pseudomonas sp.* DSM 2874 revealed that glycerol as carbon source and entrapment in calcium alginate polymers were most suitable [87, 153]. A process for continuous rhamnolipid production in a fluidised-bed reactor, including isolation of the products on Amberlite XAD-2 columns and recycling of the medium, has been developed by Matulovic [111, 147]. The immobilised biocatalyst could be regenerated several times (brief growth in nutrient medium) and reused successfully [147].

Continuous cultivation and rhamnolipid production with free cells were mainly carried out with *P. aeruginosa* PG 201 (DSM 2659) and with glucose as carbon source [56, 57]. Experiments in a chemostat were carried out with and without cell feedback. At this, cell feedback increases significantly the biocatalyst concentration in the reactor and makes it possible to decouple the substrate residence time from the growth rate of the cells. A continuously stirred reactor was coupled to two membrane units, one serving for cell retention and product stream preparation, the other one for gas exchange/O_2 replacement and CO_2 removal, by Fiechter et *al.* [48]. The important factors for an economic process, the volumetric productivity P_v and the product yield $Y_{P/S}$, could be increased by the cell feedback process to 0.55 $g \cdot L^{-1} \cdot h^{-1}$ and 0.15 $g \cdot g^{-1}$ respectively [56, 57]. Even higher yields should be possible with hydrophobic substrates such as vegetable oils [48]. The feasibility of a continuous rhamnolipid production in a 50 L bioreactor coupled with a downstream processing plant resulting in a 90% pure product has been demonstrated by Reiling et *al.* [136].

3.2.2.5 Recovery of rhamnolipids

One task for economical rhamnolipid production is to yield higher efficiencies in downstream-processing, still responsible for up to 60% of the total production costs [38]. In general, the purification method chosen depends on the application desired. A more classic approach for batchwise separation of rhamnolipids from culture broth generally applied after previous removal of microorganisms by centrifugation includes acid precipitation [40, 165, 174], salting out with aluminium sulphate [143], solvent extraction (highest recovery with ethyl acetate [109, 143, 160]) or selective crystallisation of the di-rhamnolipids [98]. Recent developments for process integration and *in situ* product removal such as foam fractionation [111], membrane techniques [55], adsorption [44, 60, 111, 136] or ion-exchange [136] (see paragraph 3.2.2.6) enable continuous separation of rhamnolipids from culture broth and show potential for cost reductions. For high purity products, chromatographic methods

comprising normal phase or reversed phase chromatography [40, 77, 149], followed by crystallisation [77] are in most cases still the sole possibility. Using reversed phase chromatography, even rhamnolipids, only differing in hydroxy fatty acid chain length, can be separated, though serving more for calibration purposes in laboratory than for industrial application [37].

3.2.2.6 Strategies towards commercial application of rhamnolipids

During last decades intensive efforts have been made for a more lucrative production of rhamnolipids by overcoming low yields in production processes and high recovery and purification costs [117]. Some approaches adopted are the use of cheaper raw materials, optimised and efficient bioprocesses and overproducing mutant and recombinant strains for obtaining maximum productivity. The application of these strategies, particularly those using hyper-producing recombinant strains in the optimally controlled environment of a bioreactor, might lead towards a successful commercial production of rhamnolipids in near future.

A variety of cheap raw materials, including plant-derived oils, oil wastes, starchy substances, lactic whey and distillery wastes have been reported to support rhamnolipid production [10, 43, 59, 120, 158]. Especially wastes which accumulate for example in biodiesel production, oil refineries or food industry are suitable substrates and available throughout the world.

For an efficient and economical rhamnolipid production, bioprocess development is the primary step towards commercialisation. Any attempt to increase the product yield demands optimal addition of media components and selection of the optimal culture conditions that will induce the maximum or the optimum productivity. A powerful tool is therefore a statistical optimisation strategy based on surface methodology as applied by Abalos et *al.* [2]. Similarly, efficient downstream processing techniques and methods are needed for maximum product recovery (see paragraph 3.2.2.5). Process integration of up- and downstream-processing by continuous *in situ* product removal increases on the one hand product yields through avoidance of inhibitory product concentrations. On the other hand less purification steps are necessary to obtain the desired product purity, therefore inducing less product loss and reduced costs. Investigated approaches for biosurfactant elimination are removal over membranes [55], by foam fractionation [29, 33, 111] or through adsorption on XAD-resins or rather activated carbon [44, 111]. While membrane processes are less successful in rhamnolipid filtration due to membrane fowling and the peculiarity of rhamnolipids to form micelles even at very low concentrations, foam fractionation permits the complete extraction of rhamnolipids from cultivation medium (see paragraph 3.2.3.3). Additionally, immobilisation of the producing bacteria enables retention of the biocatalyst in the production medium and decouples growth from product removal rates [111].

The genetics of the producer organism is an important factor affecting the yield of all biotechnological products. Mutants with up to ten-fold productivities, produced by various

agents, for example, transposons [88], chemical mutagens such as N-methyl-N'-nitro-N-nitrosoguanidine [54, 155], radiation [76] or by selection on the basis of resistance to ionic detergents such as CTAB [146], are reported in literature. Important tools also consist in systems biology and metabolic engineering. Apart from rhamnolipid overproduction, the pathogenicity of microorganisms is interesting for industrial implementation, as *P. aeruginosa* is pathogenic to humans. Alternative strains from *Pseudomonas putida* [162], *Pseudomonas chlororaphis* [58], *Burkholderia pseudomallei* [65], etc. are also producing rhamnolipids, though in smaller quantities and with different rhamnolipid species composition. The attempts to synthesise rhamnolipids in heterologous hosts by expressing the rhlAB rhamnosyltransferase genes to replace *P. aeruginosa* by a safe industrial strain yielded lesser concentrations as wild type strains as well [127]. Finally, immobilisation of the production strain by entrapment also increases security of rhamnolipid production [79, 111].

A different approach to affect the formed product composition has been chosen by Trummler et *al.* [160], who transformed enzymatically di-rhamnolipids into mono-rhamnolipids during cultivation. The achieved product only contained the mono-rhamnolipids.

A wide range of different rhamnolipids can be designed chemically by hydrophobically assisted switching phase synthesis, but are more designed for research applications to better understand rhamnolipid regulation and impact [45, 74].

3.2.3 Foam

Biosurfactants tend to intensive foaming in an aerated bioreactor, which was used in this work for continuous product removal by foam fractionation. Foam is a colloidal dispersion of gas in a continuous liquid or solid phase. In the following only liquid foams are discussed. In bioprocesses foam is often generated during fermentation by surface-active products, by-product or substrates (e.g. proteins, biosurfactants). However, foam brings with it many disadvantages such as the need for larger bioreactors, plugging up of exhaust air filters as well as lost of producing microorganisms and solid substrate compounds due to flotation. Generally, antifoams or foam-breakers have to be applied for a stable fermentation process. Foam fractionation in contrast utilises foam for product separation and enrichment. Important fundamentals are foam formation and stability [139, 169].

3.2.3.1 Foam formation

In an aqueous phase surfactants form above a specific concentration, the so-called critical micelle concentration (CMC), micelles and vesicles and also adsorb at interfaces such as gas, non miscible liquids or solids. Different types of vesicles, which are formed depending on the present conditions, are illustrated in Fig. 3-6.

Foams are produced when air or some other gas is introduced beneath the surface of a liquid containing surfactants which adsorb at the gas-liquid interface and that expands to enclose the gas with a film of liquid (lamellae).
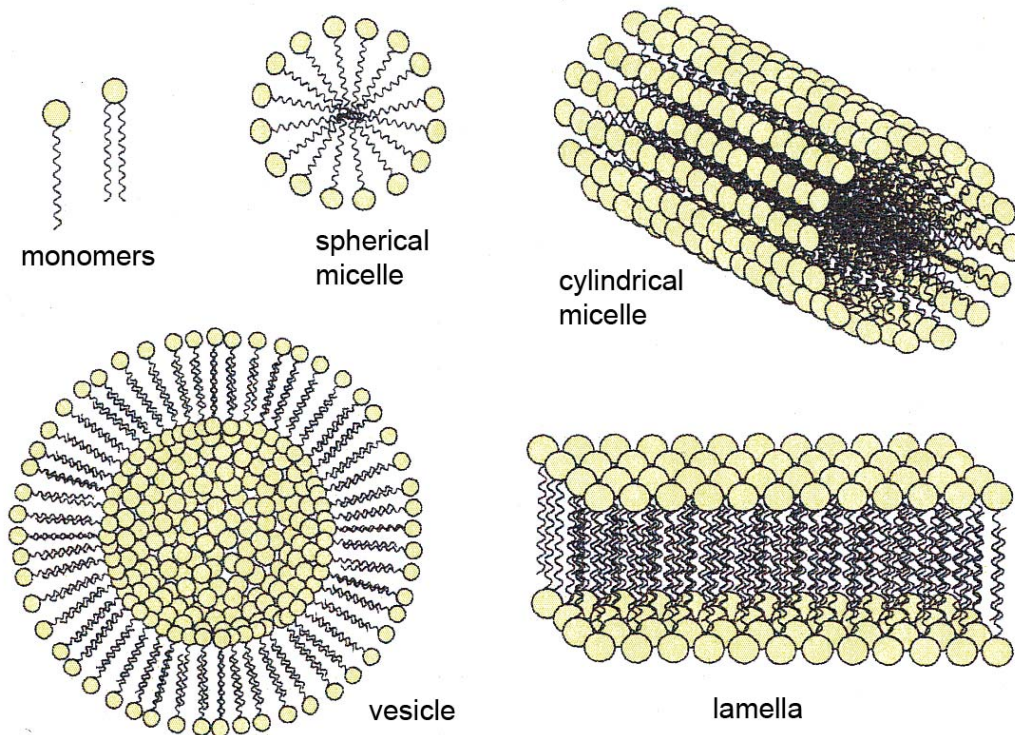
Fig. 3-6: Surfactant structures in aqueous media

The surfactant reduces surface tension of the water and stabilises foam lamellae against rupture. Directly on the liquid surface at first wet foam with spherical gas cells is formed. When the foam ascends further and starts to dry foam bubbles take the form of polyhedral cells (see Fig. 3-7 on the left).
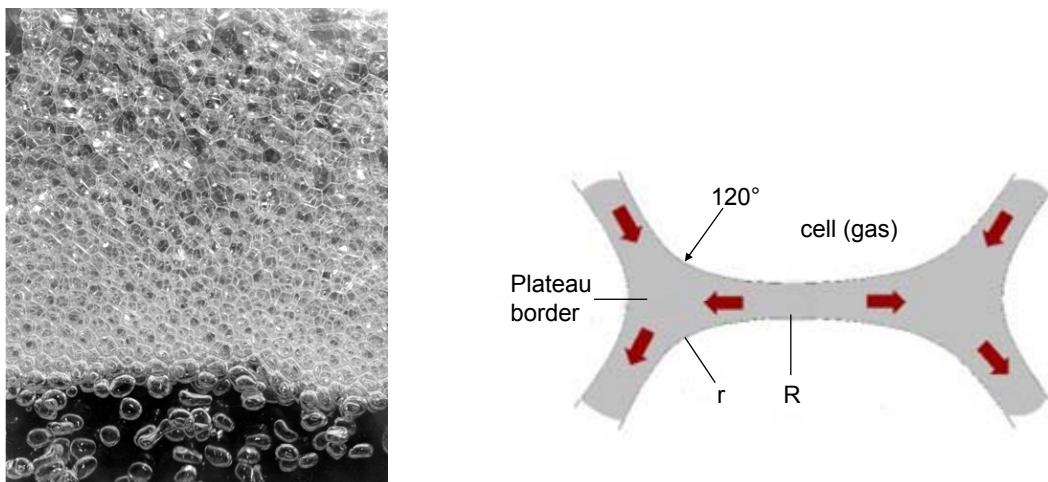
Fig. 3-7: Foam formation on liquid surface (left), schematic foam lamellae (right)

Foam films between gas cells meet at Plateau borders by an angle of 120° for dry foams and at the junction of four boarders by a vertex angle of ~109.5° (Plateau's law).

3.2.3.2 Foam stability

Foam is a thermodynamically instable system due to the high free energy at the interfaces. Surfactant foams are generally metastable foams which have a lifetime of several hours to days, as surfactants stabilise the foam through reduction of interfacial tension and therefore free energy [73]. But even metastable foams loose liquid and gas and are subjected to continuous evolution. Processes influencing foam stability are drainage and coarsening which may lead to film rupture and collapse of the foam when a critical thickness (50 - 100 Å) of the foam lamellae is reached. On the other hand, film elasticity in surfactant foams counterbalance local thinning or stretching of lamellae due to applied stress.

3.2.3.2.1 Drainage

Water drainage occurs under two influences: gravity and pressure difference. Gravity is mainly important in thick lamellae of wet foams. It can be influenced by viscosity of the medium, which increases with decreasing film thickness, or the presence of solid particles which may impede drainage. The lower pressure in the Plateau borders causes drainage of the liquid from the lamellae into the Plateau borders which is especially important in thin lamellae (see Fig. 3-7 on the right). The pressure difference is due to a different curvature of the foam lamellae and can be described by the Laplace equation (see Eq. 3-1).

$$\Delta P = \gamma \cdot \left(\frac{1}{R} + \frac{1}{r} \right)$$

Eq. 3-1

with the surface tension γ and the curvature radii of the foam lamellae R and r (see Fig. 3-7).

3.2.3.2.2 Coarsening

Another factor influencing foam stability is the rate of diffusion of gas from one bubble to another through the lamellae separating them. The rate of diffusion q is given by the following correlation (see Eq. 3-2):

$$q = -J \cdot A \cdot \Delta P = -J \cdot A \cdot 2\gamma \cdot \left(\frac{1}{R_1} - \frac{1}{R_2} \right)$$

Eq. 3-2

with the permeability of the diffusion path J, the effective perpendicular area A, the bubble radii R_1 and R_2 and the gas pressure difference of the two bubbles ΔP.

As gas pressure in smaller bubbles is higher than in larger bubbles, gas diffuses in larger bubbles and causes them to grow at the expense of smaller ones. Coarsening implies thus a structure change of the bubbles to polyhedral gas cells and a reduced amount of gas

bubbles in the foam through disappearance of smaller bubbles and rupture of lamellae due to rearrangement of bubbles in the foam. Closer packing of surfactant molecules is supposed to reduce gas transfer between bubbles, stabilising therefore foam structure.

3.2.3.2.3 Film elasticity

Elasticity, by definition, is the ratio of stress to strain and is a measure of the property of returning to an initial form or state following deformation. Foam stability is only possible if surfactants are present which are responsible for foam elasticity. In consequence of film elasticity, thinning or stretching of the bubble membranes due to applied stress are counterbalanced by restoring forces. This stabilisation of foam lamellae is described by the Gibbs-Marangoni-effect (see Fig. 3-8).
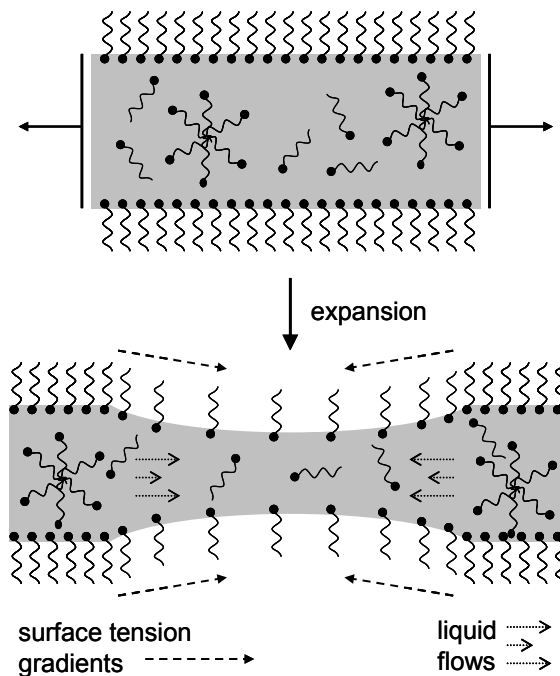
Fig. 3-8: The Gibbs-Marangoni-effect

If foam lamellae are stretched abruptly, surface concentration of adsorbed surfactant molecules is reduced, leading to a higher surface tension (Gibbs-effect). The foam elasticity *E* is defined by Gibbs as the ratio change in surface tension to change in film surface area *A* according to Eq. 3-3.

$$E = 2 \cdot A \cdot \frac{d\gamma}{dA}$$

Eq. 3-3

The induced surface tension gradient provokes diffusion of surface active molecules from regions with lower surface tension to the narrowed region of the lamella. Interlamellar liquid

is entrained with the surfactant molecules due to friction resistance and consequently restores the initial conditions of the foam lamellae (Marangoni-effect).

3.2.3.3 Foam fractionation

Foam fractionation, an adsorption process, serves as a means to separate surface active compounds or particles from a solution by foaming. It is generally performed in a so-called fractionation column. Gas is blown into a surfactant solution and surfactants adsorb at the surface of the formed bubbles. They are entrained with the foam through the fractionation column and can be collected in a separate recipient after foam collapse (e.g. through addition of acids or mechanical break-up). Due to mechanisms such as drainage or coarsening which reduce foam humidity and therefore the quotient of surface area to bubble volume as described in paragraph 3.2.3.2, surfactants are enriched at the air/liquid interface leading to higher concentrated surfactant solutions after foam collapse. Foam fractionation has already been applied for water purification by removal of solid particles, proteins and other surface active compounds in bubble columns [16, 115, 151]. The same process has also been used for concentration of a desired surface active product such as proteins or surfactants [19, 20, 36, 55]. As higher product concentrations during fermentation of microorganisms often inhibit further production of the desired compound, foam fractionation may be a tool for continuous product removal permitting continuous fermentation strategies. Several authors described fermentation processes removing surfactants directly out of the bioreactor by foam fractionation over the normal gas-flow channel or a fractionation column on top of the fermenter [28, 29, 33, 36]. They stated process feasibility, but observed an optimisation issue concerning product enrichment vis-à-vis recovery. Surfactant enrichment of about 50 or even higher has been achieved in collapsed foam compared to culture broth [29, 114].

3.2.3.3.1 Factors influencing foam fractionation

The main criteria describing the performance of foam fractionation are enrichment and recovery of the desired product (see paragraph 3.2.4.2). These two factors are in general contrariwise influenced by different process parameters. Thus optimum operation conditions have to be found between a high concentrated product and complete rhamnolipid removal from the fermentation process. A summary of parameters influencing foam fractionation of rhamnolipids based on literature [19, 55, 128] is depicted in Tab. 3-2. These parameters have either an effect on adsorption of surfactant molecules to gas bubbles (e.g. bubble size, pH, ionic strength, competitive molecules) or on water drainage (e.g. foam height, effect of particles, temperature) which has only a significant effect above a certain residence time in the foam fractionation column [55].

Tab. 3-2: Parameters influencing foam fractionation

process variables	enrichment	recovery	foam formation rate
RL-feed concentration ↑	↓	↑	↑
foam height ↑	↑	↓	
gas flow ↑	↓	↑	↑
bubble size ↑ (sparger)	↑	↓	↓
stirring speed ↑	↓	↑	↑
foam stabilizing component ↑	↓		↑
competitive adsorption	↓	↓	
effects of cells	↓	cells show higher enrichment than RLs	
pH value ↑	↑	purification better with pH > 6	
temperature ↑	↑	↓	

The residence time is calculated by Eq. 3-4 and depends on gas velocity u_G, cross section A_{column} and volume V_{column} of the fractionation column.

$$\tau = \frac{V_{column}}{u_G \cdot A_{column}} \, [s]$$

Eq. 3-4

Ionic strength and pH influence the area occupied by rhamnolipids and thereby rhamnolipid enrichment as well as product composition. As mono-rhamnolipids are more compact in the air/water interface, their partitioning in foam is higher compared to di-rhamnolipids. This competing adsorption of different rhamnolipid species leads to changes in product composition during cultivation. If rhamnolipids are separated directly from culture broth, other compounds (substrates or products) may also influence foam and thus final product composition through competitive adsorption. Productivity and purification factors (see paragraph 3.2.4.2) consider purity aspects of the desired product. These are of minor importance for rhamnolipid production with resting cells as fewer by-products compared to growing cells accrue. However, bacteria are generally more enriched in foam as surfactant molecules and may therefore contaminate collapsed foam [55]. Removal of microorganisms also takes away the biocatalyst and reduces rhamnolipid production. A remedy is found in effective cell immobilisation and retention of the immobilisates in the bioreactor.

3.2.3.3.2 Design of foam fractionation processes

In practice different concepts of foam fractionation have yet been studied, trying to improve enrichment of surface active compounds. Among these attempts for a better liquid drainage are introduction of several stages of foam fractionation instead of only one fractionation column [16, 34, 114, 115], use of fixtures in the column such as perforated plates [161] or bubble cap trays [16] and operation with a liquid reflux [115, 161]. But even under optimised operating conditions enrichment ratios of only about twice as much have been achieved

[115, 161]. These decrease rapidly with higher aeration rates and surfactant concentrations as drainage in comparatively wet foams is slower [115].

3.2.4 Relevant parameters for rhamnolipid production, separation and purification

For the development of a continuous rhamnolipid production process with continuous product recovery definition of several parameters is necessary in order to compare different fermentations. Parameters can be defined for rhamnolipid production, separation and purification.

3.2.4.1 Rhamnolipid production

The most important parameter concerning rhamnolipid production is the so-called space time yield (STY). It describes the produced rhamnolipid amount m_{RL} per reactor volume V_{RL} and time t and represents a productivity factor (see Eq. 3-5).

$$STY = \frac{m_{RL}}{t \cdot V_{bioreactor}} \left[g \cdot L^{-1} \cdot h^{-1} \right]$$

Eq. 3-5

As *P. aeruginosa* cells are immobilised and employed as resting cells, diffusion limitations and therefore a reduced rhamnolipid production rate may occur. The efficiency factor η gives an idea about the degree of rhamnolipid formation that is still achieved in immobilised systems (see Eq. 3-6).

$$\eta = \frac{\text{specific RL - production rate of cells in immobilisates}}{\text{specific RL - production rate of free cells}} \left[- \right]$$

Eq. 3-6

3.2.4.2 Rhamnolipid separation and purification

The produced rhamnolipid is separated by foam fractionation from culture broth during the fermentation process. The performance of this separation and purification method is illustrated especially by two opposed factors: the recovery R_{RL} and the enrichment ratio E_r (see Eq. 3-7 and Eq. 3-8).

$$E_r = \frac{c_{RL,foam}}{c_{RL,medium}} \left[- \right]$$

Eq. 3-7

$$R_{RL} = \frac{m_{RL,foam}}{m_{RL,medium} + m_{Rl,foam}} \cdot 100 \left[\% \right]$$

Eq. 3-8

For rhamnolipid separation during fermentation a compromise has to be made between high enrichment ratios and the total recovery of the formed rhamnolipids. Given that higher

rhamnolipid concentrations in the production medium may lead to product inhibition and therefore lower formation rates, rhamnolipid enrichment in the bioreactor should be avoided. Therefore the rhamnolipid separation rate $\dot{m}_{RL}$, based on the volumetric foaming rate $\dot{V}_{foam}$, is another important criterion (see Eq. 3-9) for description of rhamnolipid separation from culture broth.

$$\dot{m}_{RL} = c_{RL,foam} \cdot \dot{V}_{foam} \; [g \cdot h^{-1}]$$

Eq. 3-9

Product purity of rhamnolipids P_{RL} (see Eq. 3-10) has an influence on purification factors *PF* (see Eq. 3-11) and determines the efficiency of a production process.

$$P_{RL} = \frac{m_{RL}}{m_{other\ compounds}} \; [-]$$

Eq. 3-10

$$PF = \frac{P_{RL,foam}}{P_{RL,medium}} \; [-]$$

Eq. 3-11

Apart from purity, product composition and especially its alteration during cultivation plays an important role for future commercialisation and proceeding purification steps. The partitioning ratio $P_{r(A/B)}$ of compound A and B to foam bubbles accounts for this aspect (see Eq. 3-12).

$$P_{r(A/B)} = \frac{E_{r,A}}{E_{r,B}} \; [-]$$

Eq. 3-12

3.3 Fed-batch fermentation for biomass production

3.3.1 Challenge

As rhamnolipid biosynthesis is quorum sensing regulated (see paragraph 3.2.2.2), high cell densities enhance rhamnolipid formation. Concurrently, rhamnolipids are secondary metabolites, permitting separation of biomass production and rhamnolipid synthesis into two different phases. To achieve higher cell densities of bacteria, several difficulties have to be countered. Among these are solubility of solid substrates and oxygen in cultivation medium, limitation and/or inhibition of substrates with respect to growth, accumulation of products or metabolic by-products to a growth-inhibitory level, degradation of products, high evolution rates of CO_2 and heat, high oxygen demand as well as the increasing viscosity of the medium in very dense cultures [138]. For the case of *P. aeruginosa* DSM 2875, this bacterium shows sensitivities to higher salt concentrations, necessitating therefore a fed-batch process with re-feeding of required substrates. Furthermore, oxygen demand and temperature control require special strategies such as aeration with oxygen-enriched air and increase of agitation speed to ensure optimal growth conditions. Temperature is an important

variable that can be used to control cell metabolism. By lowering the culture temperature from 37°C to 30°C, nutrient uptake and growth rate can be reduced, thus reducing the formation of toxic by-products and the generation of metabolic heat [97]. Lowering culture temperature also reduces cellular oxygen demand and rhamnolipid biosynthesis, which is not desired during biomass production. As rhamnolipid formation can not be completely eliminated and antifoams inhibit subsequent rhamnolipid synthesis, efficient mechanical foam destruction (e.g. foam disc from Sartorius) facilitates a stable process control. Suitable fed-batch strategies are presented in the following paragraph.

3.3.2 Fermentation strategies

Fed-batch strategies used for high cell density cultivations (HCDC) generally consist of two phases: a batch phase with a maximum specific growth rate ($\mu = \mu_{max}$) and a fed-batch phase with a reduced specific growth rate ($\mu < \mu_{max}$) or maximum specific growth rates with a well-balanced substrate feeding through direct feedback control of the concentration of the principal carbon source [138]. Feedback control is necessary as specific growth rate may deviate when unexpected conditions arise during culture.

Tab. 3-3: Feeding strategies in fed-batch culture according to Lee [97]

	Nutrient feeding	Specific growth rate
Without feedback control **Constant feeding**	predetermined (constant) rate	continuously decreases
Increased feeding	increasing (gradual, stepwise, or linear) rate	decrease is compensated
Exponential feeding	exponential rate	constant
With feedback control **Indirect feedback control** **DO-stat**	when there is a rise in concentration of dissolved oxygen (DO) due to substrate depletion	~ constant
pH-stat	when pH rises as a result of depletion of the principal carbon source	~ constant
Carbon dioxide evolution rate (CER)	controlled by on-line measurement with mass spectrometry, CER is proportional to growth	~ constant
Cell concentration	rate is determined from cell concentration, measured on-line by a laser turbidimeter	~ constant
Direct feedback control **Substrate concentration control**	directly controlled by the concentration of the principal carbon source	~ constant

Possible feeding strategies during fed-batch phase are summarised in Tab. 3-3. Depending on control equipment of the bioreactor, open-loop strategies or feedback control approaches are applied. If appropriate monitoring equipment is lacking, fed-batch processes are generally based on an open-loop strategy with a stepwise exponential feeding. Given that during exponential growth of microorganisms nutrient requirements are also increasing exponentially, the feeding rate has to be adjusted accordingly to achieve a constant specific growth rate μ. The calculation of the exponential feeding rate as a function of time is given in Eq. 3-13 according to Wilms et *al.* [173],

$$F(t) = \left(\frac{\mu}{Y_{X/S}} + m \right) \cdot \frac{c_{X_0}}{c_{S_0}} \cdot V_0 \cdot e^{\mu \cdot (t - t_0)} \; [\mathrm{L} \cdot \mathrm{h}^{-1}]$$

Eq. 3-13

with specific growth rate μ, specific biomass/substrate yield coefficient $Y_{X/S}$, specific maintenance coefficient m, biomass concentration at start of feeding c_{X_0}, glycerol concentration in feeding solution c_{S_0} and reactor volume at start of feeding V_0.

For the case of *P. aeruginosa*, nitrate concentration has to be maintained at a higher level than glycerol concentration through constant feeding at an earlier moment to prevent induction of rhamnolipid biosynthesis.

3.4 *Immobilisation of living bacteria*

3.4.1 Classification of immobilisations

Immobilisation means a restricted motility of microorganisms or biomolecules (e.g. enzymes) by chemical or physical methods through human actions. Different methods are available depending on the application and can be divided in four main groups: Immobilisation through surface attachment, self aggregation, entrapment within porous matrices and containment behind a barrier as illustrated in Fig. 3-9. Advantages are a continuous process management, easier downstream-processing of the product, longer viability and better protection of the immobilised microorganisms as well as a higher space-time yield through higher spatial concentration of the biocatalyst [172]. The shorter residence time of substances in up- and downstream-processing also preserves better the product. The choice of immobilisation method especially depends on the substrate as its diffusion properties influence product formation. Transport of molecules only through molecular diffusion often entails oxygen limitations and therefore impedes cultivation of entrapped strict aerobic microorganisms. As *P. aeruginosa* is facultative anaerobic this shouldn't hamper rhamnolipid production. Another important point is the biocompatibility of the immobilisation material especially if living bacteria are immobilised as performed in this work. Immobilisation

methods investigated for rhamnolipid production are generally based on entrapment of bacteria which will be discussed further in the following paragraphs.
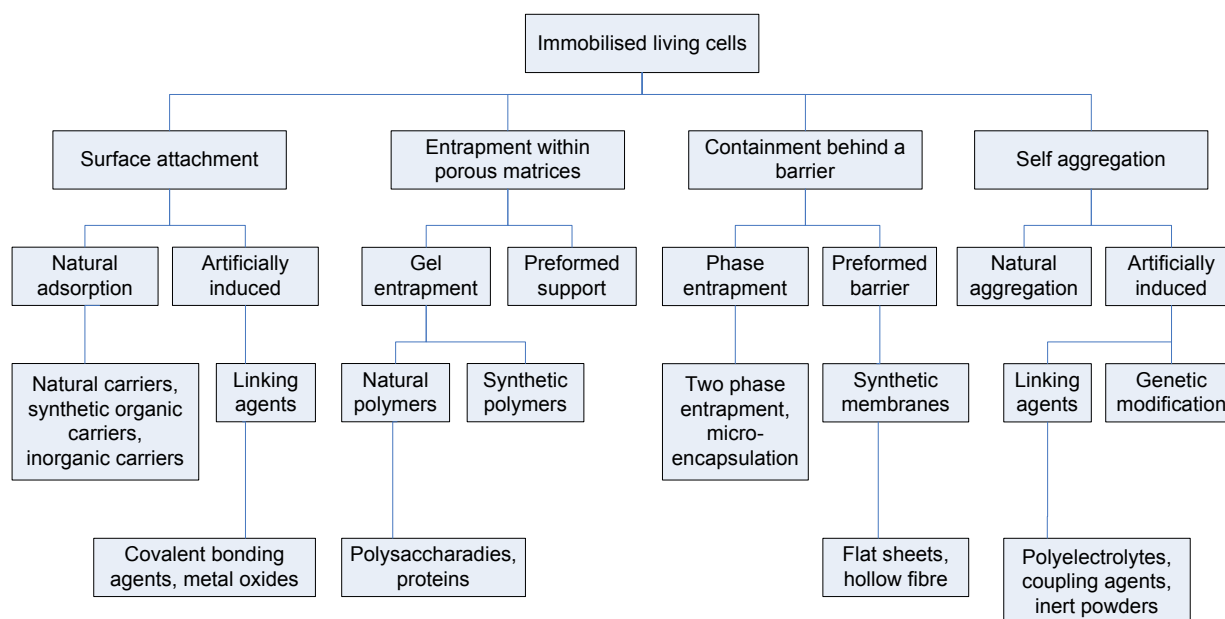
Fig. 3-9: Classification of immobilisation methods according to Willaert et *al.* [172]

3.4.1.1 Gel entrapment

Compared to simple immobilisation by adsorption, gel entrapment permits a complete separation of the immobilised bacteria from the surrounding medium and generally a better retention in the gel matrix. It is one of the most studied immobilisation technique used for living bacteria. The gel matrix can be formed of natural or synthetic polymers by ionotropic gelation (e.g. alginate, chitosan, pectine), thermal gelation (e.g. agar, gelatine, κ-carrageenan), cross-linking (e.g. PVAL), polycondensation (e.g. polyurethane) and a lot more mechanisms. In general, natural polymers are less toxic for microorganisms, but also less stable vis-à-vis mechanical stress, pH changes or certain chemical substances.

3.4.1.1.1 Natural polymers

Natural polymers are composed of polysaccharides extracted from algae and proteins. In this work only alginate has been used in rhamnolipid production processes, as other natural polymers are less stable at neutral pH values (such as pectin and chitosan), more difficult to manipulate (e.g. gelatine, agarose) or more expensive.

Alginate is one of the most studied immobilisation material for living microorganisms [172]. The starting material sodium alginate, an extract from cell walls of brown algae, is composed of a linear copolymer of 1,4-linked β-D-mannuronic (M) and α-L-guluronic acid (G) whose composition and sequence varies depending on the producer organism [21]. The polymer

structure contains homopolymeric regions (M and G blocks) and regions of alternating structures of the monomers (MG blocks). At neutral and basic pH values the alginate is charged highly negative.
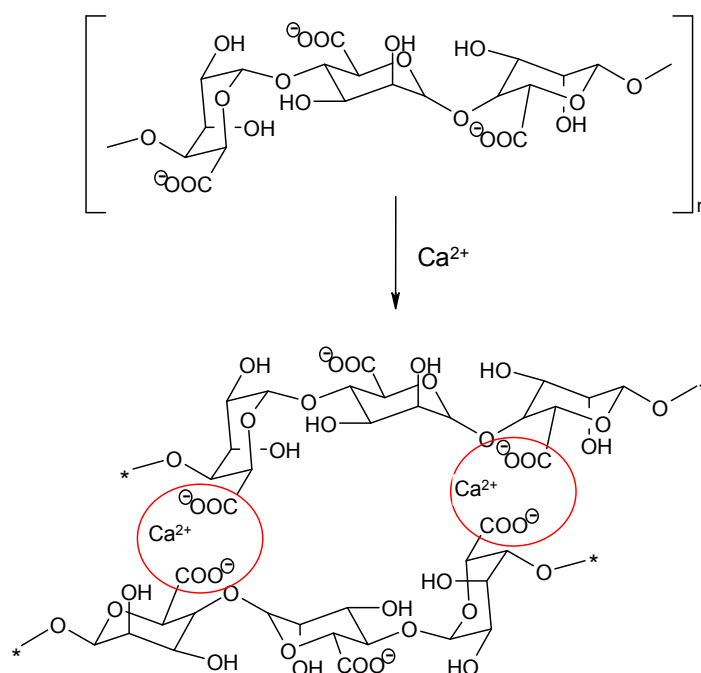
Fig. 3-10: Ionotropic gelation with Ca^{2+} ions

Reversible gelation takes place with divalent cations (generally Ca^{2+}), which bind preferably to the G blocks. The formed structure is often referred to as the egg-box model, where the calcium ions are placed inside the electronegative cavities [148].

For production of calcium alginate beads two different methods (external and internal gelation) exist to make calcium ions available for gelation. In the external gelation process sodium alginate is dropped into a stirred calcium chloride solution and calcium ions diffuse from outside into the alginate drops [21]. Gels of this extrusion procedure show an inhomogeneous structure with a smaller mash size at the bead borders than in the core due to the calcium gradient during fabrication [14]. By internal gelation calcium ions are supplied through acidification of calcium carbonate, which is mixed beforehand with the sodium alginate solution [25, 131]. Bead formation is possible over dispersion in oil (suspension polymerisation) or by dropping in acid calcium chloride solution (combined gelation).

Physical properties of calcium alginate beads depend on the composition of the sodium alginate, the gelation mechanism and the molecular size. Thus, higher stabilities are obtained with higher molecular weight of the sodium alginate molecules. A higher degree of guluronic acid (> 70%) or longer G block sequences increase mechanical strength as well [107].

Advantages like a quick, simple and cost-effective immobilisation face certain drawbacks. The inhomogeneous alginate distribution by external gelation affects diffusion properties of molecules in the gel [108]. Furthermore, alginate beads loose their stability in presence of chelating agents such as phosphate or citrate and anti-gelling substances (e.g. Na^+, Mg^{2+}, etc.) [107]. These may even induce complete dissolution of the alginate beads and release of the immobilised microorganisms. The microorganisms themselves also reduce bead stability above a certain concentration (10^5 cells·mL^{-1}) [123]. A low Na^+/Ca^{2+}-ratio and increased concentrations of free calcium ions in the medium my impede stability losses. Some other possibilities of stability enhancement are addition of other multi-charged cations (e.g. Al^{3+}, Ti^{3+}), additional hardening with polymeric polyelectrolytes (e.g. polyethylenimine) or supplement of silicates as well as partial drying of the beads [172]. Sterilisation of sodium alginate should preferably be performed by membrane filtration as high temperatures combined with non-neutral pH values lead to hydrolysis of the alginate [42].

3.4.1.1.2 Synthetic polymers

Compared to natural polymers, the application of synthetic polymers shows several advantages. As the properties of the entrapment matrix can be easily and artificially designed, it is possible to adjust gel porosity as well as the ionic and hydrophilic / hydrophobic properties depending on the destined application. Additionally, the mechanical strength and longevity of the gels are generally superior to those from natural polymers. However, the toxicity of many monomers and severe immobilisation conditions often reduce drastically the living cell concentrations in the immobilisates. For this reason, only two synthetic polymers have been explored in this work: polyurethane (PU) and polyvinyl alcohol (PVAL).

3.4.1.1.2.1 Polyurethane

Hydrophilic polyurethane foam is formed by mixing MDI polyurethane prepolymer (e.g. Hypol JM 5002) with the same or up to twofold amount of an aqueous phase forming urea linkages with liberation of carbon dioxide (see Fig. 3-11).

$$2\ OCN-R + H_2O \longrightarrow R\underset{H}{\overset{}{N}}\overset{\overset{O}{\|}}{C}\underset{H}{\overset{}{N}}R + CO_2$$
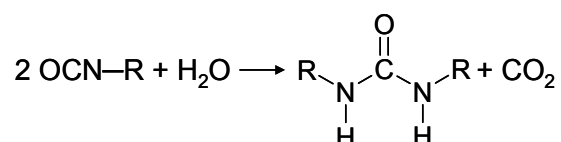
Fig. 3-11: Chemical reaction of polyurethane from prepolymer

The prepolymer contains isocyanate and urethane groups and arises from the reaction of a polyether polyol composition having nominal hydroxyl functionalities with methylene

diphenylisocyanate (MDI) [159]. The reaction product still contains monomer MDI to some extent. In general the polyether polyol is obtained by reacting ethylene oxide and propylene oxide with an initiator having active hydrogen atoms. The hydrophilic or hydrophobic properties of the polymer can be adjusted through the ratio of ethylene oxide to propylene oxide making it adaptable to many applications. High extents of ethylene oxide give hydrophilic polymers.

As spherical beads are more suitable as immobilisation system of *Pseudomonas aeruginosa* for rhamnolipid production in a stirred tank reactor, reversed-phase suspension polymerisation is applied. To allow a good dispersion of the polymer mixture in vegetable oil, MDI prepolymer and resuspended biomass has to be cooled down beforehand, as polycondensation reaction rate depends on temperature and only represents about five minutes at room temperature. Polyurethane beads are more rigid and chemically resistant than natural polymers with at the same time a clearer pore structure. The usage of prepolymers reduces toxic effects on entrapped bacteria.

3.4.1.1.2.2 Polyvinyl alcohol

Polyvinyl alcohol is a non-toxic polymer and as a low-cost material well suited for entrapment of living cells. The monomer of polyvinyl alcohol is shown in Fig. 3-12.
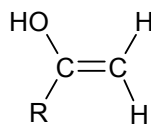
Fig. 3-12: Monomer of polyvinyl alcohol

Two different gelation mechanisms have been reported forming hydrogen bond between the polyvinyl alcohol chains. On the one hand, an elastic hydrogel is formed through repeated freezing and thawing without addition of other chemicals. As quite low temperatures are necessary to yield stable gels this mechanism hasn't been applied. A second gelation possibility consists in cross-linking with boric acid [30, 31] by dropping in a stirred saturated boric acid solution. Problems due to the high acidity of the boric acid solution reducing cell viability and the tendency of the immobilisates to agglomerate can be overcome by two approaches. Addition of low concentrated sodium alginate to the polyvinyl alcohol and hardening in mixed boric acid and calcium chloride solution reduces stickiness of the beads. Short cross-linking in boric acid followed by solidification of the gel beads by esterification of polyvinyl alcohol with phosphate prevents severe damage of the entrapped microorganisms. Jeong et *al.* [79] demonstrated the successful application of polyvinyl alcohol immobilisates of *Pseudomonas aeruginosa* for rhamnolipid production in an airlift bioreactor using a continuous culture.

3.4.1.2 Magnetic additives

Addition of magnetic or magnetisable particles to the polymer matrix permits a selective separation of the immobilisates from the reaction medium and easier handling by reuse of them. Separation of immobilisates is even possible for very small bead sizes, where classical methods such as filtration are no more applicable. By application in rhamnolipid production the great advantage lies in the retention of the magnetic immobilisates in the bioreactor facilitating a continuous production process.

For a stable and homogeneous embedding of the magnetic particles in the gel matrix these should be hydrophilic and of maximum ~1 µm size. In this work only magnetite (Fe_3O_4) particles (ferrimagnetic or super-paramagnetic) have been used. Through functionalisation of their surface (e.g. with acid groups) a stronger integration in the gel beads and maybe a more facile bead manufacturing is possible. Influence of magnetic properties and particle size on magnetic separation is described in more detail in paragraph 3.5.1.3 and 3.5.1.4.

3.4.2 Bead generation processes

Generation of spherical particles can be achieved through suspension polymerisation processes or extrusion methods dropping the polymer into a cross-linking solution. The choice of an appropriate process depends on the viscosity of the polymer solution, the hydrophobic / hydrophilic properties of the polymer, the surface tension, the gelation type and the addition of particles for entrapment. In this work reversed-phase suspension polymerisation has been used for the production of spherical polyurethane, and alginate immobilisates. Calcium alginate beads were also produced by the JetCutting®-technology as well as polyvinyl alcohol beads.

3.4.2.1 Suspension polymerisation

In a suspension polymerisation process a monomer is dispersed as liquid droplets in a suspension medium, in which it is relatively insoluble, by vigorous stirring and if necessary by a suitable stabiliser to produce polymer particles as dispersed solid phase. The reaction initiator is soluble in the monomer but not in the suspension medium [7]. Sodium alginate and polyurethane prepolymer Hypol JM 5002 are both water soluble and can be dispersed in vegetable oil or paraffin as so-called water-in-oil or reversed-phase suspensions.

Particle size distribution of beads produced by suspension polymerisation is generally rather broad. Physical factors affecting the particle size distribution are geometry and size of the reaction vessel, type of stirrer, stirrer diameter and installation, presence or absence of internal fittings and amount of energy supplied to the fluid through the impeller rotation [5]. Among these parameters, stirrer speed is the most convenient means of controlling particle size [7]. Due to turbulent pressure fluctuations or viscous shear forces the monomer phase is

cleaved in small spherical droplets. Collisions of these droplets lead to coalescence. Without stabilisers a dynamic equilibrium with a constant median particle size is reached after a certain time [15]. Addition of stabilisers can hinder coalescence and reduce therefore droplet sizes. Viscosity of the monomer phase compared to the suspension medium also influences particle size. For example, non homogeneous mixing combined with quite different viscosities of monomer phase and suspension medium leads to a bimodal particle size distribution due to satellite drops [130, 167]. As viscosity changes during polymerisation, slower reaction times may lead to broader particle size distributions. This phenomenon especially appears during production of polyurethane beads which already have a quite high viscosity in the beginning and whose reaction rate depends on temperature. In contrast, the instantaneous gelification of alginate through liberation of calcium ions after addition of acetic acid leads to smaller particle size distributions.
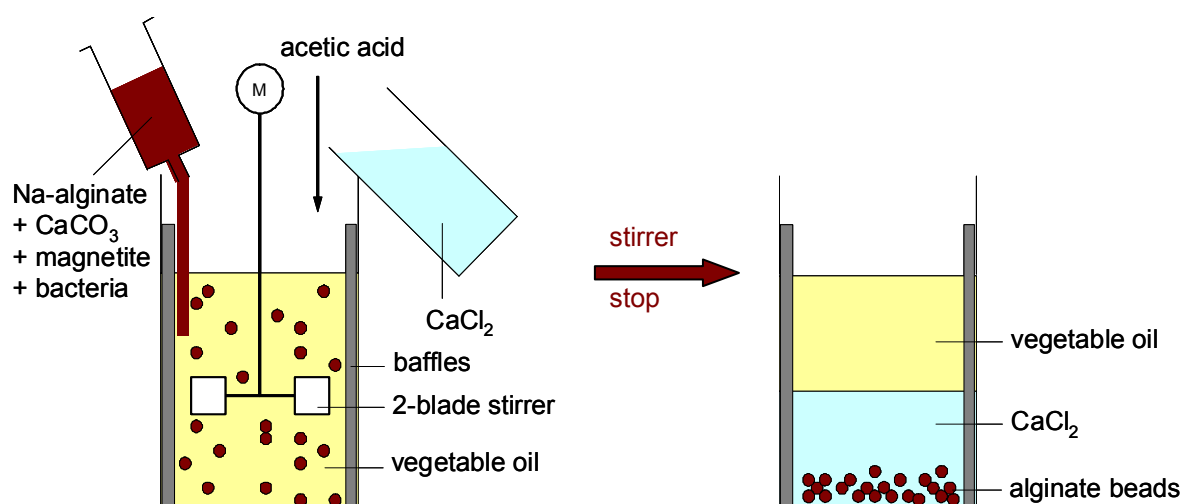
Fig. 3-13: Suspension polymerisation process of alginate beads according to Poncelet et *al.* [131]

In reversed-phase suspension polymerisation recovery of hardened immobilisates from the oily suspension medium and reuse in aqueous media is quite difficult. A device for alginate beads has been proposed by Poncelet at *al.* [131], who increased the aqueous volume ratio through addition of calcium chloride solution till the phase inversion stage with an intense coalescence of water droplets. After stopping of the stirrer phase separation occurs with alginate beads accumulated in the aqueous phase (see Fig. 3-13). The same procedure can also be adopted for polyurethane bead production.

3.4.2.2 Extrusion using JetCutting[®]-technology

The JetCutting[®] method described by Prüße et *al.* [132] is a bead production technology yielding quite monodisperse beads with a high production rate. In addition, not only low but also medium- and high-viscosity fluids can be used.

For the production of spherical particles by JetCutting[®] the fluid is pressed out of a nozzle as a solid jet. Directly underneath the nozzle the jet is cut into cylindrical segments by a rotating cutting tool made of small wires fixed in a holder. Driven by the surface tension, these segments form spherical beads while falling down into a cross-linker solution where they harden out. A scheme of the JetCutter[®] on the example of calcium alginate beads is shown in Fig. 3-14.
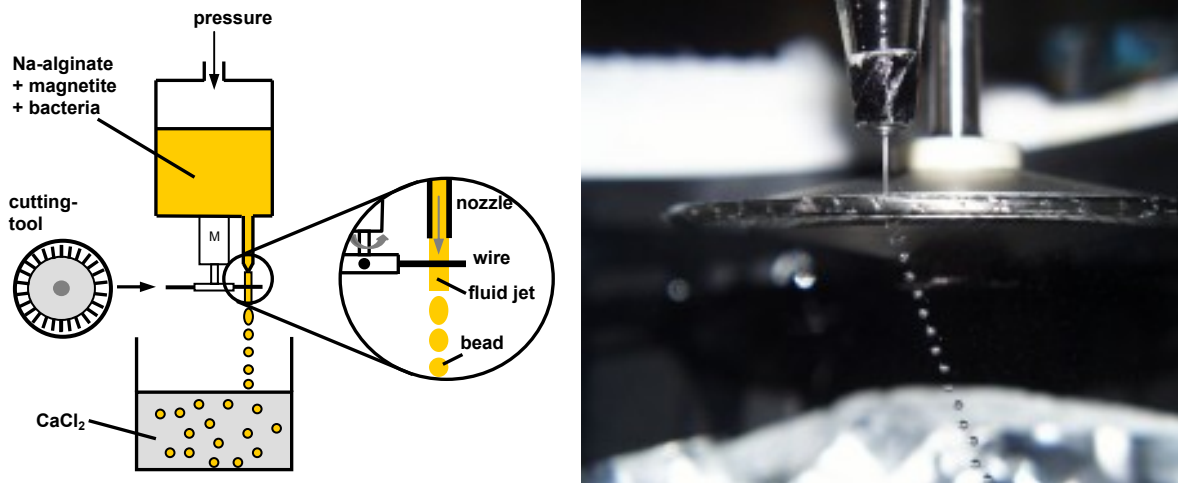
Fig. 3-14: Principle of the JetCutting[®]-technology (left) and a photograph of a cut fluid jet (right)

The size of the beads can be adjusted within a range between approximately 150 µm to several millimetres by adjusting the nozzle diameter, the flow rate through the nozzle, the number of cutting wires or the rotation speed of the cutting tool. Size limitations may although occur through higher viscosities or particle contents such as magnetite who may plug up filters and nozzles of the device.
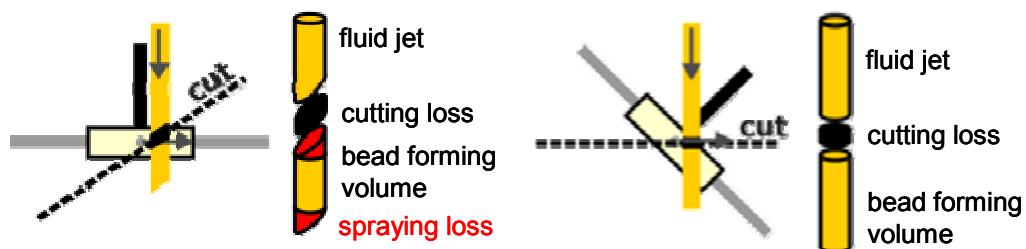
Fig. 3-15: Cutting loss by diagonal cutting of the fluid jet (left) and with inclined cutting plane

During the cutting process, losses formed when the wire cuts the fluid jet cannot be avoided. However, the inclination of the nozzle vis-à-vis the cutting tool may reduce additional spraying losses due to diagonal cutting of the jet as illustrated in Fig. 3-15. Bead diameters can be calculated for the optimum cutting angle according to Eq. 3-14.

$$d_{bead} = \sqrt[3]{\frac{3}{2} \cdot d_{nozzle}^2 \cdot \left(\frac{u_{fluid}}{n \cdot z} - d_{wire} \right)} \, [\mu m]$$

<div align="right">Eq. 3-14</div>

3.4.3 Characterisation of immobilisates

For the choice of an appropriate immobilisation method and the application of the most suited material several aspects have to be considered (see Tab. 3-4). These parameters include influences of immobilisation on product formation, viability of bacteria and stability of the immobilisation material. Assuring an economic production process, prices of immobilisation materials, immobilisation processes and disposal of waste material should also be compared beforehand. In the following subchapters several important parameters are discussed.

Tab. 3-4: Requirements of immobilisation matrices for rhamnolipid production

properties	desired value
chemical	
hydrophilicity / hydrophobicity	according to substrate und product properties
swelling properties	low
chemical stability/ solubility	high / low
microbiological stability	good
toxicity for microorganisms	low
mechanical	
compressive strength / compressibility	good / low
abrasion	none
morphological	
particle size / particle size distribution	approx. 100 µm / narrow distribution
pore size	approx. 30 - 60 nm

3.4.3.1 Chemical and mechanical stability

During production of rhamnolipids with immobilised bacteria in a stirred bioreactor combined with magnetic retention of the immobilisates through high gradient magnetic separation, compression and shear forces are always present. Therefore mechanically robust immobilisates are necessary to withstand the exposed stresses. Compression and shearing strain tests under defined conditions enable comparison of different immobilisations matrices and estimation of stability effects through additives such as magnetite.

Regarding compression of a single spherical particle between two plates, a typical stress-strain curve for viscoelastic materials (e.g. alginate) is presented in Fig. 3-16.
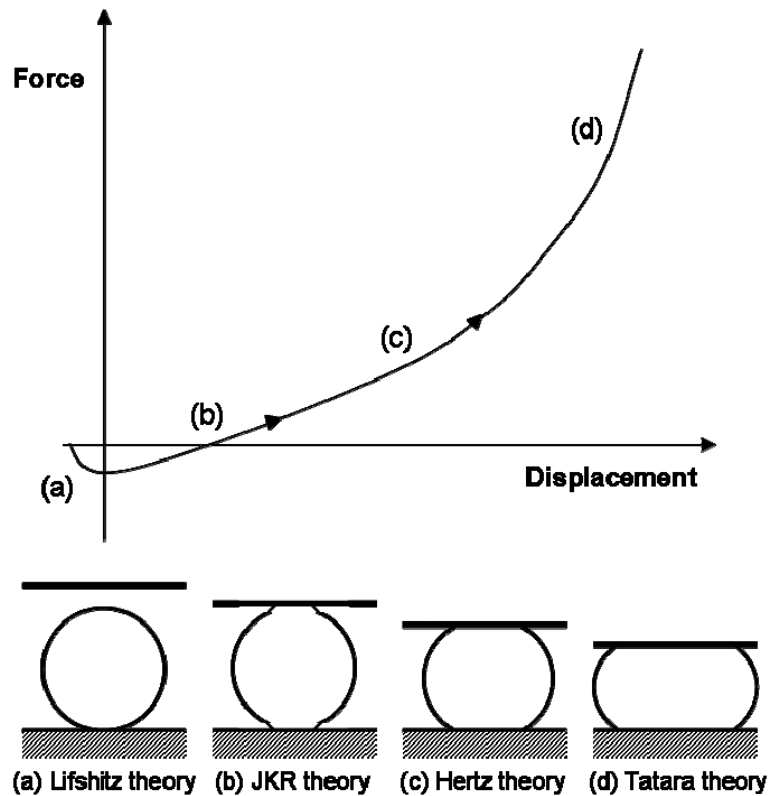
Fig. 3-16: Stress-strain curve of viscoelastic spheres compressed between two parallel plates and different theories which may be applied for the description of sequential stages

It is mainly influenced by adhesive (small deformations) and mechanical forces (large deformations). Different theories have been developed depending on the displacement of the sphere and therefore the influence of different forces [103]. Negative forces may occur in the beginning when the plate nearly touches the sphere, the so-called 'jump in contact' phenomenon. For calculation of the Young's modulus, Hertz theory is applicable for smaller strains up to 10%, whereas Tatara theory generally fits well up to relatively large strains (60%).
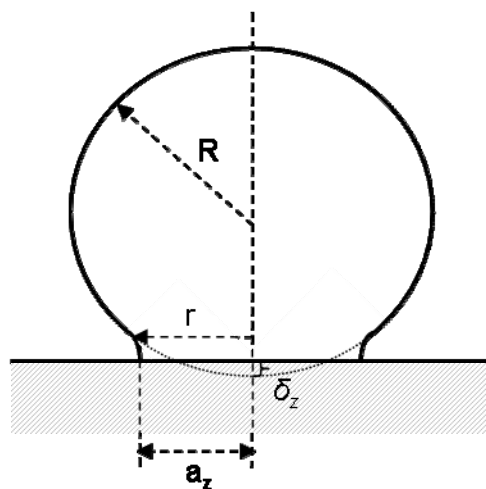
Fig. 3-17: Sketch of a sphere pressed against a plate

According to Hertz [68] and provided that linear elastic spheres are compressed between two plates having frictionless contact between the surfaces and only small deformations are investigated (see Fig. 3-17), the compressive displacement of the sphere is described as dimensionless approach δ_z by Eq. 3-15.

$$\delta_z = \frac{a_z^2}{R} = \left(\frac{3}{4 \cdot E' \cdot \sqrt{R}}\right)^{\frac{2}{3}} \cdot P^{\frac{2}{3}} \ [-]$$

Eq. 3-15

With a_z the circular contact zone of the sphere, R the initial radius of the sphere and the plane Young's modulus E' defined as a function of Poisson's ratio v and Young's modulus E (see Eq. 3-16).

$$E' = \frac{E}{(1 - v^2)} [N \cdot mm^{-2}]$$

Eq. 3-16

For deformations above 10%, according to the Tatara theory [157], load P is proportional to δ_z cubed and for even larger deformations to δ_z by the power of five taking into account a strain-dependent Young's modulus.
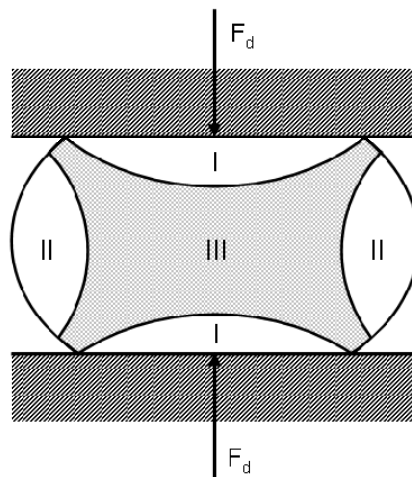
Fig. 3-18: Deformation zones of a compressed sphere, I) small deformations (friction interference), II) moderate tensile deformation, III) high compression deformation

During compression of immobilisates between two plates of a rheometer forces are measured as a function of displacement in axial direction. In material science it is conventional to plot so-called 'true' yield stress σ_t, which considers also the change of active cross-section during compression due to lateral displacement of the gel bead, as a function of deformation degree φ (see Eq. 3-17 and Eq. 3-18). This is necessary as different tensile and compression stresses occur inside the bead during compression (see Fig. 3-18). Calculations are based on the applied deformation force F_d, the initial bead height h_0, the bead deformation Δh and the initial bead diameter d_0.

$$\sigma_t = \frac{F_d \cdot h}{A_0 \cdot h_0} = \frac{F_d}{\frac{\pi}{4} \cdot d_0^2} \cdot \left(1 - \frac{|\Delta h|}{h_0}\right) \left[N \cdot mm^{-2}\right]$$

Eq. 3-17

$$\varphi = \ln\frac{h_0}{h} = \ln\frac{1}{1 - \frac{|\Delta h|}{h_0}} \ [-]$$

Eq. 3-18

As hydrogel-beads applied for immobilisation are losing water during compression measured forces depend on intrinsic mechanical properties of the matrix itself and its permeability. Therefore Young's modulus varies greatly depending on time scale of compression and particle size. This may be overcome with higher compression speeds (above 600 µm·s^{-1}), yielding stable results for Young's modulus [168]. Otherwise, only relative comparison of bead compression measurements with equal bead sizes and experiment times is possible.
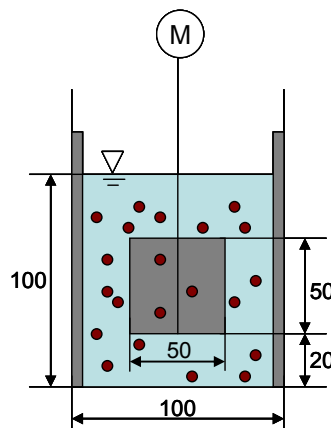
Fig. 3-19: Dimension [mm] and installation conditions of a two-blade agitator for abrasion experiments according to Zlokarnik [176]

Even more deleterious for immobilisates than compression loads are in general shearing strains, especially if chemical agents, promoting partial dissolution of gel structures on bead surfaces, are present. Stresses on immobilisates emerge from hydrodynamic interactions, collisions against other particles or reactor parts and strains during magnetic separation. In literature, abrasion experiments are often performed in bubble columns as fluidised bed reactors are frequently used for cultivation of immobilised microorganisms. Due to missing literature for shearing strain experiments regarding stirred bioreactors, experiments of this work are carried out under defined stirring and reactor conditions (see Fig. 3-19).

These permit calculations of the volumetric power input *P/V* based on literature and scale-up under equal shearing conditions (see Eq. 3-19), as shearing rates $\dot{\gamma}$ are proportional to the volumetric power input.

$$\varepsilon = \frac{P}{\rho \cdot V} = idem$$

Eq. 3-19

In turbulent flows (Re $>10^4$ and >50 with baffles respectively) the power input is calculated according to Eq. 3-20.

$$P = Ne \cdot \rho \cdot n^3 \cdot d_{stirrer}^5 [W]$$

Eq. 3-20

With Ne = 9.8 for stirring speeds n above 500 rpm under the defined conditions in Fig. 3-19. Experiments with different suspension media show the influence of chemical agents or pH conditions on etching or dissolution of immobilisates under strain conditions, approaching more reality in stirred bioreactors during rhamnolipid production than simple dissolution tests.

3.4.3.2 Particle size and diffusion properties

Utilising immobilised bacteria, diffusion properties of substrates in the pores of gel beads and transport of products out of the gels highly influence reaction rates of the desired product and in some cases also product spectrum [52, 81]. Diffusion limitations of substances may be due to limited pore sizes and physical interactions with the immobilisation matrix. It has been demonstrated [111] that larger particle diameters of gel beads almost annihilate rhamnolipid production of immobilised bacteria due to decreasing substrate concentrations towards the bead centre. It is therefore advisable to generate small particles with a homogeneous size distribution. Measurements by a laser diffraction method provide statistical ranges of surface areas in the sample which can be either illustrated as equivalent particle sizes in cumulative Q_2 or range q_2 diagrams (see Eq. 3-21).

$$Q_2(x) = \int_0^x q_2(x)dx$$

Eq. 3-21

As diffusion constitutes the most important factor influenced by particle size of immobilisates, comparison of particle ranges based on the mean particle size related to the volume specific surface of the particles $\overline{x}_{AV}$ is most suited.

Theoretical equations for measurement and calculation of effective diffusion coefficients D_{eff} by uptake and release of studied substances from particles are based on the second Fick's Law (see Eq. 3-22), where c is the concentration of the studied substance, t the experiment time and x the diffusion distance.

$$\frac{\partial c}{\partial t} = -D_{eff} \cdot \frac{\partial^2 c}{\partial x^2}$$

Eq. 3-22

Immobilisates are first saturated with rhamnolipids and then transferred to a rhamnolipid free medium or buffer, monitoring the concentration augmentation of the released rhamnolipids. For the case of spherical particles including some simplifications, Fick's Law can be transformed into Eq. 3-23, with the initial c_0, the actual c_t and the infinite c_∞ rhamnolipid concentrations in medium and r the median bead radius of the immobilisates [12].

$$\frac{c_t - c_\infty}{c_0 - c_\infty} = \frac{6}{\pi^2} \sum_{n=1}^{\infty} \frac{1}{n^2} \exp\left(-\frac{\pi^2 \cdot n^2 \cdot D_{eff} \cdot t}{r^2} \right) \qquad \text{Eq. 3-23}$$

If diffusion times are sufficiently high, the sum in Eq. 3-23 can be simplified to the following approximated solution (see Eq. 3-24). When plotting the logarithmic relative concentration change over the diffusion time, the effective diffusion coefficient can be calculated from the slope.

$$\ln\left(\frac{c_t - c_\infty}{c_0 - c_\infty} \right) \approx -\frac{\pi^2 \cdot D_{eff} \cdot t}{r^2} + const. \qquad \text{Eq. 3-24}$$

Apart from matrix material, internal diffusion is also influenced by microorganism concentrations in the immobilisates. As in this work cell-leakage of bacteria is countered with repeated cell growth after a certain production period, influence of bacteria on diffusion by clogging pores may be decisive for a continuous use of bacterial immobilisates. Hence, diffusion in gels containing immobilised microorganisms is a function of cell volume fraction ϕ_c and effective diffusion coefficient within the cells D_c [171]. For the case of impermeable cells this function is reduced to Eq. 3-25.

$$D_{eff} = (1 - \phi_c) \cdot D_{eff,0} [cm^2 \cdot s^{-1}] \qquad \text{Eq. 3-25}$$

3.4.3.3 Surface charges and adsorption phenomena

Apart from pore sizes, diffusion of solutes in immobilisates is principally influenced by interactions of molecules with immobilisation matrices or embedded material, depending on surface energy of the molecule and surface charges present. Charged particles show a difference in potential of their surface and electrolyte potential, the so-called surface potential. As counter-ions accumulate immediately around charged particles, an electrochemical double layer, composed of a stable stern layer and a diffuse layer, is formed. If this double layer is sheared between the two layers, a relative electric potential between stern layer and dispersion medium, the Zeta potential, can be measured. Determination of Zeta potentials of magnetite particles give an idea about the nature of interactions of rhamnolipids [122] or maybe certain substrates with embedded magnetite. Neutral potentials at working pH are less suspected of adsorption phenomena than charged magnetic particles.

Adsorption effects are therefore studied by saturation of immobilisates with rhamnolipids in a concentrated solution and comparison of their release properties after transfer of the immobilisates in a new rhamnolipid free medium (as for diffusion coefficient determination).

3.4.3.4 Magnetisation

For magnetic retention of immobilised bacteria during rhamnolipid production, stable incorporation of magnetic particles (e.g. magnetite) is necessary. The obtained magnetic immobilisates should furthermore possess a specific saturation magnetisation $M_{s,g}$ of the humid bead of minimum 2 $A \cdot m^2 \cdot kg^{-1}$, which does not decline too much during cultivation due to oxidation or lost. For an effective magnetic separation and back-flushing of beads from the filter matrix, these should have at most a moderate remanence (remaining magnetisation in absence of an external magnetic field). Magnetic particles without a remanence are superparamagnetic, whereas ferrimagnetic magnetite always shows a remanence (see paragraph 3.5.1.4).
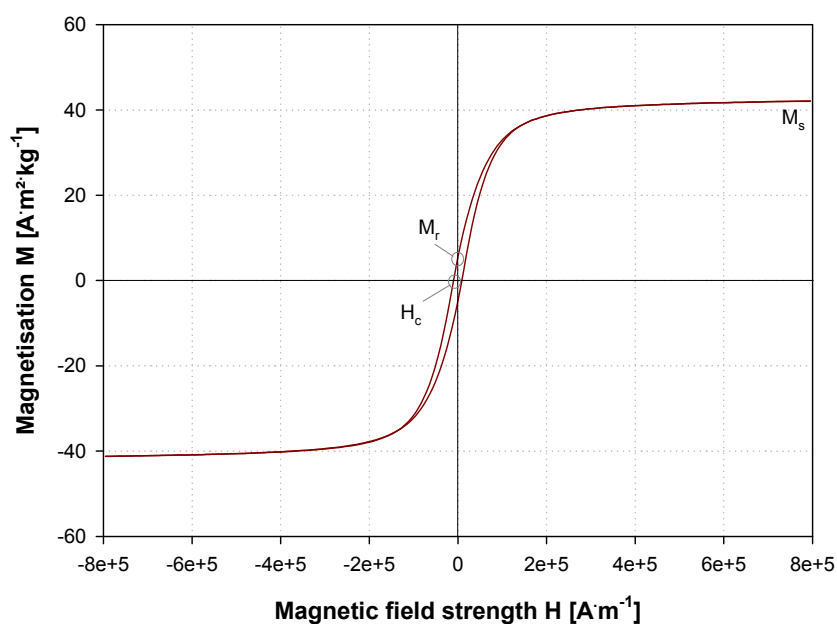
Fig. 3-20: Hysteresis curve of dried magnetic alginate beads, [M_s] saturation magnetisation, [M_r] remanence magnetisation, [H_c] coercitivity field strength

These magnetic properties are measured by an alternating-gradient magnetometer. The sample is magnetised by a static magnetic field and at the same time overlaid by an alternating magnetic field. The resulting field gradient is proportional to the magnetic moment of the sample and can be measured due to deflexion of a piezoelectric element from which the sample is suspended. An example of a magnetisation curve is illustrated in Fig. 3-20.

3.4.3.5 Biocompatibility, cell-leakage and rhamnolipid production

Finally, immobilisation material and method have to be biocompatible, which is not the case for many synthetic polymers due to toxic monomers (e.g. acrylates, urethanes, etc.) or organic dispersion media. Already during immobilisation process, high losses of viable microorganisms are possible through stressing immobilisation conditions or cell-leakages, especially for highly swelling materials (e.g. polyurethanes) and slow gelification or polymerisation processes. Later on leakage of *P. aeruginosa* cells during rhamnolipid production is also undesirable, which may be promoted unfortunately by the produced rhamnolipids (see subchapter 3.2.2.1). Concerning rhamnolipid production, several factors such as pH, substrate, product and cell concentrations or availability of promoting factors, are influencing production rates (see subchapter 3.2.2.3). These conditions may be different in immobilisates compared to medium conditions for free cells. The impact of immobilisation on physiology of entrapped microorganisms is discussed in the next chapter 3.4.4.

3.4.4 Influence of immobilisation on physiology of bacteria

Several authors [52, 70, 81] have suggested a profound influence of immobilisation on metabolism of entrapped microorganisms. Observed changes in metabolism are often caused by a change in local concentrations due to mass transfer limitations. These differences in metabolic behaviour highly depend on the examined microorganisms, leading somewhat to contradictory results in literature. Lower pH values in immobilisates due to diffusion limitations can entail increased catabolism by fermentative degradation ways and change therefore glucose consumption degrees [52]. As rhamnolipid production also depends on pH [56, 153] immobilisation may change the rhamnolipid yield and also the entire product spectrum of *P. aeruginosa*.

Additionally, the distinction between single cells and micro-colonies is necessary given that micro-colonies show more frequently different behaviour patterns in immobilisates than single cells [70]. This fact may be due to symbiotic effects or proximity of external substrates, growth factors, enzymes, etc. Concerning *P. aeruginosa*, a common biofilm inhabitant, rhamnolipid formation (as well as accumulation of certain other substances of the quorum sensing system) is intensified by higher cell densities and nutrition deprivation [163, 164].

Differences in specific growth rates of immobilised cells compared to free cells are more pronounced under anaerobic growth conditions, whereas reaction kinetics of aerobically growing microorganisms are quite similar within or without immobilisates if no mass transfer limitations occur (e.g. very small immobilisates) [61]. Osmotic pressure in immobilisates and protection from toxic compounds or inhibitors may also influence microbial growth, product formation and cell morphology [81].

3.5 Magnetism and magnetic separation

In the following paragraphs fundamentals of magnetism and the functional principle of magnetic separation are presented based on Franzreb [51]. For the separation of magnetic cell immobilisates out of foam the influence of immobilisates size, magnetisation and separator parameters on magnetic separation efficiency are important.

3.5.1 Magnetism

Magnetism is an inherent property of materials, arising from the orbital and spin magnetic moments of the nucleus and the electrons. Depending on the arrangement of these magnetic moments different forms of magnetism in matter are discerned (see Fig. 3-21).
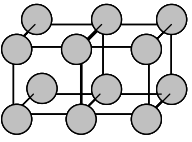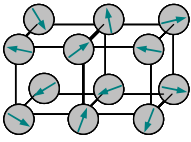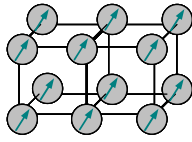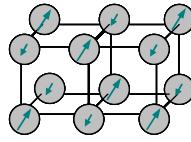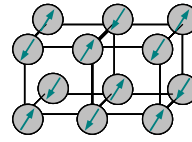
	diamagnetic	paramagnetic	ferromagnetic	ferrimagnetic	antiferromagneti
Magnetic moments					
Permeability	$\mu_r < 1\ (\approx 1)$	$\mu_r > 1\ (\approx 1)$	$\mu_r \gg 1$	$\mu_r \gg 1$	$\mu_r > 1\ (\approx 1)$
Susceptibility	$\kappa < 0\ (\approx 0)$	$\kappa > 0\ (\approx 0)$	$\kappa \gg 0$	$\kappa \gg 0$	$\kappa > 0\ (\approx 0)$

Fig. 3-21: Forms of magnetism in matter

3.5.1.1 Magnetic field and magnetic flux density

Magnetic fields are produced by electric currents, which can be macroscopic currents in wires, or microscopic currents associated with electrons in atomic orbits (permanent magnets). These magnetic fields generate forces which are characterised in vacuum through the vector of the magnetic field strength H. The impact of a magnetic field occurring in matter is rather described through the magnetic flux density B (see Eq. 3-26) which also takes into account magnetic material properties (permeability μ). Permeability is the degree of magnetisation of a material with μ_0 the permeability constant of the vacuum) and μ_r the material dependent permeability. In vacuum and by approximation in air μ_r is equal to 1.

$$B = \mu_0 \cdot \mu_r \cdot H\ [T]$$

Eq. 3-26

with $\mu_0 = 4 \cdot \pi \cdot 10^{-7} V \cdot s \cdot A^{-1} \cdot m^{-1}$

3.5.1.2 Polarisation and susceptibility

If a substance is introduced into a magnetic field, the magnetic flux density changes inside the material. The change in magnetic flux density ΔB is called the magnetic polarisation J (see Eq. 3-27).

$$J = \Delta B = B_{material} - B_{vacuum} = \kappa \cdot \mu_0 \cdot H \ [T]$$

Eq. 3-27

Except for ferro- and ferrimagnetic substances, magnetic polarisation is proportional to the present magnetic field strength by a factor called magnetic volume susceptibility $\kappa = \mu_r - 1 \ [-]$. Classification of substances corresponding to their magnetic properties is effected by the values of μ_r and κ according to Fig. 3-21. For the case of ferro- or ferrimagnetic substances, the material dependent permeability μ_r is a function of the magnetic field strength. Hence, magnetic polarisation reaches a maximum, the saturation polarisation J_s, at high magnetic field strengths.

3.5.1.3 Magnetisation

In practice, the effect of a magnetic field on ferro- or ferrimagnetic substances often is described by the apparent increase of magnetic field strength, the so-called magnetisation M (see Eq. 3-28).

$$M = \Delta H = H_{material} - H_{vacuum} = \kappa \cdot H \ [A \cdot m^{-1}]$$

Eq. 3-28

Respectively, saturation magnetisation M_s is reached, when the atomic magnetic dipoles are completely aligned through the influence of the magnetic field. Magnetic properties of ferro- or ferrimagnetic substances are visible in magnetisation curves as illustrated exemplary in Fig. 3-20 for dried magnetic immobilisates.

3.5.1.4 Influence of particle form and size

Magnetic susceptibility is not only a material property, but also depends on particle size and particle form. In the case of a finite particle, the external magnetic field induces a different intrinsic magnetic field in the particle, generally leading to an attenuation of the overall magnetic field. Dependency on particle form is described by the so-called demagnetisation factor D_m with $0 < D_m < 1$. The magnetic volume susceptibility can be calculated from the demagnetisation factor of the material and the intrinsic magnetic susceptibility κ_i (which is measured with a sample not exhibiting any demagnetisation, e.g. an annulus) according to Eq. 3-29.

$$\kappa = \frac{\kappa_i}{1 + D_m \cdot \kappa_i} \ [-]$$

Eq. 3-29

Very small particles of ferro- or ferrimagnetic material which contain only one or few magnetic domains show a completely different behaviour than macroscopic samples with constant values of remanence magnetisation (magnetisation in absence of a magnetic field). These small particles behave like paramagnetic material, but show considerably higher absolute magnetisation values, therefore called superparamagnetic. For magnetite, the magnetic susceptibility varies with particle size according to Fig. 3-22. The transition from ferrimagnetic to superparamagnetic behaviour is situated at about 2 nm for spherical magnetite particles.
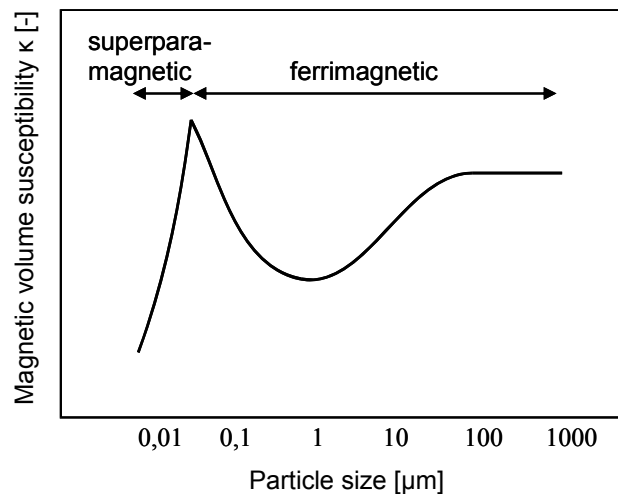
Fig. 3-22: Dependency of magnetic volume susceptibility on particle size of magnetite [152]

3.5.2 Physical fundamentals of magnetic separation

Magnetic separators are separating magnetic as well as magnetisable particles from a suspension or foam. All types of magnetic separators are based on the principle that magnetic fields are exerting a force on matter. The general relation of this magnetic force F_m is specified in Eq. 3-30.

$$F_m = \mu_0 \cdot V_P \cdot M_P \cdot \nabla H \; [N]$$

Eq. 3-30

Concerning immobilisates, separation improves with larger particle volume V_P and higher magnetisation of humid immobilisates M_P. For rhamnolipid production, these parameters can only be varied in a relatively small range, as they are limited through their influence on diffusion properties and applicable immobilisation procedures. To ensure magnetic separation of immobilisates out of foam, strong magnetic fields and therefore high gradients of magnetic field strength ∇H are necessary. These are especially achieved in high gradient magnetic separation (HGMS) with field gradients up to 10^5 T·m^{-1} [51].

3.5.3 High gradient magnetic separation

The separation principle of high gradient magnetic separation, depicted on the example of immobilisates separation from foam in Fig. 3-23, is similar to deep bed filtration. A filter chamber, filled with a magnetisable separation matrix, is placed in the scope of an external magnetic field. In Fig. 3-23 the separation matrix is illustrated by a single wire cross-section, which may consist in the simplest case of a loosely packed steel wool or, as generally applied, a stack of ordered wire meshes. The matrix wires concentrate the external magnetic field in their vicinity, yielding magnetic field gradients which originate sectors on the wire surfaces that highly attract para-, ferri- or ferromagnetic particles. Foam with magnetic immobilisates enters bottom-up, the immobilisates are accumulated on the wire surface and the purified foam leaves the separation chamber at the top. If the separation capacity of the filter matrix is exhausted, the external magnet is switched off / removed and the immobilisates are backflushed.
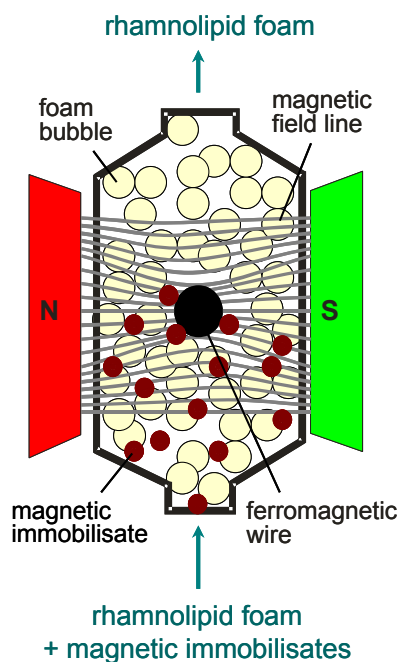
Fig. 3-23: Separation principle of HGMS

Principally, three different arrangements for foam flow, separation wire and external magnetic field are possible (see Fig. 3-24), influencing particle accumulation patterns.
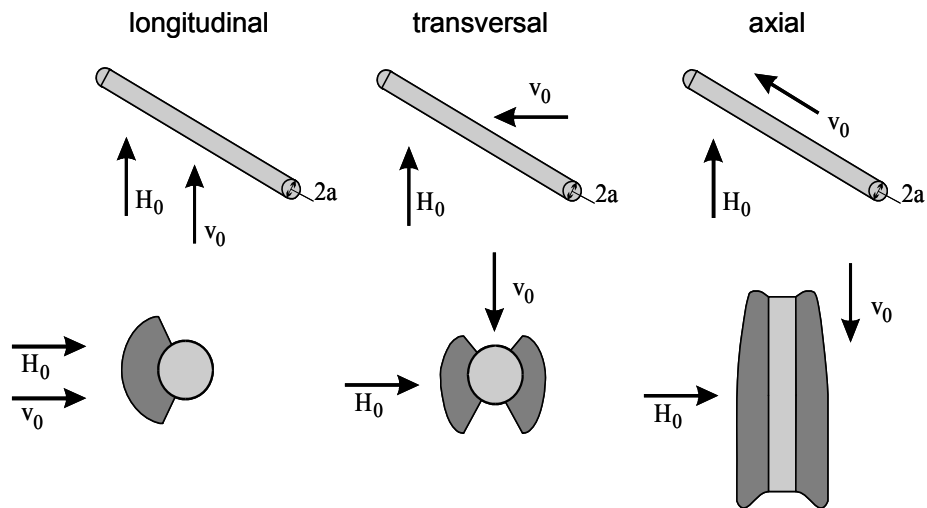
Fig. 3-24: Geometrical configuration of foam flow direction (v_0), separation wire and magnetic field (H_0) with their corresponding particle accumulation [51]

3.5.3.1 HGF 10

Magnetic separation during rhamnolipid production has to be effected constantly with at most small interruptions for backflushing as foam is generated constantly due to the produced rhamnolipid. Therefore, only permanent magnets, which can operate continuously (e.g. carousel-type HGMS) or be "switched-off" during backflushing, are suitable. A high gradient magnetic filter, called HGF 10, was developed by Hoffmann et *al.* [72] using "switchable" permanent magnets. The filter operates in a cyclic fashion making it suitable for separation of immobilisates out of foam. Fig. 3-25 shows a schematic drawing of the filter build by Steinert Elektromagnetbau GmbH (Germany).
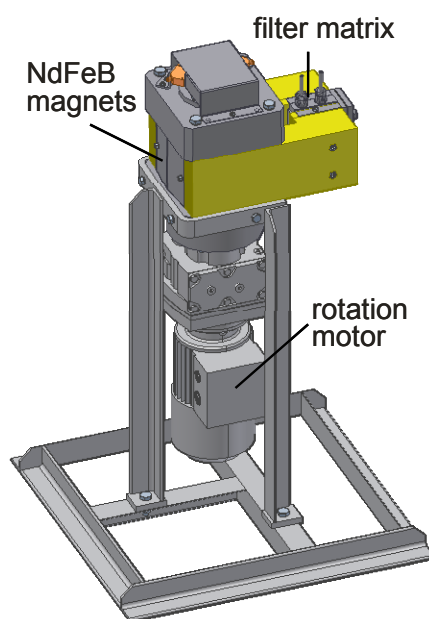
Fig. 3-25: Engineering drawing of HGF 10

Between the pole shoes of an iron yoke a filter matrix filled with ferromagnetic wire meshes is placed. During operation the foam flows bottom-up through the filter as described in paragraph 3.5.3. As the actual magnet units are placed into the centre of a cylinder which can be rotated along its axis, the magnet system can be switched "off" during backflushing in counter flow direction. The effect of rotating the permanent magnets on the magnetic field distribution for the two states is visualised in Fig. 3-26, based on calculations with a finite element program.
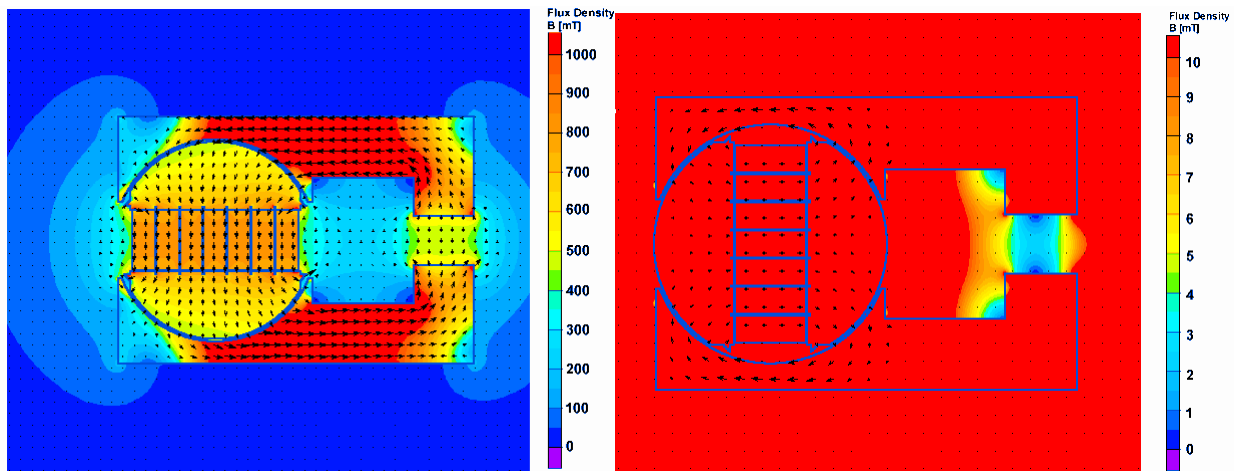
Fig. 3-26: Magnetic field distribution in the iron yoke of HGF 10
(a) field-on position, (b) "field-off" position

In the "field-on" position the system resembles a conventional magnet yoke generating a flux density between the magnetic poles of almost 500 mT. However, if the cylinder is rotated through 90°, the north and south poles of the permanent magnet formed by the cylinder are short-circuited by the iron yoke, switching the magnetic field "off". The ratio between the flux densities at the filtration matrix in the "on" and "off" position is more than 100.

The wires of the superposed meshes in the filter chamber are arranged in transversal and axial configuration to yield maximum field utilisation together with high filter capacities. To allow for almost complete backflushing of the separated immobilisates, a pneumatic ball vibrator is installed on the front side of the filter chamber facilitating immobilisates detachment of the wire meshes.

For process control of magnetic separation the rotation motor, the valves for fluid distribution and the backflushing pump are connected to a control program realised in LabVIEW from National Instruments (see Fig. 3-27). In this program are entered desired step times of the separation cycle and pumping speeds.
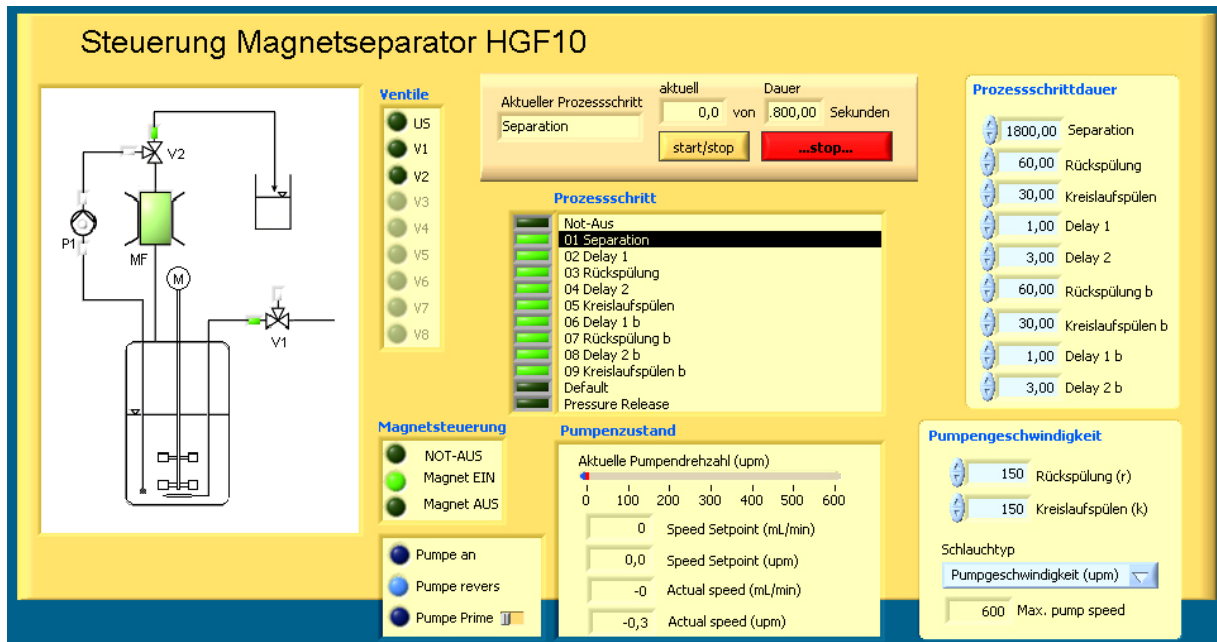
Fig. 3-27: Operator interface of the HGF 10 control program realised in LabVIEW

4 Whole-cell immobilisation of *Pseudomonas aeruginosa* in different magnetic matrices for continuous biosurfactant production

4.1 Abstract

Up to now, whole-cell immobilisation has successfully been used in many bioprocesses, especially to enable continuous production processes, higher production rates and reuse of the biocatalyst. In some cases, effective retention of immobilisates in the bioprocess is not feasible by membranes or sieves due to pore plugging or undesired losses of immobilisates. In the present publication magnetic immobilisates of *Pseudomonas aeruginosa* were examined for application in continuous biosurfactant production of rhamnolipids by foam fractionation and retention of entrained immobilisates by high gradient magnetic separation from foam. Different materials were tested in respect to important parameters such as stability, diffusion properties, biosurfactant production or magnetic separation. Good magnetic separation of immobilisates was possible with 5% magnetite loading. Best results concerning homogeneous embedding, good diffusion properties and stability enhancement vis-à-vis pure alginate beads was achieved with Bayoxide® magnetite and MagPrep® Silica particles. Although polyurethane immobilisates showed higher stabilities compared to alginate beads, rhamnolipid synthesis was superior in magnetic alginate beads. A cyclic rhamnolipid production process was suggested with cell growth between rhamnolipid production phases to re-induce the slowed down rhamnolipid synthesis and maintain high viable cell concentrations. However, still some efforts have to be made for effective cell growth inside the immobilisates, whereas specific rhamnolipid synthesis rates related to the viable cell concentration maintained at the initial level.

4.2 Introduction

Since the early 70s, whole-cell immobilisation has successfully been introduced in biotechnology processes [134] and since that various microbial fermentation processes utilising immobilised biocatalysts have been published. Advantages arise from continuous process management, easier downstream-processing of the product, longer viability and better protection of the immobilised microorganisms as well as a higher space-time yield through higher spatial concentration of the biocatalyst [13]. For immobilisation of living microorganisms, generally entrapment in gel beads or micro-encapsulation is preferred due to a better cell retention in the immobilisates and biocompatible bead generation processes [172].

The choice of an immobilisation method especially depends on nutrients and the desired product as their diffusion properties influence product formation and extraction from

immobilisates. Therefore, beads for cell entrapment should be rather small to reduce negative effects due to transport limitations in the immobilisates. Typically, retention of immobilisates in stirred bioreactors is realised by membranes or sieves, which should not retain the desired product and therefore entail limitations in bead sizes of the immobilisates [55, 111]. For the case of biosurfactant production, membrane processes are less suitable, as the passage of surfactant molecules through smaller membranes is impeded due to the peculiarity of rhamnolipids to form micelles even at very low concentrations [55]. In contrast, foam fractionation permits the complete extraction of rhamnolipids from cultivation medium, but entrains microbial immobilisates [36].

An approach facilitating retention of even very small immobilisates in a stirred bioreactor with foam fractionation consists in embedding of magnetic particles such as magnetite (Fe_3O_4) in the matrix polymer and magnetic separation of the immobilisates from foam. Separation of magnetic particles even from complex media is already well studied for high gradient magnetic separation (HGMS) [75, 112, 144].

In the present publication magnetic immobilisates of *Pseudomonas aeruginosa* DSM 2874 are studied for application in continuous microbial rhamnolipid production with *in situ* product removal by foam fractionation and immobilisates retention through HGMS (see chapter 5). Rhamnolipids, some of the most extensively studied biosurfactants, are composed of one or two rhamnose molecules and up to three molecules of hydroxy fatty acids, whereas their chain length can vary from 8 up to 14 carbon molecules [40, 58, 60]. *P. aeruginosa*, mostly producing rhamnolipids, are immobilised in magnetic matrices that allow retention of the biocatalyst in the bioreactor by magnetic separation during continuous rhamnolipid production. Potential immobilisation matrix materials, immobilisation methods as well as different types of entrapped magnetite have been analysed in respect of particle size distribution, stability, magnetic and diffusion properties, biocompatibility and of course their influence on rhamnolipid production.

4.3 Materials and Methods

4.3.1 Experimental methods

4.3.1.1 Bacterial strain and cultivation conditions

4.3.1.1.1 Microorganism

The gram-negative, under certain conditions (nitrate source) facultative anaerobic *Pseudomonas aeruginosa* DSM 2874 strain was used for all experiments. This wild-type strain has been isolated from water samples and characterised by Syldatk et *al.* [153]. The

strain is supplemented after over-night culture in Luria Broth agar with 25% glycerol and conserved at -80°C.

4.3.1.1.2 Media composition

The following media were used for biomass production, during rhamnolipid synthesis tests with immobilised bacteria in shake flasks and for shearing strain tests:

VK2   7.73 g·L^{-1} NaNO$_3$, 0.4 g·L^{-1} MgSO$_4$ x 7H$_2$O, 0.4 g·L^{-1} CaCl$_2$ x 2H$_2$O,
          3.72 g·L^{-1} Na$_2$HPO$_4$ x 2H$_2$O, 6.24 g·L^{-1} KH$_2$PO$_4$, 30 g·L^{-1} glycerol, 1 mL·L^{-1} TES

TES   100 g·L^{-1} Na-citrate x 2H$_2$O, 0.28 g·L^{-1} FeCl$_3$ x 6H$_2$O, 1.2 g·L^{-1} CoCl$_2$ x 6H$_2$O,
          1.4 g·L^{-1} ZnSO$_4$ x 7H$_2$O, 1.2 g·L^{-1} CuSO$_4$ x 5H$_2$O, 0.6 g·L^{-1} MnSO$_4$ x H$_2$O

B1   6.96 g·L^{-1} NaNO$_3$, 0.36 g·L^{-1} MgSO$_4$ x 7H$_2$O, 0.36 g·L^{-1} CaCl$_2$ x 2H$_2$O,
          3.72 g·L^{-1} Na$_2$HPO$_4$ x 2H$_2$O, 6.24 g·L^{-1} KH$_2$PO$_4$, 30 g·L^{-1} glycerol, 1 mL·L^{-1} TES

R1   0.45 g·L^{-1} NaNO$_3$, 0.18 g·L^{-1} MgSO$_4$ x 7H$_2$O, 0.18 g·L^{-1} CaCl$_2$ x 2H$_2$O,
          0.19 g·L^{-1} Na$_2$HPO$_4$ x 2H$_2$O, 0.31 g·L^{-1} KH$_2$PO$_4$, 10 mM MOPS,
          30 g·L^{-1} glycerol, 0.1 mL·L^{-1} TES

A1   1.8 g·L^{-1} NaNO$_3$, 0.72 g·L^{-1} MgSO$_4$ x 7H$_2$O, 0.72 g·L^{-1} CaCl$_2$ x 2H$_2$O,
          0.74 g·L^{-1} Na$_2$HPO$_4$ x 2H$_2$O, 1.25 g·L^{-1} KH$_2$PO$_4$, 10 mM MOPS, 0.1 mL·L^{-1} TES

A2   18 g·L^{-1} NaNO$_3$, 7.2 g·L^{-1} MgSO$_4$ x 7H$_2$O, 7.2 g·L^{-1} CaCl$_2$ x 2H$_2$O,
          7.4 g·L^{-1} Na$_2$HPO$_4$ x 2H$_2$O, 12.5 g·L^{-1} KH$_2$PO$_4$, 10 mM MOPS, 0.1 mL·L^{-1} TES

S1   2.88 g·L^{-1} NaNO$_3$, 0.13 g·L^{-1} MgSO$_4$ x 7H$_2$O, 0.5 g·L^{-1} CaCl$_2$ x 2H$_2$O,
          0.62 g·L^{-1} Na$_2$HPO$_4$ x 2H$_2$O, 1.04 g·L^{-1} KH$_2$PO$_4$, 1 mL·L^{-1} TES

For all media, mineral salts and buffer substances together with glycerol (as 10x buffer) were prepared and autoclaved separately at 121°C. Chemicals used in the formulation of growth media were purchased from Merck (Darmstadt, Germany) and Carl Roth (Karlsruhe, Germany).

4.3.1.1.3 Biomass production

Firstly, a colony of cells, grown on a cetrimid agar plate, was added to 10 mL sterile nutrient broth (Luria Broth, Miller) in a 15 mL falcon tube. After incubation at 37°C over night on an orbital shaker (194 rpm), 5 mL of culture broth were added to a 500 mL shake flasks containing 100 mL of mineral salt medium VK2 and cultivated under the same conditions for 10 h. Biomass production was performed in a 10 L bioreactor (Biostat *Bplus*, Sartorius Stedim Biotech, Melsungen, Germany), equipped with two 6-blade disc impellers (70 mm ø, 1. impeller: 50 mm above bioreactor base, 2. impeller: 125 mm distant to 1.), a foam-disc for foam destruction (10 mm above liquid level), a sparger ring for aeration and probes for pH,

pO_2 as well as temperature measurements. The 6 L of mineral salt medium B1 in the bioreactor were inoculated with 100 mL pre-culture (equal to 16,7% of the medium volume) and cultivated for about 21 h at 37°C and 1000 rpm. The pH in the bioreactor was maintained at 6.5 by the automatic addition of 2 M NaOH or 2 M HCl. In the case of intensive foaming, antifoam (Contraspum, Zschimmer & Schwarz, Lahnstein / Rhein, Germany) was added. Trace element solution TES (1 $g \cdot L^{-1}$) was supplemented approx. every 10 hours. After depletion of supplied nitrate, biomass was harvested by centrifugation at 7000 rpm and 4°C for 15 min (Coulter Avanti Centrifuge J-25 I, Beckmann, Krefeld, Germany). Bacteria were washed once with 3-(N-morpholino)propanesulfonic acid (MOPS) buffer at pH 6.5 and recentrifuged. Then, the biomass was charged into 50 mL falcons as aliquots of about 10 g and stored at -80°C until utilisation for rhamnolipid production experiments.

4.3.1.1.4 *Rhamnolipid formation*

The bacteria from the biomass fermentation process (see paragraph 4.3.1.1.3), which had been stored at -80°C, were unfrozen at room temperature and entrapped in magnetic immobilisates (see paragraph 4.3.1.5). Then, rhamnolipid synthesis was tested in 500 mL shake flasks with 100 mL of mineral salt R1 with pH 6.5 by cultivation at 37°C and 194 rpm on an orbital shaker. The pH was controlled via a disinfected pH probe and adjusted to a value of 6.5 every day by addition of 1M HCl or NaOH. Medium samples of 1 mL were taken once a day for rhamnolipid analysis. As rhamnolipid production slowed down after several days, a semi-continuous production was simulated by exchange of production medium R1 after one week. For this purpose, immobilisates were retained on a small permanent magnet, the medium decanted and replaced by new mineral salt medium A1. For influence studies of different medium compositions and remaining by-products, rhamnolipids were removed by addition of 4 g XAD-16 adsorber for 30 minutes and subsequent separation by sieving. Afterwards, 10 µL of TES solution and 10 mL of different nutrients (30 $g \cdot L^{-1}$ glycerol, 30 $g \cdot L^{-1}$ glycerol + 20 $g \cdot L^{-1}$ nitrate or growth medium A2) were added in tenfold concentrations compared to medium A1. Immobilisates of these shake flask experiments were analysed with regard to particle size distribution, magnetisation and compression stability.

4.3.1.2 Immobilisation materials

Employed matrix materials for immobilisation were alginate (Sigma-Aldrich, Taufkirchen, Germany) and polyurethane (PU) prepolymer Hypol JM 5002 (Dow, Schwalbach, Germany). Gelation of alginate occurs in the presence of divalent cations (in our case Ca^{2+}). For preparation, sodium alginate was dissolved in pre-heated 10 mM MOPS buffer on a magnetic stirrer and partly sterilised at 95°C for 30 min. Finally, PU foams were formed from PU-prepolymer by polycondensation with water and the associated release of carbon dioxide.

Different magnetite species were only incorporated into calcium alginate beads. As commercial ferromagnetic magnetite were purchased Bayoxide® E 8710 (Lanxess, Leverkusen, Germany) and MagPrep® Silica particles (Merck, Darmstadt, Germany). Superparamagnetic magnetite has been self-synthesised and activated or coated (see paragraphs 4.3.1.3 and 4.3.1.4). Mainly all other chemicals used during magnetite synthesis and immobilisation of bacteria were purchased from Merck.

4.3.1.3 Magnetite production

Superparamagnetic magnetite with a size of about 10 nm was synthesised by basic precipitation of $FeCl_2$ and $FeCl_3$. 17.2 g of $FeCl_2·4 H_2O$ and 28.2 g of $FeCl_3$ were dissolved under in 800 mL of water and 54 mL of 25% ammonia, yielding about 20 g of magnetite according to the following formula.

$$2\ FeCl_3 + FeCl_2 \cdot 4\ OH_2 + 8\ NH_3 \rightarrow \underbrace{Fe_3O_4 \downarrow}_{magnetite} + 8\ NH_4Cl$$
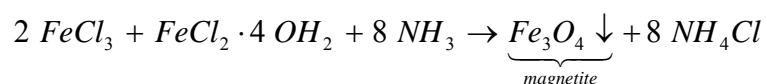
Remaining salts were removed by several washing steps with deionised water and decantation over a permanent magnet.

4.3.1.4 Magnetite activation or coating

For better incorporation of magnetite into the gel matrix of immobilisates, superparamagnetic magnetite was activated by ammonium oleate. First, a magnetfluid was produced by dropwise addition of 32 mL of oleic acid to the precipitated magnetite suspension (see paragraph 4.3.1.3). Afterwards, salts were also washed out by several washing steps with deionised water. Surplus water was removed by repeated decantation over a permanent magnet. Ammonium oleate was formed by adding 33 µL of ammonia per g of magnetfluid [145].

A second assayed modification of magnetite consisted in coating with aminosilane. 60 g of humid superparamagnetic magnetite were resuspended by ultrasonication in 500 mL of Milli-Q water and transferred to a slender 2 L reactor with baffles. After addition of 1.5 L of ethanol, 2 mL of tetramethylammonium hydroxide were supplemented as stabiliser and the solution heated to 50°C under a nitrogen flow and agitation by an overhead stirrer (2 x 4-blade impellers) at 1000 rpm. The pH value was adjusted with perchloric acid to pH 5, which was repeated regularly during the coating process. In a first reaction step, 28 mL of tetraethylorthosilicate (TEOS) were added dropwise by syringes equipped with cannulas of 0.4 mm diameter over a period of two hours. Evaporated ethanol was replaced during reaction. After two hours reaction time 28 mL of 3-(triethoxysilyl)-propylamine (APTES) were added in portions of 4 mL every 5 min and the magnetite was stirred for further two hours. Afterwards, the aminosilanised magnetite was washed several times with Milli-Q water over a permanent magnet. The reactor was rinsed with 25% hydrochloric acid after each magnetite

preparation. Both types of magnetite modifications result in amino groups on the particle surface and the magnetite was used humid in further immobilisation processes. Thus, solids contents were determined prior to immobilisation and parent sodium alginate concentrations were modified according to the measured solids content.

4.3.1.5 Bead production and bacterial entrapment

Two different methods were used for bead production, partly depending on the gelification mechanism. If rhamnolipid production was studied in shake flasks, resuspended biomass of *P. aeruginosa* fermentation was supplemented to the polymer solution. All other characterisation tests of immobilisates were made without bacteria.

4.3.1.5.1 Extrusion by JetCutting® technology

With the so-called Jet-Cutting® process from geniaLab (Braunschweig, Germany) [132], gel beads were produced by extrusion of the initial polymer mixture with high pressure through a nozzle (see paragraph 3.4.2.2). Beneath the nozzle a rotating cutting tool cleft the fluid jet into cylindrical segments, which formed spheres due to the surface tension. These polymer drops were collected in a stirred cross-linking solution and hardened out. This method has only been employed for alginate immobilisates.

In practice, a sodium alginate solution in 10 mM MOPS buffer pH 6.5 was mixed with magnetite and resuspended biomass (with 10 mM MOPS buffer pH 6.5) for cell immobilisates, yielding final concentrations of 3% (w/w) sodium alginate, 5% (w/w) magnetite and 15.8% (w/w) humid biomass (corresponds to about 3% cdw). This suspension was filled into the sterilised pressure vessel of the JetCutter® and beads were produced with the following settings: 230 µm nozzle, 4 bar pressure, 8000 rpm of cutting tool and 20% nozzle inclination. The generated beads were collected in a bowl filled with 2 L of a 0.1 M calcium chloride solution, which was agitated by a 4-blade overhead stirrer. After 30 min of hardening the cross-linking solution was removed by decantation over a magnet and the immobilisates were washed several times with sterile MOPS buffer. Parts of the JetCutter® which can not be autoclaved at 121°C, had been sterilised in a bath of 3% Mucasol® solution or with Bacillol® beforehand. After each immobilisation charge, the JetCutter® was flushed with hot deionised water and 2% (w/v) sodium citrate solution to avoid clogging of the inline filter and the nozzle.

4.3.1.5.2 Suspension polymerisation

The second process for alginate bead production consisted in suspension polymerisation by internal gelation modified from Poncelet et *al.* [131] (see paragraph 3.4.2.1).

Sodium alginate in 10 mM MOPS buffer pH 7.8 was mixed with magnetite, calcium carbonate and optional resuspended bacteria to yield final concentrations of 3% (w/w)

sodium alginate, 5% (w/w) magnetite, 1% (w/w) $CaCO_3$ and 15.8% (w/w) humid biomass. 100 g of homogeneous suspension were pressed by means of a pressure vessel or 50 mL syringes into 300 mL of vegetable oil, stirred at 500 rpm with a 4-blade stirrer in a 1 L glass beaker with baffles. After dispersion of the polymer solution, gelification was started through addition of 0.5 mL of acetic acid which liberates calcium ions from $CaCO_3$. One minute later about 100 mL of 0.05 M $CaCl_2$ solution were poured carefully into the reaction beaker and curing of the gel beads continued for 30 min. To achieve a more homogeneous mixing, stirrer height was adapted to the new filling level. Thereafter, the stirrer was stopped and phase separation awaited. As magnetic immobilisates accumulated in the lower aqueous phase, the oil phase could be decanted and beads were washed several times with 0.5% (w/v) Tween 20 aqueous solution and 10 mM MOPS buffer pH 6.5 to get rid of remaining oil droplets. During washing steps, the immobilisates were also retained in the reaction beaker by means of a permanent magnet.

For production of polyurethane foam beads by suspension polymerisation, cold PU-prepolymer was mixed with Bayoxide® magnetite (final concentration in beads of 5%) in a 50 mL syringe under a hood. Then, cold (4°C) 10 mM MOPS buffer pH 6.5 or resuspended biomass was added at a ratio of 1:2 and quickly homogenised with an overhead stirrer. 100 mL of suspension were pressed into 300 mL of stirred vegetable oil (500 rpm) and dispersed into small droplets. As polymerisation reaction of PU-prepolymer starts immediately after addition of water, the mixture had to be handled quickly. After 30 min of reaction time, about 100 mL of 10 mM MOPS buffer pH 6.5 was added, mixed and then the stirrer stopped to allow phase separation. Washing steps were performed as for alginate beads.

A third type of immobilisates was produced as a mixture of polyurethane and alginate beads to benefit from positive features of both materials. Therefore, a cold suspension of sodium alginate in 10 mM MOPS buffer pH 7.8, calcium carbonate and if necessary biomass was added to the cold mixture of PU-prepolymer and magnetite at the ratio of 1:2 instead of buffer to yield a final concentration of 0.6% (w/w) alginate and 1% (w/w) $CaCO_3$. Afterwards, the polymer suspension was treated equally to alginate bead production.

4.3.2 Analytical methods

4.3.2.1 Particle characterisation

Magnetite particles and immobilisates were characterised with respect to several parameters in order to compare different magnetite types, activations or coatings as well as different immobilisation methods and materials. For magnetite particles only zeta potentials and magnetisation saturations have been determined.

4.3.2.1.1 Zeta potential

Zeta potentials of magnetite particles give an idea about the nature of interactions of rhamnolipids [122] or maybe other substrates with embedded magnetite. They were measured for magnetite particles in a Zetasizer (Zetasizer 5000, Malvern Instruments, Herrenberg, Germany) over a pH range from pH 9 to 3 by titration of 0.05 M HCl. Measurements were made in triplicate in intervals of 0.25 pH units.

4.3.2.1.2 Magnetisation

Magnetisation was measured by an alternating-gradient magnetometer (MicroMag 2900, Princeton Measurements, USA). In this case, the sample is magnetised by a static magnetic field and at the same time overlaid by an alternating magnetic field. The resulting field gradient is proportional to the magnetic moment of the sample and can be measured due to deflexion of a piezoelectric element from which the sample is suspended. Magnetite or whole immobilisates were first dried in a freeze drier (BETA 1-8K, Christ, Osterode am Harz, Germany) and then a defined amount of particles was incorporated in a 100 µm glass capillary tube, which has been closed on both ends. The capillary tube was horizontally fixed on a specimen holder with silicon grease and the holder attached to the piezoelectric element before being symmetrically adjusted in the magnetic field. Measurements were performed as hysteresis curves beginning at the highest positive field strength ($8 \cdot 10^5$ A·m^{-1}). To calculate saturation magnetisations of humid immobilisates, their solids content was determined by weighing of immobilisates before and after freeze drying during sample preparation.

4.3.2.1.3 ESEM micrographs of immobilisates

Despite the utilisation of an environmental SEM, immobilisates samples were dehydrated before examination under the microscope. First, immobilisates were charged into 2 mL Eppendorf tubes and the bacteria fixed with 4% glutaraldehyde in 10 mM MOPS buffer pH 6.5 for 24 h. Then, the liquid was decanted over a permanent magnet and the beads washed several times by resuspension in 10 mM MOPS buffer pH 6.5 for 20 min respectively. Subsequent dehydration was achieved by an ascending series of acetone solutions from 20% (v/v) to 100% (v/v) in deionised water. Immobilisates suspended in pure acetone were finally fixed with adhesive tape on the sample carriers and examined under the ESEM (Phillips, Hamburg, Germany).

4.3.2.1.4 Particle size distribution

Particle size distributions of the immobilisates were determined by the particles sizer CIS 100 (Galai, Israel) in a measurement range from 10 to 2000 µm. The measurement principle is

based on the particle size dependent shading of a laser beam (660 nm). Samples were prepared by adding a layer of about 4 mm of immobilisates into a 3 mL cuvette filled with deionised water, which was pipetted up and down during measurements to prevent settling of the immobilisates.

4.3.2.1.5 Bead compression

Stability of immobilisates was tested by compression of a single spherical bead between two plates of a rheometer (Physica MCR 301, Anton Paar, Ostfildern, Germany). An immobilisate of approximately 1.5 mm diameter was placed on the compression table below a movable stamp and excessive water dapped off. Afterwards, the immobilisate was compressed at a constant speed of 600 µm·s^{-1} until a gap of 100 µm and the applied normal force recorded as a function of gap width. Three to five replications of each immobilisates type were made. Immobilisates from rhamnolipid production tests were always measured before and after cultivation. For comparison of different immobilisates, normal forces were related to the active cross-section of the bead by converting them into the so-called 'true' yield stress σ_t, which considers also the change of active cross-section during compression due to lateral displacement of the gel bead. σ_t was plotted as a function of deformation degree φ (see Eq. 5-4 and Eq. 5-5).

$$\sigma_t = \frac{F \cdot h}{A_0 \cdot h_0} = \frac{F}{\frac{\pi}{4} \cdot d_0^2} \cdot \left(1 - \frac{|\Delta h|}{h_0}\right) \; [N \cdot mm^{-2}]$$

Eq. 4-1

$$\varphi = \ln \frac{h_0}{h} = \ln \frac{1}{1 - \frac{|\Delta h|}{h_0}} \; [-]$$

Eq. 4-2

4.3.2.1.6 Shearing strain tests

Shearing strain experiments were accomplished in glass beakers equipped with three baffles under defined stirring conditions and a determinated experimental setup (see Fig. 3-19). These specifications permitted calculations of power density ε based on literature [176] and scale-up under equal shearing conditions ($\varepsilon = \frac{P}{\rho \cdot V} = idem$), as shearing rates $\dot{\gamma}$ are proportional to volumetric power input. In turbulent flows (Re >10^4 and >50 with baffles respectively) power input is calculated according to Eq. 4-3.

$$P = Ne \cdot \rho \cdot n^3 \cdot d_{stirrer}^5 \; [W]$$

Eq. 4-3

The Newton number equalled 9.8 for stirring speeds above 500 rpm under the defined conditions as presented in paragraph 3.4.3.1. With these values and an estimated medium

density of about 1000 kg·m^{-3} ε was calculated to 2.3 W·kg^{-1} for the shearing strain experiments.

In practice, 60 g of immobilisates without bacteria (produced by suspension polymerisation) were charged into the beaker and the medium level filled up to 100 mm height with the following media: (a) 10 mM MOPS buffer pH 6.5, (b) 10 mM MOPS buffer pH 4 and (c) mineral salt medium S1 (see paragraph 4.3.1.1.2). Different suspension media were chosen to study the influence of chemical agents or pH conditions on etching or dissolution of immobilisates under strain conditions. Particle suspensions were stirred at 500 rpm for one week. Samples withdrawn once a day and the optical density measured twice at 600 nm in a photospectrometer (UV-VIS-spectral-photometer G1103A, Agilent, Böblingen, Germany). Each type of immobilisates was tested twice in shearing stain experiments. The optical density of the different magnetite particles, which leaked out of the immobilisates, was calibrated with defined magnetite suspensions in Milli-Q water.

4.3.2.1.7 Rhamnolipid diffusion and adsorption in immobilisates

Adsorption and diffusion tests of rhamnolipids were realised in 500 mL shake flasks equipped with baffles for cell free immobilisates with different types of magnetite. Immobilisates were produced by suspension polymerisation. For these test series, a rhamnolipid mixture JBR 425 from Genail (Baiersdorf, Germany) had been partially purified over XAD-16 resins according to Reiling et al. [136]. Afterwards, the methanol had been evaporated and the remaining aqueous solution freeze-dried to yield a rhamnolipid powder.

10 g of immobilisates were charged into a shake flask with 100 mL of 10 mM MOPS buffer pH 6.5 supplemented by 2 g·L^{-1} of the partially purified rhamnolipid (corresponding to about 0.5 g·L^{-1} Rha-C$_{10}$-C$_{10}$ and 0.6 g·L^{-1} Rha-Rha-C$_{10}$-C$_{10}$). 500 µL of sample were taken immediately to determine the initial rhamnolipid concentration. Shake flasks were subsequently incubated at 37°C and 194 rpm for 24 hours on an orbital shaker. Then, a second sample was taken and the adsorbed rhamnolipid amount calculated as the concentration difference of the two samples.

For diffusion coefficient determination, immobilisates were filtrated over a membrane filter (6 µm pore diameter), flushed quickly with water and transferred into 100 mL of rhamnolipid free 10 mM MOPS buffer pH 6.5. Samples were taken after 0, 0.5, 1, 1.5, 2, 3, 4, 5, 10, 15 and 20 min. Rhamnolipid concentrations were measured by HPLC-MS analysis after direct dilution with a 50:50 solvent mixture of acetonitrile (ACN, Merck) and 10 mM ammonium acetate buffer (NH$_4$OAc, Sigma) to the calibration range.

Effective diffusion coefficients are defined for this experimental setup by Eq. 4-4 based on Fick's law. In practice, this equation can be simplified for higher effusion times to Eq. 4-5, which has been used for calculations in this work.

$$\frac{c_t - c_\infty}{c_0 - c_\infty} = \frac{6}{\pi^2} \sum_{n=1}^{\infty} \frac{1}{n^2} \exp\left(-\frac{\pi^2 \cdot n^2 \cdot D_{eff} \cdot t}{r^2} \right)$$

Eq. 4-4

$$\ln\left(\frac{c_t - c_\infty}{c_0 - c_\infty} \right) \approx -\frac{\pi^2 \cdot D_{eff} \cdot t}{r^2} + const.$$

Eq. 4-5

4.3.2.2 Growth determination

For growth determination different parameters were measured during cultivation such as optical density (OD), viable cell counts on agar plates, cell dry weight (cdw), CTC/DAPI-staining and process parameters such as pO_2 or dosage of acid.

4.3.2.2.1 Optical density

Optical density of culture broth was measured as absorbance at 600 nm compared to pure medium (UV-VIS-spectral-photometer G1103A, Agilent, Böblingen, Germany). Samples were diluted if absorbance was above 0.8. This procedure was only applied during biomass fermentation.

4.3.2.2.2 Viable cell counts

Concentrations of viable bacteria were determined through appropriate dilution of samples with phosphate buffered saline (PBS) pH 6.5 and spreading of 100 µL of 2-3 different sample dilutions on LB agar plates in triplicate with a Drigalski spatula. The agar plates were incubated at 30°C for 24 hours and the grown colonies counted.

For determination of viable cell concentrations in alginate immobilisates, immobilisates were filtered and washed with sterile PBS pH 6.5. About 0.1 g of immobilisates were then dissolved in 1 mL of 2% sodium tri-polyphosphate solution during 10 min on a vortex mixer and treated thereupon as mentioned above

4.3.2.2.3 Cell dry weight

During biomass fermentation, 40 mL of culture broth were pipetted into a weighed 50 mL centrifuge tube and centrifuged at 4°C and 10000 rpm for 15 min (Centrifuge Hermle ZK 401, Eppendorf, Hamburg, Germany). The supernatant was discarded and the pellet dried for 24 hours at 100°C. Before weighing, the centrifuge tubes were cooled down to room temperature in an exsiccator. The cdw ($g \cdot L^{-1}$) was calculated as the weight difference divided by 40 mL.

4.3.2.2.4 CTC/DAPI-staining

The distribution of viable and dead bacteria inside the immobilisates was visualised through staining with 5-cyano-2,3-ditolyltetrazoliumchloride (CTC) for metabolising bacteria and binding of 4',6-diamidino-2-phenylindoledihydrochloride-dilactate (DAPI) on DNA of all bacteria. CTC is incorporated into cells during cell respiration by transformation into the fluorescent CTF form. To 1 mL of culture medium with immobilisates were added 300 µL of 4 mM CTC solution (Polyscience, Eppelheim, Germany) and incubated for at least three hours at 37°C and 194 rpm in the dark. Thereafter, immobilisates were filtered over a 0.2 µm membrane and washed several times with PBS pH 6.5. By incubation with 1 mL of 4.4 µg·mL^{-1} DAPI solution (Polyscience) for 5 min in the dark, immobilisates were counterstained. Then, immobilisates were again washed with PBS and the filter transferred on a microscope slide. Under the microscope (Axioplan 2 imaging, Zeiss, Oberkochen, Germany), CTC-staining is visible at 450 nm in red colour and DAPI-staining at 364 nm in intensive blue.

4.3.2.3 Rhamnolipid quantification

4.3.2.3.1 Extraction

Before rhamnolipid quantification, rhamnolipids had first to be extracted from aqueous production medium. To 500 µL of sample 10 µL 1 M HCl and 500 µL ethyl acetate (Merck) were added, mixed on a vortex and centrifuged at 13000 rpm for 30 s to achieve phase separation. The upper ethyl acetate phase was transferred into a separate Eppendorf tube. After a second extraction step with ethyl acetate, the ethyl acetate phases were combined and used for further rhamnolipid analysis.

4.3.2.3.2 TLC

Normal thin layer chromatography (TLC) was used for fast qualitative rhamnolipid determination. 6 µL of extracted samples were applied with a 2 µL glass capillary to 0.2 mm silica gel plates (silica gel F254, 20 x 10 cm, Merck) and separated by a solvent mixture of chloroform / methanol / water (65:15:2, v/v/v). Visualisation of the separated compound spots was realised by dipping the TLC plates into cer-ammonium-molybdenumacid solution and developing the colours at 110°C for 10 minutes. Rhamnolipids appear in green and fatty acids as well as oil in brown colouration.

4.3.2.3.3 HPLC

Quantitative rhamnolipid concentrations were determined by reversed-phase HPLC coupled with MS. First, ethyl acetate of extracted samples was evaporated and the rhamnolipid pellet resuspended in an equal volume of a 50:50 solvent mixture of acetonitrile (ACN, Merck) and

10 mM ammonium acetate buffer (NH$_4$OAc, Sigma) (further referred to as L14). Samples were diluted (generally 1:2000 in total) to a concentration of the calibration range. Chromatographic separation was carried out by an Agilent HPLC-system using a LiChrospher RP18 column (5 µm, 125 x 3 mm, Merck) with a gradient of the mobile phase from 30% - 70% ACN in 10 mM NH$_4$OAc during 16 min and isocratic conditions of 70% ACN for 3 min by a flow rate of 0.4 mL$\cdot$min^{-1}. Thereafter, the column was equilibrated for 15 min at 30% ACN. A sample of 20 µL was injected by an autosampler including a needle-wash and the eluted rhamnolipids were monitored by an API 4000 tandem-mass spectrometer (Applied Biosystems). Analytes were ionised by electrospray ionisation in a turbo ion spray interface by -4500 V in negative mode and a temperature of 400°C. Detection of the rhamnolipids (Rha-C$_{10}$-C$_{10}$ and Rha-Rha-C$_{10}$-C$_{10}$) was performed in MRM-mode with the following specific pseudomolecular ions (PI) for Rha-C$_{10}$-C$_{10}$: m/z 503.3 → 59.0, 103.2, 169.1, 333.2 and Rha-Rha-C$_{10}$-C$_{10}$: m/z 649.3 → 142.9, 169.0, 204.9, 479.2 with retention times of 10 min and 12 min respectively. Rhamnolipid concentrations were calculated by the peak areas of PI m/z 503.3 → 169.1 and m/z 649.3 → 479.2 based on a calibration curve of pure rhamnolipids with a concentration range of 0.01 µg$\cdot$mL^{-1} to 2 µg$\cdot$mL^{-1} in L14. Maximum standard deviations for rhamnolipid concentration measurements of 9% have been observed.

4.3.2.4 Substrate analysis

Glycerol and nitrate were analysed during biomass cultivation in the supernatant of the culture broth. Medium samples were therefore centrifuged at 13000 rpm and 4°C for 5 min (Centrifuge 5415 R, Eppendorf) and the supernatant stored at -20°C until substrate analysis.

4.3.2.4.1 Glycerol

Glycerol concentrations in culture broth were determined by an UV-diagnostic test from r-biopharm (Darmstadt, Germany). Quantification is based on the amount of consumed NADH during the enzymatic conversion of glycerol with a set of enzymes.

4.3.2.4.2 Nitrate

Nitrate analysis was effected by ion exchange chromatography (DX-500, Dionex, Idstein, Germany) on an ION PAC AS 11 column (4 x 250 mm, Dionex). Samples were diluted 1:100 and filtered over 0.45 µm filters beforehand. After injection of a 10 µL sample, nitrate ions were eluted with a gradient of 8 to 30 mM NaOH by a flow rate of 1 mL$\cdot$min^{-1} and a runtime of 13 min. Ions were detected by conductivity measurements at 35°C and a suppressor current of 100 mA and quantified in a calibration range of 2.5 - 25 mg$\cdot$L^{-1} nitrate by peak areas at a retention time of 3.4 min.

4.4 Results and discussion

4.4.1 Choice of an adequate entrapment process

For retention biocatalyst in the rhamnolipid production process, the production strain *P. aeruginosa* DSM 2874 has to be safely entrapped in a magnetic polymer matrix. Principally, two different immobilisation processes were suited for bead production: extrusion by the JetCutting® technology and suspension polymerisation. Concerning the extrusion process, it was only used for alginate bead generation by so-called external gelation in calcium chloride solution, yielding immobilisates with a less dense polymer structure in the bead core [14]. Bead sizes were limited through the nozzle size and the rotational speed of the JetCutting® tool beneath the nozzle. Additionally, the supplementation of magnetite to the initial polymer solution quickly plugged up inline filters of the JetCutter® system even if the particle size of the magnetite (e.g. ~10 nm for superparamagnetic magnetite) was largely inferior to the mesh size of the filters. This was mainly due to agglomeration of particles in the polymer solution and could partly be prevented by suitable activation or coating of superparamagnetic magnetite as it is discussed in paragraph 4.4.2. Advantages of the extrusion process by JetCutting® were the generation of large bead quantities in a short time with small particle size distribution and little waste, as it was necessary for rhamnolipid production in stirred bioreactors (see chapter 5). However, especially by processing of pathogenic strains such as *P. aeruginosa* certain security measures were necessary due to the generation of aerosols during JetCutting®.

In contrast, this problem did not occur during bead production by suspension polymerisation. Moreover, magnetite particles were easily entrapped and did not hamper the polymerisation process. Suspension polymerisation in vegetable oil was applicable for alginate and polyurethane. Concerning alginate, calcium ions were provided by acidification of supplemented $CaCO_3$ directly in the polymer solution, leading to very homogeneous hydrogel bead structures. Particle loadings of the suspension medium of more than 50% of the vegetable oil volume were possible.

For the case of polyurethane, which was produced on the basis of a MDI prepolymer, reaction already started at room-temperature, necessitating cold materials and quick handling for a rather homogeneous droplet dispersion in stirred vegetable oil. Additionally, PU beads tended to agglomerate during production, which can be reduced by addition of a surfactant (e.g. Tween 20) to the oil. Particle size distributions of the suspension polymerisation process were more difficult to handle in a small range and necessitated a homogeneous power input during dispersion. As small immobilisates were desired for low diffusion limitations, suspension polymerisation was more suited as bead production process, influencing median particle sizes by adjustment of stirrer speed (Fig. 4-5). Easy separation of

the immobilisates from suspension medium was possible by addition of calcium chloride solution (alginate beads and mixed beads) or buffer (PU beads), yielding a phase separation with immobilisates accumulating in the aqueous phase. The vegetable oil can be decanted or pumped off; however, has to be disposed as waste. In regard to the easier handling and higher process security, the suspension polymerisation process was chosen for rhamnolipid production experiments.

4.4.2 Embedding of magnetite for magnetic separation

For continuous biosurfactant production with in situ product removal, an approach consists in embedding of magnetic particles such as magnetite (Fe_3O_4) in the matrix polymer and magnetic retention of the immobilisates in the bioreactor. For this purpose, magnetite particles have to be securely embedded in the matrix polymer with a magnetic saturation of the humid beads of minimum 2 to 3 $Am^2 \cdot kg^{-1}$. Different types of ferrimagnetic and superparamagnetic magnetite have been studied for entrapment.

magnetite	saturation magnetisation [$Am^2 \cdot kg^{-1}$]
Bayoxide® magnetite	88
MagPrep® Silica magnetite	88
superparamagnetic magnetite	84
aminosilanised magnetite	52
ammonium oleate magnetite	31
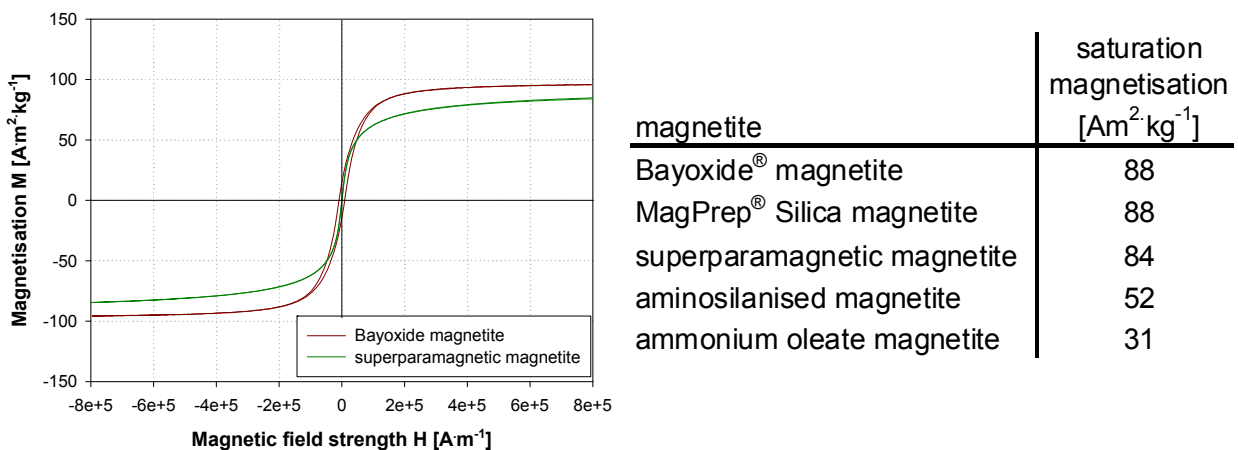
Fig. 4-1: Magnetisation curve of ferrimagnetic and superparamagnetic magnetite (left) and saturation magnetisation values of different magnetite types (right)

Due to the small size of superparamagnetic particles (~10 nm), these show no remaining magnetisation in the absence of an external magnetic field (see Fig. 4-1), facilitating therefore their removal from cyclic working magnetic separators after a separation cycle. In contrast, utilisation of ferrimagnetic particles needed in contrast further efforts to prevent plugging of magnetic filter chambers (see chapter 5). On the other hand, the small particle sizes of superparamagnetic magnetite made secure entrapment of the particles in alginate or PU beads more difficult. For bead generation by extrusion, especially these particles plugged up inline filters of the JetCutter® device by agglomeration. Thus, superparamagnetic magnetite was either activated with ammonium oleate groups on its surface or coated with aminosilane for better miscibility with hydrophilic sodium alginate or PU-prepolymer.

Tab. 4-1: Zeta potentials of magnetite particles measured at a pH of ~6.5

magnetite	pH value [-]	zeta potential [mV]
Bayoxide® magnetite	6.3	4.3
MagPrep® Silica magnetite	6.9	0.4
ammonium oleate magnetite	6.7	-27.8
basic aminosilanised magnetite	6.5	24.0
acidic aminosilanised magnetite	6.5	31.9
simple silanised magnetite	6.6	-18.2
simple aminosilanisied magnetite	6.3	27.0

Secondly, electrostatic interactions of the amino groups on the magnetite surface with the matrix polymer should reduce leakage of particles out of the immobilisates during biosurfactant production (see shearing strain tests). Zeta potential measurements of the magnetite particles show that ferrimagnetic magnetite with (MagPrep® Silica, Merck) and without silica coating (Bayoxide®, Lanxess) was almost neutral at a pH of 6.5, contrary to activated or coated superparamagnetic particles with highly positive or negative charges on the surface (see Tab. 4-1). As discussed for diffusion properties, these charges also influenced the diffusion of substrates or biosurfactants in the immobilisates and hence the production yield.
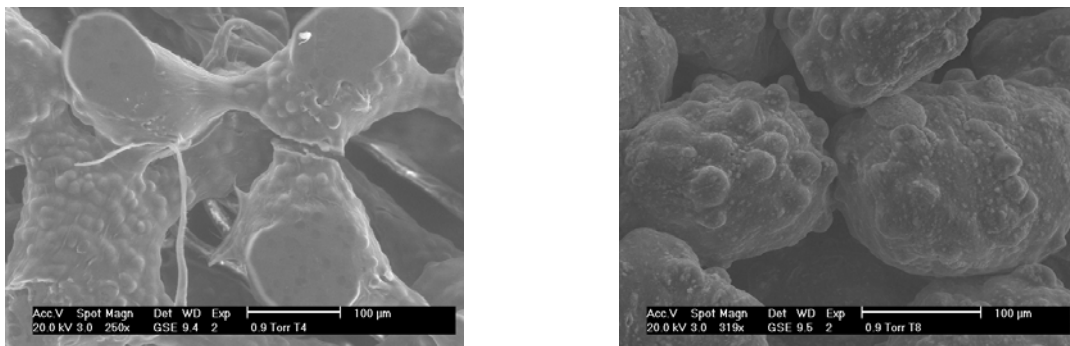
Fig. 4-2: ESEM micrographs of immobilisates of *P. aeruginosa* in pure alginate beads (left) and beads with embedded Bayoxide® magnetite (right) after RL production on vegetable oil

Concerning saturation magnetisations of the immobilisates, a final concentration of 5% (w/w) magnetite in the immobilisates turned out to be sufficient for bead separation in a high gradient magnetic separator. Saturation magnetisations of the humid beads were between 2.7 to 7.0 $Am^2 \cdot kg^{-1}$ and decreased for the case of Bayoxide® magnetite by 6% during 20 days of biosurfactant production. In the case of magnetite particles themselves, values ranged from ~31 $Am^2 \cdot kg^{-1}$ for ammonium oleate magnetite to ~88 $Am^2 \cdot kg^{-1}$ for Bayoxide® magnetite (see Fig. 4-1).

Finally, magnetite supplementation to hydrogel beads also influenced gel stability of immobilisates vis-à-vis chemical agents (e.g. fatty acids originating from vegetable oil

substrates) as demonstrated in Fig. 4-2 and also by compression tests (see paragraph 4.4.3.3).

4.4.3 Characterisation of immobilisates

To be able to compare immobilisation materials and processes in regard to stability, particle size distribution, diffusion properties, biocompatibility and their influence on rhamnolipid production, different parameters have been analysed. These are discussed in the following paragraphs.

4.4.3.1 Appearance and internal structure

First, immobilisates were compared according to their appearance and internal structure. In Fig. 4-3 are shown microscope pictures of immobilisates with different types of magnetite.
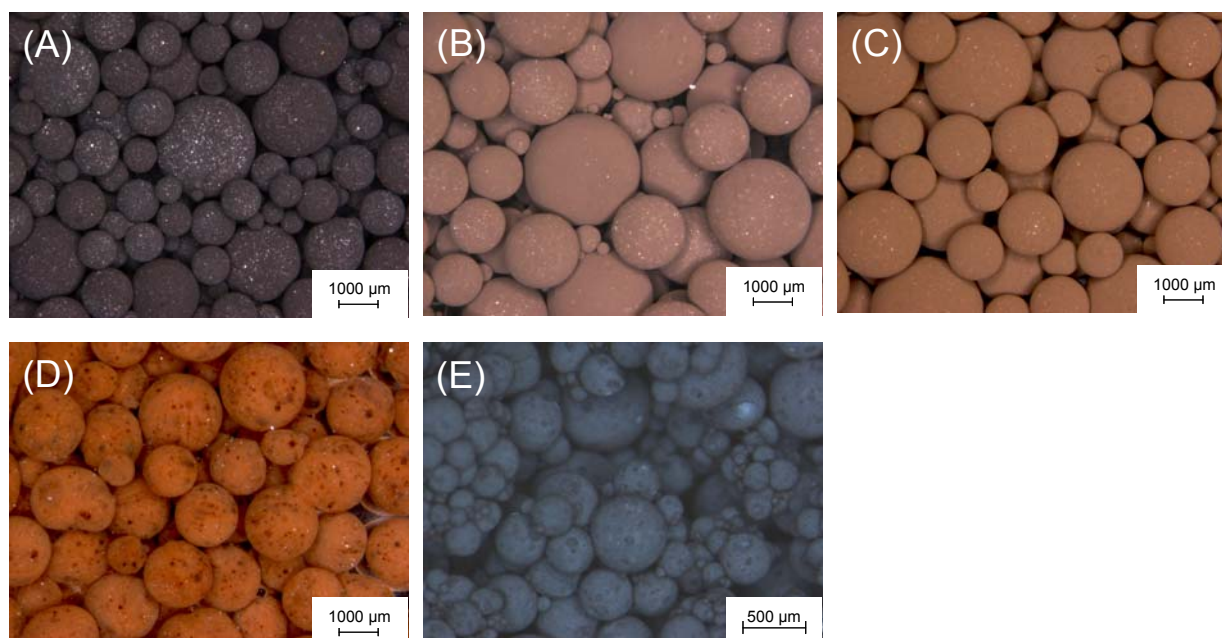
Fig. 4-3: Calcium alginate beads with different types of magnetite: (A) Bayoxide®, (B) silica coated magnetite (MagPrep® Silica, Merck), (C) aminosilanised magnetite, (D) ammonium oleate activated magnetite, (E) mixed polyurethane – alginate beads + Bayoxide® magnetite

Alginate beads with embedded Bayoxide® magnetite, silica coated magnetite and aminosilanised magnetite resulted in homogeneous beads, whereas superparamagnetic magnetite activated with ammonium oleate formed agglomerates (see spots on bead surface) and was not homogeneously dispersed in the matrix polymer. Concerning synthetic polyurethane principally uniform dispersions of magnetite particles in the beads were possible. However, as polyurethanes are foams, also larger pores were formed during the polymerisation process by CO_2 formation (see Fig. 4-4). The addition of small alginate concentrations to the initial polymer suspension and simultaneous hardening by calcium ions

was intended for pore size regulation of the immobilisates to prevent higher cell-leakage out of the immobilisates.
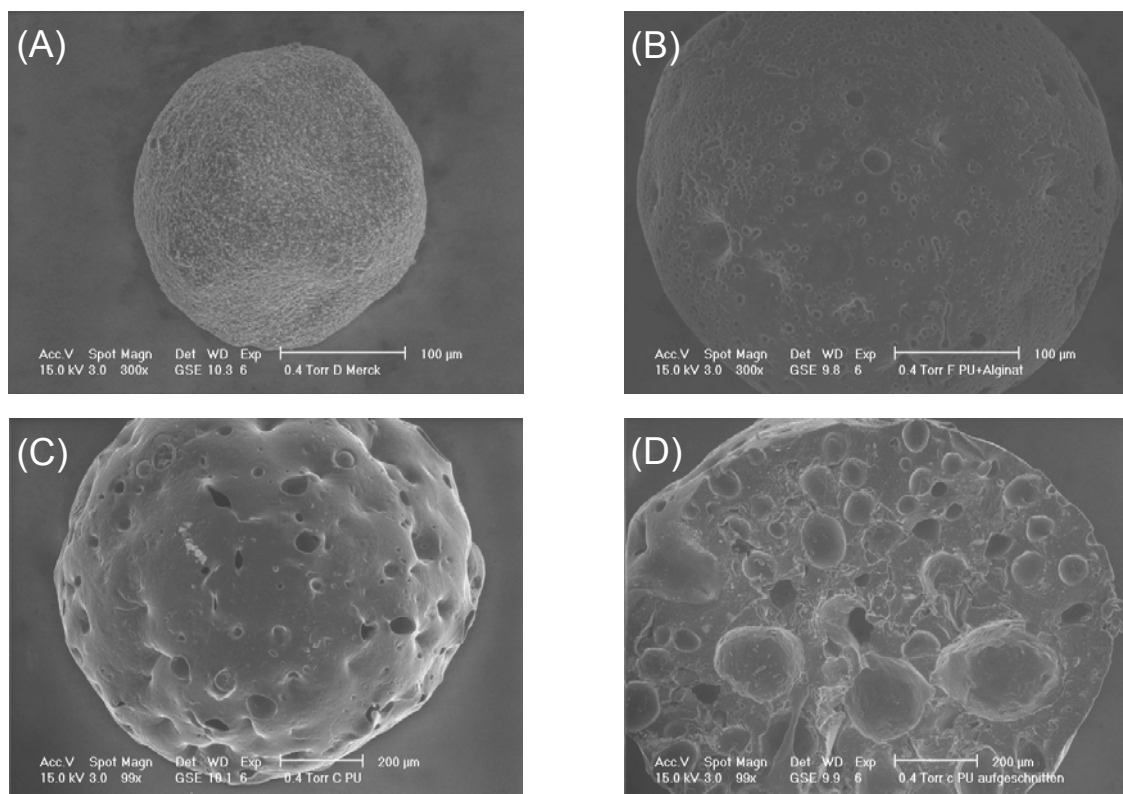
Fig. 4-4: ESEM micrographs of beads with embedded magnetite: (A) alginate, (B) PU + alginate, (C) PU, (D) sliced PU bead

These differences in pore size distribution were also visible in ESEM micrographs (see Fig. 4-4). Alginate beads with embedded magnetite possessed a very homogeneous bead surface (A) as well as uniform dispersion in the bead core (not shown). In contrast, ESEM micrographs of PU beads showed large pores on the surface (C) and even larger inside the beads (D). Pore sizes of mixed PU-alginate polymers were placed between those of the other matrix materials (B). Concerning magnetite embedding, PU beads seemed to integrate magnetite better inside the polymer as almost no magnetite particles were visible on the bead surface contrary to alginate beads. Additionally, PU beads only slightly reduced volume by dehydration during sample preparation due to their more rigid matrix structure.

4.4.3.2 Particle size distribution

Conversion rates of substrates in immobilisates highly depend on bead sizes, which influence concentrations of substrates and products in the beads through diffusion limitation. For determination of diffusion coefficients, the mean particle size related to the volume specific surface of the particles $\overline{x}_{AV}$, also called Sauter mean diameter, was used.
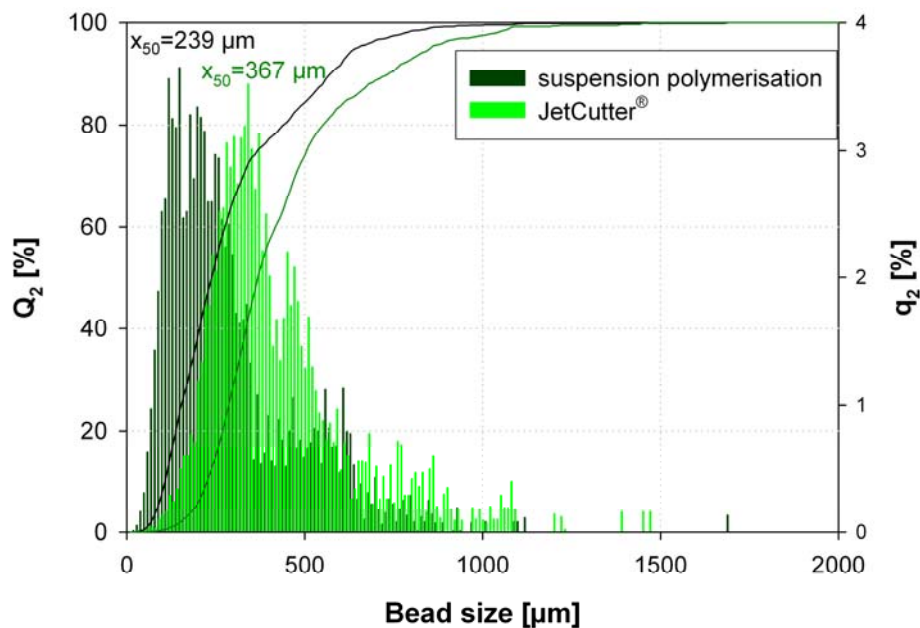
Fig. 4-5: Particle size distributions of immobilisates produced by the JetCutting® technology (3 bar, 230 μm nozzle, 8000 rpm) and suspension polymerisation (500 rpm)

In Fig. 4-5 particle size distributions of immobilisates produced by extrusion (JetCutter® device) and suspension polymerisation are comparatively presented for optimum immobilisation conditions. Due to plugging up of inline filters and nozzles with magnetite particles, smaller mean sizes (x_{50}) than about 370 μm could not be achieved without great efforts by droplet extrusion. In contrast, suspension polymerisation yielded larger and bimodal size distributions, which could yet be adjusted to smaller median bead sizes. Smaller size distributions of polymer beads produced by suspension polymerisation are principally possible through optimisation of reactor design, stirrer geometry and polymerisation conditions [6, 7, 15, 82, 83].

4.4.3.3 Gel stability

For gel stability determination two different tests have been performed. First, immobilisates were examined in a compression test between two plates to determine their relative rigidity in form of 'true' yield stresses as a function of deformation degree. These parameters also consider the change of active cross-section during compression due to lateral displacement of the gel beads. In Fig. 4-6 are depicted compression curves of different matrix materials at compression speeds of 600 μm·s^{-1}, which were necessary to prevent water lost during compression and yield thus stable Young's moduli [168].
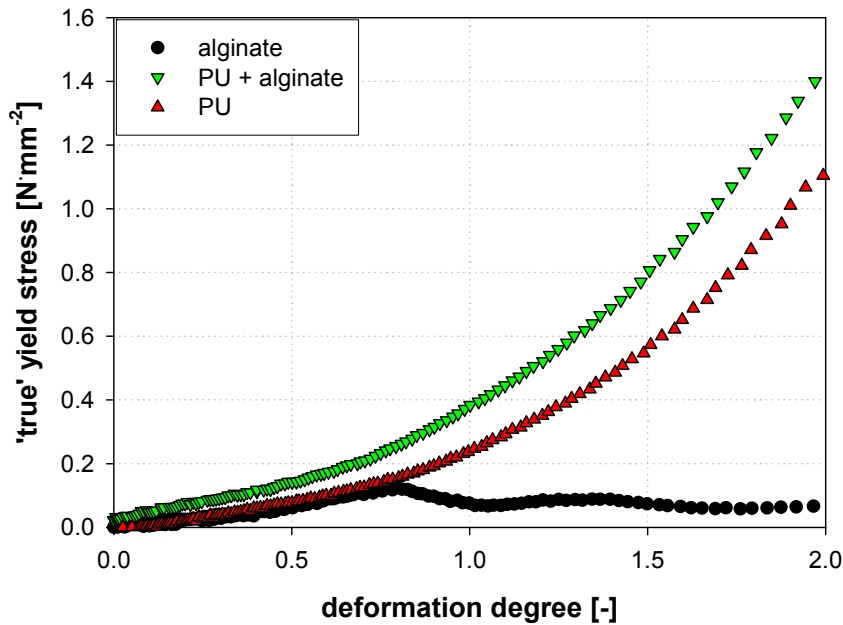
Fig. 4-6: Yield stresses as a function of deformation degree of beads with different matrix materials and embedded Bayoxide® magnetite obtained by compression tests at 600 µm·s⁻¹

Yield stresses increased with higher deformation degrees for all materials almost linearly until a deformation degree of about 0.5. Above this value yield stresses rose more strongly for PU beads or mixed PU-alginate beads, whereas they decreased and rested almost stable for alginate beads. This fact is due to the breaking of the alginate beads at a certain deformation degree (here ~0.7). PU beads and especially PU-Alginate beads not only supported much higher loads, but also regained their initial shape after stress relaxation. In contrast, alginate beads were much less elastic and remained flat after a certain deformation or even burst.

Tab. 4-2: Yield stresses σ_t at a deformation degree φ of 0.5 of different immobilisates determined by compression tests at 600 µm·s⁻¹

	alginate + Bayoxide® magnetite	alginate + silica magnetite	alginate + aminosilanised magnetite	alginate + ammonium oleate magnetite	PU + alginate + Bayoxide® magnetite	PU + Bayoxide® magnetite
σ_t mean [N·mm⁻²]	0.07	0.18	0.16	0.09	0.11	0.09
σ_t range [N·mm⁻²]	0.04 - 0.09	0.10 - 0.22	0.09 - 0.26	0.06 - 0.12	0.06 - 0.18	0.08 - 0.12

In practice, during rhamnolipid production in a stirred bioreactor only small bead deformation occurred. Therefore, immobilisates with different embedded magnetite were compared by yield stresses at a deformation degree of 0.5 (see Tab. 4-2). As yield stresses at this low deformation degree vary in a certain range, mean values have been calculated out of five measurements. Of the four magnetite types tested, MagPrep® Silica magnetite and aminosilanised magnetite revealed to result in the most rigid beads based on alginate polymer. This effect may be due to the silica coating of the magnetite. However, compared to

pure alginate beads, which did only achieve negative yield stresses at a deformation degree of 0.5, addition of magnetite always leaded to an increase of stability, as it has also been observed vis-à-vis chemical agents by ESEM micrographs (see paragraph 4.4.3.1). For small deformations, PU and PU-alginate beads did not reach much higher values than alginate beads, as deformations were mainly still in the elastic region of alginate polymer.

Apart from compression stability, immobilisates must also withstand shearing strains and influences of chemical agents, which may dissolve the matrix polymer (e.g. phosphates with alginate). Therefore, shearing strain tests of immobilisates with embedded magnetite were performed in glass beakers with different stirred media. The amount of leaked out magnetite was monitored as a function of incubation time (see Fig. 4-7).
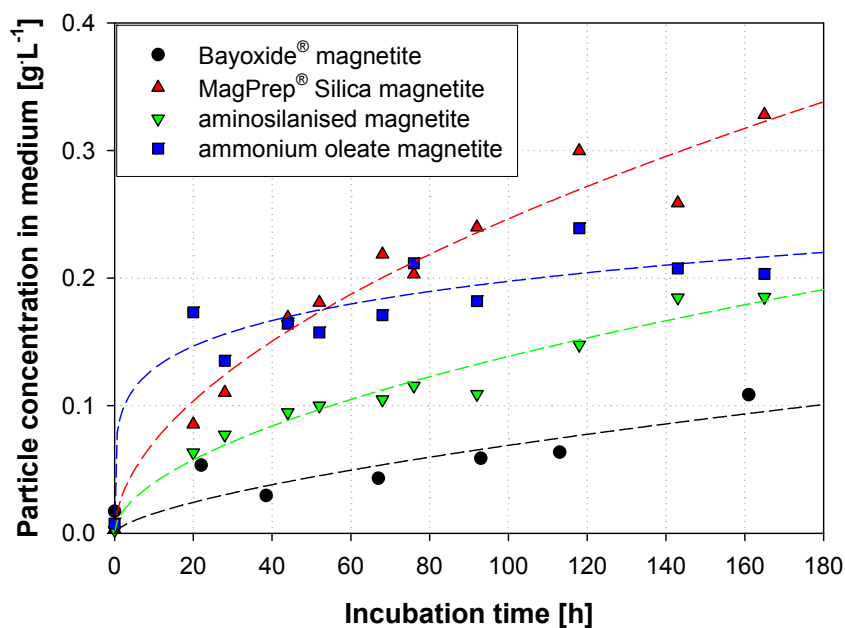
Fig. 4-7: Leakage of magnetite particles out of immobilisates during a shearing strain test in 10 mM MOPS buffer for seven days

During the whole monitoring time, magnetite concentrations increased in the suspension medium with higher magnetite leakage in the beginning of the test. Highest magnetite values in the medium were achieved for MagPrep® Silica particles, which have an almost neutral zeta potential at a pH of 6.5 and thus did not interact with the alginate polymer leading to a higher leakage. Contrary to the other magnetite types, ammonium oleate magnetite quickly diffused out of immobilisates especially in the presence of rhamnolipids (data not shown). It was the sole material, which was negatively charged at all studied pH values, which probably promoted quicker leakage of the magnetite particles. At a pH of 4, all other materials were positively charged, leading to lower magnetite leakage due to electrostatic interactions of the magnetite particles with the matrix polymer (see Tab. 4-3).

As the alginate gel of the beads still seemed absolutely intact after one week of incubation time for all studied pH values, magnetite leakage out of immobilisates was mainly influenced by their surface charge at the actual pH, with lowest leakage of positively charged particles.

Tab. 4-3: Concentration [g·L^{-1}] of magnetite particles leaked out of immobilisates after ~100 h of shearing strain test with different suspension media

suspension medium	Bayoxide$^®$ magnetite	MagPrep$^®$ Silica magnetite	aminosilanised magnetite	ammonium oleate magnetite
MOPS buffer pH 6.5	0.06	0.24	0.11	0.18
MOPS buffer pH 4	0.01	0.13	0.11	0.30
growth medium	0.15	0.25	n.d.	n.d.

The stability of immobilisates vis-à-vis low concentrations of chemical agents which are known to destabilise alginate gels by complexation or exchange of bound calcium ions (e.g. phosphate, citrate, sodium ions) [107] was estimated by a mineral salt medium, which was used for cell growth in immobilisates during rhamnolipid production. This growth medium contained at the same time higher concentrations of calcium chloride to stabilise the alginate gel. After an incubation time of 100 h, slightly higher magnetite concentrations were obtained in the suspension medium. However, the immobilisates still remained quite intact. Altogether, magnetite leakage out of alginate beads is generally higher than of mixed PU-alginate beads, which accumulate even in growth medium only 0.02 g·L^{-1} of Bayoxide$^®$ magnetite after 100 h.

4.4.3.4 Diffusion properties

Contrary to biosurfactant production with 'free' bacterial cells, diffusion limitations of substrates or products may reduce rhamnolipid yields with immobilised bacteria and diminish therefore efficiencies of rhamnolipid production. Principally, diffusion in gel beads is influenced on the one hand by pore sizes of the matrix polymer and on the other hand by physical interactions with the polymer or other embedded substances such as magnetite. For the case of substrates, mainly glycerol was used as carbon source, which should not interact with the matrix of the immobilisates and is also smaller than the produced rhamnolipids [156].

Tab. 4-4: Adsorption of RL in immobilisates after incubation in a rhamnolipid solution measured in µmol RL per g immobilisates for different immobilisates with embedded magnetite

immobilisates	Rha-C$_{10}$-C$_{10}$	Rha-Rha-C$_{10}$-C$_{10}$	mean bead size [µm]
alginate	1.2 ± 0.5	0.5 ± 0.3	630
alginate + Bayoxide$^®$ magnetite	1.5 ± 0.0	0.8 ± 0.1	670
alginate + MagPrep$^®$ Silica magnetite	1.1 ± 0.1	0.5 ± 0.1	730
alginate + aminosilanised magnetite	3.5 ± 1.0	1.9 ± 1.2	630
alginate + ammonium oleate magnetite	8.5 ± 0.1	6.0 ± 0.2	630
PU + alginate + Bayoxide$^®$ magnetite	1.5 ± 0.8	1.2 ± 0.6	300

Therefore, rhamnolipid adsorption of immobilisates and their effusion out of saturated gel beads was studied as the limiting factor for different types of embedded magnetite and different matrix polymers. In Tab. 4-4 are assorted the results of rhamnolipid adsorption in immobilisates after incubation over night in a 1.9 mM rhamnolipid solution. The mean particle sizes ($\overline{x}_{AV}$) of the alginate beads were quite similar for all magnetite types; however mixed PU-alginate beads had only about half the size of the alginate beads. The obtained bead saturations with rhamnolipids were in the same order of magnitude for pure alginate and alginate with embedded Bayoxide® / MagPrep® Silica magnetite with about twice the amount of the mono-rhamnolipid compared to the di-rhamnolipid, adsorbing preferentially the smaller Rha-C_{10}-C_{10} due to its smaller size and its more hydrophobic character. In contrast, aminosilanised magnetite and ammonium oleate activated magnetite, which were both charged at the present pH of 6.5, increased the adsorbed rhamnolipid amount by a factor of three to eight with larger quantities of adsorbed di-rhamnolipid. As these magnetite types were smaller in size than the ferrimagnetic magnetites, they also offered a higher surface for interactions with rhamnolipids. Additionally, ammonium oleate activated magnetite leaked increasingly into the suspension medium, supposing physical interactions between rhamnolipids and the magnetite particles. Comparison of rhamnolipid adsorption by mixed PU-alginate beads to alginate beads is difficult due to the different bead sizes and porosities, but bead saturation values might be higher than for alginate beads and also the rhamnolipid ratio of mono- to di-rhamnolipids was apparently altered to almost equal amounts of the two rhamnolipid species.
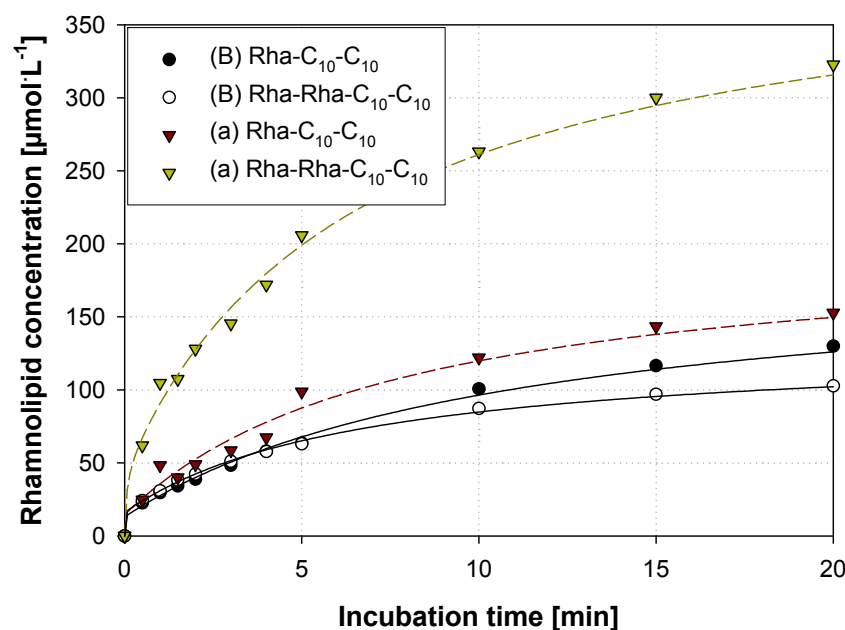
Fig. 4-8: Effusion of rhamnolipids out of alginate immobilisates with embedded magnetite: (B) Bayoxide® magnetite, (a) ammonium oleate activated magnetite

In a second step, diffusion of rhamnolipids in the immobilisates was monitored by effusion experiments. Comparably to rhamnolipid adsorption, immobilisates with embedded ammonium oleate activated magnetite also differed from the other magnetite types. As depicted in Fig. 4-8, rhamnolipid effusion from immobilisates with Bayoxide® magnetite was almost equal for both monitored rhamnolipid species and similar to alginate beads without magnetite. In contrast, rhamnolipid effusion profiles of beads with ammonium oleate activated magnetite reached much higher concentrations of Rha-Rha-C_{10}-C_{10} in the suspension medium in spite of its smaller amounts in the immobilisates. This may be explained by a better adsorption of the smaller Rha-C_{10}-C_{10} to the surface of embedded magnetite particles. At the present pH of 6.5 ammonium oleate magnetite as well as the rhamnolipids were negatively charged, maybe enforcing higher rhamnolipid effusion due to physical repulsion.

On the other hand, diffusion coefficients of rhamnolipids out of these immobilisates were also lower compared to the other embedded magnetite types (see Tab. 4-5).

Tab. 4-5: Diffusion coefficients [10^{-6} $cm^2 \cdot s^{-1}$] of rhamnolipids in different immobilisates with embedded magnetite measured by effusion tests

immobilisates	Rha-C_{10}-C_{10}	Rha-Rha-C_{10}-C_{10}
alginate	1.4 ± 0.3	1.6 ± 0.1
alginate + Bayoxide® magnetite	1.7 ± 0.3	1.7 ± 0.0
alginate + MagPrep® Silica magnetite	1.3 ± 0.2	1.3 ± 0.1
alginate + aminosilanised magnetite	1.5 ± 0.0	1.5 ± 0.1
alginate + ammonium oleate magnetite	1.0 ± 0.3	1.1 ± 0.0
PU + alginate + Bayoxide® magnetite	0.3 ± 0.0	0.3 ± 0.0

Best results have been obtained for alginate beads with Bayoxide® magnetite with slightly higher diffusion coefficients than for the other compositions. For all materials, diffusion coefficients for both rhamnolipid species were quite the same. Compared to values reported in literature for diffusion of smaller substances in alginate beads, the measured diffusion coefficients for rhamnolipids were in the same order of magnitude as for other molecules of similar size ($6.6 \cdot 10^{-6}$ $cm^2 \cdot s^{-1}$ for L-tryptophan, $1.0 \cdot 10^{-6}$ $cm^2 \cdot s^{-1}$ for α-lactoalbumin and $2.89 \cdot 10^{-6}$ $cm^2 \cdot s^{-1}$ for vitamin B12) [100, 156]. Contrary to alginate beads, diffusion of rhamnolipids in mixed PU-alginate polymer was considerably higher limited with diffusion coefficients of only $0.3 \cdot 10^{-6}$ $cm^2 \cdot s^{-1}$. This fact may also explain the lower rhamnolipid yields of shake flask experiments for rhamnolipid production as discussed in paragraph 4.4.3.5.

4.4.3.5 Rhamnolipid production

Aim of the immobilisation of the rhamnolipid production strain *P. aeruginosa* DSM 2874 was a continuous biosurfactant production process with retention of the immobilisates in the

bioreactor by magnetic separation. To determine the suitability of different immobilisation materials and magnetite types for application in a rhamnolipid production process, shake flask experiments were performed to determine rhamnolipid yields in comparison with the rhamnolipid production of free bacteria. In Fig. 4-9 is represented the specific rhamnolipid synthesis as a function of time for 'free' cells and immobilised cells in alginate beads with embedded aminosilanised magnetite.
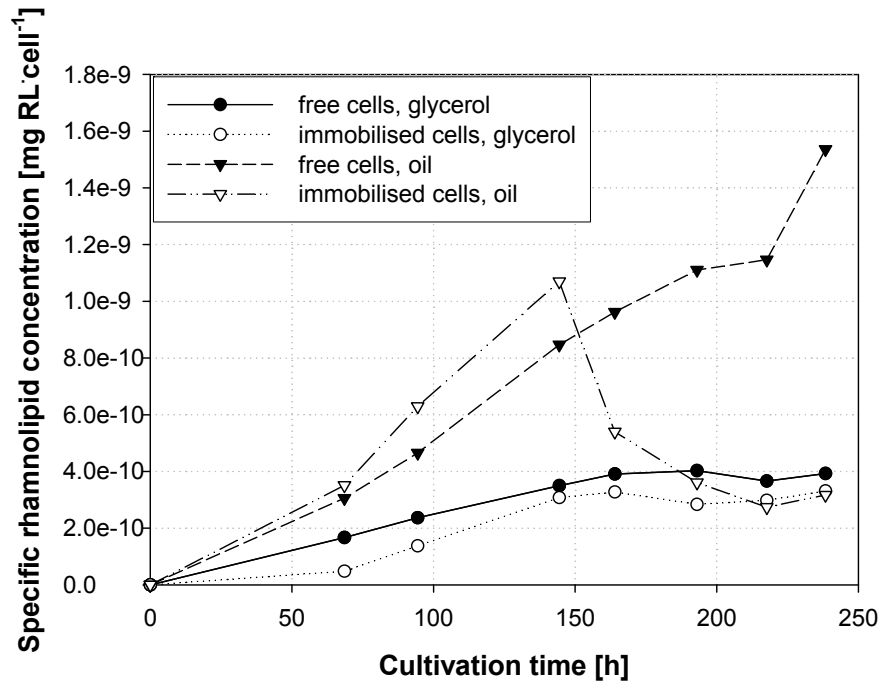
Fig. 4-9: Rhamnolipid production in shake flasks by free cells and immobilised bacteria in alginate beads with embedded aminosilanised magnetite and glycerol or vegetable sunflower oil as substrate

For 'free' cells rhamnolipid synthesis on the basis of vegetable oil was higher than on glycerol, which corresponds to results of other research groups [79, 102, 110, 149]. During the first 150 hours of cultivation this situation was the same for immobilised bacteria. However, rhamnolipid concentrations in the cultivation medium decreased after a certain cultivation time by utilisation of vegetable oil as carbon source, whereas no significant difference appeared in rhamnolipid synthesis for immobilised and free cells during cultivation with glycerol. At the same time, immobilisates have swollen in the cultivation medium with vegetable oil and the aminosilanised magnetite has changed from almost dark to a brown colour probably due to an interaction with the fatty acids, which accumulated by oil hydrolysis. As oil also destabilised the alginate matrix by formation of calcium soaps, whereas glycerol permitted almost equal rhamnolipid yields with free and immobilised bacteria and maintained stable immobilisates even over several production cycles, only glycerol was used as carbon source in the following experiments. Furthermore, previous shake flask cultivations revealed an optimal cell load of the immobilisates between 10 to 20%

to yield highest specific rhamnolipid yields (data not shown), which corresponds also to literature values [79, 111], therefore using a medium value of ~16% cell load in the following studies.

Fig. 4-10: Rhamnolipid production in shake flasks by immobilised bacteria in alginate (Alg) or PU beads with embedded magnetite (mag) and glycerol as substrate, medium exchange after 164 hours (vertical bar)

In a second shake flask experiment, different types of magnetite and matrix polymer have been compared with regard to their impact on rhamnolipid production (see Fig. 4-10). From the four different magnetite types utilised in alginate beads, MagPrep[®] Silica magnetite showed the highest rhamnolipid synthesis rates in the beginning and also highest final rhamnolipid concentrations after 164 hours of cultivation time. It was followed by Bayoxide[®] magnetite, for which rhamnolipid concentrations slightly decreased in the end of the first cultivation step. For all other magnetite types, a longer lag phase was observed for rhamnolipid production (data not shown for aminosilanised magnetite). Taking into consideration previous results of ammonium oleate and aminosilanised magnetite (e.g. diffusion properties), physical interactions of rhamnolipids and magnetite presumably led to reduced rhamnolipid concentrations in cultivation medium during the first hours.

For the case of different matrix polymers with embedded Bayoxide[®] magnetite, the lower diffusion coefficients of rhamnolipid in PU or mixed PU-alginate beads compared to alginate beads also became noticeable in lower rhamnolipid synthesis rates. While rhamnolipid yields after 164 hours cultivation time for PU immobilisates achieved the same order of magnitude as for alginate immobilisates, rhamnolipid production of the combination of the two materials stayed at a specific rhamnolipid concentration of 0.5 $g \cdot L^{-1} \cdot chw^{-1}$ in the cultivation medium. This material seemed to be too dense for adequate mass transfer inside the immobilisates. A

second reason may be a lower cell content in the immobilisates due to foaming of the material during the polymerisation process [86].

After 164 hours, the cultivation medium was exchanged with a new one to simulate a second production cycle, as rhamnolipid production decreased due to substrate consumption. Specific rhamnolipid yields during the second cultivation step were smaller due to cell-leakage out of immobilisates in the course of rhamnolipid production and reduced immobilisates amounts because of immobilisates sampling for analysis. However, a main difference to the first cultivation step was the relatively high rhamnolipid concentrations for alginate immobilisates with embedded ammonium oleate magnetite. This fact may be due to larger pore sizes and fewer interactions between rhamnolipids and magnetite in the immobilisates during the second production cycles, as ammonium oleate magnetite has highly leaked into the production medium in response to rhamnolipid formation.

4.4.3.6 Repeated production cycles and cell-leakage

During rhamnolipid production by *P. aeruginosa*, biosynthesis of rhamnolipids slowed down after a certain cultivation time due to lacking of some necessary mineral salts for cell maintenance and enzyme synthesis. In the case of an integrated bioprocess with continuous rhamnolipid removal by foam fractionation, the total bacterial concentrations decreased as a consequence of cell flotation with the foam.

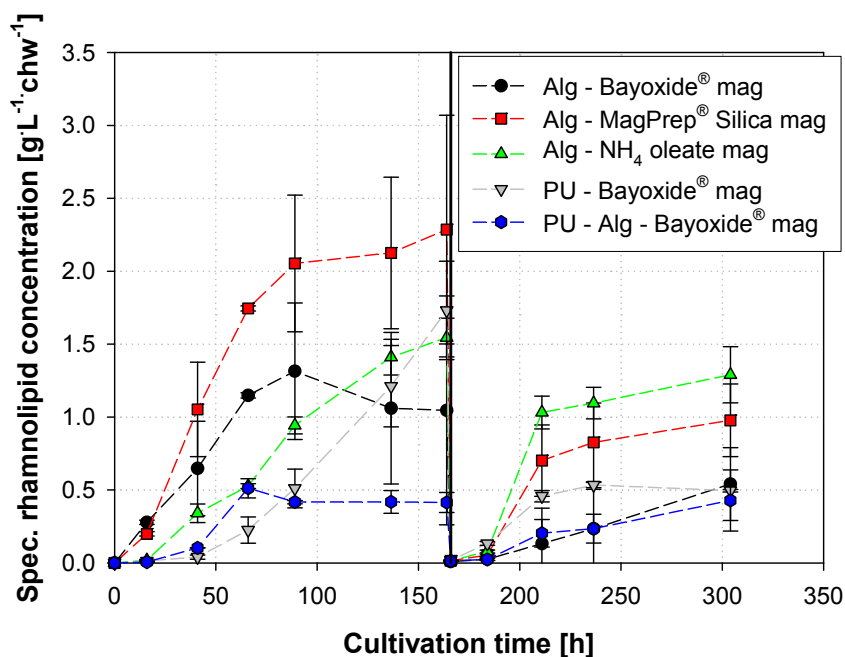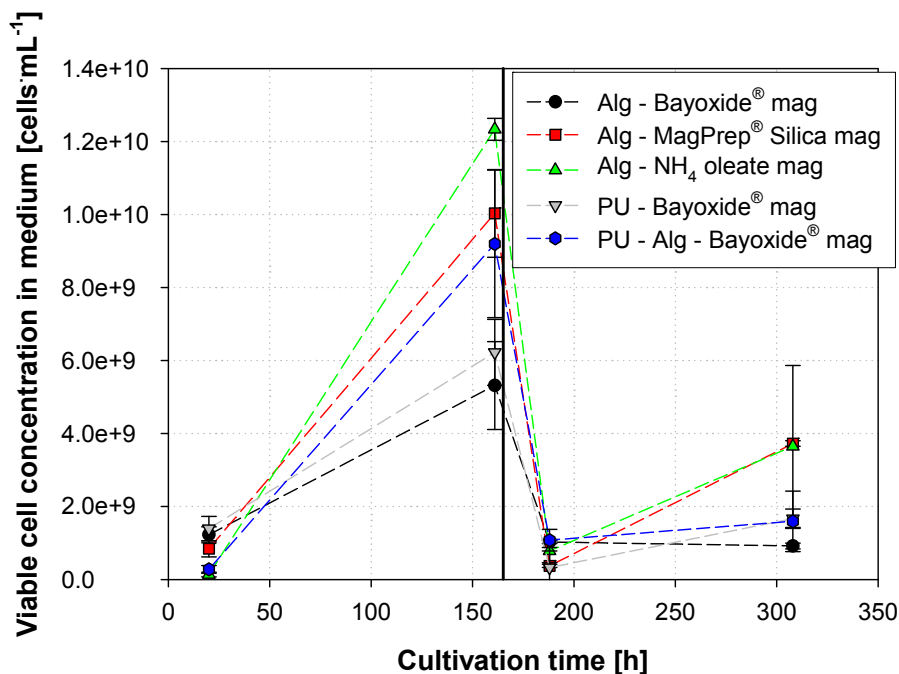**Fig. 4-11: Viable cell concentration developing in cultivation medium during rhamnolipid production in shake flasks by immobilised bacteria in alginate (Alg) or PU beads with embedded magnetite (mag) and glycerol as substrate, medium exchange after 164 hours (vertical bar)**

As depicted in Fig. 4-11 for the viable cell concentrations in the cultivation medium, bacteria leaked out of the immobilisates to a certain extent during rhamnolipid production. This effect was most pronounced during the first rhamnolipid production step due to initial cell growth and highest for immobilisates with embedded ammonium oleate magnetite and MagPrep® Silica magnetite. These materials already showed the highest magnetite leakage during shearing strain tests at pH 6.5 (see paragraph 4.4.3.3). All attempts (e.g. coating of alginate beads or other matrix materials) to prevent cell-leakage had not shown great improvements on cell-leakage (see results of PU and mixed PU-alginate beads). On the other hand supplementary coating or smaller pore sizes of immobilisates also reduced diffusion rates of rhamnolipids and therefore rhamnolipid yields in production medium as measured for PU polymer beads (see paragraphs 4.4.3.4 and 4.4.3.5). It was therefore necessary to introduce supplementary growth steps between several rhamnolipid production cycles.

The effect of cell-leakage on quasi continuous rhamnolipid production was simulated in shake flask experiments by exchange of cultivation medium after about seven to nine days of rhamnolipid production (see Fig. 4-12).
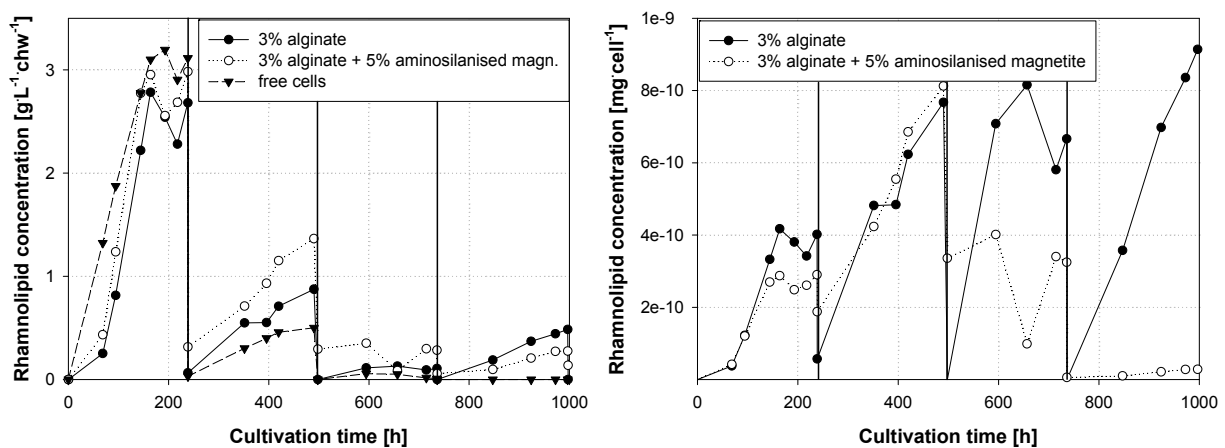
Fig. 4-12: Rhamnolipid production in shake flasks by free cells and immobilised bacteria in alginate and alginate + aminosilanised magnetite beads relating to cell humid weight immobilised in the beginning (left) and bacterial concentrations (right) with medium exchange (vertical bars) between several production cycles

If rhamnolipid concentrations in the cultivation medium were related to the initial cell humid weight in the immobilisates after cell immobilisation, rhamnolipid yields significantly decreased over several production cycles. However, if the specific rhamnolipid concentration is related to the viable cell concentrations in the immobilisates (see Fig. 4-12, right), rhamnolipid yields even increased after the first production cycle and maintained quite stable for bacteria immobilised in pure alginate beads. This signified that bacteria still produced the same quantities of rhamnolipids per cell. The decrease in rhamnolipid synthesis for immobilisates with aminosilanised magnetite after several cycles was principally due to the

aminosilanisation of the magnetite and would be smaller for other more neutral magnetite types (e.g. MagPrep® Silica or Bayoxide®) at the working pH 6.5.
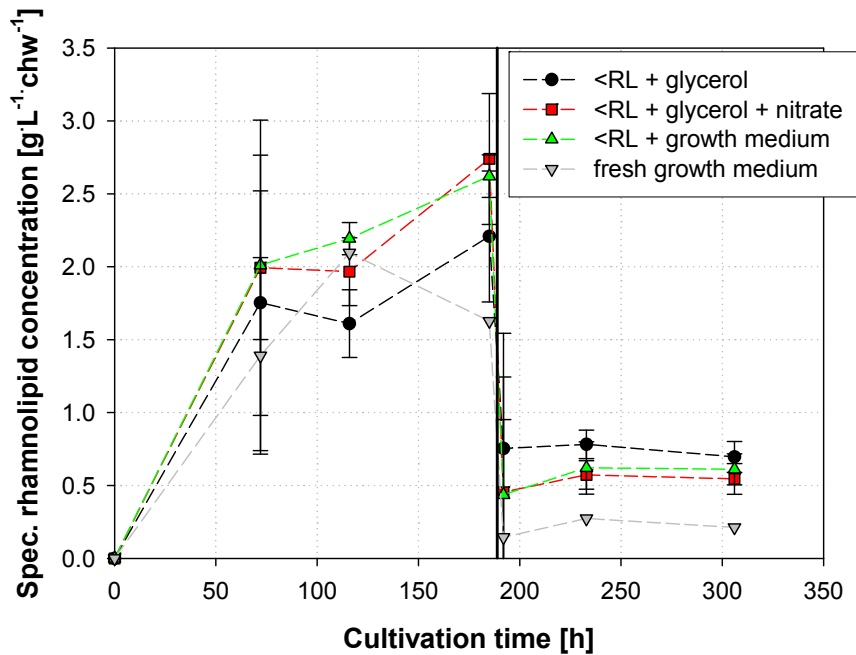
Fig. 4-13: Rhamnolipid production in shake flasks by immobilised bacteria in alginate beads with embedded Bayoxide® magnetite and glycerol as substrate, rhamnolipid removal by XAD-16 resin (<RL) and nutrient addition or complete medium exchange after 190 hours

Finally, the influence of different nutrients added by simultaneous elimination of rhamnolipids after an initial rhamnolipid production cycle was studied with the aim of subsequent cell growth and re-induction of rhamnolipid synthesis. Therefore bacteria were immobilised in alginate beads with embedded Bayoxide® magnetite. After a first rhamnolipid production phase of 190 h, produced rhamnolipids (between 10 and 18 $g^.L^{-1}$) were removed from the medium by adsorption on XAD-16 resins and different nutrient components were added or the cultivation medium was completely exchanged. Concerning rhamnolipid concentrations in the cultivation medium, only slight rhamnolipid synthesis occurred during the second production cycle (see Fig. 4-13). The higher rhamnolipid concentrations for cultures without complete medium exchange were due to an incomplete rhamnolipid adsorption on XAD resin.

These findings were elucidated by the viable cell concentration developing in immobilisates and production medium (see Fig. 4-14). After an initial cell growth in the beginning of the first rhamnolipid production cycle, viable cell concentrations in the immobilisates decreased continuously to about three decimal powers of the initial concentrations resulting in only poor rhamnolipid concentrations in the production medium. This progression was similar for all medium compositions studied and due to cell-leakage out of immobilisates as well as cell lysis (visible in CTC/DAPI-stainings). Contrary to the first cycle, no visible cell growth

occurred in the beginning of the second cycle despite addition of necessary nutrients. Concentrations in the cultivation medium also increased in the beginning due to cell-leakage and stayed at high levels until rhamnolipid removal. The high death rates during the second rhamnolipid production step for all cultures without complete medium exchange were presumably due to accumulation of toxic by products. These had been partly removed in the forth culture by complete medium exchange, therefore maintaining higher cell concentrations in the medium for a longer time span.
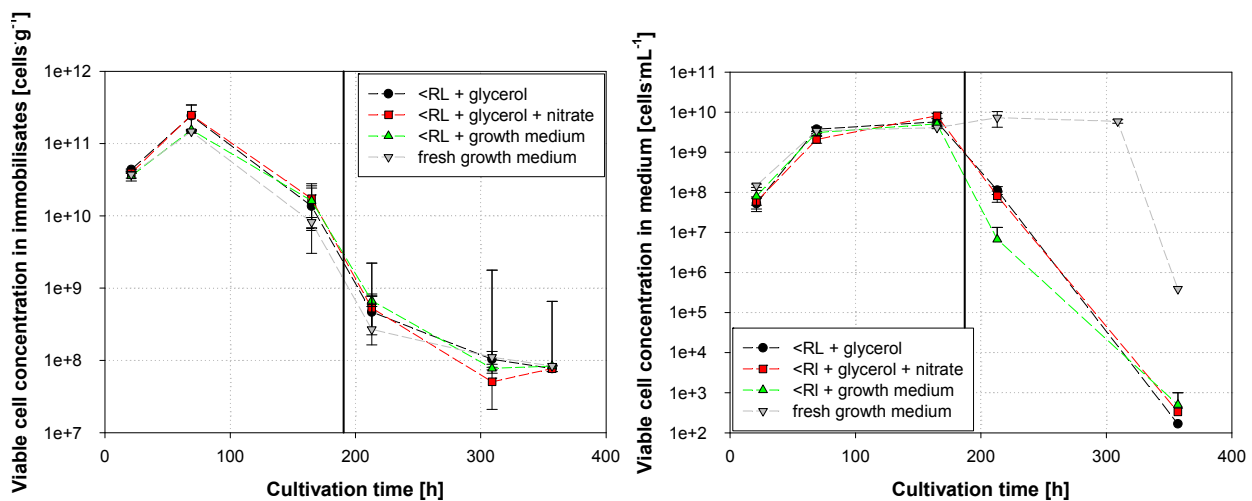
Fig. 4-14: Viable cell concentration developing in immobilisates (left) and cultivation medium (right) during rhamnolipid production in shake flasks by immobilised bacteria in alginate beads with embedded Bayoxide® magnetite and glycerol as substrate, rhamnolipid removal by XAD-16 resin (<RL) and nutrient addition or complete medium exchange after 190 hours

As a conclusion of these experiments can be drawn, that still great efforts have to be undertaken concerning cell growth in immobilisates to maintain a high level of viable cell concentrations for a continuous rhamnolipid production process.

4.5 Conclusions

In this study, we have demonstrated that immobilisation of *P. aeruginosa* cells in magnetic hydrogel beads can provide a good mean for continuous biosurfactant production by retention of the biocatalyst in the production process by high gradient magnetic separation and in situ product removal by foam fractionation. For this purpose, different immobilisation matrices, magnetic materials and immobilisation processes were investigated with regard to their application potential in a continuous rhamnolipid production process. Properties analysed were particle size distribution, stability, diffusion properties and of course their influence on rhamnolipid production.

Concerning, the immobilisation process for the studied materials, suspension polymerisation with facilitated bead separation from suspension medium by an oil/water emulsion revealed certain advantages compared to droplet extrusion by the JetCutting® device. Smaller bead

sizes were possible and additionally entrapment of magnetite particles was easier and without plugging problems especially for higher bead quantities.

From the investigated materials, Bayoxide® magnetite and MagPrep® Silica magnetite were homogeneously embedded in alginate beads. They also showed the best properties with highest saturation magnetisation for good magnetic separation, an almost neutral zeta potential at working pH for reduced interactions with rhamnolipids and good diffusion properties, not changing the product composition of effused rhamnolipids.

Alginate immobilisates with embedded magnetite possessed an improved mechanical as well as chemical stability compared to pure alginate beads, but their stability still was inferior to polyurethane beads, which stayed elastic even with relatively high deformations and were inert to all kinds of chemical agents. However, rhamnolipid synthesis by polyurethane beads was lower than for alginate immobilisates with embedded MagPrep® Silica magnetite, which revealed highest rhamnolipid production closely followed by Bayoxide® magnetite.

Principally, re-induction and cell growth of immobilised bacteria was necessary after a certain production time as rhamnolipid synthesis slowed down. For continuous rhamnolipid production in a cyclic process still some efforts have to be undertaken concerning cell growth in immobilisates between different cycles to maintain a high level of viable cell concentrations over a longer production time. In contrast, specific rhamnolipid synthesis rates related to the viable cell concentration maintained at the initial level over several production cycles.

Nevertheless, magnetic immobilisates are a promising tool for easier handling of biocatalysts in a continuous biological production process.

5 Continuous rhamnolipid production with process integration by foam fractionation and magnetic separation of immobilised *Pseudomonas aeruginosa*

5.1 Abstract

Increasing interest in biological surfactants has intensified research on cost-effective production of biosurfactants compared to traditional surface active components based on petrochemical feedstock. The present publication describes a new process for continuous rhamnolipid production by process integration. Rhamnolipid was synthesised by *Pseudomonas aeruginosa* DSM 2874 and removed continuously in situ by foam fractionation. To prevent losses of the biocatalyst through foaming, bacteria were entrapped in magnetic alginate beads. Entrained immobilisates were retained by high gradient magnetic separation from foam and backflushed in the bioreactor in constant intervals. It has been demonstrated that continuous rhamnolipid production in a 10 L bioreactor over several cycles with intermediate growth periods is feasible. Complete separation of rhamnolipids from production medium with an average enrichment of 15 in the collapsed foam was demonstrated, yielding a final rhamnolipid amount of 70 g after four production cycles. However, improvements still have to be made to reduce substrate consumption and to maintain high and active concentrations of entrapped *P. aeruginosa* in the bioreactor.

5.2 Introduction

During the last decades extensive research has been performed on biosurfactants [95, 101, 120], which are surface-active metabolites produced by microorganisms. Surfactants are widely used in larger quantities in detergents, pharmaceuticals, cosmetics and in food industry [9, 38, 85]. As traditionally used surfactants are based on petroleum feedstock, they are only partially biodegradable and pollute enduringly the environment. Biosurfactants, such as rhamnolipids, show high effectiveness coupled with good biodegradability [9, 38]. Some of the most extensively studied biosurfactants are the rhamnolipids (RL), mostly produced by *Pseudomonas aeruginosa*. Rhamnolipids are composed of one or two rhamnose molecules and up to three molecules of hydroxy fatty acids, whereas their chain length can vary from 8 up to 14 carbon molecules [40, 58, 60]. The most commonly produced rhamnolipids by *P. aeruginosa* are Rha-C_{10}-C_{10} and Rha-Rha-C_{10}-C_{10} also known as RL 1 and RL 3 [154].

Even though biotechnological production of biosurfactants is already established for several years, high production costs due to intense foaming, expensive downstream processing and high substrate costs impede their bulk use up to now [38]. Especially foaming creates problems including the undesirable stripping of product, nutrients, and cells into the foam [55]. Additionally, foaming complicates process containment, making it necessary to operate

bioreactors with excess headspace and suppress foam by the addition of chemical antifoams. This raises the costs of the bioprocess and lowers the productivity of the system due to often reduced oxygen transfer rates and possible adverse effects on the cell's physiology [89].

New attempts are made to overcome these difficulties by the use of cheaper substrates, process optimisation to improve yields and process integration to reduce downstream steps [48, 119, 166]. Concerning process integration of up- and downstream-processing by continuous in situ product removal, product yields may be increased through avoidance of inhibitory product concentrations. On the other hand less purification steps are necessary to obtain the desired product purity, therefore inducing less product loss and reduced costs. Investigated approaches for biosurfactant elimination are removal over membranes [55], by foam fractionation [29, 33, 111] or through adsorption on XAD-resins or rather activated carbon [44, 111].

Exclusively, foam fractionation permits the complete extraction of surface active components from cultivation medium [19, 36]. As bacteria are also entrained with the foam, immobilisation of the producing bacteria is necessary for retention of the biocatalyst in the production medium and decouples at the same time growth from product removal rates [111]. Entrapment of bacteria in a magnetic matrix facilitates biocatalyst retention through utilisation of magnetic forces. A magnetic separation process already well studied for magnetic retention of immobilised biomolecules even from complex media constitutes the high gradient magnetic separation (HGMS) [75, 112, 144]. The high-gradient magnetic separator designed by Hoffmann et *al.* [72] operates in a cyclic fashion using "switchable" permanent magnets. It is therefore well suited for continuous separation processes just as for immobilisates out of foam.

In this study we established a continuous production process of rhamnolipids by *P. aeruginosa* in an integrated reactor system. A 10 L bioreactor was first used for biomass production and then for rhamnolipid formation with magnetically immobilised bacteria (see paragraph 3.1). For the first step an exponential feeding-concept was adopted to yield higher cell densities. Then, the obtained biomass was immobilised in magnetic matrices that will allow retention of the biocatalyst by magnetic separation. In a second fermentation step rhamnolipid production with immobilised bacteria in the same 10 L bioreactor were studied for implementation of a continuous process with in situ product removal. The product / foam was continuously removed by foam fractionation and the liquid level completed by a controlled substrate feed. As immobilisates were also carried along with the foam, a high gradient magnetic separator (as designed by Hoffmann et *al.* [72]) was interconnected after the fractionation tube to retain them in the fermentation process. Glycerol from biodiesel

production was used as carbon source from renewable raw material to reduce furthermore process charges.

5.3 Materials and Methods

5.3.1 Experimental methods

5.3.1.1 Microorganism

The gram-negative, under certain conditions (nitrate source) facultative anaerobic *Pseudomonas aeruginosa* DSM 2874 strain was used for all experiments. This wild-type strain has been isolated from water samples and characterised by the working group of Syldatk [153]. The strain is supplemented after over-night culture in Luria Broth agar with 25% glycerol and conserved at -80°C.

5.3.1.2 Media and culture conditions

5.3.1.2.1 Media composition

The following media were used during the different stages of integrated rhamnolipid production as described below:

VK2   7.73 $g \cdot L^{-1}$ $NaNO_3$, 0.4 $g \cdot L^{-1}$ $MgSO_4$ x $7H_2O$, 0.4 $g \cdot L^{-1}$ $CaCl_2$ x $2H_2O$,
     3.72 $g \cdot L^{-1}$ Na_2HPO_4 x $2H_2O$, 6.24 $g \cdot L^{-1}$ KH_2PO_4, 30 $g \cdot L^{-1}$ glycerol, 1 $mL \cdot L^{-1}$ TES

TES   100 $g \cdot L^{-1}$ Na-citrate x $2H_2O$, 0.28 $g \cdot L^{-1}$ $FeCl_3$ x $6H_2O$, 1.2 $g \cdot L^{-1}$ $CoCl_2$ x $6H_2O$,
     1.4 $g \cdot L^{-1}$ $ZnSO_4$ x $7H_2O$, 1.2 $g \cdot L^{-1}$ $CuSO_4$ x $5H_2O$, 0.6 $g \cdot L^{-1}$ $MnSO_4$ x H_2O

B1   6.96 $g \cdot L^{-1}$ $NaNO_3$, 0.36 $g \cdot L^{-1}$ $MgSO_4$ x $7H_2O$, 0.36 $g \cdot L^{-1}$ $CaCl_2$ x $2H_2O$,
     3.72 $g \cdot L^{-1}$ Na_2HPO_4 x $2H_2O$, 6.24 $g \cdot L^{-1}$ KH_2PO_4, 20 $g \cdot L^{-1}$ glycerol, 1 $mL \cdot L^{-1}$ TES

N-Feed   350 $g \cdot L^{-1}$ $NaNO_3$, 70 $g \cdot L^{-1}$ $MgSO_4$ x $7H_2O$

C-Feed   37.17 $g \cdot L^{-1}$ Na_2HPO_4 x $2H_2O$, 62.37 $g \cdot L^{-1}$ KH_2PO_4, 600 $g \cdot L^{-1}$ glycerol

R1   0.36 $g \cdot L^{-1}$ $NaNO_3$, 0.02 $g \cdot L^{-1}$ $MgSO_4$ x $7H_2O$, 0.5 $g \cdot L^{-1}$ $CaCl_2$ x $2H_2O$,
     0.31 $g \cdot L^{-1}$ Na_2HPO_4 x $2H_2O$, 0.52 $g \cdot L^{-1}$ KH_2PO_4, 30 $g \cdot L^{-1}$ glycerol,
     0.1 $mL \cdot L^{-1}$ TES

Prod-Feed   0.5 $g \cdot L^{-1}$ $CaCl_2$ x $2H_2O$, 5 - 10 $g \cdot L^{-1}$ glycerol

A1   14.4 $g \cdot L^{-1}$ $NaNO_3$, 0.65 $g \cdot L^{-1}$ $MgSO_4$ x $7H_2O$, 3.1 $g \cdot L^{-1}$ Na_2HPO_4 x $2H_2O$,
     5.2 $g \cdot L^{-1}$ KH_2PO_4, 1 $mL \cdot L^{-1}$ TES

     (+ 100 $g \cdot L^{-1}$ $CaCl_2$ x $2H_2O$ separately in 60 mL Milli-Q water)

For all media, mineral salts and buffer substances + glycerol (as 10x buffer) were prepared and autoclaved separately at 121°C. Chemicals used in the formulation of growth media were purchased from Merck (Darmstadt, Germany) and Carl Roth (Karlsruhe, Germany).

5.3.1.2.2 *Biomass production process*

Firstly, a colony of cells, grown on a cetrimid agar plate, was added to 30 mL nutrient broth (Luria Broth, Miller) in a 50 mL falcon tube. After incubation at 30°C over night on an orbital shaker (194 rpm), 5 mL of culture broth were added respectively to six 500 mL shake flasks containing each 100 mL of mineral salt medium VK2 and cultivated under the same conditions for about 24 h. Biomass production was performed in a 10 L bioreactor (Biostat *Bplus*, Sartorius Stedim Biotech, Melsungen, Germany), equipped with two 6-blade disc impellers (70 mm ø, 1. impeller: 50 mm above bioreactor base, 2. impeller: 125 mm distant to 1.), a foam-disc for foam destruction (10 mm above liquid level), a sparger ring for aeration and probes for pH, pO_2 as well as temperature measurements. The 6 L of mineral salt medium B1 in the bioreactor were inoculated with 600 mL pre-culture (equal to 10% of the medium volume) and cultivated for about 28 h at 30°C and 600 rpm in the beginning. During fermentation, the dissolved oxygen concentration was controlled at 20% saturation by oxygen enrichment up to 60% of supplied air at 1 $L \cdot min^{-1}$ and afterwards by stirrer speed adjustment up to maximum 1200 rpm. The pH in the bioreactor was maintained at 6.5 by the automatic addition of 2 M NaOH or 2 M HCl. In the case of intensive foaming, antifoam (Contraspum, Zschimmer & Schwarz, Lahnstein / Rhein, Germany) was added. Trace element solution TES (1 $g \cdot L^{-1}$) was supplemented approx. every 10 hours. After a batch phase up to an optical density of about 12 at 600 nm, the fed-batch was started with two different nutrient supplies. The N-Feed (120 mL) was added at a constant speed of 0.69 $mL \cdot min^{-1}$, whereas the C-Feed (containing the carbon source) was fed step-wise exponential in steps of 30 min according to Eq. 5-1 until the end of fermentation.

$$F(t) = \left(\frac{\mu}{Y_{X/S}} + m \right) \cdot \frac{c_{X_0}}{c_{S_0}} \cdot V_0 \cdot e^{\mu \cdot (t - t_0)} \ [\text{L} \cdot \text{h}^{-1}]$$

Eq. 5-1

The time dependent feeding rate F(t) was calculated with the following parameter settings: specific growth rate μ = 0.15 h^{-1}, specific biomass/substrate yield coefficient $Y_{X/S}$ = 0.275 $g \cdot g^{-1}$, specific maintenance coefficient m = 0.027 $g \cdot g^{-1} \cdot h^{-1}$, biomass concentration at start of feeding c_{X0} = 5 $g \cdot L^{-1}$, glycerol concentration in feeding solution c_{S0} = 600 $g \cdot L^{-1}$, and reactor volume at start of feeding V_0 = 6 L.

After depletion of supplied nitrate, biomass was harvested by centrifugation at 7000 rpm and 4°C for 15 min (Coulter Avanti Centrifuge J-25 I, Beckmann, Krefeld, Germany). For later immobilisation, bacteria were resuspended at the ratio of 4:1 with 3-(N-morpholino)-propanesulfonic acid (MOPS) buffer at pH 7.8.

5.3.1.2.3 *Rhamnolipid production process*

5.3.1.2.3.1 Shake flasks

Several parameters for highest rhamnolipid production were first investigated in 500 mL shake flasks with 100 mL of buffer supplemented with 20 $g^.L^{-1}$ of vegetable oil (High oleic sunflower oil 90 plus, T+T Oleochemie, Alzenau, Germany) or glycerol. One to four grams of biomass from batch fermentations were added and cultivated on a rotary shaker for 15 days at 120 rpm and 37°C. Samples were taken every day and analysed for rhamnolipid content.

5.3.1.2.3.2 10 L bioreactor

The bacteria from the biomass fermentation process (see paragraph 5.3.1.2.2) were first immobilised in magnetic alginate beads (see paragraph 5.3.1.3) and then employed in a 10 L bioreactor, which was modified for a continuous rhamnolipid production (see paragraph 5.3.1.4). In some experiments bacteria were directly transferred to the bioreactor as "free" resting cells in a simple production medium composed of 30 $g^.L^{-1}$ glycerol in 10 mM MOPS buffer. Rhamnolipids were produced in a closed loop system with recirculation of foam. In all other cases, bacteria were first grown in 6 L of a low concentrated mineral salt medium R1 to increase cell activity for rhamnolipid formation, especially after the stressful immobilisation process. Cultivation conditions were 37°C, pH 6.5, 1 $L^.min^{-1}$ gassing rate and a pO_2 of 20% which is maintained by stirrer speed adjustment between 400 and 800 rpm. Owing to subsequent rhamnolipid synthesis and foam fractionation, which started after nitrate depletion, the medium level had to be replenished by production feed (Prod-Feed) according to the signal of the level probe. If rhamnolipid production slowed down, 600 mL of mineral salt medium A1 and, for the case of low glycerol concentrations, glycerol was added for cell growth. Immediately after addition of nutrients, 60 mL of 100 $g^.L^{-1}$ $CaCl_2$ solution were supplemented to prevent dissolution of immobilisates. Samples of medium, foam and collapsed foam were taken once a day for rhamnolipid and glycerol analysis.

5.3.1.3 Immobilisation in magnetic beads

Biomass from the first immobilisation process was immobilised in magnetic calcium alginate beads by internal gelation modified from Poncelet et *al.* [131]. 410 g of 3.7% sodium alginate (Sigma-Aldrich, Taufkirchen, Germany) in 10 mM MOPS buffer pH 7.8 were mixed with 25 g of magnetite (Bayoxide® E 8710, Lanxess, Leverkusen, Germany) in a beaker. A blend of 5 g $CaCO_3$ and 105.6 g resuspended bacteria was added to the mixture and homogenised by an overhead stirrer. The obtained suspension was pressed by means of a pressure vessel into 2 L of vegetable oil, stirred at 500 rpm with two 4-blade stirrers in a 5 L plastic beaker. After dispersion of the polymer solution, gelification was started through addition of 2 mL of acetic acid. One minute later 1 L of 0.05 M $CaCl_2$ solution was poured carefully into the reaction

beaker and curing of the gel beads continued for 30 min. To achieve a more homogeneous mixing, stirrer height is adapted to the new filling level. Thereafter, the stirrer was stopped and phase separation awaited. As magnetic immobilisates accumulated in the lower aqueous phase, the oil phase could be decanted and beads washed several times with 0.5% Tween 20 aqueous solution and 10 mM MOPS buffer pH 6.5 to get rid of remaining oil droplets. For transfer of the immobilisates into the 10 L bioreactor, beads were resuspended in part of the cultivation medium (R1). Final composition of the immobilisates was 3% alginate, 5% magnetite, 16% cell load and 1% $CaCO_3$.

5.3.1.4 Design of the integrated bioreactor

For rhamnolipid production, the same 10 L bioreactor was used in a modified manner. To inactivate the foam disc, it was untightened and fitted above the stirrer blades. A foam fractionation column was installed on top of the bioreactor instead of the exhaust air cooler. Foam, which pressed out of the bioreactor via the foam fractionation column, was collected as collapsed foam in a separate receptacle (see Fig. 5-1). If necessary, foam was collapsed by addition of citric acid. Two different designs of foam fractionation columns have been studied: a column of 1000 mm height and a cross-section of 30 mm and a second column of 660 mm height, a cross-section of 60 mm and fixtures in the shape of a newel (see Fig. 5-1).
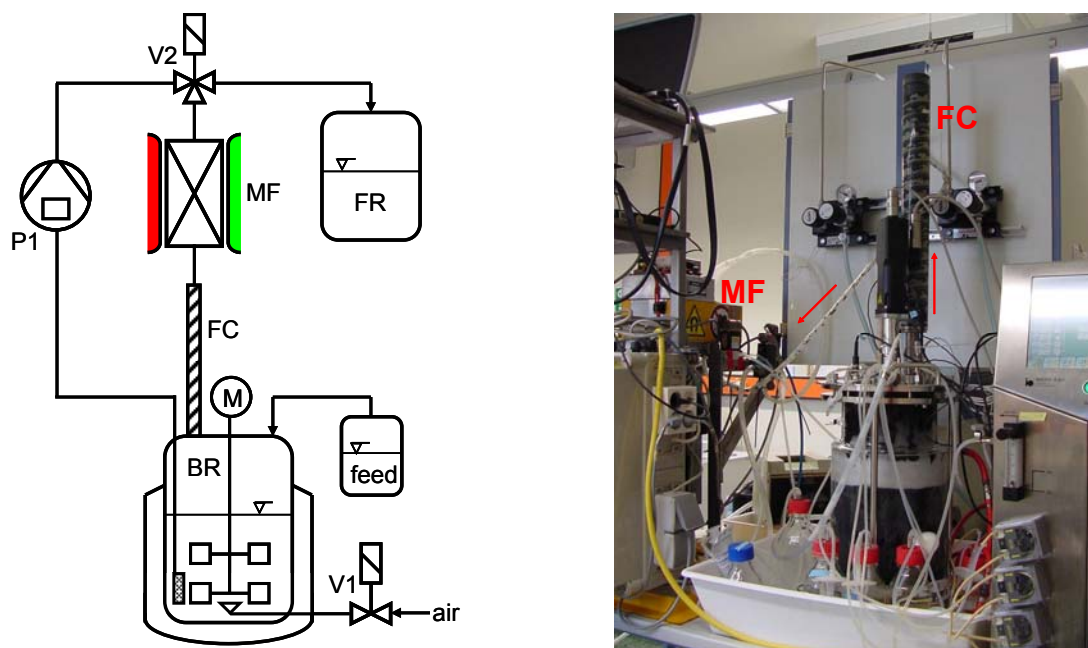
Fig. 5-1: Scheme of integrated rhamnolipid production process management (left): [BR] bioreactor, [P1] pump, [V1/V2] valves, [FC] fractionation column, [MF] magnetic filter, [FR] foam collection receptacle, photograph of integrated bioreactor (right)

Entrained immobilisates were retained by high gradient magnetic separation in the magnetic filter HGF10, developed by Hoffmann et *al.* [72] (see Fig. 5-2). The filter chamber of the magnetic separator, which was filled with a magnetisable stack of wire meshes, was placed

in the scope of an external magnetic field of rotatable NdFeB permanent magnets. Foam with magnetic immobilisates entered bottom-up, the immobilisates were accumulated on the wire surface and the purified foam left the separation chamber at the top. If the separation capacity of the filter matrix was exhausted, the external magnet was rotated by 90°C, which "switched off" the magnetic field in the filter matrix, and the immobilisates were backflushed by pumping production medium out of the bioreactor in reverse direction through the filter matrix at 0.82 L·min^{-1}.
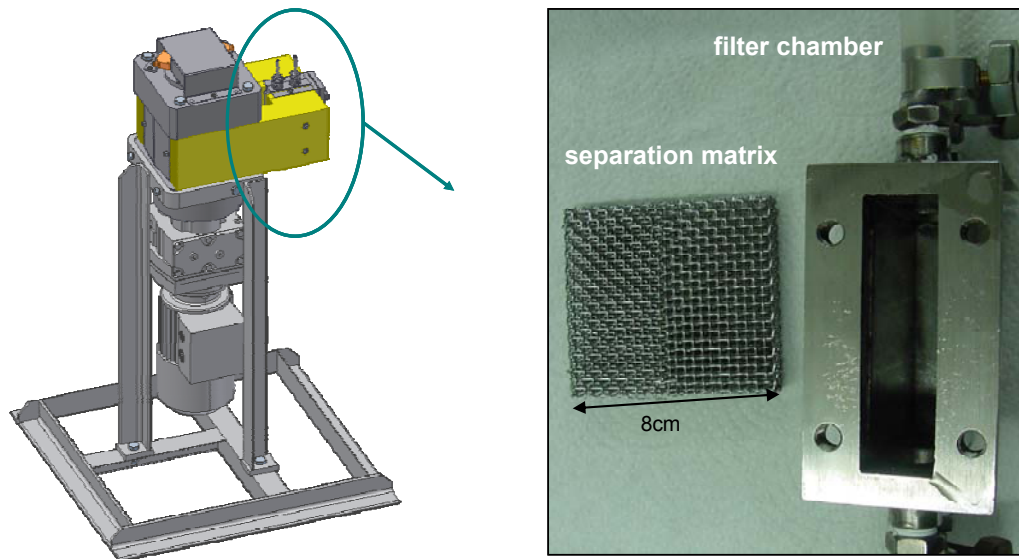
Fig. 5-2: Engineering drawing of the magnetic separator HGF 10 (left) and photograph of the filter matrix and the separator chamber (right)

For better release of the immobilisates a pneumatic ball vibrator (H10, Aldak, Troisdorf, Germany) was installed on top of the filter chamber. Entrainment of immobilisates out of the bioreactor was inhibited through a 30 µm membrane, which has been fixed around a small punnet at the end of the pump out tube.

Tab. 5-1: Configuration of magnetic separation process cycles

	cycle	duration [s]	valve 1	valve 2	pump	magnetic field
	separation	900	open	position a	off	on
I.	backflushing	60	closed	position b	on →	off
	tubing clearance	6	closed	position b	on ←	on
II.	backflushing	60	closed	position b	on →	off
	tubing clearance	30	closed	position b	on ←	on

For process control of magnetic separation the rotation motor, the valves for fluid distribution and the backflushing pump were connected to a control program realised in LabVIEW from

National Instruments. In this program were entered desired step times of the separation cycle and pumping speeds. General cycle times and configurations are presented in Tab. 5-1.

5.3.1.5 Non-integrated batch experiments

5.3.1.5.1 *Foam fractionation studies*

Parameters influencing foam fractionation behaviour of rhamnolipids were examined in a 1 L glass reactor equipped with fractionation tubes by application of experimental design. Tested experimental factors were varied within the following values: stirrer speed from 150 to 400 rpm, gas-flow rate from 0.05 to 0.15 L·min⁻¹ and foam fractionation height from 125 to 415 mm. Values of stirrer speed and gas-flow rate corresponded to the possible proportionate operating range of the 10 L bioreactor used for rhamnolipid production, for what they have been calculated based on a constant specific power input P/V by the stirrer and a constant volumetric gas-flow rate ($\dot{V}_{G}/V_{liquid}$). The specific power input is proportional to stirrer speed and diameter (see Eq. 5-2).

$$P/V \square \; \rho_L \cdot n^3 \cdot d_{stirrer}^3$$

Eq. 5-2

Values of the 10 L bioreactor were 0.5 to 1.5 L·min⁻¹ gas-flow rate and 200 - 550 rpm stirrer speed. As during experiments the rhamnolipid concentration in the medium decreased due to foaming, tracing of rhamnolipid concentrations permitted the study of an additional parameter. Experiments were configured pursuant to a Box-Behnken design with three centre-points and one replicate. Rhamnolipid enrichment, recovery and mass flow rate were chosen as response variables.

Each experiment was started with an initial rhamnolipid concentration in the model solution of about 0.8 g·L⁻¹. Procedure was as follows: 2.4 mL of Genail solution JBR 475 (a commercial aqueous rhamnolipid mixture, Genail, Baiersdorf, Germany) was added to 600 mL of 10 mM MOPS buffer pH 6.5 with 20% glycerol, filled into a 1 L test-reactor and tempered at 37°C with low stirrer speeds to avoid foaming.

The experimental setup is depicted in Fig. 5-3. Fractionation columns of different height were installed depending on the actual experiment. With the adjustment of desired stirrer speeds and gassing rates (operated by a mass-flow controller), the experiment was started. Foam, which was pressed out via the fractionation column was collected in a separate receptacle on a balance. In regular intervals, medium and foam samples were drawn off and analysed for rhamnolipid concentration.
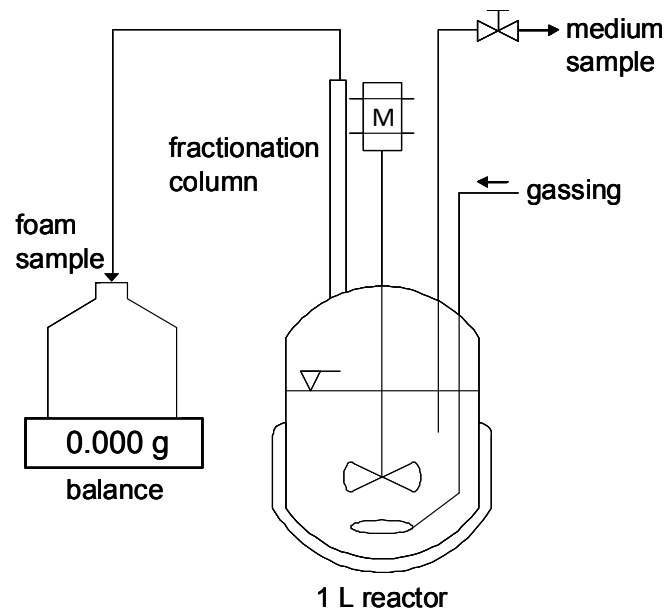
Fig. 5-3: Experimental setup of foam fractionation experiments

5.3.1.5.2 *Magnetic separation test*

Before application of the high gradient magnetic separation concept to the integrated rhamnolipid production process, tests were made beforehand with a model surfactant solution and immobilisates with different types of magnetite. A small cylindrical laboratory magnetic separator was used for experiments with varying number and distance of filter meshes (30 mm diameter, 3 µm mesh size) to examine their influence on filter capacity and backflushing of immobilisates. The above mentioned 1 L glass reactor was filled with 600 mL of 0.1% dishwashing detergent in water and 10% loading of alginate beads with 5% magnetite (Bayoxide$^®$ E 8710 from Lanxess or alternatively aminosilanised superparamagnetic magnetite, self-synthesised, see chapter 4). Foam was generated at a gas-flow rate of 0.15 L·min^{-1} and a stirrer speed of 250 rpm and led bottom up through the magnetic separator, which was placed between the pole shoes of a permanent magnet. For capacity determinations, the magnetic separator was completely loaded and then backflushed after moving the separator out of the external magnetic field by pumping water in opposite direction. Magnetic beads were quantified in the remaining surfactant solution of the glass reactor and the backflushing solution by weighing. Complete separation of magnetic immobilisates was checked at gas-flow rates varying from 0.05 to 0.15 L·min^{-1} and stirrer speeds of 150 to 400 rpm. Magnetic separation of immobilisates out of foam was also verified with the automated HGF 10 system and the 10 L bioreactor at different gas-flow rates and stirrer speeds.

5.3.2 Analytical methods

5.3.2.1 Growth determination

For growth determination different parameters were measured during cultivation such as optical density (OD), viable cell counts on agar plates, cell dry weight (cdw), CTC/DAPI-staining and process parameters such as pO_2 or dosage of acid.

5.3.2.1.1 Optical density

Optical density of culture broth was measured as absorbance at 600 nm compared to pure medium (UV-VIS-spectral-photometer G1103A, Agilent, Böblingen, Germany). Samples were diluted if absorbance was above 0.8. This procedure was only applied during biomass fermentation.

5.3.2.1.2 Viable cell counts

Concentrations of viable bacteria were determined through appropriate dilution of samples with phosphate buffered saline (PBS) pH 6.5 and spreading of 100 µL of 2-3 different sample dilutions on LB agar plates in triplicate with a Drigalski spatula. The agar plates were incubated at 30°C for 24 hours and the grown colonies counted.

For determination of viable cell concentrations in alginate immobilisates, immobilisates were filtered and washed with sterile PBS pH 6.5. About 0.1 g of immobilisates were then dissolved in 1 mL of 2% sodium tri-polyphosphate solution during 10 min on a vortex mixer and treated thereupon as mentioned above.

5.3.2.1.3 Cell dry weight

During biomass fermentation, 40 mL of culture broth were pipetted into a weighed 50 mL centrifuge tube and centrifuged at 4°C and 10000 rpm for 15 min (Centrifuge Hermle ZK 401, Eppendorf, Hamburg, Germany). The supernatant was discarded and the pellet dried for 24 hours at 100 °C. Before weighing, the centrifuge tubes were cooled down to room temperature in an exsiccator. The cdw ($g \cdot L^{-1}$) was calculated as the weight difference divided by 40 mL.

5.3.2.1.4 CTC/DAPI-staining

The distribution of viable and dead bacteria inside the immobilisates was visualised through staining with 5-cyano-2,3-ditolyltetrazoliumchloride (CTC) for metabolising bacteria and binding of 4',6-diamidino-2-phenylindoledihydrochloride-dilactate (DAPI) on DNA of all bacteria. CTC is incorporated into cells during cell respiration by transformation into the fluorescent CTF form. To 1 mL of culture medium with immobilisates were added 300 µL of 4 mM CTC solution (Polyscience, Eppelheim, Germany) and incubated for at least three

hours at 37°C and 194 rpm in the dark. Thereafter, immobilisates were filtered over a 0.2 µm membrane and washed several times with PBS pH 6.5. By incubation with 1 mL of 4.4 µg·mL^{-1} DAPI solution (Polyscience) for 5 min in the dark, immobilisates were counterstained. Then, immobilisates were again washed with PBS and the filter transferred on a microscope slide. Under the microscope (Axioplan 2 imaging, Zeiss, Oberkochen, Germany), CTC-staining is visible at 450 nm in red colour and DAPI-staining at 364 nm in intensive blue.

5.3.2.2 Rhamnolipid quantification

Medium samples for rhamnolipid analysis were taken from the bioreactor. Foam samples were collected behind the magnetic separator and centrifuged to collapse foam. Finally, samples were also taken from collapsed rhamnolipid foam of the foam collection receptacle.

5.3.2.2.1 Extraction

Before rhamnolipid quantification, rhamnolipids had first to be extracted from aqueous production medium. To 500 µL of sample 10 µL 1 M HCl and 500 µL ethyl acetate (Merck) were added, mixed on a vortex and centrifuged at 13000 rpm for 30 s to achieve phase separation. The upper ethyl acetate phase was transferred into a separate Eppendorf tube. After a second extraction step with ethyl acetate, the ethyl acetate phases were combined and used for further rhamnolipid analysis.

5.3.2.2.2 TLC

Normal thin layer chromatography (TLC) was used for fast qualitative rhamnolipid determination. 6 µL of extracted samples were applied with a 2 µL glass capillary to 0.2 mm silica gel plates (silica gel F254, 20 x 10 cm, Merck) and separated by a solvent mixture of chloroform / methanol / water (65:15:2, v/v/v). Visualisation of the separated compound spots was realised by dipping the TLC plates into cer-ammonium-molybdenumacid solution and developing the colours at 110°C for 10 minutes. Rhamnolipids appear in green and fatty acids as well as oil in brown colouration.

5.3.2.2.3 HPLC

Quantitative rhamnolipid concentrations were determined by reversed-phase HPLC coupled with MS [69]. First, ethyl acetate of extracted samples was evaporated and the rhamnolipid pellet resuspended in an equal volume of a 50:50 solvent mixture of acetonitrile (ACN, Merck) and 10 mM ammonium acetate buffer (NH$_4$OAc, Sigma) (further referred to as L14). Samples were diluted (generally 1:1000 in total) to a concentration of the calibration range. Chromatographic separation was carried out by an Agilent HPLC-system using a LiChrospher RP18 column (5 µm, 125 x 3 mm, Merck) with a gradient of the mobile phase

from 30% - 70% ACN in 10 mM NH$_4$OAc during 16 min and isocratic conditions of 70% ACN for 3 min by a flow rate of 0.4 mL·min^{-1}. Thereafter, the column was equilibrated for 15 min at 30% ACN. A sample of 20 µL was injected by an autosampler including a needle-wash and the eluted rhamnolipids were monitored by an API 4000 tandem-mass spectrometer (Applied Biosystems). Analytes were ionised by electrospray ionisation in a turbo ion spray interface by -4500 V in negative mode and a temperature of 400°C. Detection of the rhamnolipids (Rha-C$_{10}$-C$_{10}$ and Rha-Rha-C$_{10}$-C$_{10}$) was performed in MRM-mode with the following specific pseudomolecular ions (PI) for Rha-C$_{10}$-C$_{10}$: m/z 503.3 → 59.0, 103.2, 169.1, 333.2 and Rha-Rha-C$_{10}$-C$_{10}$: m/z 649.3 → 142.9, 169.0, 204.9, 479.2 with retention times of 10 min and 12 min respectively. Rhamnolipid concentrations were calculated by the peak areas of PI m/z 503.3 → 169.1 and m/z 649.3 → 479.2 based on a calibration curve of pure rhamnolipids with a concentration range of 0.01 µg·mL^{-1} to 2 µg·mL^{-1} in L14. Maximum standard deviations for rhamnolipid concentration measurements of 9% have been observed.

5.3.2.3 Substrate analysis

Glycerol and nitrate were analysed during biomass cultivation in the supernatant of the culture broth. Medium samples were therefore centrifuged at 13000 rpm and 4°C for 5 min (Centrifuge 5415 R, Eppendorf) and the supernatant stored at -20°C until substrate analysis.

5.3.2.3.1 *Glycerol*

Glycerol concentrations in culture broth were determined by an UV-diagnostic test from r-biopharm (Darmstadt, Germany). Quantification is based on the amount of consumed NADH during the enzymatic conversion of glycerol with a set of enzymes. Samples of supernatant were first heated at 80°C for 15 min in a thermomixer (Eppendorf) to coagulate proteins, which were subsequently removed by centrifugation at 13000 rpm for 5 min. Before analysis, samples were diluted appropriately with Milli-Q water to a concentration of the calibration range (0.04 - 0.4 g·L^{-1}). Then, 50 µL of diluted samples were mixed with 500 µL of solution 1 (coenzyme/buffer mixture), 950 µL of Milli-Q water and 5 µL of suspension 2 (pyruvate kinase, L-lactate dehydrogenase) and the absorbance measured photometrically after 20 min at 340 nm (UV-VIS-spectral-photometer G1103A, Agilent), corresponding to A$_1$. 5 µL of suspension 3 (glycerokinase) was added, the solution homogenised and the absorbance measured again after 30 min of reaction (A$_2$). The same procedure was performed for a blank, consisting of Milli-Q water. Glycerol concentrations, which are proportional to the consumed NADH, were finally calculated by Eq. 5-3 with the absorbance difference ΔA = (A$_1$ - A$_2$)$_{sample}$ - (A$_1$ - A$_2$)$_{blank}$.

$$c(glycerol) = \frac{V \cdot MW}{\varepsilon \cdot d \cdot v \cdot 1000} \cdot \Delta A \; [g \cdot L^{-1}]$$

Eq. 5-3

Addition of an internal standard permitted to control the correct performance of the test and to exclude influences of interfering substances.

5.3.2.3.2 Nitrate

Nitrate analysis was effected by ion exchange chromatography (DX-500, Dionex, Idstein, Germany) on an ION PAC AS 11 column (4 x 250 mm, Dionex). Samples were diluted 1:100 and filtered over 0.45 µm filters beforehand. After injection of a 10 µL sample, nitrate ions were eluted with a gradient of 8 to 30 mM NaOH by a flow rate of 1 mL$\cdot$min^{-1} and a runtime of 13 min. Ions were detected by conductivity measurements at 35°C and a suppressor current of 100 mA and quantified in a calibration range of 2.5 - 25 mg$\cdot$L^{-1} nitrate by peak areas at a retention time of 3.4 min.

Qualitative determination of nitrate was quickly possible by the so-called brown-ring test. If nitrate containing samples are mixed with a ferrous sulphate or chloride solution and concentrated sulphuric acid is layered below the aqueous solution, a brown ring is formed immediately at the interface based on a redox reaction of Fe^{2+} and NO^{3-}. In practice, 1 mL of sample was acidified by 100 µL 1 M HCl and mixed with 100 µL of 200 g$\cdot$L^{-1} Fe(II)Cl$_2$ solution. Then, 500 µL of concentrated sulphuric acid was carefully layered below the sample mixture. For concentration estimations, a blank, 0.7 g$\cdot$L^{-1} and 7 g$\cdot$L^{-1} nitrate solution were tested as well and compared to the colour intensity of the sample.

5.3.2.4 Immobilisates characterisation

5.3.2.4.1 Particle size distribution

Particle size distributions of the immobilisates were determined by the particles sizer CIS 100 (Galai, Israel) in a measurement range from 10 to 2000 µm. The measurement principle is based on the particle size dependent shading of a laser beam (660 nm). Samples were prepared by adding a spatula tip of immobilisates into a 3 mL cuvette filled with deionised water, which was pipetted up and down during measurements to prevent settling of the immobilisates.

5.3.2.4.2 Magnetisation

Magnetisation was measured by an alternating-gradient magnetometer (MicroMag 2900, Princeton Measurements, USA). In this case, the sample is magnetised by a static magnetic field and at the same time overlaid by an alternating magnetic field. The resulting field gradient is proportional to the magnetic moment of the sample and can be measured due to deflexion of a piezoelectric element from which the sample is suspended. Immobilisates were first dried in a freeze drier (BETA 1-8K, Christ, Osterode am Harz, Germany) and then a defined amount of particles was incorporated in a 100 µm glass capillary tube, which has

been closed on both ends. The capillary tube was horizontally fixed on a specimen holder with silicon grease and the holder attached to the piezoelectric element before being symmetrically adjusted in the magnetic field. Measurements were performed as hysteresis curves beginning at the highest positive field strength ($8 \cdot 10^5$ A·m^{-1}). To calculate saturation magnetisations of humid immobilisates, their solids content is determined by weighing of immobilisates before and after freeze drying during sample preparation.

5.3.2.4.3 Bead compression

Stability of immobilisates was tested by compression of a single spherical bead between two plates of a rheometer (Physica MCR 301, Anton Paar, Ostfildern, Germany). An immobilisate of approximately 1.5 mm diameter was placed on the compression table below a movable stamp and excessive water dapped off. Afterwards, the immobilisate was compressed at a constant speed of 600 µm·s^{-1} until a gap of 100 µm and the applied normal force recorded as a function of gap width. For comparison of different immobilisates, normal forces were related to the active cross-section of the bead by converting them into the so-called 'true' yield stress σ_t, which considers also the change of active cross-section during compression due to lateral displacement of the gel bead. σ_t was plotted as a function of deformation degree φ (see Eq. 5-4 and Eq. 5-5).

$$\sigma_t = \frac{F \cdot h}{A_0 \cdot h_0} = \frac{F}{\frac{\pi}{4} \cdot d_0^{\,2}} \cdot \left(1 - \frac{|\Delta h|}{h_0} \right) \; [N \cdot mm^{-2}]$$

Eq. 5-4

$$\varphi = \ln \frac{h_0}{h} = \ln \frac{1}{1 - \frac{|\Delta h|}{h_0}} \; [-]$$

Eq. 5-5

5.4 Results and discussion

5.4.1 Biomass production in fed-batch process

Rhamnolipid synthesis is induced by nitrate or phosphate depletion or by limitation of multivalent cations [94]. Experiments of rhamnolipid production in shake flasks were performed to determine the right harvest time for highest rhamnolipid production with resting cells (see Fig. 5-4).

Biomass from *Pseudomonas aeruginosa* DSM 2874 harvested at different times of a batch fermentation in a 10 L bioreactor was employed for rhamnolipid production in shake flasks with vegetable oil as carbon source. Highest specific rhamnolipid production rates and final concentrations (corresponding to 5.6 g·L^{-1}·BFM^{-1} at 18 hours cultivation time) were achieved

with bacteria harvested at the end of the exponential phase. Therefore, biomass was henceforth harvested at the end of the exponential phase.
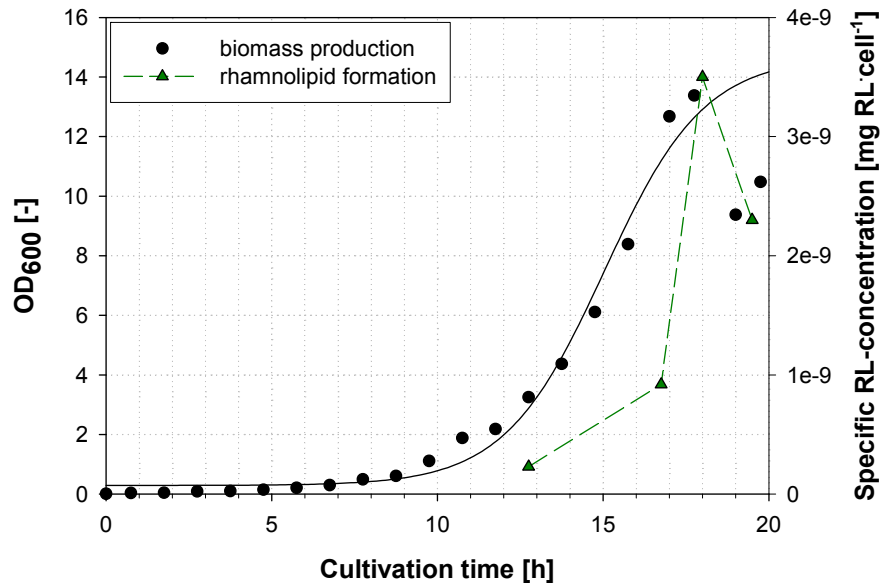
Fig. 5-4: Produced specific rhamnolipid concentrations for different harvest times during a batch cultivation of *P. aeruginosa* DSM 2874

Secondly, as rhamnolipid biosynthesis is quorum sensing regulated [125, 126], high cell densities also enhance rhamnolipid formation. Difficulties to overcome were the sensitivity of DSM 2874 to higher salt concentrations, necessitating therefore a fed-batch process with re-feeding of required substrates. Furthermore, to avoid oxygen and thus growth limitations, especially as *P. aeruginosa* is also capable of anaerobic growth on nitrate, the dissolved oxygen was controlled above 20% by pro rata aeration with oxygen and stirrer speed adjustments. Undesired metabolic by-products should be avoided by slowed down growth at 30°C [138], also reducing the generation of metabolic heat [97] and rhamnolipids during the fed-batch phase. As rhamnolipid formation could not be completely eliminated and antifoams decrease subsequent rhamnolipid synthesis, efficient mechanical foam destruction with a foam disc (Sartorius Stedim Biotech, Melsungen, Germany) facilitated a stable process control.

The fed-batch strategy applied consisted of two phases: a batch phase with a maximum specific growth rate ($\mu = \mu_{max}$) during exponential phase and a fed-batch phase with a constant specific growth rate ($\mu = 0.15$ h^{-1}). Due to a lack in appropriate monitoring equipment, fed-batch processes in this work were based on an open-loop strategy with a stepwise exponential feeding. Given that during exponential growth of microorganisms nutrient requirements are also increasing exponentially, the feeding rate was adjusted accordingly to achieve a constant specific growth rate. The calculation of the exponential feeding rate as a function of time is given in Eq. 3-13 according to Wilms et *al.* [173].

$$F(t) = \left(\frac{\mu}{Y_{X/S}} + m \right) \cdot \frac{c_{X_0}}{c_{S_0}} \cdot V_0 \cdot e^{\mu \cdot (t - t_0)} \; [\text{L} \cdot \text{h}^{-1}]$$

Eq. 5-6

The parameters for cultivation of *P. aeruginosa* were based on prior experience or estimations with the specific growth rate $\mu = 0.15$ h^{-1}, the specific biomass/substrate yield coefficient $Y_{X/S} = 0.275$ $\text{g} \cdot \text{g}^{-1}$, the maintenance coefficient $m = 0.027$ $\text{g} \cdot \text{g}^{-1} \cdot \text{h}^{-1}$ (estimation according to values of other *Pseudomonades*), the initial biomass concentration $c_{X0} = 5$ $\text{g} \cdot \text{L}^{-1}$, the glycerol concentration in the feeding solution $c_{S0} = 600$ $\text{g} \cdot \text{L}^{-1}$ and the medium volume $V_0 = 6$ L. In practice, the available equipment only allowed a stepwise change of feeding rate, which was adjusted every 30 minutes pursuant to the exponential equation.
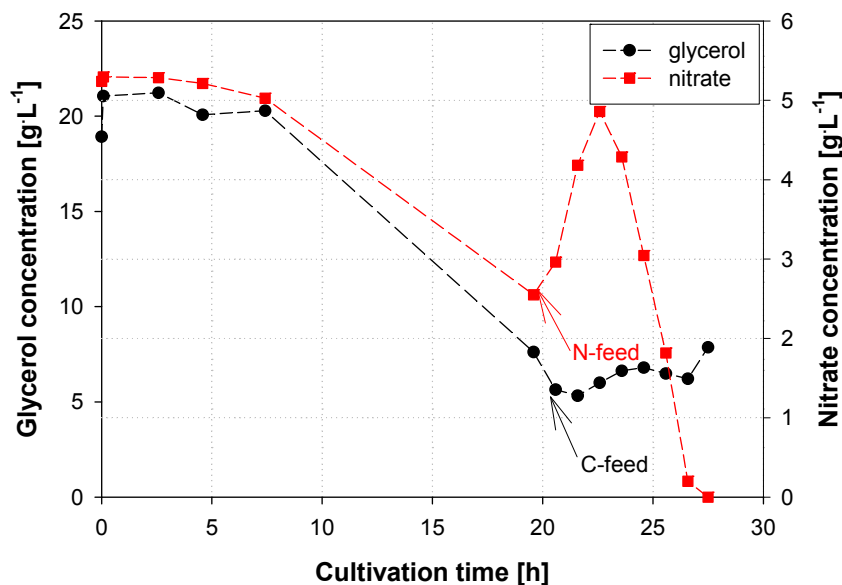
Fig. 5-5: Substrate consumption profiles during fed-batch cultivation of *P. aeruginosa* DSM 2874

Feeding was started at 20 h cultivation time after depletion of the carbon source (glycerol) at an optical density of about 13 (see Fig. 5-5 and Fig. 5-6) and continued for about seven hours. During this time the remaining glycerol concentration stayed between 5 and 6 $\text{g} \cdot \text{L}^{-1}$. To prevent induction of rhamnolipid biosynthesis, nitrate concentration was maintained on a higher level than glycerol concentration through constant feeding at an earlier moment (OD equal to 10). The nitrate concentration first increases up to almost the initial concentration and then constantly decreases after feeding stop due to bacterial growth until depletion. By this means, formation of white waxy particles, which occurs with higher nitrate concentrations, could be prevented. Afterwards, biomass was harvested for subsequent immobilisation and application in a continuous rhamnolipid production process at the onset of nitrate depletion.

Different cell growth parameters are depicted in Fig. 5-6. For growth pursuance during fermentation, acid dosage proved to be a suitable parameter as it fluctuated less than optical density and was online available contrary to cell dry weight and viable cell concentration determinations. During fed-batch phase, growth was exponential until nitrate depletion, yielding a final cell dry weight of 15 $g \cdot L^{-1}$. This concentration is higher than biomass concentrations generally reported in literature for rhamnolipid production [2, 59, 96, 153, 155], which vary from 4 $g \cdot L^{-1}$ to maximum 12 $g \cdot L^{-1}$ cdw except for rather slow cell growth on n-alkanes or vegetable oil [154]. Even higher concentrations may be possible with longer nitrate feed, but are finally limited through the bacterial oxygen demand. Moreover, the yielded biomass was absolutely adequate for the rhamnolipid production step with immobilisates.
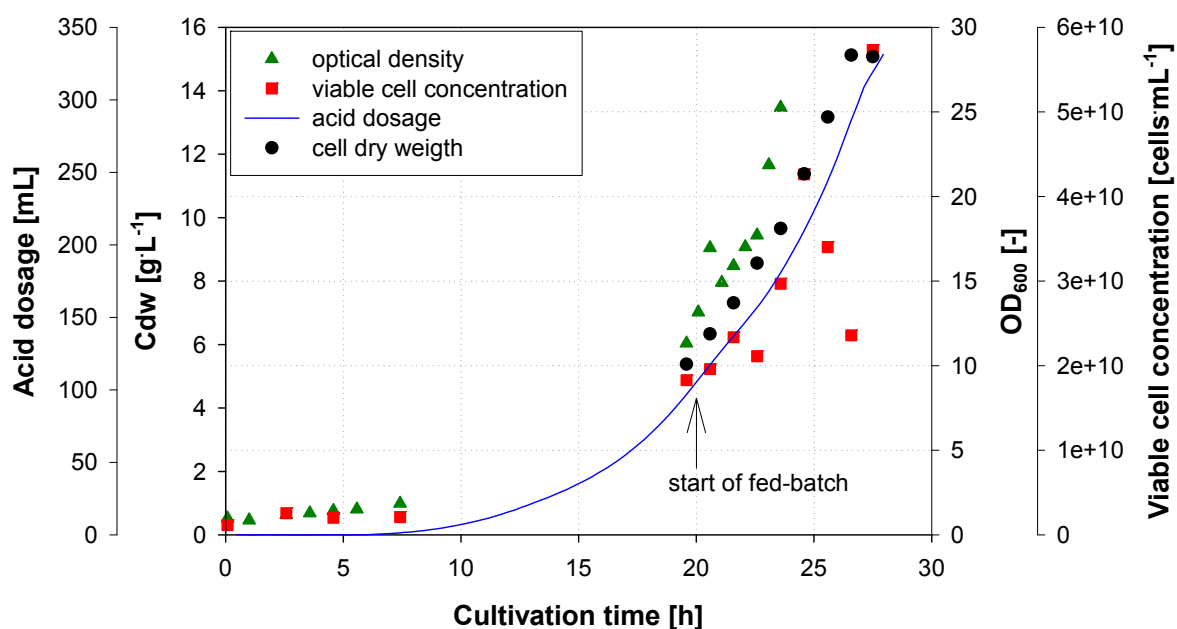
Fig. 5-6: Progress of cell growth parameters during fed-batch cultivation of *P. aeruginosa* DSM 2874

5.4.2 Immobilisation

Biomass from the first fermentation step was immobilised in calcium alginate beads with concurrently embedded ferromagnetic Bayoxide® magnetite. The immobilisation materials had been chosen on basis of comprehensive tests with different matrix materials and species of magnetite as reported in chapter 3. To handle large quantities of immobilisation material a suspension polymerisation process in 5 L beakers proved to be the more suited than an extrusion process especially as magnetite particles easily plugged up nozzles or filters. To yield a relatively narrow particle size distribution the two 4-blade stirrers had to be continuously adapted to the actual filling height for a homogeneous flow profile. As produced immobilisates were magnetic, washing of the beads could be easily effected by bead

retention with a permanent NdFeB magnet. However, bead quantities in a beaker were limited to the effective radius of the magnetic field.
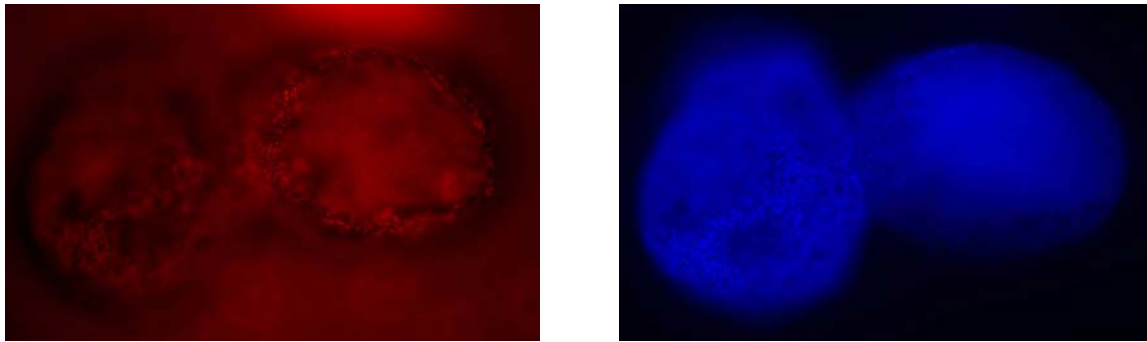
Fig. 5-7: CTC-staining (left) for visualisation of viable bacterial cells and DAPI-staining for all bacteria in alginate-Bayoxide® immobilisates at the end of an integrated rhamnolipid production process with *P. aeruginosa* DSM 2874

The produced immobilisates had a particle size distribution ranging from about 30 µm to 640 µm (for 95% of beads) with a medium volume related particle size of approximately 240 µm ($x_{AV,50}$). The initial specific saturation magnetisation of the humid immobilisates was ~5 Am²·kg^{-1} and so more than sufficient for magnetic separation in a high gradient magnetic separator. Depending on the concentration of added growth medium, immobilisates lost between 5 to 16% of their saturation magnetisation over a rhamnolipid production period of 22 days. The marginal quantities of magnetite in the production medium already give an impression about the adequate stability of the immobilisates and their suitability for continuous rhamnolipid production. As alginate beads are known to be instable vis-à-vis chelating agents or higher concentrations of monovalent ions [172], chemical stability was assured during cultivation by a higher level of $CaCl_2$ (0.5 g·L^{-1}) in the production medium [107]. This measure was especially necessary after addition of growth medium for reactivation of rhamnolipid production (see paragraph 5.4.4.3).

Secondly, bead compression tests were performed to examine mechanical stability of immobilisates. Immobilisates reached yield stresses at a deformation degree of 0.5 of 0.11 N·mm^{-2} before application in the rhamnolipid production process. These initial values decreased during cultivation to about 0.06 N·mm^{-2} due to repeated cell growth. However, magnetite embedding made immobilisates more robust than pure alginate beads, which can also be observed in the still relatively high bacterial concentrations and homogeneous distribution inside the immobilisates at the end of a rhamnolipid production process (see Fig. 5-7 and Fig. 5-16). Furthermore, the use of Bayoxide® magnetite should guarantee the lowest interactions of rhamnolipids with magnetite particles compared to other types of magnetite due to the almost neutral Zeta potential of +4.3 mV at pH 6.5.

5.4.3 Non-integrated batch experiments

Before realisation of the integrated rhamnolipid production concept, several parameters of foam fractionation as well as the functionality of magnetic separation were tested in experimental setups without bacteria.

5.4.3.1 Foam fractionation

In foam fractionation experiments, the influence of stirrer speed, gas flow rate, fractionation column height and rhamnolipid concentration in the medium on rhamnolipid enrichment, recovery, rhamnolipid mass flow rate and partitioning ratio of different rhamnolipid species were studied. The measurement variables are defined according to the following equations (see Eq. 5-7 to Eq. 5-10). In this case, rhamnolipid enrichment describes the degree of liquid volume reduction in regard to downstream processing, whereas recovery and mass flow rate characterise the degree and the rate of product separation from the bioreactor.

RL enrichment

$$E_r = \frac{c_{RL,foam}}{c_{RL,medium}} \, [-]$$

Eq. 5-7

RL recovery

$$R_{RL} = \frac{m_{RL,foam}}{m_{RL,medium} + m_{Rl,foam}} \cdot 100 \, [\%]$$

Eq. 5-8

RL mass flow rate

$$\dot{m}_{RL} = c_{RL,foam} \cdot \dot{V}_{foam} \, [g \cdot h^{-1}]$$

Eq. 5-9

partitioning ratio

$$P_r = \frac{E_{r,A}}{E_{r,B}} = \frac{E_{r,Rha-C_{10}-C_{10}}}{E_{r,Rha-Rha-C_{10}-C_{10}}} \, [-]$$

Eq. 5-10

Aim of the rhamnolipid fractionation process is continuous separation of rhamnolipids from culture broth to prevent product inhibition and at the same time concentration of rhamnolipids to reduce the handling volume of the desired product. Generally, surfactant enrichment by foam fractionation is achieved through adsorption of surfactant molecules to the bubble-water interface and subsequent water drainage when the foam ascends in the foam fractionation column, making the foam drier. The cell free foam fractionation tests revealed an antithetic behaviour of rhamnolipid enrichment and mass flow rate thus often leading to smaller rhamnolipid recoveries (see Tab. 5-2 and Fig. 5-9).

Tab. 5-2: Influence of different process parameters on rhamnolipid enrichment, recovery and mass flow rate

parameters	enrichment	mass flow rate	recovery
RL concentration ↑	↓↓↓	↑	-
stirrer speed ↑	↓↓	↑↑	↓↓
gas flow rate ↑	↓	↑↑	↑↑
dwell time ↑	↔	-	-

This fact is concordant with foam fractionation literature of other surfactants [19, 36, 55]. Primarily, rhamnolipid enrichment is influenced by rhamnolipid concentration in the production medium (see Fig. 5-8) [19, 55]. This effect is strongly pronounced at low rhamnolipid concentrations, where fewer molecules compete for adsorption space at the bubble interface. Additionally, foam is already drier, reinforcing drainage of production medium between the foam lamellae [169]. Maximum rhamnolipid enrichment ratios of more than 50 have been achieved.
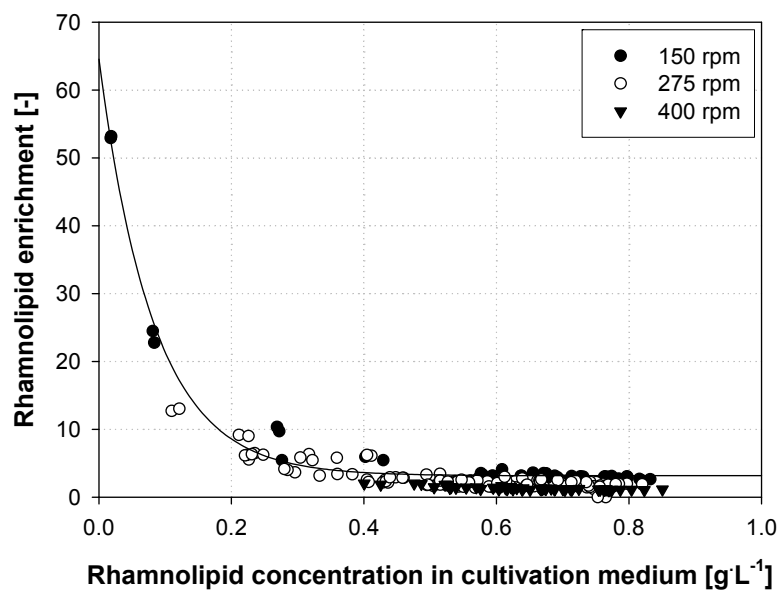
Fig. 5-8: Influence of rhamnolipid concentration in cultivation medium and stirrer speed on rhamnolipid enrichment

In contrast, other parameters such as stirrer speed or gas flow rate, which changed bubble size and therewith adsorption space at the bubble interface as well as foam humidity, showed less influence on rhamnolipid enrichment than initial rhamnolipid concentration. However, their antithetic behaviour of rhamnolipid enrichment and mass flow rate demanded a compromise between high enrichment ratios and mass flow rates (see Fig. 5-9).
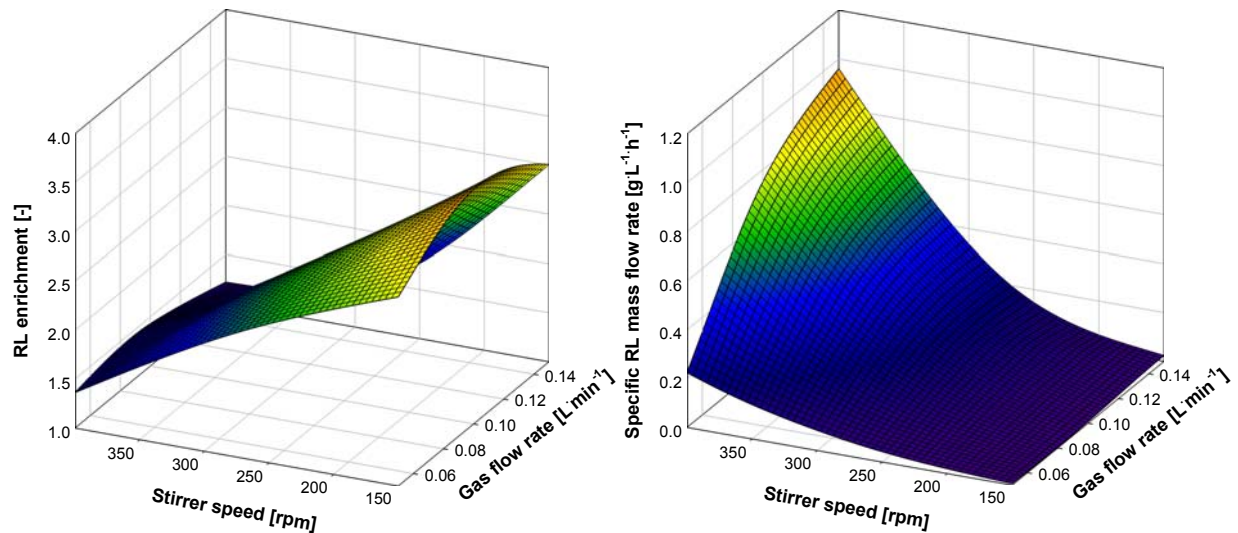
Fig. 5-9: Rhamnolipid enrichment (left) and rhamnolipid mass flow rate (right) as a function of stirrer speed and gas flow rate in a 1 L glass reactor

In practice, fermentation conditions should be chosen in a way that produced rhamnolipid is completely separated from production medium with minimum stirrer speeds and gas flow rates, yielding at the same time higher rhamnolipid enrichments through lower rhamnolipid concentrations in the medium.
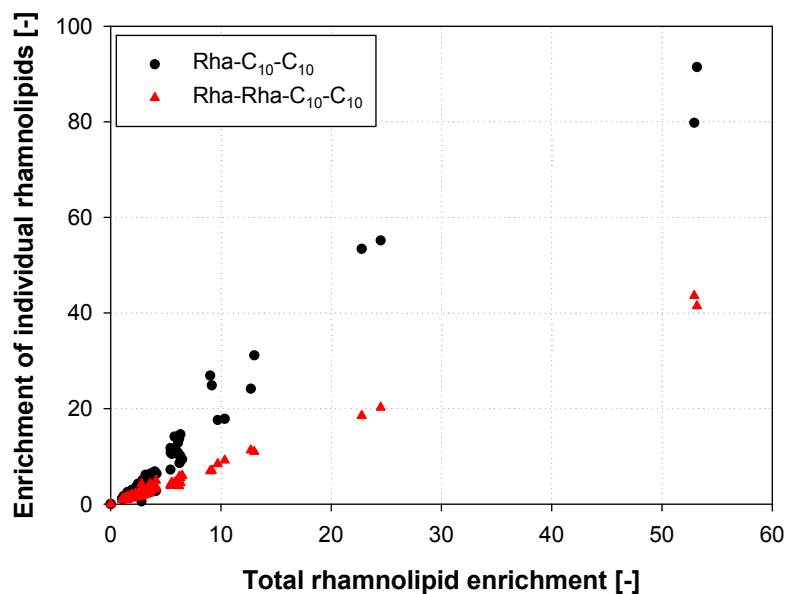
Fig. 5-10: Foam enrichment behaviour of different rhamnolipid species

Dwell time of foam in the fractionation column is on the one hand determined by the column height and on the other hand also by gas flow rates. As often reported, higher dwell times should improve rhamnolipid enrichment ratios through longer drainage times of production medium [19, 55]. Though, column heights utilised in the foam fractionation tests showed no

significant influence on rhamnolipid enrichment ratios [114]. This is due to the fact that dwell times were still very low with three to four minutes.

Finally, another aspect to consider is the foam partitioning behaviour of different rhamnolipid species, which may lead to changes in product spectrum during fermentation. The main species synthesised by *P. aeruginosa* DSM 2874 are $Rha-C_{10}-C_{10}$ and $Rha-Rha-C_{10}-C_{10}$ [Syldatk, 1984]. The enrichment ratio of $Rha-C_{10}-C_{10}$ revealed to be about twice (medium partitioning ratio of 2.1) as much than of $Rha-Rha-C_{10}-C_{10}$, due to the more hydrophobic character of $Rha-C_{10}-C_{10}$ (see Fig. 5-10). This effect was less pronounced for lower enrichment ratios, which may be explained by the higher initial concentration of $Rha-Rha-C_{10}-C_{10}$ in the test solution. For a homogeneous product composition, rhamnolipid foam should be collected over a longer time period during rhamnolipid production.

5.4.3.2 Magnetic separation

Several magnetic separators had been tested for magnetic separation of bacterial immobilisates out of foam. Only high gradient magnetic separation proved to be effective. Prior to integrated rhamnolipid production, separation and backflushing experiments were performed in a cylindrical laboratory magnetic separator with different types of magnetic immobilisates (ferromagnetic Bayoxide® magnetite and superparamagnetic aminosilanised magnetite, see Tab. 5-3).

Tab. 5-3: Separation capacity of magnetic immobilisates out of foam and backflushing efficiency of a high gradient magnetic separator

configuration of filter elements	number of filter blanks	magnetite	separation capacity	backflushing efficiency
(FFFFFF)	20	Bayoxide®	4.5 g	85 %
(F-F-F-)	10	Bayoxide®	2.8 g	89 %
(F-F-F-)	20	Bayoxide®	5.2 g	90 %
(F--F--)	20	Bayoxide®	5.8 g	91 %
(F--F--)	20	a.s.	5.9 g	99 %
(F--F--)	25	a.s.	6.2 g	98 %

F: filter blank, -: spacer ferrule, a.s.: aminosilanised magnetite

Separation capacity increased with the number of filter blanks and the number of spacers between them. However, with too large spacing between the filter mashes, separation capability decreased. Larger space between the filter blanks also increased backflushing efficiency, which was particularly higher (up to 99%) with superparamagnetic immobilisates due to the lacking remanence of the particles in absence of an external magnetic field. To improve backflushing even with ferrimagnetic immobilisates, a pneumatic ball vibrator was

installed afterwards for the switchable HGF 10 magnetic separator on the front side of the filter chamber facilitating detachment of immobilisates from the wire meshes.

Principally a magnetic separation cycle was composed of three process steps: magnetic separation, backflushing and tubing clearance to remove remaining production medium from the tubes between the bioreactor and the magnetic separator (see Tab. 5-1). Backflushing of the immobilisates was realised by pumping production medium from the bioreactor in reverse direction through the magnetic separator. As the magnetic field has to be switched off during backflushing, the permanent magnet could be either removed or the magnetic field diverted. In contrast, magnetic coils are not suited due to the long production times of rhamnolipids. Thus, a magnetic separator with a "switchable" permanent magnet, the HGF 10 system, was used for the integrated reactor concept, where the magnetic field was short-circuited by a rotation of the magnets for 90°C. Separation tests with the integrated reactor system also turned out to be applicable for magnetic separation out of foam. During rhamnolipid production one adaptation of the separation cycle had to be made, as the pressure in the bioreactor was higher with foaming and hampered backflushing. A magnetic separation step of 15 min was followed by two consecutive steps of backflushing and tubing clearance to ensure a complete return of the magnetic immobilisates into the bioreactor.

5.4.4 Rhamnolipid production

As rhamnolipids are secondary metabolites, a separation of biomass and rhamnolipid production was possible and enabled the use of immobilisates and therefore a continuous rhamnolipid production process. In order to compare results from the integrated rhamnolipid production system with magnetic immobilisates of *P. aeruginosa* and a continuous production process, rhamnolipids were first produced by free resting cells in a closed loop system.

5.4.4.1 Closed loop process with free cells

During rhamnolipid production, intensive foaming led to a discharge of surface active compounds (e.g. rhamnolipids) and particles (e.g. bacteria) out of the bioreactor. With higher gas flow rates and stirrer speeds, the bioreactor was quickly depleted of its biocatalyst and rhamnolipid production would rapidly slow down. Hence, to maintain higher bacterial concentrations in the bioreactor, pressed out foam was collected in a separate receptacle and pumped back into the bioreactor (see Fig. 5-11). Glycerol concentrations were regularly adjusted to ~30 g$\cdot$L^{-1} by addition of the necessary amount of 60% glycerol.

Rhamnolipid synthesis started after a short lag-time of several hours with a linear production rate of 0.2 g RL$\cdot$h^{-1} between 40 and 170 h for an initial cell dry weight of 19.8 g (see Fig. 5-12). After ~170 h rhamnolipid formation slowed down, leading finally to almost equal rhamnolipid concentrations in foam and production medium with a total rhamnolipid

concentration of $9\,g{\cdot}L^{-1}$ and a rhamnolipid yield of 55 g. During the main synthesis rhamnolipid enrichments in the foam of maximum 5.6 for Rha-C_{10}-C_{10} and 2.3 for Rha-Rha-C_{10}-C_{10} have been observed, which were higher for Rha-C_{10}-C_{10} due to its more hydrophobic character and its smaller spatial dimensions. The specific biomass/substrate yield amounted to 0.15 g RL per g glycerol with a space time yield of $0.038\,g{\cdot}h^{-1}{\cdot}L^{-1}$., which were similar to values obtained in literature for rhamnolipid production with glycerol as carbon source [4, 154].
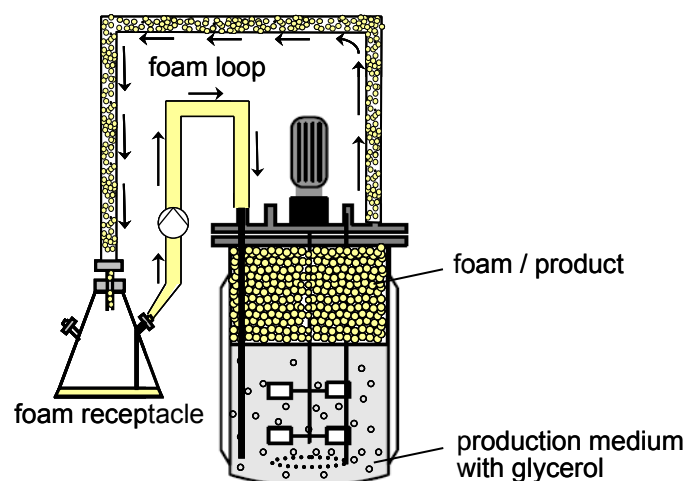
Fig. 5-11: Schematic illustration of closed-loop rhamnolipid production process with free cells

Fermentations based on vegetable oils or n-alkanes with a suitable fermentation strategy generally leaded to even higher rhamnolipid yields as reported in literature [54, 149, 154]. However, these substrates proved to be not suitable as carbon source for immobilised bacteria [111], as water solubilities are low and impeding interactions with immobilisation matrix may occur.

During cultivation time, biomass concentrations decreased through flotation and cell lysis to less than 60% of the initial concentration, reducing thus final rhamnolipid yield. As rhamnolipids were accumulated in the production medium, harvest of the medium and consecutive separation of rhamnolipids from culture broth (e.g. by extraction with ethyl acetate) followed by concentration and if necessary purification was required for product recovery. Quasi continuous rhamnolipid production would therefore only be possible as sequential fed-batches with considerable cell growth prior to rhamnolipid synthesis. In comparison, cell immobilisation and retention of the immobilisates in the bioreactor as realised in the integrated reactor concept should facilitate a continuous rhamnolipid production through in situ rhamnolipid separation by foam fractionation and for ideal case already partial purification of rhamnolipids. Additionally, immobilisates permit easier process handling and implicate less contamination problems.
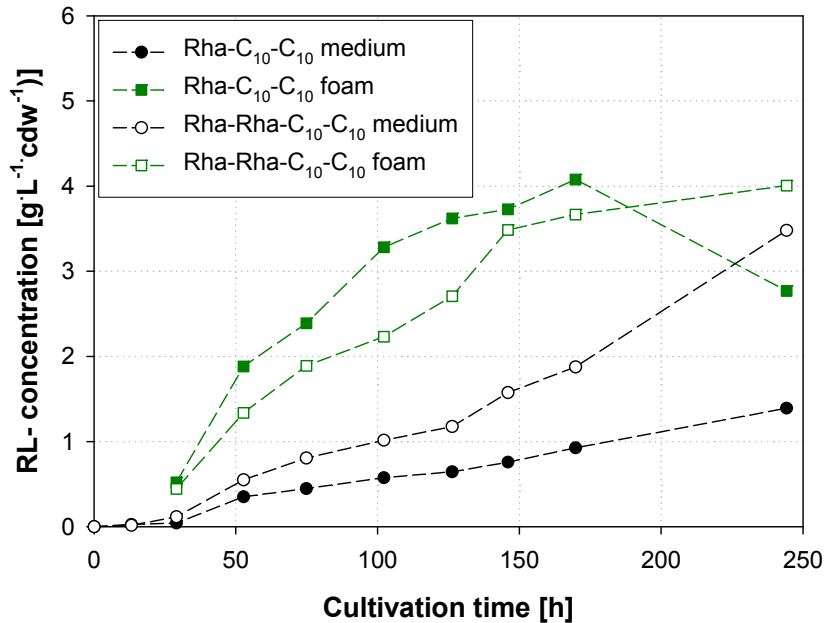
Fig. 5-12: Rhamnolipid concentration profiles in medium and foam of rhamnolipid production with free resting cells of *P. aeruginosa* DSM 2874 in a closed loop process

5.4.4.2 Integrated concept for continuous product removal

As described in materials and methods, the 10 L bioreactor was modified for an integrated rhamnolipid production process (see Fig. 5-1). Hence, generated rhamnolipid foam was pressed out of a fractionation column on top of the bioreactor and concentrated due to drainage of production medium. Continuous rhamnolipid production was ensured by magnetic retention of entrained immobilisates with a switchable high gradient magnetic separator and adjustment of the medium level by a production feed. Immobilised bacteria were first grown in a low concentrated mineral salt medium to increase cell activity for rhamnolipid formation, especially after the stressful immobilisation process. Rhamnolipid production started with nitrate depletion after several hours.

The following results are based, if not mentioned otherwise, on the fractionation column with the integrated newel. In the beginning, 2.6 kg of immobilisates were applied in the bioreactor. This quantity however diminished during rhamnolipid production (see paragraph 5.4.4.3), which could not be quantified, and gives thus only an order of magnitude of the biomass participating in rhamnolipid production.

Just as with free resting cells, rhamnolipid concentrations were higher in foam and also in collapsed foam, collected in a separate receptacle, than in production medium (see Fig. 5-13). The higher rhamnolipid concentrations in foam compared to the collapsed foam were caused by the backflushing step of magnetically separated immobilisates into the bioreactor. Although the silicon tubes between the fractionation column and the magnetic separator

were cleared from production medium by an additional pumping step after backflushing, some millilitres of medium still rested in sections with ascending tubes. These were entrained with the rhamnolipid foam into the foam receptacle, diluting the collapsed foam.
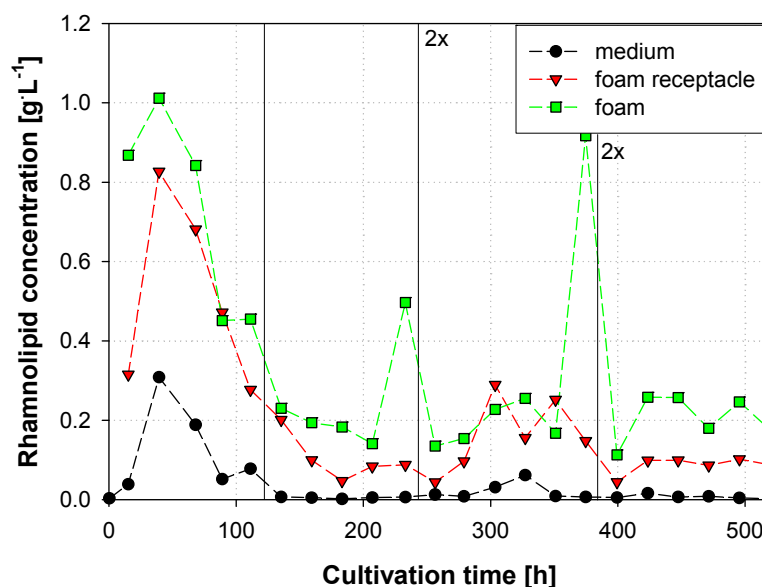
Fig. 5-13: Rhamnolipid concentration profiles in medium, foam and collapsed foam of rhamnolipid production with alginate-Bayoxide® immobilisates of *P. aeruginosa* DSM 2874 in an integrated production system with foam fractionation column and magnetic separator, vertical bars indicate growth medium addition times with 2x for double concentrated medium

For periods with high rhamnolipid production rates, enrichment factors were relatively comparable to those obtained with free resting cells (see Fig. 5-14). However, if rhamnolipid production slowed down (before addition of growth medium), rhamnolipid enrichment ratios in the foam drastically increased to values around 100 or even higher. In contrast, enrichment ratios of collapsed foam were smaller than of foam due to the backflushing step. The higher rhamnolipid enrichment can be explained on the one hand by the lower rhamnolipid concentrations in the production medium, as fewer molecules competed for adsorption space at the bubble interface and also larger and drier bubbles were formed (see foam fractionation experiments). Only in the beginning and after the second addition of growth medium, rhamnolipids accumulated to a certain extent (up to $0.3 \: g L^{-1}$) in the production medium, as cultivation conditions were not sufficient for complete rhamnolipid removal by foam fractionation. On the other hand residence times of foam in the fractionation column increased with lower rhamnolipid concentrations, leaving more time for medium drainage.

Compared to the 1 m fractionation column without fixtures, the obtained rhamnolipid concentrations and enrichment ratios were quite identical (data not shown). By forcing the foam to rise in circles with only a slight slope, better water drainage was expected as

reported by Morgan [116], who suggested an almost horizontal foam fractionation column for better water outflow and yielded enrichment increases by a factor of 1.5 to 4.8 depending on the surfactant. However, the installation of the newel inside the fractionation column did not improve visible medium drainage out of foam in our rhamnolipid production processes.
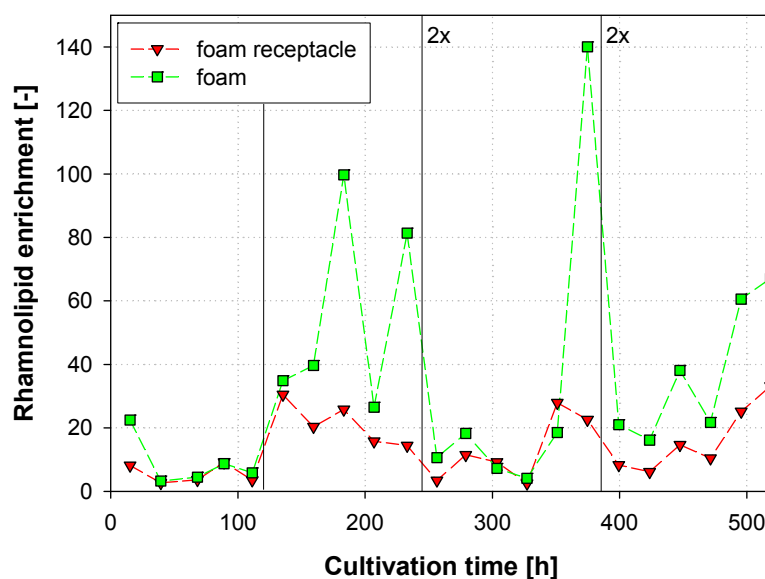
Fig. 5-14: Rhamnolipid enrichment ratios of foam and collapsed foam to production medium of rhamnolipid production with alginate-Bayoxide® immobilisates of *P. aeruginosa* DSM 2874 in an integrated production system with foam fractionation column and magnetic separator, vertical bars indicate growth medium addition times with 2x for double concentrated medium

As already mentioned above for the magnetic separation experiments with cell free immobilisates, backflushing of ferromagnetic immobilisates, used for rhamnolipid production, did not achieve 100%. Even with the improved system, including a pneumatic ball vibrator and two consecutive backflushing steps, some immobilisates remained in the filter chamber and plugged it little by little, making several exchanges of the filter matrix necessary. Additionally, polymeric material, probably attrition from alginate beads or formed by-products from bacteria, and small magnetic immobilisates partly clogged the membrane fixed around the small punnet at the end of the tube, through which medium was pumped out of the bioreactor during backflushing. This effect leaded to slower backflushing rates and required an uprating of the stirrer speed to 800 rpm after 180 h of cultivation time. Lower enrichment ratios due to the smaller bubble sizes were successfully prevented by subsequently reducing the gas flow rate to 0.5 L·min^{-1}.

In summary, complete and continuous separation of rhamnolipids from production medium, with average enrichment ratios of ~15 in the collapsed foam, have been achieved by an integrated reactor design with product removal by foam fractionation and magnetic retention of immobilisates.

5.4.4.3 Repeated production cycles

Rhamnolipid production with immobilised bacteria also slowed down (see Fig. 5-15), as with free resting cells in the closed loop system, but already after approximately 100 to 150 h (depending on the fermentation). Productivity decrease may be explained by the limitation of certain substrates (e.g. nitrate, mineral trace elements) for rhamnolipid induction, which are yet necessary for enzyme synthesis and different processes within the bacterial cells. Production feed for level adjustment in the bioreactor thus only contained glycerol as substrate and calcium chloride for stabilisation of the immobilisation matrix. Additionally, environmental conditions of immobilised bacteria may be different to that of free cells, generally leading to lower rhamnolipid formation rates for equal viable cell concentrations due to diffusion limitations, different pH values or accumulation of by-products in the immobilisates.
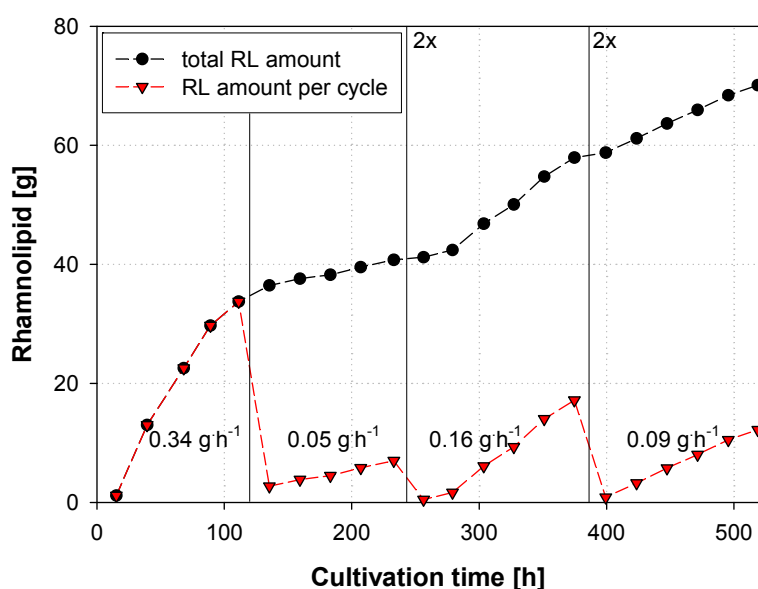
Fig. 5-15: Produced total rhamnolipid and rhamnolipid amounts per cycle during rhamnolipid production with alginate-Bayoxide® immobilisates of *P. aeruginosa* **DSM 2874 in an integrated production system with foam fractionation column and magnetic separator, vertical bars indicate growth medium addition times with 2x for double concentrated medium**

For reactivation of rhamnolipid production, mineral salt medium was added in tenfold concentration to the production medium after every 5 to 6 days. Aim of this procedure was on the one hand as mentioned an anew induction of rhamnolipid synthesis by providing the necessary mineral salts. After the first addition of growth medium, rhamnolipid synthesis rates decreased from 0.34 $g \cdot L^{-1}$ to 0.05 $g \cdot L^{-1}$. However, by addition of the double mineral salt concentrations (2x), rhamnolipid synthesis could successfully be re-induced to a production rate of 0.16 $g \cdot L^{-1}$. Directly after addition of growth medium and thus nitrate, rhamnolipid production slowed down before anew induction by nitrate depletion. The slightly lower synthesis rates for later cultivation times could partly be explained by the reduced amount of

cell immobilisates, which sometimes slipped through the magnetic separator or were removed during the exchange of a plugged up filter matrix. This fact led to an increase in the size distribution of immobilisates during cultivation, maybe implicating reduced rhamnolipid synthesis rates due to higher diffusion limitations. A second reason was definitely the reduction of viable cell concentrations in the immobilisates as well as in the production medium due to bacterial decease, cell-leakage out of the immobilisates and removal of free cells by flotation with the rhamnolipid foam (see Fig. 5-16).
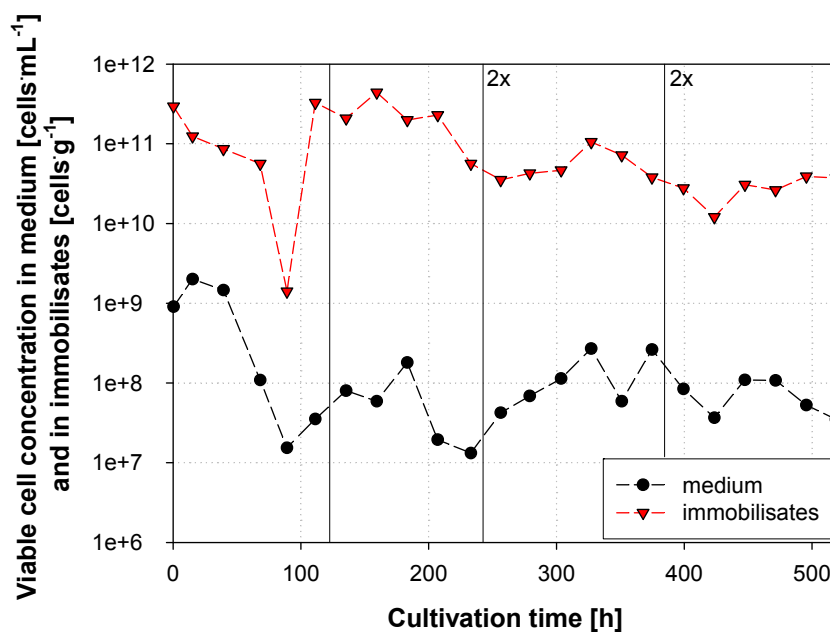
Fig. 5-16: Development of viable cell concentrations in immobilisates and medium during rhamnolipid production with alginate-Bayoxide® immobilisates of *P. aeruginosa* DSM 2874 in an integrated production system with foam fractionation column and magnetic separator, vertical bars indicate growth medium addition times with 2x for double concentrated medium

Therefore, the second aim of growth medium addition was an increase of bacterial concentration. However, even though a decrease of dissolved oxygen and glycerol concentrations in the medium indicated a higher cell activity, any significant cell growth could not be detected. Reliable statements were especially difficult, as cell counts highly fluctuated due to process conditions. Matulovic [111] demonstrated that considerable cell growth of immobilised *P. aeruginosa* DSM 2874 was possible in separate growth medium to reach initial rhamnolipid synthesis rates. For continuous rhamnolipid production, principally care has to be taken, that channels inside the immobilisates are not clogged by excessive cell growth.

After four production cycles a total rhamnolipid amount of 70 g has been achieved. From this rhamnolipid yield less than approximately 10% resulted from free bacterial cells, which leaked out of magnetic immobilisates. The specific biomass/substrate yield amounted to 0.03 g RL per g glycerol with a space time yield of 0.023 $g \cdot L^{-1} \cdot h^{-1}$. These relatively low values

result from the fact that also glycerol is partly removed from the bioreactor by foam fractionation, although glycerol concentrations in the production feed were already kept quite low. Optimisation of the yields could be possible by recirculation of collapsed foam after rhamnolipid separation (e.g. by XAD adsorber resin) or by improvement of medium drainage by significantly higher and larger fractionation columns or multistage foam fractionation [114]. Concerning the space time yield of rhamnolipid production, higher values (e.g. $0.05 \text{ g}^{\cdot}\text{L}^{-1}\cdot\text{h}^{-1}$ for the first production cycle) could presumably be obtained by higher growth medium concentrations or completion of fresh cell immobilisates to reach initial rhamnolipid synthesis rates. A conclusion of the presented results can be drawn, that continuous rhamnolipid production is principally possible by the integrated reactor design with product removal by foam fractionation and magnetic retention of immobilisates.

5.5 Conclusions

In this study, we have demonstrated that continuous rhamnolipid production with intermediate growth periods is possible by an integrated reactor design. Formed rhamnolipids were continuously separated from production medium by foam fractionation and entrained immobilisates of *P. aeruginosa* DSM 2874 retained by magnetic separation.

As rhamnolipid synthesis is quorum sensing regulated [125, 126], the basis for this concept was the production of high biomass concentrations in a first fed-batch fermentation step in a 10 L bioreactor by an exponential feed concept of the carbon source glycerol. Final concentrations of cell dry weights of $15 \text{ g}^{\cdot}\text{L}^{-1}$ have been achieved, which are higher than values reported in literature for growth of *P. aeruginosa* on glycerol [2, 59, 96, 153, 155].

This biomass was subsequently immobilised in calcium alginate beads with concurrently embedded ferrimagnetic Bayoxide® magnetite in a suspension polymerisation process, which was facile to handle and yielded large quantities of immobilisates in a short time. Immobilisation of the biocatalyst in a magnetic matrix was necessary for its retention in the production medium. In a second fermentation step rhamnolipids were produced with the immobilised bacteria in a 10 L bioreactor.

Due to their ability to form micelles, in situ removal of rhamnolipids seamed only to be enduringly possible by foam fractionation. Fractionation tests with cell free immobilisates revealed an antithetic behaviour of rhamnolipid enrichment and mass flow rate thus facing one with an optimisation task. Primarily however, rhamnolipid enrichment was influenced by rhamnolipid concentrations in the production medium, which was highest for very low concentrations. In practice, fermentation conditions were therefore chosen in a way that produced rhamnolipids were completely separated from production medium with minimum stirrer speeds and gas flow rates, yielding at the same time higher rhamnolipid enrichments through lower rhamnolipid concentrations in the medium.

As immobilisates were also entrained with the foam, their magnetic separation by a high gradient magnetic separator out of foam turned out to be well suited, compared to simple sieves or membranes [111]. In practice, the HGF 10 designed by Hoffmann et *al.* [72], which operates in a cyclic fashion using "switchable" permanent magnets, permitted a reliable separation over long production times.

For rhamnolipid production in the integrated reactor concept, complete and continuous separation of rhamnolipids from production medium with average enrichment ratios of ~15 in the collapsed foam has been achieved. A total rhamnolipid yield of 70 g over four production cycles revealed the feasibility of a continuous rhamnolipid production, yet leaving potential for further improvements regarding constantly high cell concentrations and lower substrate wastage.

6 Development and trends of biosurfactant analysis and purification using rhamnolipids as an example

6.1 Abstract

During the last decades, increasing interest in biological surfactants led to an intensification of research for the cost-efficient production of biosurfactants compared to traditional petrochemical surface-active components. The quest for alternative production strains also is associated with new demands on biosurfactant analysis. The present paper will give an overview of the analytical methods existing, based on the example of rhamnolipids. The methods reviewed range from simple colorimetric testing to sophisticated chromatographic separation coupled with detection systems like mass spectrometry, by means of which detailed structural information is obtained. HPLC coupled with mass spectrometry presents currently the most precise method for rhamnolipid identification and quantification. Suitable approaches to accelerate rhamnolipid quantification for better control of biosurfactant production are HPLC analysis directly from culture broth by adding an internal standard or FTIR-ATR measurements of culture broth as possible quasi-online quantification method in the future. The search for alternative rhamnolipid-producing strains makes a structure analysis and constant adaptation of the existing quantification methods necessary. Therefore, simple colorimetric tests based on whole rhamnolipid content can be useful for strain and medium screening. Furthermore, rhamnolipid purification from a fermentation broth will be considered depending on the following application.

6.2 Introduction

During the last decades, extensive research was performed in the field of biosurfactants [95, 101, 120, 150]. These are surface-active metabolites produced by microorganisms. Biosurfactants have the potential to be applied in detergents, pharmaceuticals, cosmetics, and in food industry [9, 38, 49, 85, 94, 104]. Contrary to traditionally produced surfactants based on petroleum feedstock, they are better biodegradable and do not permanently pollute the environment. Apart from a good effectiveness they exhibit an antimicrobial activity against other microorganisms [9, 38].

Even though the biotechnological production of biosurfactants has already been established for several years, high production costs due to intense foaming and expensive downstream processing have prevented their wide use up to now. Attempts are being made to overcome these difficulties by using cheaper substrates, optimising the process to improve yields, and integrating the process to reduce downstream process steps [48, 119, 166]. Furthermore, mutant and recombinant rhamnolipid-producing strains are developed to increase the yields

by several factors. A better understanding of the natural role of biosurfactants in biofilms for example [23, 35] may also provide for new approaches to increasing production yields.

Some of the most extensively studied biosurfactants are the rhamnolipids, mostly produced by *Pseudomonas aeruginosa* [94]. Rhamnolipids are composed of one or two rhamnose molecules and up to three molecules of hydroxy fatty acids, whereas their chain length can vary from 8 up to 14 carbon molecules [40, 58, 60]. In research related to these rhamnolipids, a large variety of analytical methods has been employed to identify and quantify the different rhamnolipid species. These methods range from simple colorimetric measurement of the rhamnose moiety after rhamnolipid hydrolysis [26] to a sophisticated analysis of sample composition by mass spectrometry [40, 41]. In order to compare the results of different research groups or to choose the appropriate method for a certain research activity (e.g. strain screening, process optimisation, etc.) and laboratory equipment some characteristics have to be considered. Among these are rapidity, the measuring range, accuracy, instrumentation, and costs of the method. The present review will compare the different methods applied in the analysis of rhamnolipids so far and give as well an overview of the purification methods existing. The advantages and disadvantages of these analytical methods will be discussed. Recent developments made to accelerate rhamnolipid analysis for a better control of biosurfactant production will be presented.

6.3 Rhamnolipid analysis techniques

6.3.1 Indirect methods

Indirect methods are based on physical properties of rhamnolipids, such as alteration of interfacial tension due to the amphiphilic character of the biosurfactant or haemolysis, the breaking open of red blood cells with the release of haemoglobin into the surrounding medium. The influence of rhamnolipids on different bacteria, fungi, and algae [60, 65, 74, 77, 162] here is not considered an analytical method.

6.3.1.1 Surface tension

Amphiphilic molecules accumulate at the interface of different media and form micelles or vesicles above a certain concentration, called the critical micelle concentration (CMC). Below this value, surface or interfacial tension depends on the concentration of the active compound and can be used for an indirect quantification of the total rhamnolipid content using a calibration curve with pure rhamnolipid for comparison. Analysis is carried out with tensiometers [56] or with mercury electrodes [47], where the differential capacity potential is changed due to an adsorption of rhamnolipids on the electrodes. Samples have to be diluted to a concentration ranging from about 1 to 50 mg·L^{-1} prior to surface tension measurement [174]. Drawbacks of this method are the susceptibility to other surface-active compounds, the

variable influence of every rhamnolipid species on surface tension, and the lack of information about sample composition. Tensiometric measurements were applied widely in the early days of rhamnolipid research [56, 136] due to their simplicity. They are still used, especially for new rhamnolipid species [65, 124, 162].

6.3.1.2 Haemolytic activity

Haemolytic activity tests (HAT) can be performed in two ways. Firstly, on blood agar plates (BAP) which contain mammalian blood (usually sheep) in differential media. β-haemolytic activity indicates a complete lysis of the red blood cells surrounding the bacteria colonies, while α-haemolysis just partially lyses haemoglobin and appears green. These ready-made agar plates can only be used for screening new biosurfactant-producing strains and not for medium optimisation as medium composition cannot be altered. Moreover, the reaction is not specific for rhamnolipids, since lytic enzymes (e.g. protease, lysozyme, etc.) undergo the same reaction [146].

Secondly, quantitative HATs are carried out using erythrocyte suspensions and by measuring the released haemoglobin absorbance at 540 nm [80]. The smallest amount of haemolysin causing a complete lysis of the blood cells is considered one haemolytic unit (HU). The disadvantages are the same as those mentioned above.

6.3.2 Colorimetric methods

Colour reactions are generally performed by binding a dye to the rhamnolipid (e.g. CTAB agar test) or by reaction of the rhamnose moiety with a coloured chemical compound (e.g. anthrone method, orcinol test, and others), which can be quantified afterwards by photometry. These assays were and still are applied most frequently in rhamnolipid analysis.

6.3.2.1 CTAB agar test

This semi-quantitative agar plate cultivation test is based on the formation of an insoluble ion pair of anionic surfactants with the cationic surfactant cetyltrimethylammonium bromide (CTAB) and the basic dye methylene blue [146]. As the constitution of the agar medium, containing 0.2 g·L^{-1} CTAB and 0.005 g·L^{-1} methylene blue, can be altered, this quick and simple test is well-suited for medium optimisation and screening new anionic biosurfactant production strains or mutants [129]. Rhamnolipids are detected as dark blue halos around the colonies, with the spot diameter being dependent on rhamnolipid concentration. Nevertheless, care has to be taken in quantification, as the spot diameter is influenced by variable cell growths of the bacteria, cultivation times, migrations of the rhamnolipids and filling levels of the agar plates.

6.3.2.2 Anthrone method

This colorimetric test is based on the reaction of rhamnose in the presence of a strong acid with anthrone (9,10-dihydro-9-oxoanthracene), forming a dye by heating, which can be measured at 625 nm by a photometer against a calibration curve with rhamnose or rhamnolipid [66, 71] (Fig. 6-1).
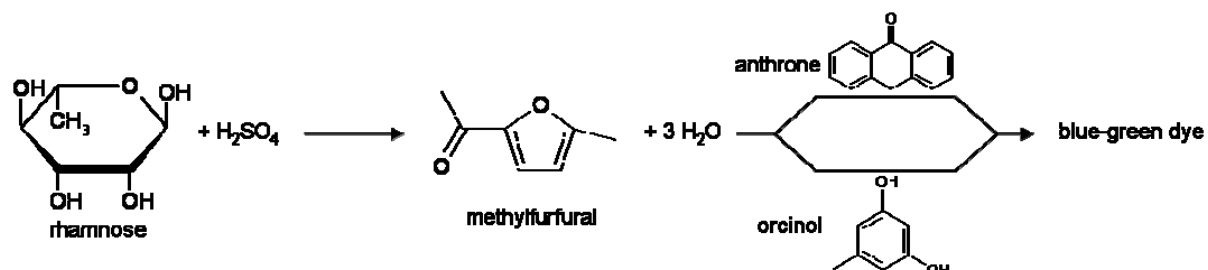
Fig. 6-1: Reaction scheme of the anthrone method and orcinol assay

As it is a quick and simple assay that does not require any expensive instrumentation, it is often used just for the detection of rhamnolipids or quantification of the total rhamnolipid content down to 20 mg·L^{-1}. For this purpose, the composition of the rhamnolipid mixture has to be known.
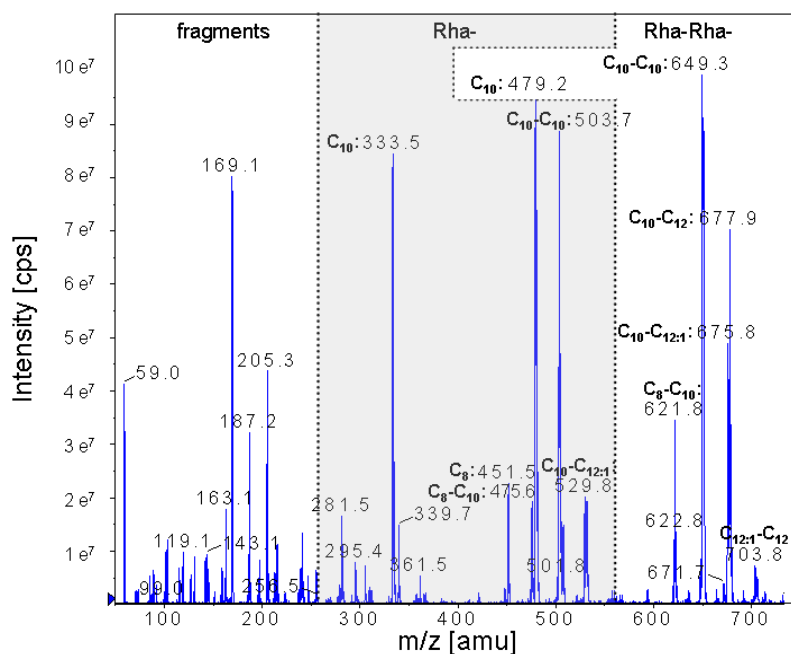
Fig. 6-2: Mass spectrometer spectrum of a rhamnolipid crude extract divided into a mass range for mono- and di-rhamnolipids with different fatty acid chain lengths (e.g. Rha-C$_{10}$-C$_{10}$) and some of their fragments

However, it generally changes during rhamnolipid production (Fig. 6-2) or in adsorption experiments [122], which may render the method inexact. Additionally, interferences of several solvents, inorganic salts (e.g. NaCl), carbonyl or oxidising compounds and proteins

with the reaction have been reported [71]. An advantage consists in the possibility of treating larger quantities of samples on the micro titre plate scale [50].

6.3.2.3 Orcinol assay

In analogy to the anthrone method, this method modified by Chandrasekaran et *al.* [26] is based on using a dye for the quantification of the rhamnolipid content in a sample by absorption measurements at 421 nm (Fig. 6-1). In this case, the rhamnose molecule of rhamnolipids reacts with sulphuric acid and orcinol (1,3-dihydroxy-5-methylbenzene) at high temperatures (30 min at 80°C) to give a blue-green colour [88].

6.3.3 Chromatographic methods

One of the main disadvantages of the indirect and colorimetric methods described above is the ignorance of sample composition and, hence, the occurrence of various rhamnolipid species. Chromatographic separation of a rhamnolipid mixture, coupled with appropriate detection methods like mass spectrometry, revealed that the hydroxy fatty acid moiety of the rhamnolipids may comprise various fatty acid chain lengths [18, 40, 60, 113, 137] (Tab. 6-1).

Tab. 6-1: Structures of rhamnolipids from *Pseudomonas aeruginosa* DSM 2874 and some of their fragments detected by MS after cultivation with sunflower oil as carbon source

compound	pseudomolecular ion (m/z)	fragment ions (m/z)
Rha-C_8	305	141
Rha-C_{10}	333	169
Rha-C_{12}	361	197
Rha-C_8-C_8	447	305, 283, 141
Rha-C_8-C_{10}	475	311, 305, 169, 141
Rha-C_{10}-C_8	475	333, 311, 169, 141
Rha-C_{10}-C_{10}	503	339, 333, 169
Rha-C_{10}-$C_{12:1}$	529	365, 333, 195, 169
Rha-$C_{12:1}$-C_{10}	529	365, 359, 195, 169
Rha-C_{10}-C_{12}	531	367, 333, 197, 169
Rha-C_{12}-C_{10}	531	367, 361, 197, 169
Rha-Rha-C_8	451	141
Rha-Rha-C_{10}	479	169
Rha-Rha-$C_{12:1}$	505	195
Rha-Rha-C_{12}	507	197
Rha-Rha-C_8-C_8	593	451, 283, 141
Rha-Rha-C_8-C_{10}	621	451,311,169,141
Rha-Rha-C_{10}-C_8	621	479, 311, 169, 141
Rha-Rha-C_8-$C_{12:1}$	647	451, 337, 195, 141
Rha-Rha-$C_{12:1}$-C_8	647	505, 337, 195, 141
Rha-Rha-C_{10}-C_{10}	649	479, 339, 169
Rha-Rha-C_{10}-$C_{12:1}$	675	479, 365, 195, 169
Rha-Rha-$C_{12:1}$-C_{10}	675	505, 365, 195, 169
Rha-Rha-C_{10}-C_{12}	677	479, 367, 197, 169
Rha-Rha-C_{12}-C_{10}	677	507, 367, 197, 169
Rha-Rha-C_{10}-$C_{14:1}$	703	479, 391, 221, 169
Rha-Rha-$C_{12:1}$-C_{12}	703	505, 393, 197, 195

Firstly, different chromatographic separation methods and, if necessary, derivation reactions of pre-purified rhamnolipid samples will be discussed. Different extraction procedures for preliminary purification will be presented in the purification chapter. Rhamnolipid detection methods for structure analysis or quantification will be outlined in more detail in the next subchapter.

6.3.3.1 Thin-layer chromatography

Thin-layer chromatography (TLC) has been used extensively for determining the composition of culture broth extracts of rhamnolipids [37, 137, 153] and for their preliminary purification on a thicker chromatographic layer.

For the separation of different rhamnolipid species (the simplest separation is that into mono- and dirhamnolipids), normal-phase or reversed-phase chromatography can be employed. Normal-phase chromatography on silica 60 plates with a solvent mixture of chloroform – methanol – water or 20% aqueous acetic acid (65:15:2) allows for the division into mono- and disaccharide polar head groups. TLC with RP-8 plates using a mixture of methanol – water – trifluoroacetic acid (90:10:0.25) results in a good separation of a rhamnolipid mixture on the basis of the length of the fatty acid alkyl chain [37].

Separate rhamnolipid spots can be detected by staining and comparison with the retention times of standard substances. Suitable staining reagents for rhamnolipids are cer-ammoniummolybdenum acid and diphenylamine or reagents specific for sugars (anthrone, 4-methoxy-benzaldehyde) and fatty acids (bromocresol green, bromothymol blue, 2',7'-dichlorofluoresceine). Densiometric quantification by the spot diameter and intensity is also possible, if the sample is prepared automatically in advance. However, this method is not very accurate and larger quantities of rhamnolipids (> 10 µg) are needed compared to other quantification methods (not suited for analysis of trace concentrations).

An alternative for rhamnolipid identification is to couple TLC analysis with a detection system based on e.g. fast atom bombardment (FAB) [37, 137]. This combination even allows to distinguish different fatty acid chains and their sequences inside the rhamnolipid that cannot be dissociated by chromatography. However, no quantification is possible. For this reason, the method is not used frequently.

Nevertheless, large numbers of samples with small volumes can be treated by TLC and less organic solvents are consumed compared to column chromatography.

6.3.3.2 Gas chromatography

As whole rhamnolipids cannot be used for gas chromatography (GC), these are hydrolysed prior to analysis. Hydrolysis of rhamnolipids can be performed with acids (e.g. triflouroacetic acid) or bases (NaOH) which do not cleave the two fatty acid chains of the di-rhamnolipid.

Separation of rhamnose or fatty acids by gas chromatography, coupled with flame ionisation detectors (FID) or mass spectrometers (MS), has been reported [4, 109, 153, 165].

Rhamnose is analysed quantitatively after conversion into trimethylsilyl esters, not giving any structural information about rhamnolipid composition [4].

In contrast to this, analysis of fatty acids or their methyl esters (after methylation with boron trifluoride for example) with GC shows the whole spectrum of hydroxy fatty acids in rhamnolipids. Contrary to many cases of HPLC-MS analysis, the exact arrangement of the fatty acids in rhamnolipids cannot be obtained by GC.

6.3.3.3 High-performance liquid chromatography

Contrary to the methods described so far, high-performance liquid chromatography (HPLC) is not only appropriate for the complete separation of different rhamnolipid species [4, 40, 99, 109, 143], but can also be coupled with various detection devices (UV, MS, ELSD) for identification and quantification of rhamnolipids.

Tab. 6-2: Gradient method for rhamnolipid separation by reversed-phase chromatography in an RP-18 column

step	time (min)	% acetonitrile	% 10 mM ammonium acetate
0	0.1	42	58
1	3	42	58
2	9	70	30
3	1	70	30
4	12	42	58

While normal-phase chromatography of rhamnolipids is quite popular in TLC, analytical column chromatography uses mostly reversed-phase silica columns with a gradient of acetonitrile (ACN) and water (30-70% ACN to 70-100% ACN) [11, 40, 41, 109, 143, 160]. For better rhamnolipid separation acids or ammonium acetate are added to the solvent, depending on the detection system used (Tab. 6-2). Structural isomers of rhamnolipids (e.g. Rha-C_{10}-C_8 and Rha-C_8-C_{10}) cannot be separated by these HPLC methods. They are distinguished by tandem-mass spectrometry (MSMS) based on their distinct fragmentation.

As rhamnolipids are only very faintly sensitive to ultraviolet light (detection limit 0.2 g), derivation to p-bromophenacyl esters for UV detection at 265 nm is recommended [143]. This derivation is achieved by a reaction of the rhamnolipid crude extract with p-bromoacetophenone and triethylamine at a molar ratio of 1:4:2 in acetonitrile at 60°C for one hour, the derivation rate being about 95%. By means of evaporative light scattering detection (ELSD, measurement of the analyte droplet size after solvent evaporation) or mass spectrometry, rhamnolipids can be detected without derivation [4, 122].

Their identification by comparison with retention times of standard substances is necessary for ELSD and UV detection. When coupled with tandem-mass spectrometry, identification

and quantification should be performed in the multiple reaction mode (MRM), which means that only defined analytes are recorded via several specific pseudomolecular ions (PI, quantifiers and qualifiers). This results in the advantage that even overlapping substances can be identified (by qualifier PI) and quantified (by quantifier PI) exactly, but only, if they are included in the MRM method. Suitable instrument settings for MS detection are a source temperature of 450°C (without split) and negative ionisation at -4800 V to obtain negative [M-H]$^-$ ions. The negative ion mode is used, because identification and quantification in the positive mode are difficult due to the formation of adducts by ammonium or sodium ions in the sample.
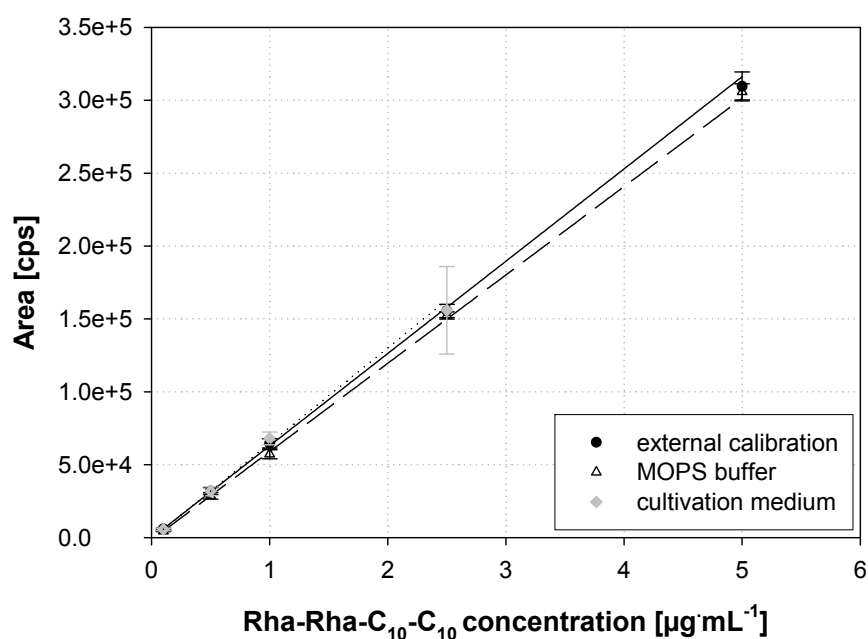
Fig. 6-3: Comparison of the external HPLC-MS calibration curve of rhamnolipid Rha-Rha-C$_{10}$-C$_{10}$ with the calibration in a buffer or cultivation medium followed by extraction with ethyl acetate and dilution

A suitable measuring range for rhamnolipid quantification with an ELSD detector lies between 0.015 and 1.5 g·L^{-1}. Linear calibration for derived rhamnolipids and UV detection is possible between 0.01 and 0.25 g·L^{-1} rhamnolipid. Even lower concentrations (approx. $1 \cdot 10^{-5}$ g·L^{-1}) were detected by HPLC-MS, with a linear correlation of the peak area and rhamnolipid concentration over a range of almost two magnitudes.

Especially when HPLC-MS is used, samples should be pre-purified, as salts and some other impurities influence rhamnolipid ionisation in the ion source of the MS and, hence, affect the signal intensities measured. During these purification steps (e.g. centrifugation, extraction, solvent evaporation), losses of analyte may occur, which are evaluated by examining the recovery rates. For derivation including UV detection pursuant the method of Schenk et al. [143], recovery rates of about 70% were estimated. If derivation is not needed (HPLC-MS),

recovery rates higher than 90% have been achieved (Fig. 6-3). Generally, care has to be taken as regards analyte losses during the extraction of small quantities, as these may be very high due to the amphiphilic character of the rhamnolipids (Fig. 6-4).
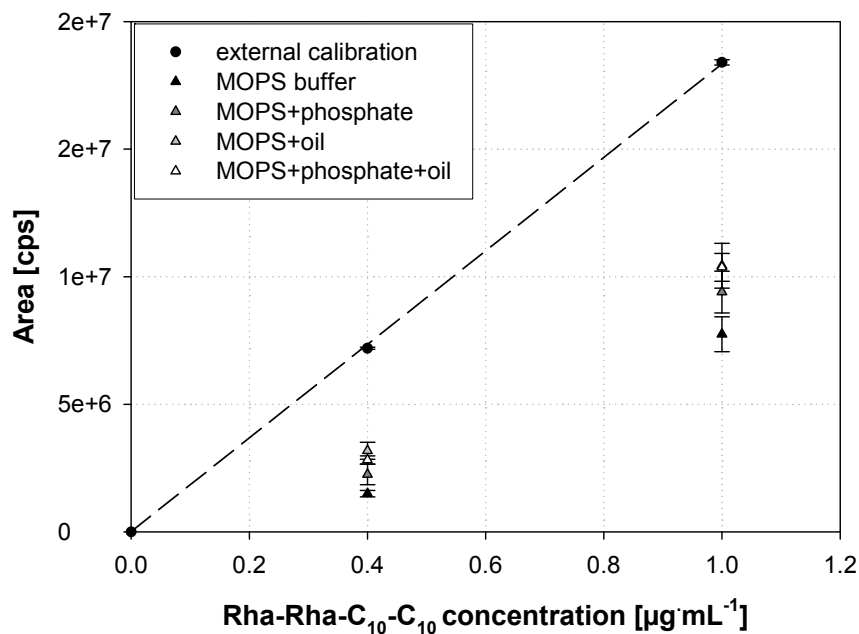
Fig. 6-4: Recovery of rhamnolipid Rha-Rha-C_{10}-C_{10} from different media compared to an external HPLC-MS calibration curve for small initial concentrations

By adding an appropriate internal standard (e.g. hydroxyatrazine for phenacyl esters [143] for UV detection and 16-hydroxyhexadecanoic acid for rhamnolipid quantification by HPLC-MS [41]), measuring errors due to losses during sample preparation and changes of analyte ionisation may be compensated. The latter problem may also be overcome by standard addition experiments. If high sample dilution is possible (for matrix reduction) and optimised geometries are available for ionisation in mass spectrometers, purification steps prior to HPLC-analysis may even be omitted by using an internal standard [41]. Own work has shown that an internal standard must exhibit properties that are equivalent to those of rhamnolipids during chromatographic separation and ionisation for MS and can be applied in a certain measuring range only.

For all detection methods described, standard substances have to be used for calibration to quantify properly - simple comparison of intensities of several species with one standard curve generally is not sufficient. Suitable calibration methods (e.g. external standard, enriched media, internal standard, etc.) are selected depending on the recovery rates and changes of sample composition.

The high sensitivity of HPLC-MS allows for an analysis down to trace concentrations. When coupled with HPLC and a proper sample preparation, it is the most precise method for

rhamnolipid identification and quantification. Another advantage is the possibility to handle a high number of samples.

6.3.4 Composition and purity analysis

For a better understanding of the relationship among the chemical structures of rhamnolipids, the composition of mixtures, and their surface-active properties, detailed structural analysis is necessary. This is achieved by mass spectrometry, infrared spectroscopy (IR), and nuclear magnetic resonance spectrometry (NMR). Mass spectrometry also allows to examine a rhamnolipid mixture composition. Compared to formerly applied methods like the hydrolysis of rhamnolipids and measurement of the fatty acid content by gas chromatography [153], the methods discussed below provide for a better insight into the structure composition of rhamnolipids, even for isomers [40, 60, 113].

6.3.4.1 Mass spectrometry

Nowadays, mixture composition and structure analysis can be performed by tandem quadrupole mass spectrometers (developed in the late 1970's). Good rhamnolipid ionisation is achieved by electrospray ionisation (ESI) for direct infusion or HPLC-MS, as it represents a "soft" method with little fragmentation of primary molecules. Ionised molecules are selected by a mass analyser according to their mass-to-charge ratio (m/z) and detected subsequently. Instrument settings are optimised by infusion experiments.
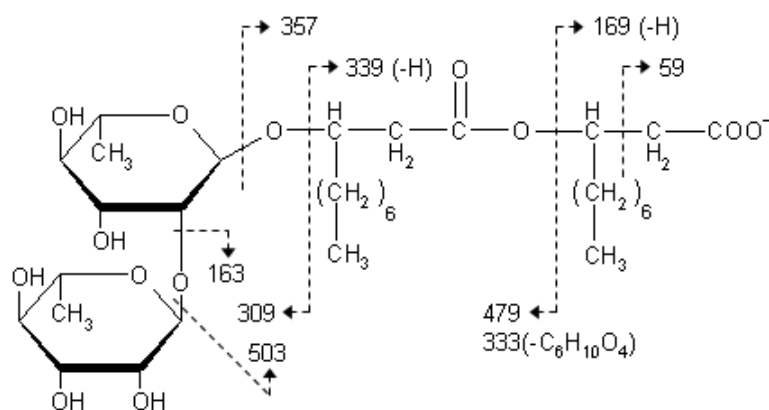
Fig. 6-5: Possible fractionation sites of rhamnolipid Rha-Rha-C_{10}-C_{10}

Scanning of the whole mass spectrum between 100 and 750 Da (Q_1 scan) in the negative MS mode allows for the selection of the target ions (different rhamnolipids). A typical mass spectrum (Q_1 scan) of a rhamnolipid mixture is presented in figure 2. Structural identification of the target ions can be accomplished by MSMS experiments (product ion scans, PIC), which means that a target ion is fractionated in the collision cell and the fragment ions (e.g. hydroxy fatty acids, rhamnose fragments, etc.) are detected. Potential sites of fracture for

rhamnolipids are marked in Fig. 6-5, with Rha-Rha-C_{10}-C_{10} being used as an example. Known rhamnolipid species typically produced by *Pseudomonas aeruginosa*, their pseudomolecular primary ions, and some corresponding fragment ions are listed in Tab. 6-1, demonstrating that even isomers (e.g. Rha-C_{10}-C_{12} and Rha-C_{12}-C_{10}) can be discriminated [40, 60].

6.3.4.2 Fourier transform infrared spectroscopy

A classical method for structure analysis is infrared spectroscopy. Irradiation of molecules with infrared light induces an oscillation of chemical bonds at characteristic frequencies and, thus, energy is absorbed. The resulting transmission of radiation is measured over a frequency spectrum from about 400 to 4000 cm^{-1}. The so-called fingerprint area between 400 to 1500 cm^{-1} shows deformation bands which are characteristic of every molecule and allow for the chemical substances to be identified by spectrum files. Partial structures are analysed by dilation oscillations in the area of 1500 to 4000 cm^{-1}, as chemical bonds generate distinct valency oscillation bands. A characteristic FTIR transmittance spectrum of Rha-Rha-C_{10}-C_{10} is shown in Fig. 6-6.
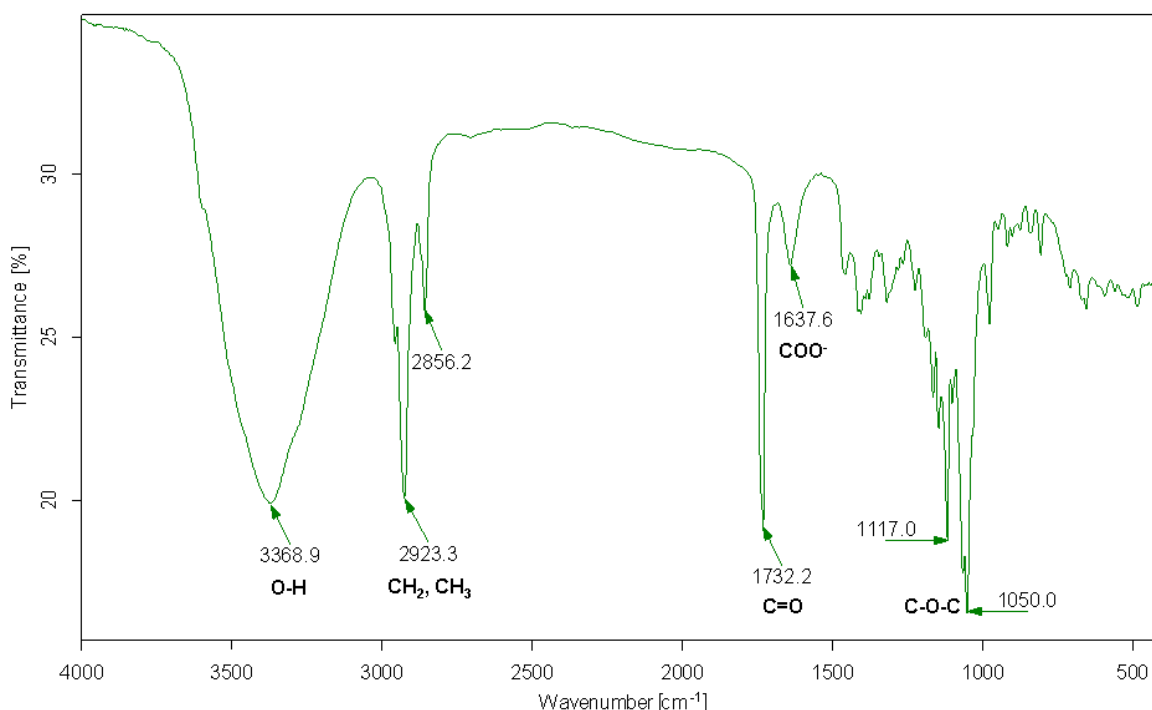
Fig. 6-6: FTIR transmittance spectrum of a potassium bromide pellet of rhamnolipid Rha-Rha-C_{10}-C_{10} from *Pseudomonas aeruginosa* measured in the FTIR spectrometer IFS 66 from Bruker

However, one of the most commonly used techniques for rhamnolipid analysis by IR is Fourier transform infrared attenuated total reflectance spectroscopy (FTIR-ATR) [17, 162]. Apart from structure analysis, it is being attempted to rapidly and simply quantify

biosurfactants even in culture broth and mixtures with a view to obtain an online method for total rhamnolipid analysis [53]. Quantification in biosurfactant model solutions is based on the peak area due to the carbonyl bond in comparison to an internal standard (anthracene carbonitrile) in a concentration range suitable for fermentation monitoring (0.2 - 3 $g \cdot L^{-1}$). Depending on other medium compounds present, use of several characteristic peaks may be more accurate. Online measurements are especially useful for the process optimization of rhamnolipid production during fermentations. ATR probes for direct introduction into bioreactors are commercially available (www.hitec-zang.de), but have not yet been used for the monitoring of rhamnolipid concentrations in bioreactors. Drawbacks of rhamnolipid quantification by FTIR may consist in a certain sensibility to other medium components and pH influence, resulting in measurement errors in excess of 50% [53]. However, analysis is much quicker than in case of HPLC as samples do not have to be treated before the measurements.

6.3.4.3 Nuclear magnetic resonance spectroscopy

NMR spectroscopy allows for an even more accurate structure and purity analysis than IR spectroscopy disposing of solid state and high resolution techniques. NMR spectroscopy is based on transitions in atoms with a magnetic moment when applying an external magnetic field. Structure information is obtained from three parameters: chemical shifts of the absorption frequency, coupling (mutual influence of adjacent nuclei), and integral height. Different techniques, such as COSY (correlation spectroscopy), HMQC (heteronuclear multiple quantum coherence), etc., can be applied for NMR [113].

Tab. 6-3: [1]H chemical shifts (ppm) of mono- and di-rhamnolipids according to Choe et *al.* [32]

residue	proton	Rha-C_{10}-C_{10}	Rha-Rha-C_{10}-C_{10}
rhamnose 1	H-1	4.89	4.93
	H-2	3.87	4.05
	H-3	3.72	3.78
	H-4	3.39	3.44
	H-5	3.70	3.72
	CH_3 (ring)	1.28	1.27
rhamnose 2	H-1		4.95
	H-2		3.87
	H-3		3.70
	H-4		3.40
	H-5		3.80
	CH_3 (ring)		1.27
lipid A	CH	4.12	4.09
	CH_2	2.64	2.61
	CH_2	1.60	1.59
	$(CH_2)_5$	1.28	1.27
	CH_3	0.88	0.85

lipid B	CH	5.28	5.23
	CH_2	2.51	2.47
	CH_2	1.63	1.61
	$(CH_2)_5$	1.28	1.27
	CH_3	0.88	0.85

One and two-dimensional ^1H and ^{13}C NMR spectroscopy have already been performed for pure rhamnolipids [32, 113]. Measurements of deuterium-exchanged samples are generally carried out in chloroform-deuterated methanol (2:1 v/v) using tetramethylsilane as the internal standard. The chemical shifts and coupling constants obtained by the ^1H NMR of rhamnolipids are listed in Tab. 6-3 and Tab. 6-4, see Choe et *al.* [32]. In the last years, NMR spectroscopic analysis [113, 155, 170] was performed in principle to confirm the structure of rhamnolipids produced by recently isolated or mutant bacteria strains compared to rhamnolipids mentioned in literature [77, 78, 153].

Tab. 6-4: Coupling constants (Hz) of mono- and di-rhamnolipids according to Choe et *al.* [32]

residue	proton	$Rha-C_{10}-C_{10}$	$Rha-Rha-C_{10}-C_{10}$
rhamnose 1	$J(1,2)$	2.4	2.5
	$J(2,3)$	3.4	3.2
	$J(3,4)$	9.5	9.4
	$J(4,5)$	9.9	9.7
	$J(5,6)$	6.4	6.4
rhamnose 2	$J(1,2)$		2.2
	$J(2,3)$		3.7
	$J(3,4)$		9.8
	$J(4,5)$		9.9
	$J(5,6)$		6.4

6.4 Rhamnolipid purification procedures

6.4.1 Batch-wise separation of rhamnolipids from culture broth

After rhamnolipid production, a high expenditure is required for purification procedures to achieve a pure product. First, the production medium has to be separated from the microorganisms and the liquid volume has to be reduced. On the laboratory scale, microorganisms are generally removed by centrifugation prior to further purification steps. Preliminary purification can be performed in batches by precipitation, solvent extraction or selective crystallisation.

6.4.1.1 Precipitation

Two different kinds of precipitation can be discriminated: acid [40, 165, 174] or aluminium sulphate precipitation [143]. Through acidification of the medium to a final pH between 2 and

3, rhamnolipids are existent in their acid form and are therefore less soluble in an aqueous solution. The precipitate can be collected by centrifugation (after several hours at 4°C) and resuspended in an appropriate buffer (e.g. bicarbonate). Aluminium sulphate also lowers the pH and precipitates rhamnolipids through salting-out.

6.4.1.2 Solvent extraction

Rhamnolipid extraction is often used for removing hydrophilic compounds prior to rhamnolipid analysis. Different solvents and solvent mixtures like ethyl acetate or chloroform/ methanol (2:1) are applied [109, 143, 160]. In general, the extraction yield can be improved by an acidification of the sample prior to extraction, as rhamnolipids are present in their protonated form and, hence are less soluble in water.

6.4.1.3 Selective crystallisation

Selective crystallisation may be applied after precipitation or extraction of rhamnolipid mixtures from culture broth and re-dissolution in an organic solvent (e.g. ethyl acetate). As rhamnolipids are concentrated in the solvent mixture, the addition of hexane or another comparable solvent, combined with a temperature reduction, results in the selective crystallisation of a rhamnolipid species due to the reduced solubility of the rhamnolipid in the solvent. This has already been observed for Rha-Rha-C_{10}-C_{10} which often is the most abundant rhamnolipid in mixtures [106].

Secondly, a crystallization process is used to obtain pure crystals of Rha-Rha-C_{10}-C_{10} after chromatographic purification steps. Lyophilisation in 0.05 M sodium bicarbonate solution causes the formation of crystals of mono-rhamnolipids, which cannot be obtained by solvent evaporation in the presence of water.

6.4.2 Continuous separation of rhamnolipids from culture broth

As product inhibition occurs at higher rhamnolipid concentrations, continuous separation of rhamnolipids from culture broth is desired in some cases for a continuous rhamnolipid production with a permanent product removal to achieve higher product yields. Several options are available for this purpose, including rhamnolipid adsorption on a resin or activated carbon, ion exchange chromatography, membrane filtration, or foam fractionation after cell separation or immobilisation. Combination of several purification processes, as proposed by Reiling et *al.* [136] for adsorption and ion exchange columns, improves the results of the downstream processing of larger culture broth quantities.

6.4.2.1 Adsorption

Most frequently, Amberlite XAD 2 or 16 polystyrene resin that absorb and release hydrophobic and amphiphilic substances (e.g. rhamnolipids) due to basically hydrophobic

interactions are used [1, 55, 60, 111, 136]. For primary enrichment, cell-free culture broth is directly applied to the adsorbent column and equilibrated with 0.1 M phosphate buffer at pH 6.1. Exhaustion of the adsorbent resin can be monitored by surface tension or UV absorption measurements for example [111, 136]. Washing of the resin with distilled water removes some pigments and free fatty acids [1]. Finally, rhamnolipids are eluted with methanol and the solvent is evaporated subsequently. Further purification of the crude rhamnolipid mixture can be performed by chromatographic methods after re-dissolving the rhamnolipids in an appropriate buffer. The adsorbent is regenerated with 1 M NaOH as described by Reiling et al. [136].

An adsorption material studied more recently is wood activated carbon (WAC) [44]. Adsorption is possible at a pH ranging from 5 to 10 and a temperature of 40°C, desorption (and regeneration) takes place with acetone at 30°C to recover almost 90% of rhamnolipids. The WAC can be re-used several times and in particular allows for the separation of water-soluble pigments from the rhamnolipids.

Adsorption chromatography represents a good alternative to solvent extraction, the advantages being a continuous process and smaller solvent consumption.

6.4.2.2 Ion exchange

Another purification step of the rhamnolipid mixture is anion exchange chromatography [110, 136, 143]. Rhamnolipids are charged negatively at higher pH values, so that they can be separated by a weak anion exchanger (e.g. DEAE-Sepharose). The anion exchanger is equilibrated with a tris hydrochloride buffer (pH 8 or higher) containing 10% (v/v) ethanol. According to own results, rhamnolipids are released from the resin by adding at least 0.6 M NaCl to the equilibration buffer. A second adsorption step or extraction removes the salt from the rhamnolipid fractions. Subsequent solvent evaporation and freeze-drying yield a solid and quite hygroscopic rhamnolipid mixture, still containing some fatty acids and pigments. The ion exchange resin can be regenerated with a buffer containing 2 M NaCl and 20% ethanol (or methanol for pigment ejection) [136].

6.4.2.3 Membrane filtration

Membrane filtration is another alternative for rhamnolipid enrichment and pre-purification [55, 65, 119]. Generally, ultra-filtration with a membrane cut-off of 10 kDa leads to an almost complete retention of rhamnolipids even at a neutral pH [55]. But also with bigger pores (e.g. 0.2 µm), high rhamnolipid retention rates are be obtained under certain conditions. Low pH values, rhamnolipid concentrations above the critical micelle concentration, proteins and other culture broth ingredients can promote rhamnolipid aggregation to micelles [55, 142]. By the direct filtration of culture broth, a gel layer forms on the membrane due to fouling, which also acts like a membrane. Consequently, in-situ product removal concepts for cell retention

and continuous rhamnolipid removal failed due to micelle formation [55]. In contrast to this, smaller medium components can be separated from rhamnolipids [118].

6.4.2.4 Foam fractionation

Foam fractionation by contrast uses the peculiarity of rhamnolipids of forming micelles and, thus, of foaming. When applied for the continuous removal of rhamnolipids during fermentations, foam is allowed to press out of the bioreactor through a fractionation column. Afterwards, it collapses in a separate recipient by acids or shear forces [55, 111].

Rhamnolipids adsorb on the interface of air bubbles and medium depending on the pH, the ionic strength and the concentration of other surface active compounds [67, 128]. With increasing residence time of the foam in the fractionation column, gravitational forces result in the drainage of the liquid in the foam lamellae, thus enriching rhamnolipids in the foam up to approximately 12 g$\cdot$L^{-1} [55]. As recovery decreases at the same time, foam fractionation conditions have to be traded off depending on the pre-purification desired. Factors influencing rhamnolipid enrichment, recovery, and the foam formation rate are given in Tab. 6-5.

Tab. 6-5: Factors influencing enrichment, recovery, foam formation rate, and purification of rhamnolipids by foam fractionation (flashes indicate a change of direction) based on literature [19, 55, 128]

process variables	enrichment	recovery	foam formation rate
RL feed concentration ↑	↓	↑	↑
foam height ↑	↑	↓	
gas flow ↑	↓	↑	↑
bubble size ↑ (sparger)	↑	↓	↓
stirring speed ↑	↓	↑	↑
foam-stabilising component ↑	↓		↑
competitive adsorption	↓	↓	
effects of cells	↓	cells show higher enrichment than RLs	
pH value ↑	↑	purification better with pH > 6	
temperature ↑	↑	↓	

As regards rhamnolipid purification, adsorption of bacteria in foam is higher than that of rhamnolipids and proteins [55]. Hence, immobilisation of the bacteria and retention of the immobilisates in the bioreactor are necessary for product enrichment. Given that a higher enrichment of rhamnolipids is possible with low rhamnolipid concentrations in the culture medium (Fig. 6-7) and long residence times in the fractionation column only [55], this method is more effective in continuous rhamnolipid removal during fermentation (to achieve higher rhamnolipid production yields) than in purification.
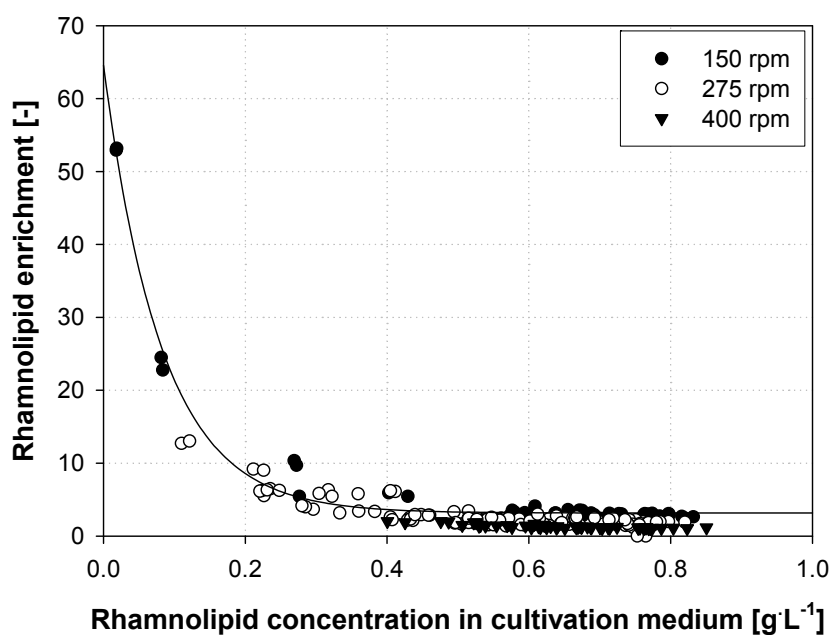
Fig. 6-7: Rhamnolipid enrichment by foam fractionation as a function of rhamnolipid concentration in the cultivation medium

6.4.3 Chromatographic separation of rhamnolipid mixtures

After rhamnolipid separation from bacterial cells and some water-soluble substances, chromatographic methods are applied to obtain pure rhamnolipids. For smaller volumes, preparative thin-layer chromatography may be applied, whereas larger quantities are separated by column chromatography (e.g. silica gel or reversed-phase material).

6.4.3.1 Preparative thin-layer chromatography

The process of preparative thin-layer chromatography is similar to analytical TLC. Generally, preparative silica gel plates are used with a solvent mixture of chloroform – methanol – water / acetic acid (e.g. 65:15:2) or mixtures of equivalent polarities. As one chromatographic run is not sufficient to achieve pure rhamnolipids, TLC often is performed several times with solvents of different polarities [40, 165] or after column chromatography for precision cleaning [113, 149]. Samples are applied onto TLC plates after extraction from culture broth and concentration. The separated rhamnolipids are eluted from silica by methanol or chloroform-methanol [113, 149, 165]. Advantages of TLC are its simple feasibility and the need of less equipment than for preparative column chromatography. On the other hand, only smaller quantities of samples can be treated. Consequently, it is suited in particular for analytical calibration standard purification and not for industrial downstream processing.

6.4.3.2 Normal phase

Normal phase column chromatography using silica is a standard purification method for rhamnolipid separation if larger volumes have to be treated [77, 113, 143, 149]. The acidified rhamnolipid mixture, in a solvent like chloroform, is fed into the column after various pre-purification steps (e.g. centrifugation and extraction or adsorption on a resin) to separate bacterial cells (generally *Pseudomonas aeruginosa*) and some water-soluble compounds. Flushing of silica with chloroform removes neutral lipids and some pigments [77, 149]. Rhamnolipids can be eluted with chloroform – methanol at the ratio of 50:3 for Rha-C_{10}-C_{10} (RL 1) and 50:5 for the remaining RL 1 to achieve a better separation, as it was done in our group. Ultimate scrubbing at a ratio of 50:50 removes Rha-Rha-C_{10}-C_{10} (RL 2). Thereafter, the solvent of the red-brown coloured rhamnolipid fractions is evaporated. Dissolution of the residue in alkaline solution, followed by acidification and recrystallisation yields crystalline rhamnolipids according to their number of sugar and hydroxy fatty acid molecules [77]. Apart from recrystallisation, pure rhamnolipids can also be obtained by re-application to column or thin-layer chromatography [77, 149].

6.4.3.3 Reversed phase

As already described for the analytical separation of rhamnolipids, mixtures are separated by reversed-phase chromatography according to the chain length of the hydroxy fatty acids [37]. Pre-purified rhamnolipid mixtures are acidified and fed into an RP18 column. Our group separated the rhamnolipids isocratically using 70% acetonitrile and 30% distilled water. The resulting fractions of the main rhamnolipids (RL 1, RL 2) are free from fatty acids or pigments and give a white powder after crystallisation. Hence, a secondary treatment is not necessary. However, column material is more expensive than normal silica. Therefore, it is used for semi-preparative purposes only.

6.5 Conclusions

Rhamnolipid analysis is carried out by methods ranging from simple colorimetric tests to sophisticated chromatographic separation, coupled with detection systems like mass spectrometry to provide detailed structural information. Most commonly, rhamnolipids are extracted from culture broth and then subjected to HPLC analysis. In this case, HPLC coupled with mass spectrometry presents for the moment the most precise method for rhamnolipid identification and quantification. Recently, efforts were made to accelerate rhamnolipid quantification for better control of biosurfactant production. Suitable approaches are HPLC analysis directly from culture broth by adding an internal standard or FTIR-ATR measurements of culture broth as quasi-online quantification method. Concerning FTIR-ATR, further efforts for application to complex rhamnolipid solutions have to be made. The search

for alternative rhamnolipid-producing strains makes a structure analysis and constant adaptation of the existing quantification methods necessary. Therefore, simple colorimetric tests based on whole rhamnolipid content can provide a useful tool for strain and medium screening.

For downstream processing, the purification method chosen depends on the application desired. As costs of biosurfactant production have to be reduced for the latter be applied widely as detergents or emulsifiers, different approaches to process integration with a continuous removal of rhamnolipids from the bioreactor are being investigated, such as foam fractionation, membrane techniques or adsorption. For high-purity products, chromatography followed by crystallisation still is the method of choice.

7 References

1. Abalos, A., A. Pinazo, M.R. Infante, M. Casals, F. Garcia, and A. Manresa, *Physicochemical and antimicrobial properties of new rhamnolipids produced by Pseudomonas aeruginosa AT10 from soybean oil refinery wastes.* Langmuir, 2001. 17(5): p. 1367-1371.

2. Abalos, A., F. Maximo, M.A. Manresa, and J. Bastida, *Utilization of response surface methodology to optimize the culture media for the production of rhamnolipids by Pseudomonas aeruginosa AT10.* J Chem Technol Biot, 2002. 77(7): p. 777-784.

3. Al-Tahhan, R.A., T.R. Sandrin, A.A. Bodour, and R.M. Maier, *Rhamnolipid-induced removal of lipopolysaccharide from Pseudomonas aeruginosa: Effect on cell surface properties and interaction with hydrophobic substrates.* Appl Environ Microbiol, 2000. 66(8): p. 3262-3268.

4. Arino, S., R. Marchal, and J.-P. Vandecasteele, *Identification and production of a rhamnolipidic biosurfactant by a Pseudomonas species.* Appl Microbiol Biot, 1996. 45(1 - 2): p. 162-168.

5. Arshady, R., *Microspheres and microcapsules: A survey of manufacturing techniques. Part 1: Suspension cross-linking.* Polym Eng Sci, 1989. 29(24): p. 1746-1758.

6. Arshady, R., *Beaded polymer supports and gels : I. Manufacturing techniques.* J Chromatogr A, 1991. 586(2): p. 181-197.

7. Arshady, R., *Suspension, emulsion, and dispersion polymerization - a methodological survey.* Colloid Polym Sci, 1992. 270(8): p. 717-732.

8. Banat, I.M., *Biosurfactants production and possible uses in microbial enhanced oil-recovery and oil pollution remediation - a review.* Bioresource Technol, 1995. 51(1): p. 1-12.

9. Banat, I.M., R.S. Makkar, and S.S. Cameotra, *Potential commercial applications of microbial surfactants.* Appl Microbiol Biot, 2000. 53(5): p. 495-508.

10. Benincasa, M., J. Contiero, M.A. Manresa, and I.O. Moraes, *Rhamnolipid production by Pseudomonas aeruginosa LBI growing on soapstock as the sole carbon source.* J Food Eng, 2002. 54(4): p. 283-288.

11. Benincasa, M., A. Abalos, I. Oliveira, and A. Manresa, *Chemical structure, surface properties and biological activities of the biosurfactant produced by Pseudomonas aeruginosa LBI from soapstock.* Anton Leeuw Int J G, 2004. 85(1): p. 1-8.

12. Berensmeier, S., M. Ergezinger, M. Bohnet, and K. Buchholz, *Design of immobilised dextransucrase for fluidised bed application.* J Biotechnol, 2004. 114(3): p. 255-267.

13. Berger, R., *Immobilisierung mikrobieller Zellen und deren Nutzung zur Substratwandlung - Eine Literaturstudie.* Acta Biotechnol, 1981. 1(1): p. 73-102.

14. Bienaimé, C., J.-N. Barbotin, and J.-E. Nava-Saucedo, *How to build an adapted and bioactive cell microenvironment? A chemical interaction study of the structure of Ca-alginate matrices and their repercussion on confined cells.* J Biomed Mater Res A, 2003. 67A(2): p. 376-388.

15. Bieringer, H., K. Flatau, and D. Reese, *Industrielle Aspekte der Suspensionspolymerisation.* Angewandte Makromolekulare Chemie, 1984. 123(1): p. 307-334.

16. Boonyasuwat, S., S. Chavadej, P. Malakul, and J.F. Scamehorn, *Surfactant recovery from water using a multistage foam fractionator: Part I - Effects of air flow rate, foam*

height, feed flow rate and number of stages. Sep Sci Technol, 2005. 40(9): p. 1835-1853.

17. Borgund, A.E., K. Erstad, and T. Barth, *Normal phase high performance liquid chromatography for fractionation of organic acid mixtures extracted from crude oils.* J Chromatogr A, 2007. 1149(2): p. 189-196.

18. Bosch, M.-P., J.L. Parra, M.-A. Manresa, F. Ventura, and J. Rivera, *Analysis of glycolipids by fast atom bombardment mass spectrometry.* Biol Mass Spectrom, 1989. 18(12): p. 1046-1050.

19. Brown, A.K., A. Kaul, and J. Varley, *Continuous foaming for protein recovery: Part I. Recovery of beta-casein.* Biotechnol Bioeng, 1999a. 62(3): p. 278-290.

20. Brown, A.K., A. Kaul, and J. Varley, *Continuous foaming for protein recovery: Part II. Selective recovery of proteins from binary mixtures.* Biotechnol Bioeng, 1999b. 62(3): p. 291-300.

21. Bucke, C., *Cell immobilization in calcium alginate.* Method Enzymol, 1987. 135(Immobilized Enzymes and Cells Part B): p. 175-189.

22. Burger, M.M., L. Glaser, and R.M. Burton, *The enzymatic synthesis of a rhamnose-containing glycolipid by extracts of Pseudomonas aeruginosa.* J Biol Chem, 1963. 238(8): p. 2595-2602.

23. Caiazza, N.C., R.M.Q. Shanks, and G.A. O'Toole, *Rhamnolipids modulate swarming motility patterns of Pseudomonas aeruginosa.* J Bacteriol, 2005. 187(21): p. 7351-7361.

24. Cameotra, S.S. and R.S. Makkar, *Synthesis of biosurfactants in extreme conditions.* Appl Microbiol Biot, 1998. 50(5): p. 520-529.

25. Chan, L.W., H.Y. Lee, and P.W.S. Heng, *Production of alginate microspheres by internal gelation using an emulsification method.* Int J Pharm, 2002. 242(1-2): p. 259-262.

26. Chandrasekaran, E.V. and J.N. BeMiller, *Constituent analysis of glycosaminoglycans*, in *Methods in carbohydrate chemistry*, R.L. Whistler, Editor. 1980, Academic Press, Inc.: New York. p. 89-96.

27. Chayabutra, C., J. Wu, and L.-K. Ju, *Rhamnolipid production by Pseudomonas aeruginosa under denitrification: Effects of limiting nutrients and carbon substrates.* Biotechnol Bioeng, 2001. 72(1): p. 25-33.

28. Chen, C.Y., S.C. Baker, and R.C. Darton, *Continuous production of biosurfactant with foam fractionation.* J Chem Technol Biot, 2006a. 81(12): p. 1915-1922.

29. Chen, C.Y., S.C. Baker, and R.C. Darton, *Batch production of biosurfactant with foam fractionation.* J Chem Technol Biot, 2006b. 81(12): p. 1923-1931.

30. Chen, K.C., S.J. Chen, and J.Y. Houng, *Improvement of gas permeability of denitrifying PVA gel beads.* Enzyme Microb Tech, 1996. 18(7): p. 502-506.

31. Chen, K.-C. and Y.-F. Lin, *Immobilization of microorganisms with phosphorylated polyvinyl alcohol (PVA) gel.* Enzyme Microb Tech, 1994. 16(1): p. 79-83.

32. Choe, B.-Y., N.R. Krishna, and D.G. Pritchard, *Proton NMR study on rhamnolipids produced by Pseudomonas aeruginosa.* Magn Reson Chem, 1992. 30(10): p. 1025-1026.

33. Cooper, D.G., C.R. Macdonald, S.J.B. Duff, and N. Kosaric, *Enhanced production of surfactin from Bacillus subtilis by continuous product removal and metal cation additions.* Appl Environ Microb, 1981. 42(3): p. 408–412.

34. Darton, R.C., S. Supino, and K.J. Sweeting, *Development of a multistaged foam fractionation column.* Chem Eng Process, Special Issue on Distillation and Absorption, 2004. 43(3): p. 477-482.

35. Davey, M.E., N.C. Caiazza, and G.A. O'Toole, *Rhamnolipid surfactant production affects biofilm architecture in Pseudomonas aeruginosa PAO1.* J Bacteriol, 2003. 185(3): p. 1027-1036.

36. Davis, D.A., H.C. Lynch, and J. Varley, *The application of foaming for the recovery of Surfactin from B. subtilis ATCC 21332 cultures.* Enzyme Microb Tech, 2001. 28(4-5): p. 346-354.

37. de Koster, C.G., B. Vos, C. Versluis, W. Heerma, and J. Haverkamp, *High-performance thin-layer chromatography/fast atom bombardment (tandem) mass spectrometry of Pseudomonas rhamnolipids.* Biol Mass Spectrom, 1994. 23(4): p. 179-185.

38. Desai, J.D. and I.M. Banat, *Microbial production of surfactants and their commercial potential.* Microbiol Mol Biol R, 1997. 61(1): p. 47-64.

39. Deziel, E., G. Paquette, R. Villemur, F. Lepine, and J.G. Bisaillon, *Biosurfactant production by a soil Pseudomonas strain growing on polycyclic aromatic hydrocarbons.* Appl Environ Microb, 1996. 62(6): p. 1908-1912.

40. Deziel, E., F. Lepine, D. Dennie, D. Boismenu, O.A. Mamer, and R. Villemur, *Liquid chromatography/mass spectrometry analysis of mixtures of rhamnolipids produced by Pseudomonas aeruginosa strain 57RP grown on mannitol or naphthalene.* Biochim Biophys Acta, 1999. 1440(2-3): p. 244-252.

41. Deziel, E., F. Lepine, S. Milot, and R. Villemur, *Mass spectrometry monitoring of rhamnolipids from a growing culture of Pseudomonas aeruginosa strain 57RP.* Biochim Biophys Acta, 2000. 1485(2-3): p. 145-152.

42. Draget, K.I., G. Skjak-Braek, and O. Smidsrod, *Alginate based new materials.* Int J Biol Macromol, 1997. 21(1-2): p. 47-55.

43. Dubey, K. and A. Juwarkar, *Distillery and curd whey wastes as viable alternative sources for biosurfactant production.* World J Microb Biot, 2001. 17(1): p. 61-69.

44. Dubey, K.V. and A.A. Juwarkar, *Adsorption-desorption process using wood-based activated carbon for recovery of biosurfactant from fermented distillery wastewater.* Biotechnol Prog, 2005. 21(3): p. 860-867.

45. Duynstee, H.I., M.J. van Vliet, G.A. van der Marel, and J.H. van Boom, *An efficient synthesis of (R)-3-{(R)-3- 2-O-(alpha-L-rhamnopyranosyl)-alpha-L-rhamnopyranosyl oxyd ecanoyl}oxydecanoic acid, a rhamnolipid from Pseudomonas aeruginosa.* Eur J Org Chem, 1998(2): p. 303-307.

46. Edmonds, P. and J.J. Cooney, *Lipids of Pseudomonas aeruginosa cells grown on hydrocarbons and on trypticase soy broth.* J Bacteriol, 1969. 98(1): p. 16-22.

47. Emons, H., G. Werner, D. Haferburg, and H.-P. Kleber, *Tensammetric determination of a rhamnolipid at mercury electrodes.* Electroanalysis, 1989. 1(6): p. 555-557.

48. Fiechter, A., *Integrated systems for biosurfactant synthesis.* Pure Appl Chem, 1992. 64(11): p. 1739-1743.

49. Fiechter, A., *Biosurfactants: moving towards industrial application.* Trends Biotechnol, 1992. 10: p. 208-217.

50. Fox, J.D. and J.F. Robyt, *Miniaturization of three carbohydrate analyses using a microsample plate reader.* Anal Biochem, 1991. 195(1): p. 93-96.

51. Franzreb, M., *Magnettechnologie in der Verfahrenstechnik wässriger Medien*, in *Forschungszentrum Karlsruhe*. 2003, Eggenstein-Leopoldshafen.

52. Galazzo, J.L. and J.E. Bailey, *Growing Saccharomyces cerevisiae in calcium-alginate beads induces cell alterations which accelerate glucose conversion to ethanol.* Biotechnol Bioeng, 1990. 36(4): p. 417-426.

53. Gartshore, J., Y.C. Lim, and D.G. Cooper, *Quantitative analysis of biosurfactants using Fourier Transform Infrared (FT-IR) spectroscopy.* Biotechnol Lett, 2000. 22(2): p. 169-172.

54. Giani, C., D. Wullbrandt, R. Rothert, and J. Meiwes, *Pseudomonas aeruginosa and its use in process for the biotechnological preparation of L-rhamnose*, in *US patent 5,658,793.* 1997, Hoechst AG, Frankfurt am Main, Germany.

55. Gruber, T., *Verfahrenstechnische Aspekte der kontinuierlichen Produktion von Biotensiden am Beispiel der Rhamnolipide*, in *Lehrstuhl für Bioprozesstechnik.* 1991, Stuttgart. p. 121.

56. Guerra-Santos, L., O. Käppeli, and A. Fiechter, *Pseudomonas aeruginosa biosurfactant production in continuous culture with glucose as carbon source.* Appl Environ Microbiol, 1984. 48(2): p. 301-305.

57. Guerra-Santos, L.H., O. Käppeli, and A. Fiechter, *Dependence of Pseudomonas aeruginosa continous culture biosurfactant production on nutritional and environmental factors.* Appl Microbiol Biot, 1986. V24(6): p. 443-448.

58. Gunther, N.W., A. Nunez, W. Fett, and D.K.Y. Solaiman, *Production of rhamnolipids by Pseudomonas chlororaphis, a nonpathogenic bacterium.* Appl Environ Microbiol, 2005. 71(5): p. 2288-2293.

59. Haba, E., M.J. Espuny, M. Busquets, and A. Manresa, *Screening and production of rhamnolipids by Pseudomonas aeruginosa 47T2 NCIB 40044 from waste frying oils.* J Appl Microbiol, 2000. 88(3): p. 379-387.

60. Haba, E., P. Pinazo, O. Jauregui, M.J. Espuny, M.R. Infante, and A. Manresa, *Physicochemical characterization and antimicrobial properties of rhamnolipids produced by Pseudomonas aeruginosa 47T2 NCBIM 40044.* Biotechnol Bioeng, 2003. 81(3): p. 316-322.

61. Hannoun, B.J.M. and G. Stephanopoulos, *Intrinsic growth and fermentation rates of alginate-entrapped Saccharomyces cerevisiae.* Biotechnol Prog, 1990. 6(5): p. 341-348.

62. Hardegger, M., A.K. Koch, U.A. Ochsner, A. Fiechter, and J. Reiser, *Cloning and heterologous expression of a gene encoding an alkane-induced extracellular protein involved in alkane assimilation from Pseudomonas aeruginosa.* Appl Environ Microb, 1994. 60(10): p. 3679-3687.

63. Hauser, G. and M.L. Karnovsky, *Studies on the production of glycolipid by Pseudomonas aeruginosa.* J Bacteriol, 1954. 68: p. 645-654.

64. Hauser, G. and M.L. Karnovsky, *Studies on the biosynthesis of L-rhamnose.* J Biol Chem, 1958. 233: p. 287-291.

65. Haussler, S., M. Nimtz, T. Domke, V. Wray, and I. Steinmetz, *Purification and characterization of a cytotoxic exolipid of Burkholderia pseudomallei.* Infect Immun, 1998. 66(4): p. 1588-1593.

66. Helbert, J.R. and K.D. Brown, *Color reaction of anthrone with monosaccharide mixtures and oligo- and polysaccharides containing hexuronic acids.* Anal Chem, 1957. 29(10): p. 1464-1466.

67. Helvaci, S.S., S. Peker, and G. Ozdemir, *Effect of electrolytes on the surface behavior of rhamnolipids R1 and R2.* Colloids Surf B Biointerfaces, 2004. 35(3-4): p. 225-233.

68. Hertz, H., *Über die Berührung fester elastischer Körper.* J reine angew Math, 1882. 92: p. 156-171.

69. Heyd, M., A. Kohnert, T.-H. Tan, M. Nusser, F. Kirschhöfer, G. Brenner-Weiss, M. Franzreb, and S. Berensmeier, *Development and trends of biosurfactant analysis and purification using rhamnolipids as an example.* Anal Bioanal Chem, 2008. 391(5): p. 1579-1590.

70. Hilge-Rotmann, B. and H.-J. Rehm, *Comparison of fermentation properties and specific enzyme activities of free and calcium-alginate-entrapped Saccharomyces cerevisiae.* Appl Microbiol Biot, 1990. 33(1): p. 54-58.

71. Hodge, J.E. and B.T. Hofreiter, *Determination of reducing sugars and carbohydrates*, in *Methods in Carbohydrate Chemistry*, M.L. Wolfrom, Editor. 1962, Academic Press, Inc.: New York. p. 380-394.

72. Hoffmann, C., M. Franzreb, and W.H. Holl, *A novel high-gradient magnetic separator (HGMS) design for biotech applications.* Ieee T Appl Supercon, 2002. 12(1): p. 963-966.

73. Holmberg, K., *Handbook of applied surface and colloid chemistry*. 2002, New York: John Wiley & Sons. p. 217.

74. Howe, J., J. Bauer, J. Andra, A.B. Schromm, M. Ernst, M. Rossle, U. Zahringer, J. Rademann, and K. Brandenburg, *Biophysical characterization of synthetic rhamnolipids.* FEBS J, 2006. 273(22): p. 5101-5112.

75. Hubbuch, J.J. and O.R.T. Thomas, *High-gradient magnetic affinity separation of trypsin from porcine pancreatin.* Biotechnol Bioeng, 2002. 79(3): p. 301-313.

76. Iqbal, S., Z.M. Khalid, and K.A. Malik, *Enhanced biodegradation and emulsification of crude-oil and hyperproduction of biosurfactants by a gamma-ray-induced mutant of Pseudomonas aeruginosa.* Lett Appl Microbiol, 1995. 21(3): p. 176-179.

77. Itoh, S., H. Honda, F. Tomita, and T. Suzuki, *Rhamnolipids produced by Pseudomonas aeruginosa grown on n-paraffin (mixture of C_{12}, C_{13} and C_{14} fractions).* J Antibiot, 1971. 24(12): p. 855-859.

78. Jarvis, F.G. and M.J. Johnson, *A glyco-lipide produced by Pseudomonas aeruginosa.* J Am Chem Soc, 1949. 71: p. 4124-4126.

79. Jeong, H.S., D.J. Lim, S.H. Hwang, S.D. Ha, and J.Y. Kong, *Rhamnolipid production by Pseudomonas aeruginosa immobilised in polyvinyl alcohol beads.* Biotechnol Lett, 2004. 26(1): p. 35-39.

80. Johnson, M.K. and D. Boese-Marrazzo, *Production and properties of heat-stable extracellular hemolysin from Pseudomonas aeruginosa.* Infect Immun, 1980. 29(3): p. 1028-1033.

81. Junter, G.-A., L. Coquet, S. Vilain, and T. Jouenne, *Immobilized-cell physiology: current data and the potentialities of proteomics.* Enzyme Microb Tech, 2002. 31(3): p. 201-212.

82. Kichatov, B.V., A.M. Korshunov, I.V. Boiko, and P.V. Assorova, *Effect of impeller blade geometry on drop size in stirring of immiscible liquids.* Theor Found Chem Eng, 2003a. 37(1): p. 19-24.

83. Kichatov, B.V., A.M. Korshunov, and P.V. Assorova, *Particle size distribution of the product of suspension polymerization.* Theor Found Chem Eng, 2003b. 37(3): p. 306-309.

84. Kim, E.-J., W. Sabra, and A.-P. Zeng, *Iron deficiency leads to inhibition of oxygen transfer and enhanced formation of virulence factors in cultures of Pseudomonas aeruginosa PAO1.* Microbiology, 2003. 149(9): p. 2627-2634.

85.   Kitamoto, D., H. Isoda, and T. Nakahara, *Functions and potential applications of glycolipid biosurfactants - from energy-saving materials to gene delivery carriers.* J Biosci Bioeng, 2002. 94(3): p. 187-201.

86.   Klein, J., *Immobilization of microbial cells in polyurethane matrices.* Biotechnol Lett, 1981. 3(2): p. 65-70.

87.   Klein, J. and F. Wagner, *Different strategies to optimize the production phase of immobilized cells.* Ann NY Acad Sci, 1987. 501: p. 306-316.

88.   Koch, A.K., O. Käppeli, A. Fiechter, and J. Reiser, *Hydrocarbon assimilation and biosurfactant production in Pseudomonas aeruginosa mutants.* J Bacteriol, 1991. 173(13): p. 4212-4219.

89.   Koch, V., H.-M. Rüffer, K. Schügerl, E. Innertsberger, H. Menzel, and J. Weis, *Effect of Antifoam Agents on the Medium and Microbial Cell Properties and Process Performance in Small and Large Reactors.* Process Biochem, 1995. 30(5): p. 435-446.

90.   Kosaric, N., *Biosurfactants in industry.* Pure Appl Chem, 1992. 64(11): p. 1731-1737.

91.   Lang, S., E. Katsiwela, and F. Wagner, *Antimicrobial effects of biosurfactants.* Fett Wissenschaft Technologie/Fat Science Technology, 1989. 91(9): p. 363-366.

92.   Lang, S. and F. Wagner, *Bioconversion of oils and sugars to glycolipids*, in *Biosurfactants (Surfactant Science series)*, N. Kosaric, Editor. 1993, Dekker: New York Basel Hong Kong. p. 206-227.

93.   Lang, S. and D. Wullbrandt, *Rhamnose lipids - biosynthesis, microbial production and application potential.* Appl Microbiol Biot, 1999. 51(1): p. 22-32.

94.   Lang, S. and D. Wullbrandt, *Rhamnose lipids - biosynthesis, microbial production and application potential.* Applied Microbiology and Biotechnology, 1999. 51(1): p. 22-32.

95.   Lang, S., *Biological amphiphiles (microbial biosurfactants).* Curr Opin Colloid In, 2002. 7(1-2): p. 12-20.

96.   Lee, K.M., S.H. Hwang, S.D. Ha, J.H. Jang, D.J. Lim, and J.Y. Kong, *Rhamnolipid production in batch and fed-batch fermentation using Pseudomonas aeruginosa BYK-2 KCTC 18012P.* Biotechnol Bioproc E, 2004. 9(4): p. 267-273.

97.   Lee, S.Y., *High cell-density culture of Escherichia coli.* Trends Biotechnol, 1996. 14(3): p. 98-105.

98.   Leitermann, F., *personal communication.* 2008: TH Karlsruhe.

99.   Lépine, F., E. Déziel, S. Milot, and R. Villemur, *Liquid chromatographic/mass spectrometric detection of the 3-(3-hydroxyalkanoyloxy) alkanoic acid precursors of rhamnolipids in Pseudomonas aeruginosa cultures.* J Mass Spectrom, 2002. 37(1): p. 41-46.

100.   Li, R.H., D.H. Altreuter, and F.T. Gentile, *Transport characterization of hydrogel matrices for cell encapsulation.* Biotechnol Bioeng, 1996. 50(4): p. 365-373.

101.   Lin, S.C., *Biosurfactants: Recent advances.* J Chem Technol Biot, 1996. 66(2): p. 109-120.

102.   Linhardt, R.J., R. Bakhit, L. Daniels, F. Mayerl, and W. Pickenhagen, *Microbially Produced Rhamnolipid as a Source of Rhamnose.* Biotechnol Bioeng, 1989. 33(3): p. 365-368.

103.   Liu, K.K., *Deformation behaviour of soft particles: a review.* J Phys D Appl Phys, 2006. 39(11): p. R189-R199.

104.   Maier, R.M. and G. Soberon-Chavez, *Pseudomonas aeruginosa rhamnolipids: biosynthesis and potential applications.* Appl Microbiol Biotechnol, 2000. 54(5): p. 625-633.

105.   Manresa, M.A., J. Bastida, M.E. Mercadé, M. Robert, C. de Andrés, M.J. Espuny, and J. Guinea, *Kinetic studies on surfactant production by Pseudomonas aeruginosa 44T1.* J Ind Microbiol Biot, 1991. V8(2): p. 133-136.

106.   Manso Pajarron, A., C.G. Koster, W. Heerma, M. Schmidt, and J. Haverkamp, *Structure identification of natural rhamnolipid mixtures by fast atom bombardment tandem mass spectrometry.* Glycoconj J, 1993. 10(3): p. 219-226.

107.   Martinsen, A., G. Skjåk-Bræk, and O. Smidsrød, *Alginate as immobilization material: I. Correlation between chemical and physical properties of alginate gel beads.* Biotechnol Bioeng, 1989. 33(1): p. 79-89.

108.   Martinsen, A., I. Storrø, and G. Skjårk-Bræk, *Alginate as immobilization material: III. Diffusional properties.* Biotechnol Bioeng, 1992. 39(2): p. 186-194.

109.   Mata-Sandoval, J.C., J. Karns, and A. Torrents, *High-performance liquid chromatography method for the characterization of rhamnolipid mixtures produced by Pseudomonas aeruginosa UG2 on corn oil.* J Chromatogr A, 1999. 864(2): p. 211-220.

110.   Matsufuji, M., K. Nakata, and A. Yoshimoto, *High production of rhamnolipids by Pseudomonas aeruginosa growing on ethanol.* Biotechnol Lett, 1997. 19(12): p. 1213-1215.

111.   Matulovic, U., *Verfahrensentwicklung zur Herstellung grenzflächenaktiver Rhamnolipide mit immobilisierten Zellen von Pseudomonas spec. DSM 2874*, in *Institute of Biochemistry and Biotechnology*. 1987, TU Braunschweig. p. 157.

112.   Meyer, A., S. Berensmeier, and M. Franzreb, *Direct capture of lactoferrin from whey using magnetic micro-ion exchangers in combination with high-gradient magnetic separation.* React Funct Polym, 2007. 67(12): p. 1577-1588.

113.   Monteiro, S.A., G.L. Sassaki, L.M. de Souza, J.A. Meira, J.M. de Araujo, D.A. Mitchell, L.P. Ramos, and N. Krieger, *Molecular and structural characterization of the biosurfactant produced by Pseudomonas aeruginosa DAUPE 614.* Chem Phys Lipids, 2007. 147(1): p. 1-13.

114.   Morgan, G. and U. Wiesmann, *Single and multistage foam fractionation of rinse water with alkyl ethoxylate surfactants.* Sep Sci Technol, 2001. 36(10): p. 2247-2263.

115.   Morgan, G. and U. Wiesmann, *Foam fractionation of surfactant-containing rinsing water.* Chem-Ing-Tech, 2002. 74(4): p. 453-457.

116.   Morgan, G., *Foam fractionation of surfactant solutions*, in *Fortschrittsberichte VDI Reihe 3*. 2004, VDI Verlag: Düsseldorf. p. 124.

117.   Mukherjee, S., P. Das, and R. Sen, *Towards commercial production of microbial surfactants.* Trends Biotechnol, 2006. 24(11): p. 509-515.

118.   Mulligan, C.N., G. Mahmourides, and B.F. Gibbs, *Biosurfactant production by a chloramphenicol tolerant strain of Pseudomonas aeruginosa.* J Biotechnol, 1989. 12(1): p. 37-43.

119.   Mulligan, C.N. and B.F. Gibbs, *Recovery of biosurfactants by ultrafiltration.* J Chem Technol Biot, 1990. 47(1): p. 23-29.

120.   Nitschke, M., S.G.V.A.O. Costa, and J. Contiero, *Rhamnolipid surfactants: an update on the general aspects of these remarkable biomolecules.* Biotechnol Prog, 2005. 21(6): p. 1593-1600.

121. Noordman, W.H., W. Ji, M.L. Brusseau, and D.B. Janssen, *Effects of rhamnolipid biosurfactants on removal of phenanthrene from soil.* Environ Sci Technol, 1998. 32(12): p. 1806-1812.

122. Noordman, W.H., M.L. Brusseau, and D.B. Janssen, *Adsorption of a multicomponent rhamnolipid surfactant to soil.* Environ Sci Technol, 2000. 34(5): p. 832-838.

123. Nussinovitch, A., *Resemblance of immobilized Trichoderma viride fungal spores in an alginate matrix to a composite material.* Biotechnol. Prog., 1994. 10(5): p. 551-554.

124. Ochoa-Loza, F.J., W.H. Noordman, D.B. Jannsen, M.L. Brusseau, and R.M. Maier, *Effect of clays, metal oxides, and organic matter on rhamnolipid biosurfactant sorption by soil.* Chemosphere, 2007. 66(9): p. 1634-1642.

125. Ochsner, U.A., A. Koch, A. Fiechter, and J. Reiser, *Isolation and characterization of a regulatory gene affecting rhamnolipid biosurfactant synthesis in Pseudomonas aeruginosa.* J Bacteriol, 1994. 176(7): p. 2044-2054.

126. Ochsner, U.A. and J. Reiser, *Autoinducer-mediated regulation of rhamnolipid biosurfactant synthesis in Pseudomonas aeruginosa.* P Natl Acad Sci USA, 1995. 92(14): p. 6424-6428.

127. Ochsner, U.A., T. Hembach, and A. Fiechter, *Production of rhamnolipid biosurfactants.* Adv Biochem Eng Biot, 1996. 53: p. 89-118.

128. Ozdemir, G., S. Peker, and S.S. Helvaci, *Effect of pH on the surface and interfacial behavior of rhamnolipids R1 and R2.* Colloid Surface A, 2004. 234(1-3): p. 135-143.

129. Perfumo, A., I. Banat, F. Canganella, and R. Marchant, *Rhamnolipid production by a novel thermophilic hydrocarbon-degrading Pseudomonas aeruginosa AP02-1.* Appl Microbiol Biotechnol, 2006. 72(1): p. 132-138.

130. Poncelet, D., R. Lencki, C. Beaulieu, J.P. Halle, R.J. Neufeld, and A. Fournier, *Production of alginate beads by emulsification/internal gelation. I. Methodology.* Appl Microbiol Biot, 1992. 38(1): p. 39-45.

131. Poncelet, D., V. Babak, C. Dulieu, and A. Picot, *A physico-chemical approach to production of alginate beads by emulsification-internal ionotropic gelation.* Colloid Surface A, 1999. 155(2-3): p. 171-176.

132. Prüße, U., J. Dalluhn, J. Breford, and K.-D. Vorlop, *Production of spherical beads by JetCutting.* Chemical Engineering & Technology, 2000. 23(12): p. 1105-1110.

133. Rahim, R., U.A. Ochsner, C. Olvera, M. Graninger, P. Messner, J.S. Lam, and G. Soberon-Chavez, *Cloning and functional characterization of the Pseudomonas aeruginosa rhlC gene that encodes rhamnosyltransferase 2, an enzyme responsible for di-rhamnolipid biosynthesis.* Mol Microbiol, 2001. 40(3): p. 708-718.

134. Ramakrishna, S.V. and R.S. Prakasham, *Microbial fermentations with immobilized cells.* Curr Sci India, 1999. 77(1): p. 87-100.

135. Ramana, K.V. and N.G. Karanth, *Production of biosurfactants by the resting cells of Pseudomonas aeruginosa CFTR-6.* Biotechnol Lett, 1989. 11(6): p. 437-442.

136. Reiling, H.E., U. Thanei-Wyss, L.H. Guerra-Santos, R. Hirt, O. Käppeli, and A. Fiechter, *Pilot plant production of rhamnolipid biosurfactant by Pseudomonas aeruginosa.* Appl Environ Microbiol, 1986. 51(5): p. 985–989.

137. Rendell, N.B., G.W. Taylor, M. Somerville, H. Todd, R. Wilson, and P.J. Cole, *Characterization of Pseudomonas rhamnolipids.* Biochim Biophys Acta, 1990. 1045(2): p. 189-193.

138. Riesenberg, D. and R. Guthke, *High-cell-density cultivation of microorganisms.* Appl Microbiol Biot, 1999. 51(4): p. 422-430.

139. Rosen, M.J., *Surfactants and interfacial phenomena, 3rd edition*. 2004, New York: John Wiley & Sons. p. 464.

140. Rosenberg, M. and E. Rosenberg, *Role of adherence in growth of Acinetobacter calcoaceticus RAG-1 on hexadecane.* J Bacteriol, 1981. 148(1): p. 51-57.

141. Sabra, W., E.-J. Kim, and A.-P. Zeng, *Physiological responses of Pseudomonas aeruginosa PAO1 to oxidative stress in controlled microaerobic and aerobic cultures.* Microbiology, 2002. 148(10): p. 3195-3202.

142. Sanchez, M., F. Aranda, M.J. Espuny, A. Marques, J.A. Teruel, A. Manresa, and A. Ortiz, *Aggregation behaviour of a dirhamnolipid biosurfactant secreted by Pseudomonas aeruginosa in aqueous media.* J Colloid Interface Sci, 2007. 307(1): p. 246-253.

143. Schenk, T., I. Schuphan, and B. Schmidt, *High-performance liquid-chromatographic determination of the rhamnolipids produced by Pseudomonas aeruginosa.* J Chromatogr A, 1995. 693(1): p. 7-13.

144. Schultz, N., C. Syldatk, M. Franzreb, and T.J. Hobley, *Integrated processing and multiple re-use of immobilised lipase by magnetic separation technology.* J Biotechnol, 2007. 132(2): p. 202-208.

145. Shan, G.B., J.M. Xing, M.F. Luo, H.Z. Liu, and J.Y. Chen, *Immobilization of Pseudomonas delafieldii with magnetic polyvinyl alcohol beads and its application in biodesulfurization.* Biotechnol Lett, 2003. 25(23): p. 1977-1981.

146. Siegmund, I. and F. Wagner, *New method for detecting rhamnolipids excreted by Pseudomonas species during growth on mineral agar.* Biotechnol Techniques, 1991. 5(4): p. 265-268.

147. Siemann, M. and F. Wagner, *Prospects and limits for the production of biosurfactants using immobilized biocatalysts*, in *Biosurfactants (Surfactant Science series)*, N. Kosaric, Editor. 1993, Dekker: New York Basel Hong Kong. p. 99-133.

148. Sikorski, P., F. Mo, G. Skjak-Brak, and B.T. Stokke, *Evidence for egg-box-compatible interactions in calcium-alginate gels from fiber x-ray diffraction.* Biomacromolecules, 2007. 8(7): p. 2098-2103.

149. Sim, L., O.P. Ward, and Z.-Y. Li, *Production and characterisation of a biosurfactant isolated from Pseudomonas aeruginosa UW-1.* J Ind Microbiol Biotechnol, 1997. 19(4): p. 232-238.

150. Soberón-Chávez, G., F. Lépine, and E. Déziel, *Production of rhamnolipids by Pseudomonas aeruginosa.* Appl Microbiol Biotechnol, 2005. 68(6): p. 718-725.

151. Sonc, A. and V. Grilc, *Batch foam fractionation of surfactants from aqueous solutions.* Acta Chim Slov, 2004. 51(4): p. 687-698.

152. Svoboda, J., *Magnetic methods for the treatment of minerals*, in *Development in Mineral Processing, 8*. 1987, Elsevier: Amsterdam. p. 682.

153. Syldatk, C., *Mikrobielle Bildung und Charakterisierung grenzflächenaktiver Rhamnolipide aus Pseudomonas spec. DSM 2874*, in *Institute of Biochemistry and Biotechnology*. 1984, TU Braunschweig. p. 99.

154. Syldatk, C., S. Lang, U. Matulovic, and F. Wagner, *Production of four interfacial active rhamnolipids from n-alkanes or glycerol by resting cells of Pseudomonas species DSM 2874.* Z Naturforsch C, 1985. 40(1-2): p. 61-67.

155. Tahzibi, A., F. Kamal, and M.M. Assadi, *Improved production of rhamnolipids by Pseudomonas aeruginosa mutant.* Iran Biomed J, 2004. 8(1): p. 25-31.

156. Tanaka, H., M. Matsumura, and I.A. Veliky, *Diffusion characteristics of substrates in Ca-alginate gel beads.* Biotechnol Bioeng, 1984. 26(1): p. 53-58.

157. Tatara, Y., *On compression of rubber elastic sphere over a large range of displacements---Part 1: Theoretical study.* J Eng Mater-T ASME, 1991. 113(3): p. 285-291.

158. Thanomsub, B., W. Pumeechockchai, A. Limtrakul, P. Arunrattiyakorn, W. Petchleelaha, T. Nitoda, and H. Kanzaki, *Chemical structures and biological activities of rhamnolipids produced by Pseudomonas aeruginosa B189 isolated from milk factory waste.* Bioresource Technol, 2007. 98(5): p. 1149-1153.

159. Thiede, V., N.B. Lopez, L. Pellacani, and F.E. Parks, *Hydrophilic polyurethane polymers derived from a MDI-based isocyanate-terminated prepolymer,* in *US patent WO 2004/074343 A1.* 2004, Dow global technologies Inc., Midland, US.

160. Trummler, K., F. Effenberger, and C. Syldatk, *An integrated microbial/enzymatic process for production of rhamnolipids and L-(+)-rhamnose from rapeseed oil with Pseudomonas sp DSM 2874.* Eur J Lipid Sci Technol, 2003. 105(10): p. 563-571.

161. Tsubomizu, H., R. Horikoshi, K. Yamagiwa, K. Takahashi, M. Yoshida, and A. Ohkawa, *Effect of perforated plate on concentration of poly(vinyl alcohol) by foam fractionation with external reflux.* J Chem Eng Jpn, 2003. 36(9): p. 1107-1110.

162. Tuleva, B.K., G.R. Ivanov, and N.E. Christova, *Biosurfactant production by a new Pseudomonas putida strain.* Z Naturforsch C, 2002. 57(3-4): p. 356-360.

163. Van Delden, C., E.C. Pesci, J.P. Pearson, and B.H. Iglewski, *Starvation selection restores elastase and rhamnolipid production in a Pseudomonas aeruginosa quorum-sensing mutant.* Infect Immun, 1998. 66(9): p. 4499-4502.

164. van Delden, C., R. Comte, and A.M. Bally, *Stringent response activates quorum sensing and modulates cell density-dependent gene expression in Pseudomonas aeruginosa.* J Bacteriol, 2001. 183(18): p. 5376-5384.

165. Van Dyke, M.I., P. Couture, M. Brauer, H. Lee, and J.T. Trevors, *Pseudomonas aeruginosa UG2 rhamnolipid biosurfactants - Structural characterization and their use in removing hydrophobic compounds from soil.* Can J Microbiol, 1993. 39(11): p. 1071-1078.

166. Van Hamme, J.D., A. Singh, and O.P. Ward, *Physiological aspects: Part 1 in a series of papers devoted to surfactants in microbiology and biotechnology.* Biotechnol Adv, 2006. 24(6): p. 604-620.

167. VivaldoLima, E., P.E. Wood, A.E. Hamielec, and A. Penlidis, *An updated review on suspension polymerization.* Ind Eng Chem Res, 1997. 36(4): p. 939-965.

168. Wang, C.X., C. Cowen, Z. Zhang, and C.R. Thomas, *High-speed compression of single alginate microspheres.* Chem Eng Sci, 2005. 60(23): p. 6649-6657.

169. Weaire, D.L. and S. Hutzler, *The physics of foam.* 1999, Oxford: Oxford University Press. p. 246.

170. Wei, Y.-H., C.-L. Chou, and J.-S. Chang, *Rhamnolipid production by indigenous Pseudomonas aeruginosa J4 originating from petrochemical wastewater.* Biochem Eng J, 2005. 27(2): p. 146-154.

171. Westrin, B.A. and A. Axelsson, *Diffusion in gels containing immobilized cells: A critical review.* Biotechnol Bioeng, 1991. 38(5): p. 439-446.

172. Willaert, R.G. and G.V. Baron, *Gel entrapment and micro-encapsulation: Methods, applications and engineering principles.* Rev Chem Eng, 1996. 12(1-2): p. 5-205.

173. Wilms, B., A. Hauck, M. Reuss, C. Syldatk, R. Mattes, M. Siemann, and J. Altenbuchner, *High-cell-density fermentation for production of L-N-carbamoylase using an expression system based on the Escherichia coli rhaBAD promoter.* Biotechnol Bioeng, 2001. 73(2): p. 95-103.

174. Zhang, Y.M. and R.M. Miller, *Enhanced octadecane dispersion and biodegradation by a Pseudomonas rhamnolipid surfactant (biosurfactant).* Appl Environ Microbiol, 1992. 58(10): p. 3276-3282.

175. Zhang, Y.M. and R.M. Miller, *Effect of a Pseudomonas rhamnolipid biosurfactant on cell hydrophobicity and biodegradation of octadecane.* Appl Environ Microbiol, 1994. 60(6): p. 2101-2106.

176. Zlokarnik, M., *Eignung von Rührern zum Homogenisieren von Flüssigkeitsgemischen.* Chem-Ing-Tech, 1967. 39(9/10): p. 539-548.

8 Appendix

8.1 Abbreviations

Alg	alginate
APTES	3-(triethoxysilyl)-propylamine
ATR	attenuated total reflectance
BAP	blood agar plates
C_{10}	hydroxy fatty acid with 10 carbon atoms
cdw	cell dry weight
CER	carbon dioxide evolution rate
cetrimid	N-cetyl-N,N,N-ammoniumbromide
chw	cell humid weight
CMC	critical micelle concentration
COSY	correlation spectroscopy
CTAB	cetyltrimethylammonium bromide
CTC	5-cyano-2,3-ditolyltetrazoliumchloride
DAPI	4',6-diamidino-2-phenylindoledihydrochloride-dilactate
DO	dissolved oxygen
ELSD	evaporative light scattering detector
ESEM	environmental scanning electron microscopy
ESI	electrospray ionisation
FAB	fast atom bombardment
FID	flame ionisation detector
FTIR	Fourier transform infrared spectrometry
GC	gas chromatography
HAT	haemolytic activity test
HCDC	high cell density cultivation
HGMS	high gradient magnetic separation
HMQC	heteronuclear multiple quantum coherence
HPLC	high-performance liquid chromatography
HSL	homoserine lactone
HU	haemolytic unit
IR	infrared spectrometry
LC-MS	liquid chromatography coupled with mass spectrometry
mag	magnetite
MDI	methylene diphenylisocyanate

MOPS	3-(N-morpholino)propanesulphonic acid
MRM	multiple reaction monitoring
MS	mass spectrometry
MSMS	tandem-mass spectrometry
NADH	nicotinamide adenine dinucleotide
NMR	nuclear magnetic resonance
OD	optical density
PI	pseudomolecular ion
PIS	product ion scan
PU	polyurethane
PVAL	polyvinyl alcohol
QS	quorum sensing
Rha	rhamnose
RL	rhamnolipid
RP	reversed-phase
SIMS	secondary ion mass spectrometry
STY	space time yield
TDP	thymidine-diphosphate
TEOS	tetraethylorthosilicate
TES	trace element solution
TLC	thin-layer chromatography
UV	ultra violet
WAC	wood activated carbon

8.2 Symbols

8.2.1 Latin symbols

a_z	circular contact zone of sphere to plate	mm
A	area	mm^2
A_0	cross-section area in the middle of sphere at t = 0 s	mm^2
A_{column}	cross-section of fractionation column	m^2
B	magnetic flux density	T
c_{RL}	rhamnolipid concentration	$g \cdot L^{-1}$
c_{S0}	glycerol concentration in the feeding solution	$g \cdot L^{-1}$
c_{X0}	biomass concentration at start of feeding	$g \cdot L^{-1}$
c_0	concentration in the beginning	$g \cdot L^{-1}$
c_t	concentration at time t	$g \cdot L^{-1}$

c_∞	final concentration after an infinite time	$g \cdot L^{-1}$
d_0	diameter of sphere at t = 0 s	mm
d_{bead}	bead diameter	µm
d_{nozzle}	nozzle diameter of JetCutter®	µm
$d_{stirrer}$	stirrer diameter	M
d_{wire}	wire diameter of cutting tool	µm
D_{eff}	effective diffusion coefficient	$cm^2 \cdot s^{-1}$
$D_{eff,0}$	effective diffusion coefficient in cell free matrix	$cm^2 \cdot s^{-1}$
D_m	demagnetisation factor	-
E	foam elasticity	$kg \cdot s^{-2}$
E	Young's modulus	$N \cdot mm^{-2}$
E'	plane Young's modulus	$N \cdot mm^{-2}$
E_r	enrichment ratio	-
F	feeding rate	$L \cdot h^{-1}$
F	force	N
F_d	deformation force	N
F_m	magnetic force	N
h	actual sphere height	mm
h_0	sphere height at t = 0 s	mm
Δh	change in height due to compression	mm
H	magnetic field strength	$A \cdot m^{-1}$
∇H	gradient of magnetic field strength	$A \cdot m^{-2}$
J	permeability of diffusion path	$m^2 \cdot s \cdot kg^{-1}$
J	magnetic polarisation	T
m	specific maintenance coefficient	$g \cdot g^{-1} \cdot h^{-1}$
m_{RL}	rhamnolipid mass	g
$\dot{m}_{RL}$	rhamnolipid separation rate	$g \cdot h^{-1}$
M	magnetisation	$A \cdot m^{-1}$
M_P	particle magnetisation	$A \cdot m^{-1}$
M_s	saturation magnetisation	$A \cdot m^{-1}$
M_g	specific magnetisation	$A \cdot m^2 \cdot kg^{-1}$
n	number of rotations of the stirrer or the cutting tool	rpm
Ne	Newton number	-
pO_2	dissolved oxygen concentration	%
P	load by compression	$N \cdot mm^{-2}$
P	power input	W
P/V	volumetric power input	$W \cdot m^{-3}$

P_r	partitioning ratio	-
P_{RL}	purity of rhamnolipids	-
PF	purification factor	-
ΔP	gas pressure difference	Pa
q	diffusion rate	$m^3 \cdot s$
q_2	range size distribution	%
Q_2	cumulative size distribution	%
r	bead radius	cm
R	initial sphere radius	mm
R,r	curvation radii of foam lamellae	m
R_1, R_2	bubble radii	m
R_{RL}	recovery of rhamnolipids	-
Re	Reynolds number	-
STY	space time yield	$g \cdot L^{-1} \cdot h^{-1}$
t	time	s
u_{fluid}	velocity of the fluid	$\mu m \cdot min^{-1}$
u_G	gas velocity	$m \cdot s^{-1}$
V_0	initial medium volume in bioreactor before feeding	L
$V_{bioreactor}$	liquid volume in bioreactor	L
V_{column}	volume of fractionation column	m^3
$\dot{V}_{foam}$	volumetric foaming rate	$L \cdot h^{-1}$
V_p	particle volume	m^3
x	distance	m
x_{50}	mean bead size	μm
$\bar{x}_{AV}$	Sauter mean diameter	μm
$Y_{X/S}$	specific biomass/ substrate yield coefficient	$g \cdot g^{-1}$
z	number of cutting wires	-

8.2.2 Greek symbols

δ_z	dimensionless approach	-
ε	power density	$W \cdot kg^{-1}$
ϕ_c	cell volume fraction	-
φ	deformation degree	-
γ	surface tension	$kg \cdot s^{-2}$
$\dot{\gamma}$	shearing rate	s^{-1}

κ	magnetic volume susceptibility	-
κ_i	intrinsic magnetic susceptibility	-
μ	specific growth rate	h^{-1}
μ_0	magnetic field constant	$V{\cdot}s{\cdot}A^{-1}{\cdot}m^{-1}$
μ_r	material dependent permeability	-
η	efficiency factor	-
π	ratio of the circumference of a circle to its diameter	-
ρ	liquid density	$kg{\cdot}m^{-3}$
σ_t	true yield stress	$N{\cdot}mm^{-2}$
τ	residence time	S
υ	Poisson's ratio	-

9 Publications within the scope of this work

- Development and trends of biosurfactant analysis and purification using rhamnolipids as an example.
  M. Heyd, A. Kohnert, T.-H. Tan, M. Nusser, F. Kirschhöfer, G. Brenner-Weiss, M. Franzreb, and S. Berensmeier
  Analytical and Bioanalytical Chemistry, 2008. 391(5): p. 1579-1590.

- Continuous Rhamnolipid Production with Integrated Product Removal by Foam Fractionation and Magnetic Separation of Immobilized *Pseudomonas aeruginosa*.
  M. Heyd, S. Trauth, M. Franzreb, and S. Berensmeier
  Biotechnology and Bioengineering, submitted.

- Influence of Different Magnetites on Properties of Magnetic *Pseudomonas aeruginosa* Immobilizates Used for Biosurfactant Production.
  M. Heyd, P. Weigold, M. Franzreb, and S. Berensmeier
  Biotechnology Progress, submitted.

- Whole-cell Immobilization of *Pseudomonas aeruginosa* in Different Magnetic Matrices for Continuous Biosurfactant Production.
  M. Heyd, P. Weigold, M. Franzreb, and S. Berensmeier
  Journal of Biotechnology, submitted.

10 Curriculum vitae

Dipl.-Ing. Miriam Heyd

* 26. Mai 1981 in Sindelfingen
deutsch

AUSBILDUNG

seit Okt. 2005	**Doktorarbeit** im Forschungszentrum Karlsruhe (FZK, Institut für Technische Chemie, Bereich Wasser- und Geotechnologie) ‣ Continuous production of rhamnolipids by means of process integration
April – Oktober 2005	**Diplomarbeit** im Institut für Thermische und Chemische Verfahrenstechnik an der TU Braunschweig ‣ Einfluss der Festphase auf das Fest-flüssig-flüssig-Gleichgewicht bei der Extraktion von Proteinen
Sept. 2002 – Febr. 2004	**3 Auslandssemester** an der Université de Technologie de Compiègne (UTC) in Frankreich
2000 – 2005	**Studium: Bioingenieurwesen** an der TU Braunschweig
1991 – 2000	Stiftsgymnasium in Sindelfingen Abschluss: Abitur

BERUFSERFAHRUNG

Aug. – Okt. 2004	**Verfahrenstechnisches Fachpraktikum** BASF AG in Ludwigshafen ‣ Charakterisierung des blasenbegasten Reaktors ISF100 hinsichtlich des Sauerstoffeintrags
Feb. – April 2004	**Fachpraktikum** im Bereich **Umwelttechnik** Eisenmann GmbH in Holzgerlingen ‣ Bearbeitung verschiedener Aufgabenstellungen bei der Planung von Abwasseranlagen
Sept. 2003 – Feb. 2004	**Studienarbeit** Institut National de la Recherche Agronomique (INRA) in Thiverval-Grignon (F) ‣ Fabrikation von Livarot (Käse) in Pilotanlagen, Qualitätsvergleich verschiedener Bakterien- und Hefemischungen
August 2001	**Verfahrenstechnisches Praktikum** Forschungsanstalt für Landwirtschaft (FAL) in Braunschweig ‣ Produktion von sphärischen Partikeln mit Hilfe des Strahlschneiderverfahrens
Juni/ Juli 2000	Praktikum in der Central Apotheke in Sindelfingen